Nonsense Mediated Decay Inhibition under NaCl stress in *Arabidopsis thaliana*

Dissertation

Der Mathematisch-Naturwissenschaftlichen Fakultät
Der Eberhard-Karls-Universität Tübingen
zur Erlangung des Grades eines
Doktors der Naturwissenschaften
(Dr. rer. nat.)

Vorgelegt von

MSc. Biol. Hsin-Chieh Lee
aus Taipei, Taiwan

Tübingen
2019

Gedruckt mit der Genehmigung der Mathematisch-Naturwissenschaftlichen Fakultät der Eberhard Karls Universität Tübingen.

Tage der mündlichen Qualifikation:	27.09.2019
Dekan:	Prof. Dr. Wolfgang Rosenstiel
1. Berichterstatter:	Prof. Dr. Andreas Wachter
2. Berichterstatter:	Prof. Dr. Klaus Harter

Eidesstattliche Versicherung / Statement of Authorship

Ich versichere hiermit, dass ich

- die vorliegende Arbeit selbstständig verfasst habe,
- keine anderen als die angegebenen Quellen benutzt und alle wörtlich oder sinngemäß aus anderen Werken übernommenen Aussagen als solche gekennzeichnet habe,
- und dass die eingereichte Arbeit weder vollständig noch in wesentlichen Teilen Gegenstand eines anderen Prüfungsverfahrens gewesen ist.

I hereby certify that

- that I have composed this doctoral thesis by myself,
- all references and verbatim extracts have been quoted, and all sources of information have been specifically acknowledged
- this doctoral thesis has not been accepted in any previous application for a degree, neither in total nor in substantial parts.

Tübingen, 5th Oct, 2019	
Ort, Datum/Place, Date	Unterschrift/Signature

Contents

List of Figures

List of Tables

List of Abbreviations

K	Rate constant
$t_{1/2}$	Half-life
$[Ca^{2+}]_{cyt}$	Ca^{2+} in cytosol
β-Me	β-mercaptoethanol
AZF2	*ZINK-FINGER PROTEIN 2*
RS2Z33	*ARGININE/SERINE-RICH ZINC KNUCKLE-CONTAINING PROTEIN 33*
VCS-ami no. 2	*VCS*-knockdown line no. 2
VCS-ami no. 4	*VCS*-knockdown line no. 4
lba1	*Low-beta-amylase*
^{7}mG	7-methyl guanosine
4sU	4-thiouridine
5BrU	5-bromouridine
5EU	5-ethynyluridine
A. thaliana	*Arabidopsis thaliana*
AA	Amino acid
ABA	Abscisic acid
ABI	ABA INSENSITIVE
ACA	AUTOINHIBITED CA^{2+} ATPASE
amiRNA	Artificial microRNA
APX	ASCORBATE PEROXIDASE
AS	Alternative precursor mRNA splicing
AtDRH1	ARABIDOPSIS THALIANA DEAD BOX RNA HELICASE 1
ATP	Adenosine triphosphate
BSA	Bovine serum albumin
Ca^{2+}	Calcium
CAF1	CCR4 associated factor 1
CaM	Calmodulin
CAX1	Vacuolar cation/proton exchanger 1
CBC	Cap-binding complex

CBL	Calcineurin B-like
CBP	CAP-BINDING PROTEIN
CCR4	Carbon catabolite repressor 4
cDNA	Complementary DNA
CDPK	Calcium-dependent protein kinases
CHX	Cycloheximide
CI	Confidence interval
CIPK	CBL-interacting protein kinases
CML	CaM-like
Col-0	Columbia 0
Col-5	Columbia 5
cordycepin	3'-deoxyadenosine
CPK	Ca^{2+}-dependent protein kinase
Ct	Cycle threshold
$d(N)_6$	Random hexamers
$d(T)_{20}$	Oligo dTs
DCL	Dicer-like
DCP	DECAPPING
DF	Deferoxamine
DMSO	Dimethylsufoxide
DMTU	*N,N'*-dimethylthiourea
DNA	Deoxyribonucleic acid
DPI	Diphenyleneiodonium
DREB2B	Dehydration-responsive element-binding protein 2
dsRNA	Double-stranded RNA
DTT	1,4-Dithiothreitol
EDTA	Ethylenediaminetetraacetic acid
eIF2α	EUKARYOTIC INITIATION FACTOR 2α
eIF4	EUKARYOTIC INITIATION FACTOR 4
EJC	Exon junction complex
ER	Endoplasmic reticulum
eRF	EUKARYOTIC RELEASE FACTOR
EtOH	Ethanol

flg22	Flagellin peptide flg22
FLS2	FLAGELLIN-SENSING 2
GCN2	GENERAL CONTROL NON-DEREPRESSIBLE 2
h	Hours
H_2O	MilliQ water
H_2O_2	Hydrogen peroxide
HACC	Hyperpolarization-activated Ca^{2+} channel
HK	Histidine kinase
HKT1	High-affinity K^+ transporter 1
hnRNP	Heterogenous nuclear ribonucleoprotein
HO^*	Hydroxyl radical
HOS5	HIGH OSMOTIC STRESS GENE EXPRESSION 5
HSP	Heat shock protein
IC_{50}	Half maximal inhibitory concentration
K252a	Kinase inhibitor from *Nonomuraea longicatena*
kDa	Kilo Dalton
$LaCl_3$	Lanthanum (III) chloride
Ler	Landsberg erecta
LLPS	Liquid-liquid phase separation
LSM	Sm-like
m	Minutes
m^6A	N^6-methyladenosine
MeOH	Methanol
MilliQ	Ultrapure water of Type 1 laboratory use Milli-Q water (defined by ISO 3696) from the Millipore Corporation
miRNA	Micro RNA
mRNA	Messenger RNA
mRNP	MRNA-ribonucleoprotein

MUSE	MUTANT, *SNC1*-ENHANCING
N. benthamiana	*Nicotiana benthamiana*
N. tabacum	*Nicotiana tabacum*
NASC	Nottingham Arabidopsis Stock Centre
ncRNA	Non-coding RNA
NGD	No-go decay
NGS	Next generation sequencing
NHX1	Sodium/hydrogen exchanger 1
NLR	NOD-LIKE RECEPTOR
NMD	Nonsense mediated decay
NOX	NADPH oxidase
NSD	Non-stop decay
nt	Nucleotides
NUP	Nucleoporin
O_2^{*-}	Superoxide
O. sativa	*Oryza sativa*
OA	Okadiac acid
ORF	Open reading frame
P-bodies	Processing-bodies
P. patens	*Physcometrella patens*
PA	Phosphatidic acid
PABP	Poly[A]-binding protein
PAMP	Pathogen-associated molecular pattern
PAN	Poly[A]-specific nuclease
PARN	Poly[A]-specific ribonuclease
PCR	Polymerase chain reaction
PERK	Protein kinase RNA-like endoplasmic reticulum kinase
PH	Pleckstrin homology
PKS	SOS2-LIKE PROTEIN KINASE
PLD	Phospholipase D
PM	Plasma membrane
PMSF	Phenylmethylsulfonyl fluoride

poly[A]	3' polyadenylated
poly[Y]$_{15–20}$	Polypyrimidine tract
PP2A	PROTEIN PHOSPHATASE 2A
pre-miRNA	Precursor micro RNA
pre-mRNA	Precursor mRNA
PSI	Photosystem I
PTB	POLYPYRIMIDINE TRACT BINDING PROTEIN
PTC	Premature termination codon
PVDF	Polyvinylidenfluorid
q-PCR	Quantitative PCR
R. solanacearum	*Ralstonia solanacearum*
RBOH	RESPIRATORY BURST OXIDASE HOMOLOGUE
RBP	RNA-binding protein
RCD	Radical-induced cell death
RH14	DEAD-box ATP-dependent RNA helicase 14
RIN	RNA integrity number
RIP	RNA immunoprecipitation
RISC	RNA-induced silencing complex
RNA	Ribonucleic acid
RNA-seq	RNA sequencing
RNAi	RNA interference
RNase	Ribonuclease
RNP	Ribonucleoprotein
ROS	Reactive oxygen species
ROUT	Robust regression and outlier removal
rRNA	Ribosomal RNA
RSA1	SHORT ROOT IN SALT MEDIUM 1
RT	Reverse transcription
RT-qPCR	Reverse transcription and quantitative PCR
SA	Salicylic acid
SCaBP8	SOS3-LIKE CALCIUM BINDING PROTEIN 8
SD	Standard deviation

SDS	Sodium-Dodecyl-Sulfate
SDS-PAGE	Sodium dodecyl sulfate polyacrylamide gel electrophoresis
Ser5P	Serine 5 phosphorylation
SG	Stress granules
SIR	SULFITE REDUCTASE
siRNA	Short interfering RNA
SKIP	Ski-interacting protein
SMG	SUPPRESSOR OF MORPHOLOGICAL DEFECTS ON GENITALIA
snoRNA	Small nucleolar RNA
SnRK	Sucrose non-fermenting-1 (SNF1)-related protein kinases
snRNAs	Small nuclear RNAs
snRNPs	Small nuclear ribonucleoproteins
SOD	Superoxide dismutase
SOS	SALT OVERLY SENSITIVE
SPB	Sodium phosphate buffer
SR	Serine-arginine-rich
SR30	SERINE/ARGININE-RICH PROTEIN 30
ssRNA	Single-stranded RNA
T-DNA	Transfer DNA
T-DNA	Transfer DNA
TBS	Tris buffered saline
TF	Transcription factor
TIM14	MITOCHONDRIAL IMPORT INNER MEMBRANE TRANSLOCASE
TNL	TIR domain-containing, nucleotide-binding, leucine-rich repeat
TOP	5' terminal oligopyrimidine
TOR	Target of rapamycin
tRNA	Transfer RNA
U2AF	U2 small RNA auxiliary factor
uORF	Upstream open reading frame
UPF	UP FRAMESHIFT
UPR	Unfolded protein response
UTR	Untranslated region

UV	Ultraviolet
V	Volts
VCS	VARICOSE
WT	Wild-type
XRN	Exoribonuclease

‘Twas brillig, and the slithy toves
Did gyre and gimble in the wabe,
All mimsy were the borogroves,
And the mome raths outgrabe.

Lewis Carroll

1 Abstract / Zusammenfassung

Abstract Nonsense mediated decay (NMD) is an mRNA surveillance system present in all eukaryotes, which regulates large quantities of transcripts, and has a considerable impact on gene expression. NMD plays an essential role in survival and development, and is regulated in response to various signals and stresses. Salinity stress is a major threat to crop yields worldwide, and interestingly, affects NMD as well. To understand the mechanism that mediates NMD impairment under salt stress, a reliable assay to measure mRNA decay in plants was first established. Using this assay, it was demonstrated that NaCl-mediated NMD inhibition had a dose-response relationship, was specific to the NMD pathway and did not result from changes in general decay. NaCl-mediated NMD also shows specificity to NaCl, as KCl did not elicit the same degree of response. Furthermore, transcripts of several NMD core components possess NMD triggering features, and therefore NMD feedback regulation of these transcripts were examined. Using the established assay, and mutants deficient in NMD, several transcripts of the NMD core components were confirmed to be also under regulation of NMD. Under salt stress these transcripts were further stabilized in addition to the stabilization caused by the mutants, indicating the partially retained NMD function can further be shut off by additional salt. To address the upstream regulatory mechanism, abscisic acid (ABA) was found to be neither sufficient nor required for salt mediated NMD inhibition, nor were downstream SNF1-RELATED KINASES 2 (SnRK2s), as determined by analysing class I and class III SnRK2 mutants. SnRK2s and its phosphorylation target VARICOSE (VCS) were tested as they had been reported to play a role in mRNA stability under osmotic and salt stress. Downregulation of VCS in VCS artificial microRNA knockdown lines, seems to inhibit NMD target transcripts under control conditions, but exhibit little difference compared to wild type (WT) under salt stress. NMD is also tightly linked to translation. Using cycloheximide, a translation elongation inhibitor, the accumulation of NMD targets suggests NMD inhibition involves interference with translation elongation. However, analyzing components of translation initiation by inducing EUKARYOTIC INITIATION FACTOR 2α (eIF2α) phosphorylation via chlorsulfuron, or by using mutants, which lack the kinase GENERAL CONTROL NONDEREPRESSIBLE 2 (GCN2), does not seem to affect the decay of NMD targets. Other stresses such as heat stress were examined. Heat at 30 °C showed accelerated degradation and 38 °C showed the stabilization of transcripts, possibly due to heat stress granule formation at 34 °C, according to recent literature. Mutants deficient in decapping components, that are associated with UP-FRAMESHIFT 1 (UPF1), which are also P-body and stress granule components seem to regulate NMD target transcripts under control conditions, but show little difference in their

expression compared to WT under salt stress. Phosphorylation is likely involved in NaCl-mediated NMD inhibition, based on the rapid and reversible stabilization and destabilization of NMD target mRNAs in response to salt exposure. Stimulation of cytosolic Ca^{2+} influx and application of external H_2O_2 mimics the stabilization pattern of NMD targets under salt. Using paraquat, reactive oxygen species (ROS) produced at the chloroplast seemed not to affect NMD. *SALT OVERLY SENSITIVE* (*SOS*) mutants, *sos1-1* and *sos2-2*, show hyperstabilization of NMD targets, while *sos3-1* does not exhibit difference from WT control. In a Phos-tag gel, SMG7 could not be detected in *sos2-2*, but is detected on the western blot. This could indicate the phosphorylated form of SMG7 present in *sos2-2* was extracted under suboptimal conditions, and thus cannot be visualized. Taken together with data from Ca^{2+} and H_2O_2 experiments, as well as recent publications, I propose a mechanism in which SMG7 is phosphorylated in a calcium-dependent manner, which can be triggered by (but not limited to) apoplastic H_2O_2 under salt stress conditions. According to this model, changes in the phosphorylation status of SMG7 in turn affects the efficiency of NMD, allowing for dose-dependent, fine adjustments to transcript control in the cell.

Zusammenfassung Nonsense mediated decay (NMD) ist ein mRNA-Kontrollmechanismus in Eukaryoten, der eine Vielzahl von Transkripten reguliert. Daher hat er auch einen großen, direkten Einfluss auf die Expression vieler Gene. NMD spielt eine zentrale Rolle in der Pflanzenentwicklung und ist Teil von vielen Stressantworten. Salzstress ist eine große Bedrohung für Nutzpflanzen weltweit, und hat außerdem einen Einfluss auf NMD. Um die zugrundeliegenden Mechanismen der durch Salzstress vermittelten Beeinträchtigung des NMD näher zu untersuchen, wurde zuerst eine zuverlässige Methode zur Messung des RNA Abbaus etabliert. Mittels dieser Messmethode konnte gezeigt werden, dass die Salzstress-vermittelte Inhibition des NMD Dosis abhängig ist, sowie spezifisch auf den Mechanismus des NMD wirkt, und nicht von einer allgemeinen Beeinflussung der RNA Abbauprozessen her rührt. Die Salzstress vermittelte NMD Inhibition scheint spezifisch für NaCl zu sein, da andere Salze wie z.B. KCl keinen vergleichbaren Effekt zeigen. Zudem weisen einige Transkripte zentraler NMD Komponenten NMD auslösende Charakteristika auf, was uns dazu veranlasste, NMD vermittelte Rückkopplungseffekte an diesen Transkripten zu untersuchen. Mittels der von uns etablierten Methode zur Erfassung von RNA Abbauprozessen sowie verschiedenen NMD defizienten Mutanten gelang es uns zu zeigen, dass tatsächlich einige dieser Transkripte selbst einer Regulation durch NMD unterliegen. Die in NMD Mutanten auftretende Stabilisierung dieser Transkripte wurde unter Salzstress noch verstärkt. Dies weist daraufhin, dass die noch teilweise Erhaltene NMD Funktion der Mutanten durch applizierten Salzstress weiter verringert werden kann. Im Bestreben übergeordnete,

regulatorische Prozesse zu identifizieren, wurde festgestellt, dass Abszisinsäure (ABA) weder ausreicht, noch benötigt wird für Salzstress abhängige NMD Inhibition. Die untergeordneten SNF1-RELATED KINASES 2 (SnRK2s) ist ebenfalls unbeteiligt, was anhand von Analysen der Klasse I und III SnRK2 Mutanten gezeigt werden konnte. SnRK2s und das davon phosphorylierte VARICOSE (VCS) wurden überprüft, da andere Studien eine Rolle in die Regulation von mRNA Stabilität während Salzstress zeigten. Die Reduktion der VCS Expression in VCS amiRNA Linien zeigte eine Inhibition von NMD regulierten Transkripten unter Kontrollbedingungen, jedoch keinen signifikanten Effekt unter Salzstress im Vergleich zum Wildtyp (WT). Des Weiteren weist NMD eine enge Verbindung zu Translationsprozessen auf. Die Applikation des Translations-Elongations Inhibitors Cycloheximid hat die Akkumulation von NMD regulierten Transkripten zur Folge. Dies legt nahe, dass eine NMD Inhibition die Beeinträchtigung der Translations-Elongation zur Folge hat. Dennoch konnte durch die Applikation von Chlorsulfuron, einem Induktor der Phosphorylierung des EUKARYOTISCHEN INITIATIONSFAKTORS 2 α (eIF2α), kein Effekt auf den Abbau von NMD regulierten Transkripten festgestellt werden. Ein Effekt war ebenfalls nicht detektierbar in *gcn2* (*general control nondepressible 2*) Linien. GCN2 vermittelt *in-vivo* die eIF2α phosphorylierung. Auch andere Stressfaktoren wie z.B. Hitzestress wurden untersucht. Bei 30 °C konnte ein beschleunigter Abbau von regulierten Transkripten festgestellt werden, bei 38 °C hingegen eine Stabilisierung derselben. Ausgehend von jüngster Literatur, könnte dies von der Bildung von Hitzestress-Körperchen (Heat stress-granules) bei 34 °C herrühren. Unter Kontrollbedingungen scheinen Pflanzen mit mutierten Decapping Komponenten, die mit UP-FRAMESHIFT PROTEIN 1 (UPF1) interagieren, und des Weiteren Bestandteile von P-bodies und Stress-Körperchen (Stress granules) sind, NMD regulierte Transkripte beeinflussen. Unter Salzstress zeigen diese jedoch nur minimale Änderungen in Ihrer Expression im Vergleich zum WT. Basierend auf der schnellen und reversiblen (De-) Stabilisierung von NMD regulierten Transkripte, sind sehr wahrscheinlich Phosphorylierungsprozesse in die NaCl vermittelte NMD Inhibition involviert. Das Stabilisierungsmuster von NMD Transkripten unter Salzstress kann sowohl durch die Stimulation von cytosolischem Ca^{2+} Influx, als auch durch externe H_2O_2 Applikation nachgeahmt werden. Eine mittels Paraquat Behandlung ausgelöste Reaktive Sauerstoffspezies (ROS) Akkumulation in den Chloroplasten hingegen zeigte keinen Einfluss. Die *SALT OVERLY SENSITIVE* (*SOS*) Mutanten *sos1-1* und *sos2-2* zeigen eine Hyperstabilisierung von NMD regulierten Transkripten, *sos3-1* jedoch zeigen keinen Effekt. In einem Phos-Tag Gel konnte SUPPRESSOR WITH MORPHOLOGICAL DEFECTS IN GENITALIA 7 (SMG7) in *sos2-2* Pflanzen nicht nachgewiesen werden. Auf dem entsprechenden Western-Blot war der Nachweis möglich, was die Folge einer suboptimalen Extraktion des phosphoryliertem

SMG7 sein könnte. Zusammen mit den Daten der Ca^{2+} und der H_2O_2 Experimente, sowie von neuesten Publikationen, schlage ich einen Mechanismus vor, in welchem SMG7 Ca^{2+} abhängig phosphoryliert wird, was wiederum unter anderem durch apoplastisches H_2O_2 im Rahmen einer Salzstress Antwort ausgelöst wird. Ausgehend von diesem Modell wird mittels des Phosphorylierungsstatus von SMG7 die NMD Effizienz moduliert, was wiederum eine dosis-abhängige Feinjustierung der Transkriptkontrolle in der Zelle erlaubt.

2 Contributions

Several graphs in this study were the combined efforts of multiple people. They have been included to provide extra context of the reasoning behind several experimental approaches, or as control conformations (that the mutants or wild type are behaving as expected). The research was designed by Prof. Andreas Wachter and myself, data interpretation was a combined effort between Prof. Andreas Wachter and myself. If not mentioned otherwise, all data collection and analysis, including graph plotting, half-life and rate constant calculation, decay regression, statistical test calculations, were done by myself. The choice of figure display and which statistical test to use was a combined decision between Prof. Andreas Wachter and myself.

Figure 10 Data collected by Siliya Köster-Hofmann.

Figure 28 Data collected by Siliya Köster-Hofmann.

Figure 34 Data collected in collaboration with Caroline Wall. Graph reworked from Wall (2017), incorporated regression curves with rate constant calculations.

Figure 45 Data collected by Siliya Köster-Hofmann.

Figure 46 Data collected by Siliya Köster-Hofmann.

Figure 47 Data collected by Siliya Köster-Hofmann.

Figure 48 Data collected by Siliya Köster-Hofmann.

Figure B.1 Figure and text generated by Prof. Andreas Wachter, data generated by Patrizia Ricca, Natalie Faiss and others.

Figure C.1 Figure and text generated by Prof. Andreas Wachter. Data generated by others.

Figure D.1 Data and graphs generated by myself, figure assembled and figure legend written by Prof. Andreas Wachter.

Figure G.1 Figures and legend generated by Prof. Andreas Wachter. Data from (A–D) generated by others, data from (E–F) generated by myself.

Figure H.6 Data collected by Caroline Wall. Graph reworked from Wall (2017), added in error bars.

3 Introduction

Life is only possible if cells can store, retrieve, execute and regulate the genetic information required to create and maintain a living organism. This information is passed on from a cell to its daughter cells, and is encoded in genes. The journey of gene expression begins with transcription, where deoxyribonucleic acid (DNA) is transcribed into ribonucleic acid (RNA), which can either be functional, or act as an intermediate template for translation into protein. RNA biogenesis starts with transcription.

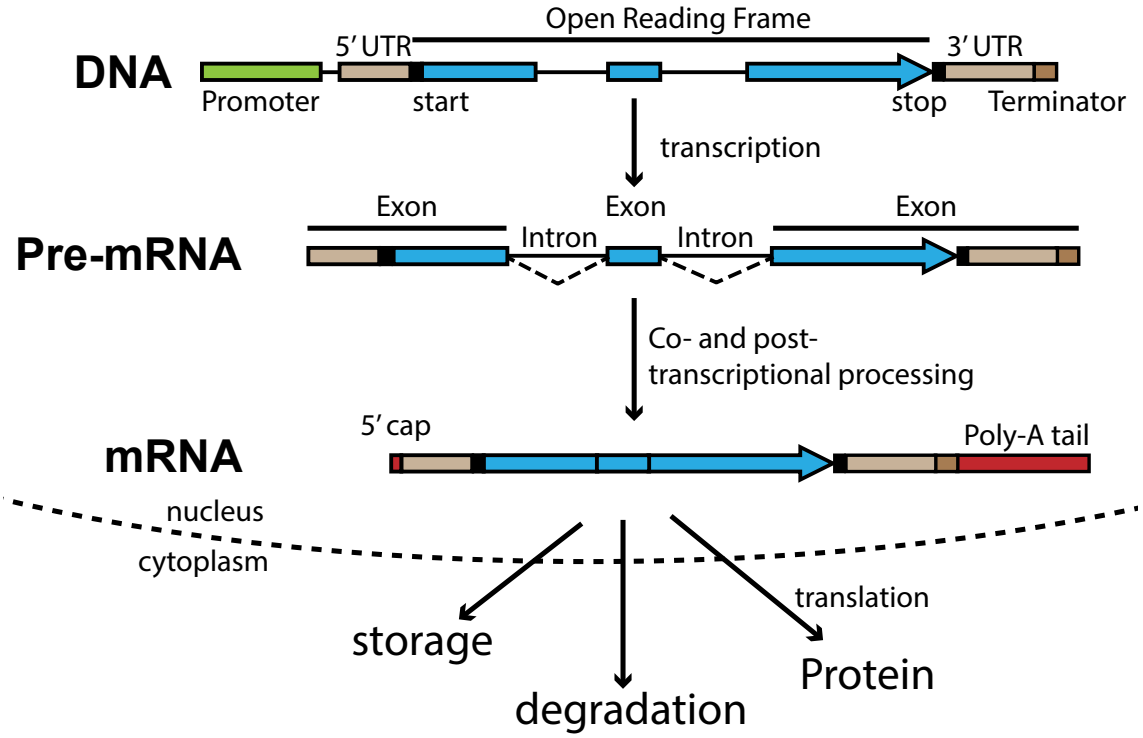

Figure 1: Overview of the biogenesis and fate of mRNA (transcripts). In eukaryotes, precursor mRNA (pre-mRNA) is created as a first product of transcription, and post-transcriptional modifications such as 5'-capping, 3'-polyadenylation, and (alternative) splicing occurs to form mature mRNA. The mRNA is then exported out of the nucleus to be translated, sometimes stored, or degraded. RNA steady state levels refers to the homeostasis resulting from RNA biogenesis and degradation. Nuclear RNA degradation can also take place, and various degradation pathways are outlined in Figure 4. The promoter is depicted in green, 5'- and 3'-UTRs are depicted in beige, and start and stop codon in black. The terminator is shown in brown and extends beyond the 3'-UTR. The open reading frame is shown as blue for exons (which can include the 5'-UTR and start codon, or 3'UTR, stop codon, and terminator), and lines for introns. The 5'-cap and poly-A tail that are added co- and post-transcriptionally are shown in red.

Transcription initiates with the binding of RNA polymerase to DNA, and the non-coding strand of the DNA is used as template for transcription. The RNA

polymerase travels on the template strand from 3'→5', synthesizing a new RNA molecule from 5'→3'. In eukaryotes, pre-mRNAs are the first product of transcription, which are then processed to form mature messenger RNA (mRNA) (Figure 1). Since Gene expression constantly undergoes fluctuations, and cellular status can change substantially, therefore, the regulation of genetic information is particularly important. RNA biogenesis and degradation are two sides of the same coin, and both are required to control RNA levels in the cell. This is called RNA (transcript) steady state levels. Several different types of RNA are produced as a result of transcription. The products of transcription are also referred to as transcripts. Apart from mRNAs, which most (but not all) are protein coding, transfer RNA (tRNA) and ribosomal RNA (rRNA), which are involved in translation, there are many non-coding RNA (ncRNA)s, that are not translated into protein. These ncRNAs, such as short interfering RNA (siRNA), micro RNA (miRNA), or ribozymes (ribonucleic acid enzymes), which are enzymatically active RNA molecules, are functionally important, and involved in many biological processes. During and after transcription, the pre-mRNA are processed. These processes include 5'-capping, 3'-polyadenylation, and (alternative) splicing.

3.1 Co- and Post-transcriptional processing

5'-capping As the nascent pre-mRNA is being synthesized, the 5'-end of the pre-mRNA is modified with a 7-methyl guanosine (^{7}mG) cap. Through a 5' to 5' triphosphate linkage, a guanine nucleotide can be connected. This guanosine is then methylated on the 7th position by a methyltransferase (Shatkin, 1976; Banerjee, 1980; Marcotrigiano et al., 1997; Sonenberg and Gingras, 1998). In the nucleus, ^{7}mG-capped RNA is bound by the nuclear cap-binding complex (CBC), which is recognized by the nuclear pore complex and exported. In the cytoplasm, after the pioneer round of translation (Section 3.4), the nuclear CBC is replaced by the cytoplasmic CBC, namely EUKARYOTIC INITIATION FACTOR 4 (eIF4)E (Maquat et al., 2010). eIF4E is part of the eIF4F complex, which consists of eIF4E, eIF4G (Results section 4.12) and eIF4A. This complex forms an RNA loop with poly[A]-binding protein (PABP) to ensure productive translation, and the eIF4E/G complex protects the mRNA from decapping enyzmes. The 5'-cap serves as a starting point where the ribosome binds, and scanning begins, and is critical for the construction of functional mRNAs (Cooper and Hausman, 2007). Removal of the cap (decapping, Section 3.3.1) will lead to degradation of the RNA (Section 3.3.1).

3'-polyadenylation Upon transcription termination, the pre-mRNA is cleaved by a set of proteins, and a stretch of adenosine monophosphates are attached to the 3'-end of the pre-mRNA (Bienroth et al., 1993; Hunt et al., 2008). This is referred

to as the 3' polyadenylated (poly[A]) tail. In some genes there are more than one possible site for the poly[A] tail to attach, and alternative polyadenylation may occur. The poly[A] tail acts as the binding site for PABP, which promotes nuclear export, translation, and cytoplasmic mRNA stability (Bernstein and Ross, 1989; Babbs et al., 1989; Sachs, 1990; Coller et al., 1998). Effective translation depends on the formation of an mRNA loop, caused by interactions between the PABP and eIF4G, which is part of the cytoplasmic CBC, which acts as a scaffolding protein, connecting PABP and eIF4E. As the tail shortens over time, or if deadenylation (Section 3.3.1) occurs, the mRNA is degraded (Guhaniyogi and Brewer, 2001). Although the poly[A] tail promotes stability in eukaryotic mRNAs, polyadenylation promotes RNA degradation in bacteria and organelles (Steege, 2000; Slomovic et al., 2006), and in some cases eukaryotic ncRNAs (Anderson, 2005; Reinisch and Wolin, 2007; Zhuang et al., 2013).

Splicing Splicing is present in both eukaryotic and prokaryotic cells. However, even though there are self-splicing introns in prokaryotes, splicing through the spliceosome is unique to eukaryotic cells. Under guidance of the spliceosome, introns are removed and exons are joined to form mature mRNA (Figure 2). Most commonly, at the 5' end of the intron that is to be removed, a splicing donor site begins with GU, and ends with AG as the acceptor site at the 3' end. These sequences are strongly conserved and mutation in the main sites would result in activation of alternative cryptic sites, or sometimes splicing inhibition. Approximately 5–40 nucleotides (nt) upstream of the 3' end of the intron is a polypyrimidine tract ($\text{poly[Y]}_{15–20}$) followed by the branch point, which always contains an adenine (A), but is loosely conserved in other respects (Black, 2003; Clancy, 2008). A general consensus would look like YNYYRAY, with Y representing a pyrimidine, N as any nucleotide, R as any purine, and A as adenine (Clancy, 2008; Taggart et al., 2012). Specific sequences of these elements and number of base pairs between the branch point and the 3' acceptor site will affect splice site selection (Corvelo et al., 2010; Taggart et al., 2012). The spliceosome consists of five small nuclear RNAs (snRNAs) and the spliceosomal proteins. Combined with protein factors, these RNA-protein complexes form small nuclear ribonucleoproteins (snRNPs) (commonly pronounced "snurps"). The snRNPs that make up the spliceosome are named U1, U2, U4, U5, and U6, due to the snRNAs being rich in uridine (U). Additional proteins such as U2 small RNA auxiliary factor (U2AF)35 and U2AF65 are required for spliceosome assembly as well (Graveley et al., 2001; Black, 2003; Matlin et al., 2005). Splicing begins as the exon borders are brought close, U1 binds to GU at the 5'-end of the intron and is cleaved, U2AF65 to the $\text{poly[Y]}_{15–20}$, and U2AF35 at the 3' splice site (Guth and Valcárcel, 2000). U2 binds to the branch point, and places 2' OH of the protruded adenosine in a favorable position (Newby and Greenbaum, 2002). U5/U4/U6 forms a trimer, with U5 binding to the 5' end of the exon, and U4/U6 binding to U2. U1 is released, U5 shifts from

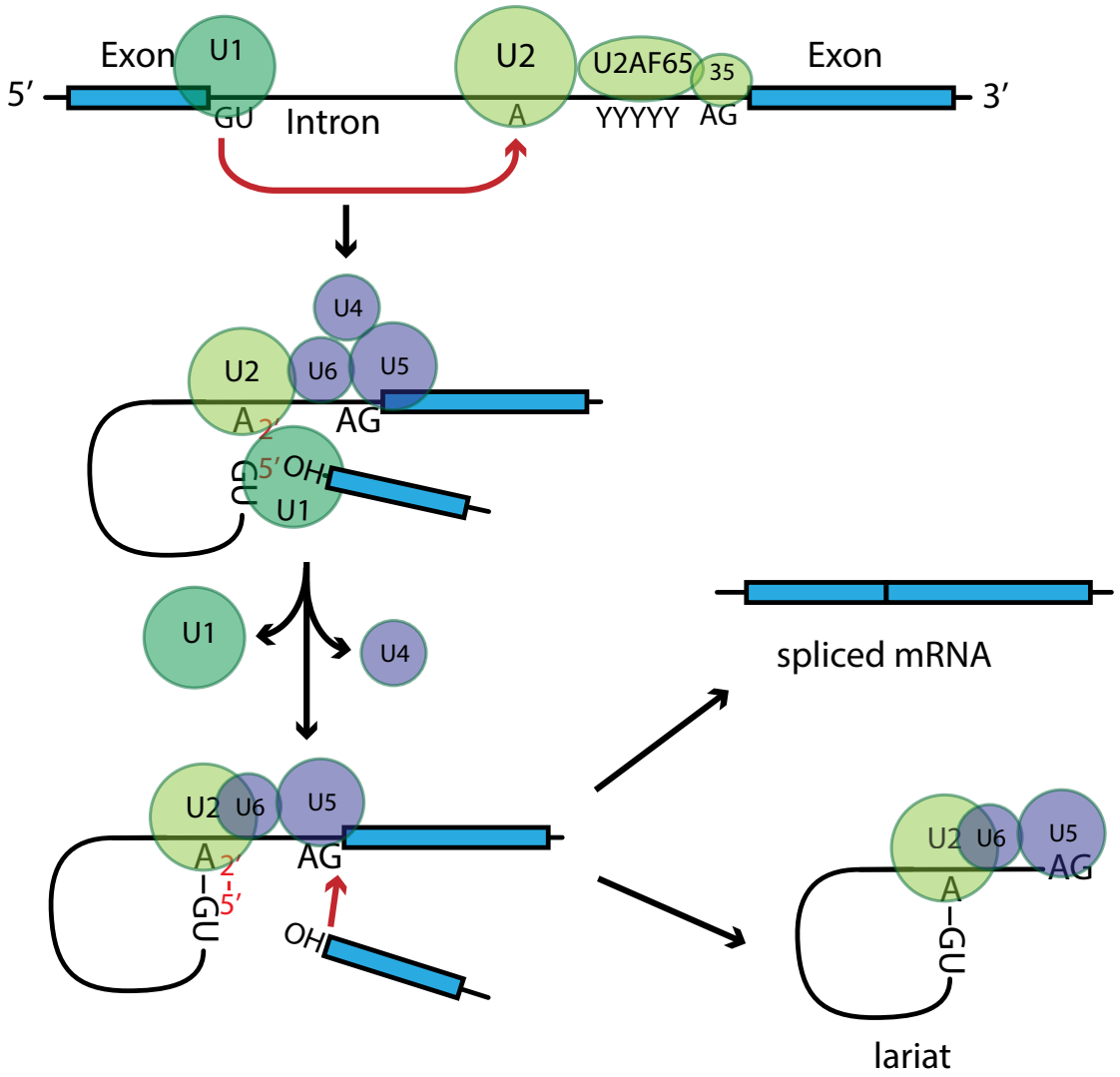

Figure 2: Overview of mRNA splicing. In the pre-mRNA within the introns, a donor site (GU) is located at the 5' end, a branch site (A) close to the 3' end, followed by a polypyrimidine stretch (YYYYY) and an acceptor site (AG) at the 3' end. Spliceosome U1 binds to the donor site and cleaves the 5'-end of intron ("p" represents phosphate at the cut site), and U2 small RNA auxilary factors (U2AF) binds to the polypyrimidine tract. U2 binds to the branch site and is bridged by U5/U4/U6 to the 3'-end. U6/U2 forms a lariat with the 2' OH of the A in the branch site and the 5' end of the donor site, and the 3' end of the intron is cleaved and the lariat is released. Exons are joined through ATP hydrolysis, and the spliceosomes are disassembled and recycled.

exon to intron, and U6 binds at the 5' splice site (Staley and Guthrie, 1998; Burge et al., 1999). U4 is released, U6/U2 ligates the 5' end of GU to the 2' end of the branch point through transesterification, and forms the lariat structure (Staley and Guthrie, 1998; Burge et al., 1999; Fica et al., 2013). The 3' site is cleaved, exons are ligated through ATP hydrolysis, the lariat is released with U2/U5/U6, which later disassembles and gets recycled (Black, 2003; Clancy, 2008; Cheng and Menees, 2011;

Fica et al., 2013; Matera and Wang, 2014).

Alternative splicing Alternative precursor mRNA splicing (AS) is a major source of transcriptome diversity in eukaryotes. According to current knowledge, genome-wide transcriptome mapping in plants shows AS events ranges anywhere from 42–61 % (Filichkin et al., 2010; Reddy et al., 2013; Marquez et al., 2012; Klepikova et al., 2016), which probably still does not include all events, and is likely a lower estimate of total occurrences. There are a couple of modes which splice sites can be joined together (Figure 3) (Black, 2003; Matlin et al., 2005; Pan et al., 2008; Sammeth et al., 2008; Xin et al., 2008; Tian and Manley, 2016):

- **Cassette exons** are exons that be skipped or included from the mRNA. Cryptic exons (cassette exons) that are included in some but not all transcripts, opposed to constitutive exons which are always included. Cryptic exons are on average shorter, and flanked by weaker splice sites than constitutive exons (Berget, 1995; Stamm et al., 2000).
- **Mutually exclusive exons**, only one of two or more exons are kept after splicing.
- **Alternative donor site** are competing 5' donor sites that change the 3' end of the upstream exon.
- **Alternative acceptor site** are competing 3' acceptor sites that change the 5' end of the downstream exon.
- **Intron retention**, where an intron is either retained or spliced out.
- **Alternative transcription start sites** resulting from multiple promoters can be used in conjunction with AS to regulate gene expression (Ayoubi and Van De Ven, 1996; Matlin et al., 2005; Xin et al., 2008), although it does not necessarily need to be at the level of splicing.
- **Alternative polyadenylation** or alternative 3' end positions can also be used in conjunction with AS to regulate gene expression (Barbas et al., 1988; Chen et al., 2017a; Li et al., 2017a), and does not need to be at the level of splicing.

Splicing decisions are complex with many components at play. Two major universal splicing regulatory factors consists of serine-arginine-rich (SR) proteins and the heterogenous nuclear ribonucleoprotein (hnRNP) protein family, which interact with splicing activators and suppressors depending on context (Wachter et al., 2012). In addition to the known factors, there are still unknown aspects of this waiting to be resolved. Physiologically, AS in plants is known to have many regulatory functions, including components of the circadian clock (Deng et al., 2010; Sanchez et al., 2010; Jones et al., 2012; Seo et al., 2012; Filichkin et al., 2015), temperature sensing and flowering (Song et al., 2012; Lee et al., 2013; Posé et al., 2013), biotic stress (Dinesh-Kumar and Baker, 2000; DeYoung and Innes, 2006; Palma et al., 2007) and abiotic stress responses (see Section 3.5).

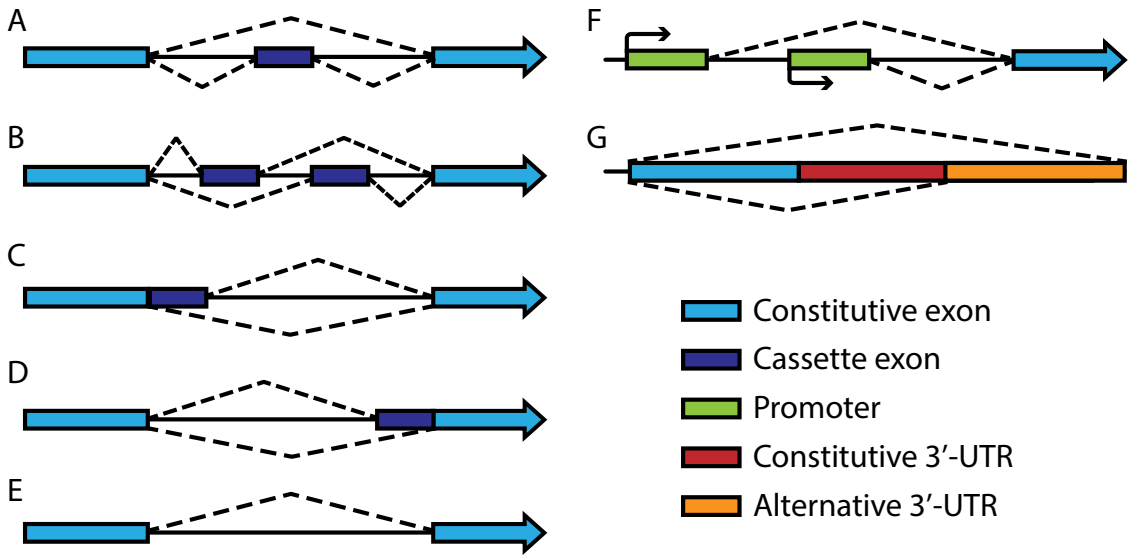

Figure 3: Different modes of alternative splicing (AS). (A) Cassette exons can be spliced out or retained, (B) one out of two or more mutually exclusive exons will be retained after splicing, (C) alternative 5' donor site or (D) alternative 3' acceptor site, as well as (E) retained introns are AS events. In combination with AS, (F) alternative transcription start sites, resulting from promoters (Xin et al., 2008) or (G) alternative 3' UTR end positions (alternative polyadenylation) can regulate gene expression (Tian and Manley, 2016). Constitutive exons or 3'-untranslated region (UTR) are exons or 3' UTRs that are consistently conserved after splicing.

3.2 Alternative splicing and abiotic stress

A large number of plant stress response genes are regulated through AS. One field of study would be heat shock induced transcriptional regulation, where 22 °C would result in a full-length transcript with a spliced out intron (*HsfA2*), but 37 °C activates a 31 bp cryptic exon within the intron and produces a premature termination codon (PTC) containing variant (*HsfA2-II*) which is degraded via nonsense mediated decay (NMD) (von Koskull-Doring et al., 2007; Sugio et al., 2009). Under extreme heat 42–45 °C , a third splice form (*HsfA2-III*) is produced by an alternative 5' splice site, at the expense of *HsfA2-II* (Liu et al., 2013b). *HsfA2-III* encodes a truncated protein which binds to the *HsfA2* promoter and forms a positive autoregulatory loop. Reactive oxygen species (ROS) (Section 3.5.2) is also linked to AS. In maize, *ZmrbohB* has two AS isoforms, *ZmrbohB-*α and an intron-retaining -β, which contains a PTC, and is a likely target of NMD. *ZmrbohB* was differentially expressed spatially and temporally, and *ZmrbohB-*α transcripts accumulate under various abiotic stresses, such as wounding, cold (4 °C), heat (40 °C), ultraviolet (UV) and salinity stress (Lin et al., 2009a). In rice, through AS, DEHYDRATION-RESPONSIVE ELEMENT-BINDING PROTEIN 2 (DREB2B) can be produced rapidly, independent of transcriptional activation. *OsDREB2B* are alternatively

spliced in heat and drought stresses. Under control conditions, *OsDRE2B1* is more abundant and contains an exon insertion that creates an open reading frame (ORF) shift. When exposed to high temperatures, the isoform which the cassette exon is spliced out (*OsDREB2B2*) dominates (Matsukura et al., 2010). A similar mechanism is also reported for its orthologues in wheat, barley and maize (Xue and Loveridge, 2004; Egawa et al., 2006; Qin et al., 2007). Abscisic acid (ABA) signaling is also associated with plant stress responses as well as RNA processing factors. Proteogenomic analysis shows AS and translation to play a role in ABA response (Zhu et al., 2017). The pre-mRNA of *HAB1* is regulated with AS by a protein that binds to the last intron. Two splice isoforms *HAB1.1* and *HAB1.2* are produced. *HAB1.1* encodes a protein which inhibits the kinase activity of sucrose non-fermenting-1 (SNF1)-related protein kinases (SnRK)2.6 and turn ABA signaling off. *HAB1.2* can still interact with SnRK2, but is unable to regulate kinase activity, leaving ABA signaling on (Wang et al., 2015; Zhan et al., 2015). Therefore, as a result of AS, two antagonistic, functional proteins are produced, showing the importance of AS for ABA signaling. Salt stress induces genome-wide AS in *Arabidopsis thaliana* as well, and influence 5'- or 3'-splice site selection, intron retention, which can contain PTCs (Ding et al., 2014; Feng et al., 2015). Knockout mutants of *HIGH OSMOTIC STRESS GENE EXPRESSION 5 (HOS5)*, *RS40*, *RS41* show salt and ABA hypersensitivity and significant intron retention in stress-related genes (Chen et al., 2013). Several hnRNPs regulates seed germination, early development, stomatal movements under cold, salt or drought stress in *A. thaliana* (Kim et al., 2007, 2008). In particular, using a RNA immunoprecipitation (RIP) analysis combined with reverse transcription (RT)-coamplified polymerase chain reaction (PCR), Streitner et al. (2012) was able to show direct binding of an hnRNP-like RNA-binding protein to mRNA, causing alternative 5'-splice site choices. CAP-BINDING PROTEIN (CBP)20 and CBP80 are also involved in salt and drought stress responses during seed germination, ABA sensitivity and stomatal closure (Hugouvieux et al., 2001; Papp et al., 2004; Kong et al., 2014; Daszkowska-Golec et al., 2017). These proteins are involved in cap-binding and found to influence AS in *A. thaliana*, particularly the 5'-splice site of the first introns (Raczynska et al., 2010). Ski-interacting protein (SKIP) is a splicing factor, which confers osmotic tolerance under salt stress through regulation of salt-tolerance genes by AS, providing further links of AS and plant salt responses (Feng et al., 2015).

3.3 mRNA Decay

Opposite of biogenesis, degradation is equally important for regulating RNA levels. RNA stabilities can differ drastically in different organisms, for example bacterial

mRNA half-lives can range from seconds to 90 minutes (m), averaging at around 1–3 m (Lewin et al., 2011). In plant cells, half-lives can range from minutes to over 24 hours (h) (Narsai et al., 2007). Degradation is a dynamic process with transitions in composition and structural elements, occuring at almost any stage, even during transcription (Brannan et al., 2012) or translation (Hu et al., 2009; Pelechano et al., 2015; Yu et al., 2016; Tat et al., 2016) (Figure 4). Considering relevancy for this study, cytoplasmic mRNA degradation will be briefly introduced here, which will be discussed as two overall groups: general and specialized degradation pathways.

3.3.1 General Decay

Ribonuclease (RNase) is a nuclease that catalyzes the degradation of RNA. It can be categorized into endoribonucleases and exoribonucleases. Exoribonucleases can further be categorized into 5'- or 3'-exonucleases, which hydrolyzes RNA starting from the 5'- or 3'-end, respectively.

3'→5' decay Deadenylation is the first step to both 3'→5' and 5'→3' decay. It is predominantly carried out by two multiprotein complexes, poly[A]-specific nuclease (PAN)2/PAN3 and carbon catabolite repressor 4 (CCR4)/NOT in yeast (Wahle and Winkler, 2013; Wolf and Passmore, 2014; Collart, 2016), which are mainly localized in the cytoplasm (Tucker et al., 2001; Cougot et al., 2004; Yamashita et al., 2005). In yeast, PAN was the first deadenylating enzyme discovered (Sachs and Deardorff, 1992), and in humans and yeast, PAN2 is a hydrolytic 3'-exonuclease and is responsible of the catalytic activity of the complex (Uchida et al., 2004; Wahle and Winkler, 2013). However, no homologues of PAN2/PAN3 have been identified in plants, and deadenylation is rather performed by the CCR4/NOT complex (Chou et al., 2014, 2017). The CCR4/NOT complex consists of two catalytic components: CCR4 and CCR4 associated factor 1 (CAF1), which are Mg^{2+}-dependent poly[A]-specific exonucleases, and NOT is thought to act as a central scaffold (Wahle and Winkler, 2013). In plants, CCR4, CAF1 and poly[A]-specific ribonuclease (PARN) are involved in embryogenesis (Chiba et al., 2004; Reverdatto et al., 2004), development, stress and defense responses (Sarowar et al., 2007; Liang et al., 2009; Walley et al., 2010a,b; Zhang et al., 2013; Yan, 2014; Chen et al., 2016). After deadenylation, the mRNA body can by degraded via the 5' pathway through decapping, or the 3' pathway through exonucleolytic digestion by the exosome (Houseley and Tollervey, 2009).

First discovered in yeast and animals, the eukaryotic exosome is essential for the 3'→5' degradation of many RNA substrates. The core of the RNA exosome (Exo9) consists of nine conserved subunits — six RNase pleckstrin homology (PH)-like proteins that form a ring-like structure (Rrp41-Rrp45, Rrp42-Mtr3, Rrp43-Rrp46 heterodimers), and three RNA binding proteins (Rrp4, Rrp40, Csl4) which forms a

"cap" to the ring (Lange and Gagliardi, 2010; Makino et al., 2013; Januszyk and Lima, 2014; Labno et al., 2016). Although structurally similar bacterial exoribonucleases exists (Janke et al., 2016), it will not be discussed here, as it does not fall in the scope of this study. Plants possess homologues of all nine subunits, and the plant core complex contains RRP4, CSL4, RRP41, RRP42, RRP43, RRP46 and MTR3, which have been purified and characterized using transgenic *A. thaliana* lines (Chekanova et al., 2007; Lange and Gagliardi, 2010). Some targets of the plant exosome include rRNA precursors, mRNAs, and intermediates of microRNA biogenesis (Chekanova et al., 2007). In contrast to yeast and animals, where Exo9 do not have phosphorolytic activity, and depend on hydrolytic ribonucleases, it has been demonstrated that Exo9 in *A. thaliana* possess phosphorolytic catalytic activity, and acts on specific rRNA maturation by-products (Sikorska et al., 2017).

5'→3' decay The 5'→3' degradation pathway is considered a major pathway for cytoplasmic RNA degradation. 5'→3' decay begins with deadenylation, resulting in a reduction in PABP binding and translational repression (Mugridge et al., 2018). One school of thought is that translation is the master regulator of mRNA decay (Section 3.4). In *A. thaliana*, decapping is activated by DECAPPING (DCP)5 and DCP1, which recruits the enzymatic DCP2 and the scaffolding protein VARICOSE (VCS) (Xu et al., 2006; Goeres et al., 2007; Xu and Chua, 2009). These proteins are localized to processing-bodies (P-bodies), and DCP5 is also required for formation of P-bodies, translational repression, and recently has been co-purified with the NMD core factor UP FRAMESHIFT (UPF)1 interactome in *A. thaliana* (Xu et al., 2006; Xu and Chua, 2009; Chicois et al., 2018). In yeast, after decapping by Dcp1-Dcp2, the cytoplasmic ScXRN1 degrades the uncapped mRNA by targeting the 5'-monophosphate ends (Parker, 2012). The XRN protein family are conserved in plants as well, and three homologues are found in *A. thaliana* — *AtXRN2*, *AtXRN3* and *AtXRN4* (Kastenmayer and Green, 2000).

AtXRN4 has been localized in the cytoplasm, particularly in the P-bodies, while AtXRN2 is localized in the nucleus (Kastenmayer and Green, 2000; Kurihara, 2017). Although there are no data to date for the subcellular localization of AtXRN3, it is speculated to localize to the nucleus, due to its function to degrade some nuclear substrates (Kurihara, 2017). AtXRNs are involved in the processing of the miRNA pathway. Using next generation sequencing (NGS), RNA sequencing (RNA-seq) analysis revealed accumulation of precursor micro RNA (pre-miRNA) 3' remnants, in *xrn3*, and *xrn2xrn3*, *xrn3xrn4* double mutants (Kurihara et al., 2012), as well as accumulation of loop remnants (products of Dicer-like (DCL)1 cleavage) in *xrn2xrn3* (nuclear AtXRN mutants) (Gy et al., 2007). Target transcripts in *AtXRN4* transfer DNA (T-DNA) lines showed accumulation of 3' cleavage products of miRNA-mediated cleavage (Souret et al., 2004). Arabidopsis decapping components are influenced by

environmental signals, such as phosphorylation of DCP1 under dehydration (Xu and Chua, 2012), or VCS under osmotic or salt stress (Soma et al., 2017). Decapping is also important for the transition of embryo to seedling development (Goeres et al., 2007), and contributes to the regulation of ABA signaling (Wawer et al., 2018). According to experimental data, AtXRN4 is involved in degradation of specific RNA substrates as a part of stress response, such as drought, high light, and heat (Estavillo et al., 2011; Rymarquis et al., 2011; Merret et al., 2013; Nguyen et al., 2015), further showing the impact of RNA stability on plant development and stress resistance. However, it is suggested that XRN4 is not essential for plant NMD, as NMD reporter transcripts show similar expression to wild-type (WT) in *xrn4* mutant plants (Merai et al., 2013).

Endoribonucleolytic decay Endoribonucleases cut RNA internally, resulting in 5'- or 3'- cleavage products. The cleavage products are then degraded by the exosome (3'→5') or XRN4 (5'→3') (Labno et al., 2016). Some endoribonuclease examples include RNaseA, which cleaves the 3'-end of pyrimidines on single- and double-stranded RNAs (Farrell, 2010), or RNaseG, which cleaves guanine residues on the 3'-end of single-stranded RNA (ssRNA) (Pace et al., 1991). An example of a well-known endoribonuclease from the RNase III family is the Dicer, which cleaves double-stranded RNA (dsRNA) or pre-miRNA into siRNA or miRNA, respectively. It plays a role in the assembly of RNA-induced silencing complex (RISC), serves as a key enzyme in RNA interference (RNAi), where it guides RISC to complementary RNAs to prevent translation or accelerate degradation (Doyle et al., 2012; Hull, 2014; Tennant et al., 2018). Relevant to NMD (Section 3.3.3), SUPPRESSOR OF MORPHOLOGICAL DEFECTS ON GENITALIA (SMG)6 is an endonuclease that cleaves mRNA in the proximity of the PTC, in metazoans as well as humans (Huntzinger et al., 2008; Schmidt et al., 2015). Although human cells rely on SMG6-mediated degradation, with SMG5-SMG7 as a backup pathway, plants do not possess SMG5 or SMG6 paralogues, and is suggested to degrade target transcripts through exonucleolytic pathways (Riehs-Kearnan et al., 2012; Kerenyi et al., 2013).

3.3.2 Processing-bodies (P-bodies) and stress granules (SG)

Eukaryotic cells contain numerous compartments that are biomolecular condensates, in which specific collections of proteins and nucleic acids are concentrated. These granules are membraneless and compartmentalized through liquid-liquid phase separation (LLPS) (Banani et al., 2017). For this study, P-bodies and SG, which are such compartments, will be introduced.

Found in yeast, flies, plants, and mammals, P-bodies are ribonucleoprotein (RNP) aggregates in the cytoplasm, usually consisting of translationally repressed mRNAs and associated proteins, including decapping proteins DCP1/DCP2, cap-binding

Table 3.1: Major protein components of P-bodies and stress granules (SG) that are involved in decay

Components	Function	Predominantly in:	Organism
Ccr4/Not	Deadenylase	P-bodies	Plant, Yeast, Human
CAF1	Deadenylase	P-bodies	Plant*
PARN	Deadenylase	P-bodies	Plant
DCP1	Decapping	P-bodies	Plant, Yeast, Fly, Human
DCP2	Decapping	P-bodies	Plant, Yeast, Fly, Human
DCP5	Decapping, P-body formation, Translation repressor	P-bodies	Plant
VCS	Decapping scaffold	P-bodies	Plant
UPF1	NMD component	P-bodies	Plant,Yeast, Human
Upf2p	NMD component	P-bodies	Yeast
UPF3p	NMD component	P-bodies	Yeast
SMG7	NMD component	P-bodies	Plant, Human
PTB1, PTB2, and PTB3	Splicing regulators involved in AS-coupled NMD	P-bodies	Plant
eIF2α	Translation initiation	SG	Mouse, Monkey, Human
eIF4G	Translation initiation	SG	Yeast, Monkey, Human
Pabp/PABP	Poly-A binding protein	SG	Plant, Yeast, Mammalian
40 S ribosomal subunit	Translation	SG	Yeast, Mammalian
eIF4E	Translation initiation	Both	Plant, Human
Xrn1	5'→3' exonuclease	Both	Yeast, Mouse, Human
XRN4	5'→3' exonuclease	Both	Plant

Sources: https://www.arabidopsis.org/; Parker and Sheth (2007); Xu and Chua (2009); Stauffer et al. (2010) Decker and Parker (2012); Merai et al. (2013); Maldonado-Bonilla (2014); Protter and Parker (2016) Chantarachot and Bailey-Serres (2018)
* Tolerance reduced to ROS, increased to NaCl in knockout (Walley et al., 2010b)

protein eIF4E, and NMD components (Table 3.1, Section 3.3.1). Stress granules, despite sharing similarities and protein components with P-bodies — such as coming into contact with each other, or being induced by cellular stress (Stoecklin and Kedersha, 2013) — are distinct in function and molecular composition in both plant and mammalian cells (Weber et al., 2008; Luo et al., 2018). In yeast and mammal studies, SG contains translation initiation factors, and typically associated with storage of untranslated mRNPs, while P-bodies in yeast, plants and mammals are linked with translational repression, RNA decay, or miRNA/siRNA silencing (Parker and Sheth, 2007; Decker and Parker, 2012; Luo et al., 2018). In yeast, it has been shown that NMD factors Upf1p, Upf2p and Upf3p can localize to P-bodies, and mRNAs that harbor PTCs accumulate in P-bodies when NMD is inhibited (Sheth and Parker, 2006). Sheth and Parker (2006) also show in yeast that Upf1p has a central role in the targeting of mRNAs to P-bodies, whether the transcript harbors NMD triggering features or not. Together with a phosphorylated AtUPF1, it is suggested that AtSMG7 recruits the NMD complex to P-bodies in for degradation (Chantarachot and Bailey-Serres, 2018), although the full degradation mechanism is not yet known, as XRN4-silenced leaves or *xrn4* mutants show similar expression of

NMD targets compared to WT (Merai et al., 2013).

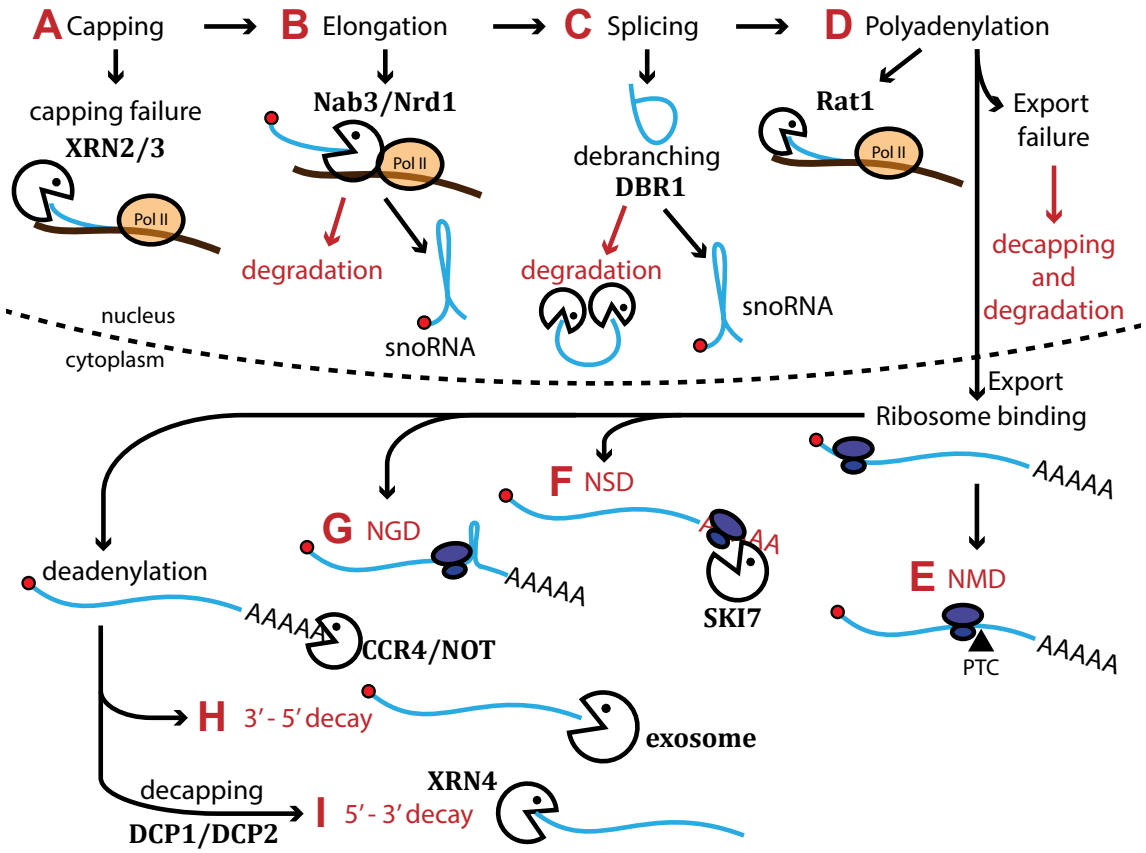

Figure 4: Decay pathways during mRNA processing in plants, unless specified "Shown in yeast" (A) Capping failure results in transcription termination from degradation by exoribonuclease (XRN)2/3 (Zakrzewska-Placzek et al., 2010). (B) Shown in yeast: If clusters of Nab3/Nrd1 are encountered during C-terminal RNA Polymerase II serine 5 phosphorylation (Ser5P) period, transcription is terminated and RNA is degraded through the 3'-pathway, forming small nucleolar RNA (snoRNA)s in some cases (Gudipati et al., 2008). Nrd1 homologue exists in *A. thaliana*. (C) The lariat is debranched by DBR1 and degraded from both ends, sometimes leading to intron-encoded snoRNAs (Wang et al., 2004). (D) Shown in yeast: Errors in cleavage and polyadenylation can leave the 3'-end stuck to the polymerase but the 5'-end no longer capped, leading to degradation by Rat1 (West et al., 2008). Plant homologue exists as XRN3, but it is unknown if this step happens in plants. After polyadenylation, the mRNA is exported out of the nucleus. Failure to export leads to decay by 5' or 3' exonucleases, and the transcript is retained at the transcription site (Rougemaille et al., 2008). After export, cytoplasmic degradation can occur (Section 3.3.1, 3.3.3). (E) NMD degrades transcripts with certain features e.g. PTCs (Section 3.3.3). (F–I) After the poly[A] tail is progressively shortened after iterative translation, deadenylation (Section 3.3.1) with CCR4/NOT can occur, leading to (H) 3'→5' degradation via the exosome, or (I) decapping with DCP1/DCP2 followed by 5'→3' degradation via XRN4 (Moore, 2005; Xu and Chua, 2011; Parker, 2012). Other specialized decay pathways involved in aberrant transcript recognition include (F) Non-stop decay (NSD), in which SKI7 recognizes transcripts lacking stop codons (Brunkard and Baker, 2018) or (G) No-go decay (NGD), which targets mRNAs upon ribosome stalling due to RNA secondary structures. Figure inspired by Houseley and Tollervey (2009). Blue lines represent transcripts, red dot the 5'-cap. Degradation enzymes are in bold and represented by PacMan-esque symbols, degradation step highlighted in red text. Ribosome represented by dark purple symbol.

3.3.3 Specialized Decay

Non-stop Decay Apart from general degradation pathways introduced in Section 3.3.1, there are many specialized pathways that recognizes specific features of a transcript, and target them for decay. For example, in yeast, NSD (Figure 4F) targets transcripts that lack a termination codon (Maquat, 2002; Wagner and Lykke-Andersen, 2002), with the purpose to detect two types of transcripts which do not have stop codons — mRNAs that contain poly[A] tails caused by premature polyadenylation, as well as mRNAs without poly[A] tails produced by endonucleolytic cleavage. NSD identifies these transcripts at the translation termination step, where under normal circumstances, as the ribosome reaches the stop codon, the EUKARYOTIC RELEASE FACTOR (eRF)1/eRF3–GTP termination complex will bind to the A-site, induce conformational changes to eRF1, and subsequently the protein is release and the ribosome is dissociated and recycled (Jackson et al., 2012; Brandman and Hegde, 2016). However, if there is no in-frame stop codon, the ribosome will reach the end of the transcript, the A-site will be empty and the termination complex will fail to bind (Frischmeyer et al., 2002; Tsuboi et al., 2012). In animal models, the NSD complex (Pelota/Hbs1–GTP) — resembles the eRF1/eRF3–GTP translation termination complex, but does not have a stop-codon identification sequence, nor a peptide release sequence — is recruited to the empty A-site, and independently of the stop-codon, can bind to the A-site and terminate translation (Shoemaker and Green, 2012; Inada, 2013). In yeast, the NSD target transcript is then degraded from 3'→5' by the SKI-exosome complex, or from 5'→3' after decapping by the XRN1 (Halbach et al., 2013; Nagarajan et al., 2013). So far in plants, the core proteins PELOTA, HBS1 and SKI2 are conserved, and the plant NSD have shown to degrade non-stop transcripts, through a transient assay (agroinfiltration) of NDS reporter constructs (no stop codon) compared to control constructs (same constructs with stop codon) (Szádeczky-Kardoss et al., 2018a). In plants, it has been proposed that the SKI-exosome complex are mainly responsible for the degradation of non-stop transcripts, or more specifically, in a transient agroinfiltration assay, non-stop reporter transcripts accumulated in SKI2-silenced lines, while the reporter constructs were barely detectable in XRN4-silenced lines (Szádeczky-Kardoss et al., 2018a). It is also suggested that NSD and NMD systems operate independently of each other in plants. In another transient assay, NSD and NMD reporter transcripts (GFP with no stop codon, and GFP with long 3'-UTR, respectively), as well as a control transcript (GFP with stop codon) were expressed in Pelota-silenced (NSD-deficient) and UPF1-silenced (NMD-deficient) plants. The NMD reporter accumulated to high levels in the UPF1-sileneced samples, while the NSD reporter was barely detectable. *Vice-versa*, the NSD reporter accumulated to high levels in PELOTA-silenced leaves while was barely detectable in UPF1-silenced

leaves (Szádeczky-Kardoss et al., 2018a).

No-go Decay Another specialized degradation pathway is through NGD (Figure 4G), which can be activated when translation elongation is inhibited, e.g. ribosomes stalled from secondary RNA structure. Recent reports in yeast and mammals suggest that the stalling of ribosomes leads to ribosome collision, and triggers ubiquitination of certain ribosomal proteins (Garzia et al., 2017; Juszkiewicz and Hegde, 2017; Matsuo et al., 2017; Simms et al., 2017; Sundaramoorthy et al., 2017). The transcript is thereafter cleaved by endonucleolytic cleavage (so far unknown), and the fragmented products are degraded by 5'- or 3'-exonucleolytic enyzmes (Doma and Parker, 2006). In yeast, it has been reported that stem-loop structures, PTCs, rare (non-optimal) codons, polybasic amino acid (AA) stretches (poly-lysine, poly-arginine tracts), and A-stretches can induce NGD. In *Nicotiana benthamiana*, these NGD-inducing elements were tested, and only long A-stretches triggered NGD. NGD-mediated cleavage was more efficient on longer A-stretches, and after endonucleolytic cleavage, the elimination of 5'- and 3'- fragments were dependent on SKI2 and XRN4, respectively (Szádeczky-Kardoss et al., 2018b).

So far, not a lot is known about NSD or NGD in plants, and available plant studies are primarily transient assays done with agroinfiltrated *N. benthamiana*. In this study, the main focus will be on NMD.

Nonsense Mediated Decay NMD is an RNA surveillance mechanism which is widespread in eukaryotes, and is a major player in quality control as well as gene regulation (He and Jacobson, 2015; Lykke-Andersen and Jensen, 2015; Nasif et al., 2018; Karousis and Muhlemann, 2019). Previously, NMD was considered mainly to function as a quality control for aberrant (faulty) mRNAs, which arise from genetic mutations, aberrant or abnormal splicing, or inaccurate transcription. In recent years, it has come to light that NMD can regulate physiological (normal) transcripts. For example, transcripts possessing upstream open reading frames (uORFs) in the 5'-UTR, PTCs, introns located over 50–55 nt downstream of a stop codon, or long 3'-UTRs independent of PTCs (Schweingruber et al., 2013; Popp and Maquat, 2013). Programmed ribosomal frameshifting, where the ribosome either skips forward, or slips back one nucleotide (for review see Ketteler (2012)), have also been shown to cause NMD targeting in yeast (Belew et al., 2008, 2011, 2014; Advani et al., 2013); however, this mechanism has not been observed in higher plants so far. Another major source of NMD targets are AS events, which can be triggered by both internal developmental regulation, as well as external stimuli (Section 3.1), and the coupling of AS with NMD is well established in plants (Kalyna et al., 2012; Drechsel et al., 2013) as well as other organisms. In *A. thaliana*, some studies show 20 % of non-coding and 1 % of coding RNAs are regulated by NMD (Kurihara et al., 2009; Rayson

et al., 2012b). However, Drechsel et al. (2013) show at least 17.4 % of all multi-exon, protein-coding genes produce splice variants that are NMD targets.

The NMD mechanism is largely conserved in eukaryotes, and a wealth of knowledge have been established primarily in yeast and metazoans. NMD activation starts with UPF1. UPF1 is an ATP-dependent RNA helicase, and a phosphoprotein that can be regulated through phosphorylation-dephosphorylation cycles. The cycle as well as its helicase activity are essential for NMD (Czaplinski et al., 1995; Weng et al., 1996; Bhattacharya et al., 2000; Ohnishi et al., 2003). Exon junction complex (EJC)-triggered NMD is one of the ways to activate this surveillance system. During splicing, an EJC is deposited approximately 20–24 nt upstream of exon-exon junctions (Le Hir et al., 2000). In mammals, the EJC consists of four core proteins as well as outer proteins, including UPF3 and UPF2. During translation, the EJC-UPF3/2 complex is removed from the mRNA by the ribosome. If the ribosome does not reach the complex, e.g. stopped by a PTC, or a regular stop codon, it will not be removed. During translation termination, a complex consisting of SMG1, UPF1 and eRFs (SURF complex) binds to the ribosome. If an EJC-UPF3/2 complex is present (i.e. has not been removed), UPF1 will bind UPF2, and UPF1 will be phosphorylated by SMG1, recruiting mRNA decay systems. The targeted transcript will then undergo deadenylation and decapping (Section 3.3.1), and degraded in the cytoplasm or P-bodies (Isken and Maquat, 2007). In the end UPF1 is dephosphorylated by SMG5, SMG6, and SMG7-recruited phosphatase, and the components are recycled. In yeast, Upf1 can also recognize delayed translation termination. PABP binds to the termination complex eRF1 and eRF3, and rapid termination is initiated. However, if a long 3'-UTR hinders the interacting between eRF3 and PABP, termination is delayed and Upf1-activated recruitment occurs.

It is proposed that plant NMD mechanism of long-3'-UTR-NMD are similar to those of yeast, whereas EJC-NMD resembles those in mammalian cells (Kerényi et al., 2008). Based on transient assays in plants, EJC-like complexes also mediate intron-based NMD (Kerényi et al., 2008). Many plant orthologues have been identified, including the EJC complex, as well as NMD core factors UPF1, UPF2, UPF3 and SMG7. SMG5 and SMG6 have not been found in plants, and SMG1 is absent from *A. thaliana*, but is present in almost all other examined plants, including *Arabidopsis lyrata* (Lloyd and Davies, 2013; Causier et al., 2017). There are several aspects of plant NMD that are unique. Unlike yeast or mammals, in transient assays, SMG7 in plants redirect UPF1 to P-bodies, where target transcripts can be subsequently degraded (Merai et al., 2013). Comparison analysis suggests that plant P-bodies are more closely related to mammals rather than yeast, with the difference that plants posses XRN4 in their P-bodies, while mammals do not (Xu and Chua, 2011). Considering new factors associated with P-bodies, such as VCS and DCPs, late stage

NMD-degradation via the XRN4 (5'→3' exonucleolytic) pathway in the P-bodies have been proposed (Xu and Chua, 2011; Dai et al., 2016) as speculation. This pathway still needs to be confirmed experimentally.

The transcripts of NMD core components are under NMD regulation. Accumulation of steady state levels and increased half-lives of *UPF1*, *UPF2*, *UPF3B*, *SMG1*, *SMG5*, *SMG6* and *SMG7* transcripts were observed in mammalian cells under NMD deficiency (Huang et al., 2011; Yepiskoposyan et al., 2011). In plants, *AtUPF3* (which contains a long 3'-UTR) was found to be regulated by NMD (Degtiar et al., 2015), as well as *SMG7* of *A. thaliana*, *N. benthamiana* and *Physcometrella patens* have intron-containing long 3'-UTRs (Kerényi et al., 2008; Lloyd and Davies, 2013). *AtUPF1*, *AtUPF3* and *AtSMG7* have been shown to have elevated steady state levels, as well as longer half-lives in NMD impaired mutants (Kesarwani, Lee, Ricca et al., 2019).

3.4 Translation and mRNA decay

Translation is tightly coupled to mRNA turnover (Pelechano et al., 2015; Yu et al., 2016; Tat et al., 2016), and the rate of translation is an important determinant of transcript lifetimes. It has been shown in yeast, zebrafish and flies, mRNA degradation rates depend on the efficiency of translation elongation, which in turn can be determined by codon optimality (Presnyak et al., 2015; Bazzini et al., 2016; Harigaya and Parker, 2016; Radhakrishnan et al., 2016; Mishima and Tomari, 2016; Jeacock et al., 2018). Transcripts which are abundant in optimal codons (codons decoded by tRNAs that are abundant in the cellular tRNA pool) are found to have longer half-lives, while transcripts containing more non-optimal codons, are more unstable. Synonymous substitution of optimal to non-optimal codons decreased mRNA half-lives by 10-fold, while synonymous substitution of non-optimal to optimal codons increased the half-life by over 7-fold (Presnyak et al., 2015). However, this pathway is separate from NMD, and NMD is the stronger degradation pathway compared to the codon-associated decay (Radhakrishnan et al., 2016). The connection between translation efficiency and mRNA stability is linked to DEAD-box helicase Dhh1/DDX6 (Radhakrishnan et al., 2016), which acts as a sensor for ribosome speed, and is coupled to deadenylation (Sun et al., 2013; Bazzini et al., 2016; Mishima and Tomari, 2016), likely through differential activities of CCR4-NOT nucleases, and modulated by PABP (Stowell et al., 2016; Mugridge et al., 2018; Webster et al., 2018). In *A. thaliana*, cotranslational RNA decay is XRN4 dependent, and the absence of ABH1 — a part of a subunit in the nuclear cap binding complex — showed an approximate 50 % decrease in cotranslational RNA decay (Yu et al., 2016).

Other ribosomal activities also link translation to decay through specialized path-

ways, for example NGD, NSD, and of course NMD. NMD is a translation dependent process (Section 3.3.3, Carter et al. (1995); Thermann et al. (1998); Karousis and Muhlemann (2019)), and can be inhibited by various translation inhibitors, one of those is cycloheximide (CHX) (Carter et al., 1995; Noensie and Dietz, 2001). CHX is an elongation inhibitor that interferes with tRNA binding (Pestova and Hellen, 2003; Schneider-Poetsch et al., 2010; Klinge et al., 2011). Under CHX treatment, NMD target transcripts show strong accumulation (Noensie and Dietz, 2001; Pereverzev et al., 2015), and is used in this study to observe the relationship between translation and NaCl treatment on NMD (Section 4.6.4).

3.5 Abiotic stress

Plants are sessile organisms, and their well-being is dependent on environmental factors. Abiotic stress is intrinsically unavoidable, and considered the most harmful factor worldwide when it comes to the growth and productivity of crops, especially when they occur in combination with each other, e.g. drought in combination with salinity and heat (Mittler, 2006; Gao et al., 2007). Common abiotic stresses include heat, drought and soil salinity. Stress response in plants first starts with signal perception, followed by downstream changes in gene expression, and eventually growth and developmental changes in physiology. In this section, the most relevant abiotic stresses for this study will be introduced.

3.5.1 Salt stress

Salt stress affects up to 932.2 million hectares of soil worldwide (Shahid et al., 2018), and threatens 19.5 % of irrigated and 2.1 % non-irrigated agricultural lands (Neto et al., 2004). Na^+ is not an essential nutrient for most plants. Accumulation of high Na^+ can cause K^+ deficiency, disrupt many enzymatic processes, and is an energetic burden to the cell due to the necessity of active export of Na^+ (Munns and Tester, 2008). Many enzymes are activated by K^+ which cannot be substituted by Na^+ (Tester and Davenport, 2003). However, low to moderate Na^+ levels are usually not harmful and sometimes can even stimulate growth of plants under K^+-deficiency (Schulze et al., 2012), likely due to displacement of K^+ from the vacuole into the cytosol (Mäser et al., 2002; Rodríguez-Navarro and Rubio, 2006; Flowers and Colmer, 2008). So far, no specific salt sensors have been identified in plants (Wu, 2018). However, there are several candidates that are involved in salt signal transduction. SALT OVERLY SENSITIVE (SOS)1, an Na^+/H^+ antiporter (Zhu, 2003), and histidine kinases (HKs) (Marin et al., 2003), for example AHK1/ATHK1 (Tran et al., 2007) have been suggested to function as osmosensors. Salt-induced extracellular adenosine triphosphate (ATP) by plasma membrane purinoceptors can induce other signaling events, such as production of ROS and elevation of

Ca^{2+} in cytosol ($[Ca^{2+}]_{cyt}$) (Sun et al., 2012). Na^+ intake can be mediated by the Na^+ transporter high-affinity K^+ transporter 1 (HKT1) against the electrochemical gradient via the proton symporter, or by non-selective cation channels (Ward et al., 2003). So far, SOS1 is the only characterized transporter for sodium exclusion from the cytosol to the apoplast (Wu, 2018).

The Salt Overly Sensitive (SOS) pathway The SOS signaling pathway was originally discovered through the role of calcineurin B-like (CBL)s in salt tolerance (Xiong et al., 2002; Shi et al., 2005). Three complementary *sos* mutants (*sos1*, *sos2* and *sos3*) were identified through a root bending assay — where lack of *SOS* genes showed hypersensitivity to salt, while overexpression increases salt tolerance (Yang et al., 2009). Interestingly, these mutants showed to be also hypersensitive to Li^+, but not to K^+ or Cs^+ (Wu et al., 1996; Liu and Zhu, 1997; Zhu et al., 1998), indicating certain ionic specificity. Through map-based cloning, the molecular identities for these three genes were identified (Liu and Zhu, 1997; Liu et al., 2000; Shi et al., 2000).

SOS3 is also known as CBL4, encodes a Ca^{2+} sensor, and is predicted to contain three typical EF-hand Ca^{2+} binding motifs (Section 3.5.3). Mutation in the *SOS3* gene and conformationally changes one of the EF-hand motifs (Liu and Zhu, 1997), and is demonstrated to have reduced Ca^{2+} binding through a gel mobility shift assay (Ishitani et al., 2000). SOS3 can interact with SOS3-LIKE CALCIUM BINDING PROTEIN 8 (SCaBP8), also known as CBL10, and together interacts with SOS2 to confer salt tolerance in plants (Quan et al., 2007). SOS3 and SCaBP8 are partially redundant in their function, and a double mutant of *sos3*/*scabp8* displays similar phenotype to *sos2* (Quan et al., 2007). SOS2 is a serine/threonine protein kinase and belongs to the SnRK3 family of protein kinases (Liu and Zhu, 1998; Halfter et al., 2000; Liu et al., 2000; Hrabak et al., 2003), and the CBL-interacting protein kinases (CIPK) family (CIPK24). SOS2 physically interacts with, and is activated by SOS3 (Halfter et al., 2000) and SCaBP8 (Quan et al., 2007) in a Ca^{2+} dependent manner. SOS2 has two major domains, the C-terminal domain is a regulatory domain, which can interact with the kinase domain at the N-terminal (Guo et al., 2001, 2004). This results in an autoinhibitory structure, which can block access to the catalytic site. Under salt stress, two calcium sensors SOS3 and SCaBP8 can accesses the regulatory domain of SOS2 and open up the catalytic site for kinase activity (Guo et al., 2001, 2004; Quan et al., 2007; Xie et al., 2009). SOS2 is also capable of phosphorylating ion transporters such as Ca^{2+}/H^+ antiporter CAX1, and the plasma membrane Na^+/H^+ antiporter SOS1 (Zhu, 2002; Shi et al., 2005), as well as vacuolar Na^+/H^+ antiporters (Qiu et al., 2004). Once the catalytic site of SOS2 is made available by Ca^{2+}-dependent binding of SOS3/SCaBP8, the SOS2 is recruited to the plasma membrane (PM) by SOS3, where SOS2 activates SOS1 through phosphorylation

(Quintero et al., 2011). SOS1 is an Na^+/H^+ antiporter located at the PM, and is essential for salt tolerance by extruding Na^+ out of the cytosol (Shi et al., 2000, 2002, 2003; Qiu et al., 2002). Overexpression of SOS1 improves salt tolerance, and *sos1* mutants show hypersensitivity to salt. SOS2 notably has many interaction partners (Table 4.2), and is also known to autophosphorylate (Fujii and Zhu, 2009b). Apart from CBLs, one interaction partner is the protein phosphatase 2C ABA INSENSITIVE (ABI)2 (Ohta et al., 2003), which is a well known regulator of ABA signaling. ABA is one of the major hormones that respond to stress. This suggests interplay between ABA and the SOS signaling pathway, as SOS2 is a kinase and ABI2 a phosphatase, and may cross-regulate their phosphorylation statuses, or have common target substrates. SOS2 is also known to interact with 14-3-3 proteins. Recently, SOS2-LIKE PROTEIN KINASE (PKS)5 have been shown to negatively regulate the SOS pathway (Yang et al., 2019). Under normal conditions PKS5 phosphorylates SOS2 and promote the interaction between SOS2 and 14-3-3 proteins, and under salt stress, inhibits SOS2 activity by increased interaction between PKS5 and 14-3-3 proteins.

3.5.2 Reactive Oxygen Species

ROS is an inevitable product of cellular aerobic metabolism. For a long time, ROS has been thought to be harmful by-products that should be eliminated as quickly as possible. However, now it is well established ROS can also act as important secondary messengers. Plants monitor the rapid changes in compartmental redox caused by environmental stimuli, as a signal for adaptive strategies to adjust metabolism or physiology accordingly. ROS — hydrogen peroxide (H_2O_2), superoxide (O_2^{*-}), and the hydroxyl radical (HO^*) — can be produced in nearly every subcellular compartment, roughly categorized: chloroplasts, mitochondria, peroxisomes and the apoplast. Each site is buffered with antioxidant systems, with the exception of the apoplast, which has a low antioxidant capacity (Foyer, 2016; Noctor et al., 2016; Waszczak et al., 2018). The lifetime of each ROS depend on the presence and activity of local dedicated scavengers (Mattila et al., 2015). For example, HO^* is highly reactive, with an estimated lifetime of nanoseconds, while more stable forms of ROS like O_2^{*-} and H_2O_2 can last from milliseconds to seconds (Waszczak et al., 2018), and therefore is more likely to diffuse from the production site and function as a signal.

Chloroplastic ROS production is strongly tied to photosynthetic reactions. O_2^{*-} produced during photosystem I (PSI) is quickly dismutated into H_2O_2 in the stromule, through superoxide dismutase (SOD)s (Asada, 2006). Chloroplastic SODs — for instance iron-SOD (FeSOD) and copper/zinc-SOD (Cu/ZnSODs) — are crucial for chloroplastic function and development (Waszczak et al., 2018). The stromal

H_2O_2 is then detoxified by ASCORBATE PEROXIDASE (APX)s and other enzymes (Asada, 2006). Apoplastic ROS accumulation often results from plant responses to the environment, as the apoplast acts as a platform for exchange of nutrients and signals between cells and the environment. ROS production in the apoplast results from stimulation of ROS-producing enzymes like apoplastic peroxidases, or the PM-localized NADPH oxidase (NOX), also known as RESPIRATORY BURST OXIDASE HOMOLOGUE (RBOH)s (Kadota et al., 2015; Sierla et al., 2016; Kimura et al., 2017). RBOHs are one of the most critical enzymes that produce ROS in

Table 3.2: Overview of relevant (to this study) AtRBOH members

Gene Name	Localization	Mutant phenotype
AtRBOHC	Root epidermis, root hairs	Short root hair, reduced O_2^{*-} production at root hair apoplast
AtRBOHD	Root maturation zone, lateral root primordia	Reduced primary root elongation, response to heat, flooding, drought
AtRBOHF	Lateral root periphery, vascular tissue in leaves, guard cells	Reduced primary root elongation, delayed casparian strip formation
	phenotype in *rbohd/f* mutants:	Increased lateral root number, reduced ABA-mediated stomatal closure, increased survival under salt or hypoxia stress

Table simplified from review from Chapman et al. (2019)

response to hormonal and environmental signals in plants (Suzuki et al., 2011). As one of the most important class of apoplastic ROS producers, RBOHs produces O_2^{*-} by transferring electrons across the PM from cytosolic NADPH to O_2 (Waszczak et al., 2018). The *RBOH* family consists of ten members, *RBOHA–RBOHJ* (Sagi and Fluhr, 2006; Torres et al., 1998), each unique in expression and functional roles under plant development or stress. In this study, *rbohd/f* double mutant and *rbohc* are explored under salt stress (Table 3.2). RBOHD/F are involved in stomatal closing (Kwak et al., 2003; Singh et al., 2017), and *rbohd/f* mutant phenotype shows increased survival under salt and multiple other abiotic stresses (Miller et al., 2009; Ma et al., 2012). RBOHC is involved in root hair formation (Foreman et al., 2003). During stress, cell-to-cell communication plays an important role in how ROS signals can affect the surrounding tissue, as well as the whole plant — and interactions between apoplastic and organelle ROS contributes to central response (Miller et al., 2009). There are several obstacles for signal transportation in plants. For example, high levels of Ca^{2+} in the apoplast makes it an unsuitable platform for conduction of Ca^{2+} signals. The apoplast also contains various ROS producers and scavengers (see review Mittler et al. (2004)), and ROS signals are under constant production and scavenging. The PM on the contrary is not a good platform for ROS signaling, due to its sensitivity to lipid peroxidation, and Ca^{2+} cannot travel long distances due to its hydrophilic properties. The cytosol on the other hand, where Ca^{2+} is tightly

controlled, is an excellent medium for conduction of Ca^{2+} signals (Section 3.5.3). Therefore, long-distance (systemic) signals through tissue could be mediated through apoplastic ROS signaling, electric signals through the PM, and $[Ca^{2+}]_{cyt}$ and ROS for short distances in the cytosol (Gilroy et al., 2016a,b).

RBOHD has been discovered to play a central role in the apoplastic movement of H_2O_2 (Miller et al., 2009), along with intricate constitutional mechanisms for NOX phosphorylation. For example, ROS-induced RBOHD phosphorylation by Ca^{2+}-dependent protein kinase (CPK)5 (Dubiella et al., 2013), and RBOHD and RBOHF phosphorylation through CIPK26, CBL1 and CBL9 (Steinhorst and Kudla, 2014), are both important discoveries. CBL1 and CBL9 are both SOS2 interaction partners (Table 4.2), and NOX-mediated ROS production leads to the stabilization of the *SOS1* transcripts (Chung et al., 2008), connecting RBOHD/F and the SOS signaling pathway (Section 3.5.1). Under salt stress, *RBOHD* and *RBOHF* expression are highly induced (Ma et al., 2012), and *RBOHF* mutants lacked ROS accumulation in the vasculature, and display Na^+ hypersensitivity in the shoots (Jiang et al., 2012). Like SOS3, RBOHs also are identified as having EF hands (Keller et al., 1998; Torres et al., 1998), classified as class B Ca^{2+} sensors, tying both ROS and the SOS pathway to Ca^{2+} signaling.

3.5.3 Calcium signaling

In response to stimuli, the calcium signal is initially perceived by binding to Ca^{2+} sensors, roughly divided into four major classes — Class A: calmodulin (CaM), Class B: CaM-like (CML) EF-hand containing Ca^{2+}-binding proteins, Class C: calcium-dependent protein kinases (CDPK), and Class D: Ca^{2+}-binding proteins without EF-hand motifs (Roberts and Harmon, 1992; Poovaiah and Reddy, 1993; Day et al., 2002). Most Ca^{2+} sensors contain a conserved structural motif the "EF hand", a common structural motif. The EF hand is a helix-loop-helix structure that can bind a single Ca^{2+} ion (Kretsinger and Nockolds, 1973). Ca^{2+} sensors can be categorized into two types, sensor relays and sensor responders (Sanders et al., 2002). For relay sensors, a conformational change occurs with Ca^{2+} binding, and is then relayed to an interaction partner. The interaction partner then undergoes changes and regulates the functions of the effectors. This type of sensor includes CaMs, CMLs and CBLs. SOS3 (Section 3.5.1) is such a sensor. For sensor responders, their own activity or structure is altered through calcium binding. CDPKs are an example of sensor responders in plants.

Calmodulins (CaM) The regulation of the ACA4 Ca^{2+} pumps by CaM seems to play an important role in salt tolerance (Geisler et al., 2000), and *AtNHX1*, which encodes a vacuolar Na^+/H^+ antiporter, also contains a CaM binding domain in its C-terminus (Yamaguchi et al., 2005). *AtNHX1* expression is upregulated through

salt stress in an ABA-dependent manner (Shi et al., 2002). AtNHX1 can interact with AtCaM15, and modify Na^+/K^+ selectivity of the antiporter, decreasing Na^+/H^+ activity (Yamaguchi et al., 2005). These studies suggest salt stress induced Ca^{2+} signaling directly regulates ion transporters important for Na^+ and K^+ homeostasis and salt tolerance in plants.

Calcineurin B-like (CBL) and CBL-interacting protein kinases (CIPK) CBLs are named after their sequence similarity with calcineurin B subunit in yeast and mammalian cells. Calcineurin is a calcium/calmodulin-dependent serine/threonine protein phosphatase (Rusnak and Mertz, 2000). Its activity is dependent on Ca^{2+} and CaM, and is one of the most common intracellular transducer of Ca^{2+} signaling pathways. The four Ca^{2+} EF-hand motifs in calcineurin B bind four Ca^{2+} molecules with high affinity, and the myristoylation (lipid modification) found in yeast is conserved even in mammals, implying a crucial physiological role (Rusnak and Mertz, 2000; Shi, 2007). In yeast, mutants deficient in the calcineurin gene confer hypersensitivity to Na^+ and Li^+, but not K^+, Ca^{2+} or Mg^{2+} (Nakamura et al., 1993; Mendoza et al., 1994). Studies of *SOS* genes has made the connection of the role of CBLs in salt tolerance (Xiong et al., 2002; Shi et al., 2005). Like yeast, the *sos* mutants show hypersensitivity to Na^+ and Li^+, but not K^+ or Cs^+ (Wu et al., 1996; Liu and Zhu, 1997; Zhu et al., 1998) (see above Section 3.5.1). The SOS3 protein (belongs to CBLs), like calcineurin B, also contains an N-terminal myristoylation site (Ishitani et al., 2000). Despite no significant difference in membrane association between myristoylated or the non-myristoylated forms of SOS3, expression of the myristoylated SOS3 can complement salt hypersensitivity in *sos3* mutants, while the non-myristoylated cannot, suggesting that myristoylation of SOS3 is required for salt tolerance in plants.

Ca^{2+}-dependent protein kinases (CDPK) CDPKs are sensor responders, unique to plants, and contain a N-terminus protein kinase domain and a C-terminus calmodulin-like domain. Ca^{2+} binding to the calmodulin-like domain causes conformational changes that modifies the kinase activity (Shi, 2007). CDPKs exists throughout the entire plant kingdom (Harmon et al., 2001; Hrabak et al., 2003), however have not yet been identified in yeast, worms, files or humans (Shi, 2007; Xiao et al., 2016). Studies have shown CDPKs are involved in hormone signaling, growth and development, biotic and abiotic responses, including salt (Monroy and Dhindsa, 1995; Berberich and Kusano, 1997; Saijo et al., 2000; Abbasi and Komatsu, 2004; Urao et al., 1994; Botella et al., 1996; Patharkar and Cushman, 2000; Chehab et al., 2004; Shi, 2007; Wang et al., 2016). CDPKs can interact with various proteins and mediate abiotic stress signaling (Shi, 2007; Asano et al., 2012), including activation by lipid messengers, phosphorylated by other kinases, and interact with 14-3-3 proteins,

which could contribute to response specificity (Cheng et al., 2002; Sanders et al., 2002; Ormancey et al., 2017).

Despite Ca^{2+} to be an essential nutrient, high concentrations of Ca^{2+} in the cytosol is toxic, and is tightly regulated by plants. There are several ways which Ca^{2+} is regulated in the cells, major ones being Ca^{2+} permeable channels, Ca^{2+} pumps, and Ca^{2+}/H^+ antiporters.

Ca^{2+} permeable channels So far not much is studied about the effects of NaCl on Ca^{2+} permeable channels, however hyperpolarization-activated Ca^{2+} channel (HACC)s have been implicated in drought stress, from studies in the guard cells in response to ABA, where the application thereof elevates $[Ca^{2+}]_{cyt}$ (Grabov and Blatt, 1998; Pei et al., 1999). Induced by drought, ABA concentration increases, HACCs activates and triggers Ca^{2+} dependent events, including $[Ca^{2+}]_{cyt}$-dependent release from intracellular stores, leading to stomatal closure (Blatt, 2000; White, 2000; Schroeder et al., 2001; White and Broadley, 2003). ABA-induced stomatal closure involves ROS (Section 3.5.2). In Arabidopsis, H_2O_2 activates HACCs and cause an increase in $[Ca^{2+}]_{cyt}$ (Pei et al., 2000). This process demands NADPH, and NOX might be a component in the signaling chain of ABA–H_2O_2–Ca^{2+} elevation during stomatal closure (Murata et al., 2001). The plasma membrane NOX AtRBOHC is required for ROS production and the generation of root hair apical $[Ca^{2+}]_{cyt}$ gradient (Monshausen et al., 2007).

Ca^{2+} pumps Ca^{2+} pumps actively transport Ca^{2+}, and are directly energized by ATP hydrolysis through Ca^{2+}-ATPase, which exports Ca^{2+} out against a steep electrochemical gradient. There is a relationship between Ca^{2+} pumps and salt stress response, and can be accentuated by the fact that the expression of many Ca^{2+}-ATPases are increased upon exposure to high salinity, and some Ca^{2+}-ATPases are only expressed under stress conditions (Geisler et al., 2000; Garciadeblas et al., 2001). For example, in yeast, the golgi-located Ca^{2+}-ATPase PMR1 regulates salt tolerance through controlling the expression of the plasma membrane Na^+-ATPase PMR2, and *pmr1* mutants are more salt tolerant (Park et al., 2001). The plasma membrane Ca^{2+}-ATPase *SCA1* from soybean is highly and rapidly induced by NaCl stress, but not by osmotic stress (Chung et al., 2000). Arabidopsis *AUTOINHIBITED CA^{2+} ATPASE (ACA)4*, which encodes a vacuolar Ca^{2+} pump is regulated upon NaCl treatment, and can enhance salt tolerance in yeast (Geisler et al., 2000). Expression of *AtACA* genes are dynamic and these Ca^{2+} pumps might be important for different stress signaling — for example *ACA1* is highly expressed under 100 mM NaCl in roots, *ACA12* and *ACA13* are induced by both cold and salt, while *ACA8* is induced by cold and ABA treatment (Cerana et al., 2006; Maathuis, 2006; Shi, 2007). The

connection of induced Ca^{2+}-ATPase genes, and increased $[Ca^{2+}]_{cyt}$ under NaCl stress suggest a link between Ca^{2+} signaling through Ca^{2+} pumps under salt stress.

Ca^{2+}/H^+ antiporters Ca^{2+}/H^+ antiporters are Ca^{2+} transporters that depend on the electrochemical gradients of H^+ to remove Ca^{2+} from the cytosol (Evans and Williams, 1998; Sanders et al., 2002). The Arabidopsis vacuolar cation/proton exchanger 1 (CAX1) has low Ca^{2+} affinity and high Ca^{2+} transport capacity (Shigaki et al., 2001), and is localized in the vacuolar membrane (Cheng et al., 2003). CAX1 has an N-terminal autoinhibitory domain that plays a role in CAX1 activity (Pittman and Hirschi, 2001), and *cax1* mutants showed a significant increased expression of other Ca^{2+}/H^+ antiporters *CAX3* and *CAX4*. *CAX4* expression is induced by Mn^{2+}, Na^+, and Ni^{2+} treatments (Cheng et al., 2002). CAX1 is implicated in salt stress response, due to a study showing its activation from SOS2, where SOS2 was able to interact with the N-terminus of CAX1 and activate its transport ability in a SOS3-independent manner in yeast (Cheng et al., 2004). Salt sensitivity was also seen in plants expressing a high level of deregulated CAX1, further implicating CAX1 might be a component of salt stress signaling, through modulating $[Ca^{2+}]_{cyt}$ and subsequent signal transduction (Cheng et al., 2004).

3.5.4 Other stresses

Heat stress Gene expression and mRNA decay can also be affected by temperature. In Arabidopsis, heat can trigger total genome changes at the transcript level (Larkindale and Vierling, 2008). Upon temperature increase, translation is one of the first processes to be downregulated through inhibition of translation initiation, and is positively correlated with the intensity and duration of stress (Munoz and Castellano, 2012; Liu and Qian, 2014). The molecular mechanism is not yet clear in plants, however in mammalian cells translation elongation can also be affected, through accumulation of misfolded proteins, causing 5'-ribosome pausing (Liu et al., 2013a; Shalgi et al., 2013). 5'-ribosome pausing is described in mouse and humans where translation elongation is paused at around codon 65, and can be triggered with severe heat stress (Liu et al., 2013a; Shalgi et al., 2013). Cytoplastic mRNA decay generally occurs in a deadenylation-dependent manner (Section 3.3.1), and is tightly tied to translation (Section 3.4). Merret et al. (2015) shows heat exposure can induce ribosome pausing, and results in co-translation decay. Although P-bodies also have mRNA decay components, and are induced by heat (Section 3.3.2), heat-induced decay are unlikely to be linked to P-bodies, due to an observation of overaccumulation of polysomal decapped mRNAs in XRN4-depleted seedlings following a treatment for heat shock protein (HSP)70 inhibition (Merret et al., 2015). However, this does not necessarily mean that P-bodies are not involved in other types of stresses.

Heat (and cold) can also change the fluidity of cellular membranes (Sangwan et al.,

2002). Integral membrane proteins, such as channels, transporters or kinases can sense these changes. In *P. patens*, changes in membrane lipid composition due to heat can regulate the Ca^{2+}-dependent heat-signaling pathway (Saidi et al., 2009, 2010, 2011). In *A. thaliana*, the ROS generating NOX RBOHD have been suggested to rapidly produce an oxidative burst by $[Ca^{2+}]_{cyt}$ increase due to heat stress (Suzuki et al., 2011).

Endoplasmic reticulum (ER) stress As one of the largest organelle in the endomembrane system, functions such as protein synthesis, folding, modification and export takes place in the endoplasmic reticulum (ER). ER homeostasis is greatly affected by environmental stimuli, and results in accumulation of misfolded or unfolded proteins, and is referred to as ER stress (Walter and Ron, 2011). The activation of intracellular signaling from ER stress is known collectively as the unfolded protein response (UPR), which includes detection of aberrant proteins, activation of chaperone, and reduction of membrane protein contents (Walter and Ron, 2011; Niu and Xiang, 2018). In mammalian systems, NMD and the UPR are known to cross-regulate (inhibit) each other (Karam et al., 2015; Goetz and Wilkinson, 2017; Li et al., 2017b). Under strong ER stress, UPR is triggered and NMD is inhibited, and under "background" ER stress NMD degrades transcripts of UPR components to prevent UPR activation (Karam et al., 2015; Goetz and Wilkinson, 2017). Without ER homeostasis, UPR triggers programmed cell death (Breckenridge et al., 2003; Hetz et al., 2006; Lin et al., 2007; Lisbona et al., 2009; Walter and Ron, 2011).

3.6 Aims of this Study

Previous data on salt-mediated NMD target accumulation, or splice ratio changes has only been described on the steady state level (Kesarwani, 2014). This means that the degradation aspect of this observation is not accurately addressed. Therefore, the first aim was to provide direct proof that it is the decay of transcripts that is affected, and remove RNA biogenesis from the equation. The main obstacle here was to establish this assay in fully developed plant cells, not protoplasts or suspension culture cells, in a fashion where the treatment does not trigger excessive general or other specialized degradation pathways. After this was successfully established, the second goal was to identify the mechanism of how NaCl causes NMD inhibition. This is completely novel and proves to be quite challenging, due to the complex network of abiotic stress signaling triggered under salt stress, as well as intricacies of the mRNA degradation systems of the cell. Lastly, finding a suitable statistical measurement is critical for data interpretation and presentation. Traditionally, half-lives ($t_{1/2}$) are used. However, due to the nature of this study, where sometimes salt causes complete stabilization, plus the imperfect integration of transcription inhibitors or other factors,

results in a negative value for half-life (increased transcript levels). This then does not allow for direct comparisons, since a negative half-life can be interpreted as having no degradation ($t_{1/2}= \infty$), while low half-lives depict very unstable transcript. Therefore, instead of half-lives, I argue to employ rate constants (K) in this study, as high K correlates to fast degradation rates and can be compared linearly. The approach used in this study to identify the underlying signaling pathway, is predominantly by stress-testing WT and/or mutants with different chemicals or conditions. Following this, through analyzing NMD targets (in some cases non-NMD targets), K is used to determine the significance of these treatments. This allows the determination of whether the NMD pathway is affected or not, with this specific treatment. By testing a wide network of possible stresses and mutants that are connected to abiotic signaling pathways, or associated with different mRNA degradation machineries, the link between salt stress and NMD inhibition can be clarified.

4 Results

4.1 Measurement of mRNA half-lives in *Arabidopsis thaliana*

Posttranscriptional mechanisms play a fundamental and intricate role in gene expression and alter the quantity and quality of mRNA. Translational repression, silencing, AS, mRNA surveillance and decay are all different examples of posttranscriptional regulations, in addition to modifications such as N^6-methyladenosine (m^6A), which for example has been shown to alter RNA structure and regulate RNA-protein interactions (Liu et al., 2015). While many researchers are focused on the synthesis via gene transcription, one particularly intriguing scope of this field is at the level of mRNA degradation, as it can also control gene expression in a rapid and effective manner. mRNA steady state levels — the sum of production and degradation — are often used to assume that the stability has altered, due to technical ease of determination. However, the changes are not necessarily caused by variations in the stability itself. It can also be affected by alterations in the mRNA biogenesis, such as transcription and processing, which can differ between developmental stages or depending on environmental stimuli. Under physiological conditions, different mRNAs show a wide range of stabilities, from minutes to over 24 h (Narsai et al., 2007). The half-lives of certain transcripts can also vary to a great degree under different environmental conditions, for example, various TIR domain-containing, nucleotide-binding, leucine-rich repeat (TNL) immune receptor transcripts are stabilized upon bacterial infection (Gloggnitzer et al., 2014). By tightly controlling mRNA metabolism, the amount and constitution of mRNAs can be controlled, and in turn regulate the expression of many proteins and manifold processes. One way to study mRNA stability is to inhibit RNA synthesis and quantify mRNA levels over time. Although seemingly straightforward, in reality there are several factors and technical difficulties hidden beneath the simple methods present in various published papers (Gutierrez et al., 2002; Gloggnitzer et al., 2014; Soma et al., 2017). One of the biggest challenges to reach our goal — to follow up on the mechanisms underlying steady state changes of NMD target transcripts under NaCl — was to establish a consistent, reproducible method for reliable mRNA stability measurements, which will be described below.

4.1.1 Comparison between transcription inhibitors

One consideration was the choice of transcription inhibitors. Here we discuss two popular choices as previously used for studies in plants and other organisms, actinomycin D and 3'-deoxyadenosine (cordycepin). Actinomycin D interferes with transcription through binding DNA at the transcription initiation complex and interferes with the movement of RNA polymerases (Sobell, 1985), while cordycepin

is an adenosine analogue, and prematurely terminates RNA elongation when incorporated into the growing RNA molecule (Siev et al., 1969). However, actinomycin D has been reported to impact cellular physiology and have been shown to alter the stability of many mRNAs (Harrold et al., 1991; Seiser et al., 1995). This was also reflected in the preliminary test we did with *A. thaliana* Columbia 0 (Col-0) suspension culture cells. The effects of these two transcription inhibitors on two transcripts *MITOCHONDRIAL IMPORT INNER MEMBRANE TRANSLOCASE (TIM14) (AT2G35795)* and *SMG7 (AT5G19400)* were analyzed. *TIM14* was predicted to have a longer half-life (Narsai et al., 2007), and *SMG7*, an NMD target, was predicted to have faster decay. Therefore, if both transcription inhibitors are effective, a rapid decay should be seen for *SMG7*, while a slower decay should be seen for *TIM14*. However, under actinomycin D treatment, both transcripts showed a prolonged stabilization over 4 hrs, compared with cordycepin, where a rapid decay of *SMG7* becomes visible, and a slower decay of *TIM14* is observed (Figure A.1). This indicates that cordycepin was successfully absorbed and incorporated, and transcription was slowed to a degree where decay was measurable. Although this transcript stabilization with actinomycin D was not as strong with plants grown in liquid culture (described below), it did affect drastically one NMD target transcript out of four that was tested (Figure 5), where the half life for *AT2G45670+* during the 1st hour was raised to 3.96 h with actinomycin D treatment, compared to 0.51 h with cordycepin (Figure 5B)). The other NMD targets *SMG7*, *POLYPYRIMIDINE TRACT BINDING PROTEIN (PTB)2+*, and *ARGININE/SERINE-RICH ZINC KNUCKLE-CONTAINING PROTEIN 33 (RS2Z33)+*, as well as the non-NMD splicing variant *RS2Z33−*, was not affected. Transcripts with "+" or "−" refer to alternative splicing variants. The PTC containing (+) isoform, is a predicted NMD target, and the non-PTC containing (−) isoform does not contain NMD target features. Considering the results from suspension culture cells (Figure A.1) and liquid culture (Figure 5), cordycepin was the transcription inhibitor of choice for all future experiments.

4.1.2 Incorporation of transcription inhibitors in plants

Unlike mammalian cells, plant cells possess cell walls, and makes infiltration of any type of solution difficult. To circumvent this problem, protoplasts or suspension cell cultures can be used. However, protoplasts, while very useful in other applications, are severely stressed and are not ideal for analyzing physiological transcripts. Suspension cells are in a much better physiological state, but are also far away from being a fully developed and differentiated plant. Thus, the ideal subject for physiological analysis are whole plants. As mentioned before, the challenge lies within penetrating the cell with desired solution, which should contain a transcription inhibitor and

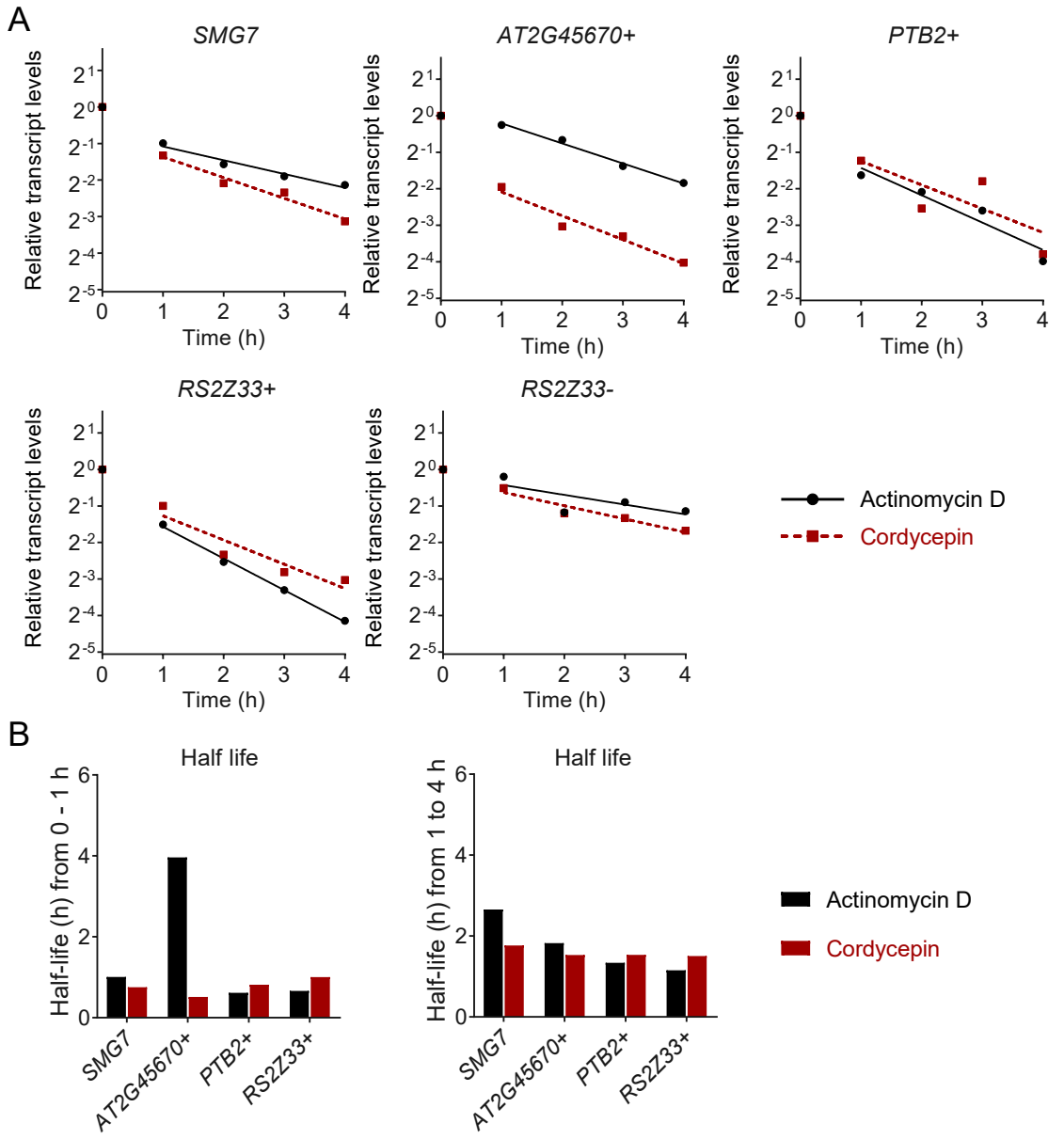

Figure 5: Slower decay of *AT2G45670+* in actinomycin D treated seedlings compared to cordycepin ($n = 1$). Transcripts with "+" or "−" refer to alternative splicing variants. The PTC containing (+) isoform, is a predicted NMD target, and the non-PTC containing (−) isoform does not contain NMD target features. (A) Comparison of actinomycin D and cordycepin in decay of predicted NMD target transcripts, with a non-NMD target isoform (*RS2Z33−*) as control. *AT2G45670+* shows slower decay during the 1st hour of treatment with actinomycin D, compared to cordycepin. Dots represent individual values, line represents least squares non-linear regression, described in Material and Methods 6.4. (B) Half lives of NMD target transcripts during the 1st hour of treatment (left) and from 1–4 h of treatment (right).

other chemicals of interest.

Vacuum Infiltration At first, several attempts were made to replicate the half-life assays with plate-grown seedlings as previously reported (e.g. Gloggnitzer et al. (2014)). An infiltration solution containing cordycepin, detergents and buffering

agents were vacuum infiltrated through the stomata and into the cell. However, using such a forceful method destroys cellular membrane properties, and compromise RNA integrity. This was demonstrated by analyzing nuclei staining through propidium iodide, as well as quality control of total RNA samples with the Bioanalyzer™. Propidium iodide is a dye that intercalates into nucleic acids. It is membrane impermeable and therefore excluded from viable cells. With just 1 min of gentle vacuum infiltration, staining of the nucleus was observed, and even stronger staining with longer periods of time (Figure 6). Using an RNA chip in the Bioanalyzer confirms the overall degradation of total RNA (Figure 7), where the RNA integrity number (RIN) decrease drastically over time. Since the goal was to measure a specific degradation pathway, vacuum infiltration should not be used, since a strong overall degradation is present and would render the measurements inaccurate.

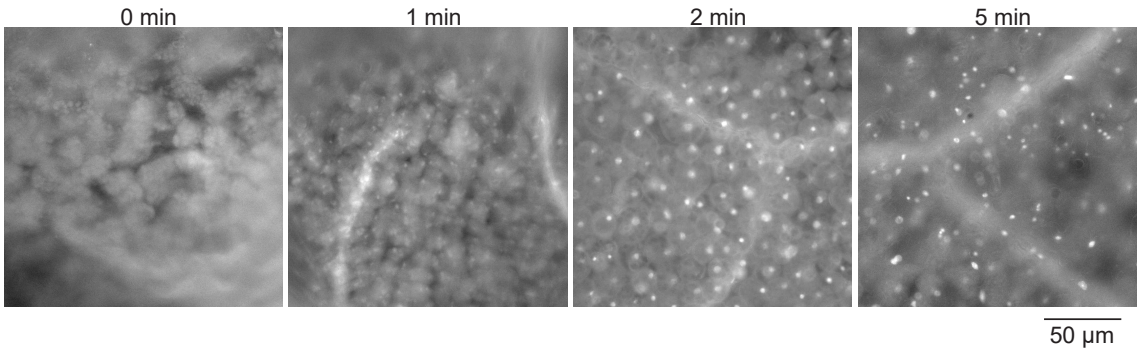

Figure 6: Cellular integrity destroyed with vacuum infiltration, leading to the staining of the nucleus. 10-d-old plate grown *A. thaliana* Col-0 plants were submerged in a propidium iodide (400 μg/ml) infiltration solution, and infiltrated at 200–250 mbar for 0, 1, 2, or 5 minutes. Solution was de-gassed for 10 min at 100–150 mbar before usage. Scale bar depicts 50 μm and applies to all pictures.

Liquid Culture The physical damage caused by vacuum infiltration can be circumvented by growing the plants directly in liquid medium. The seeds were sterilized and pipetted directly into growth medium, stratified overnight at 4 °C and germinated under growth conditions described in Material and Methods 6.1. During growth, the seedlings often clump into little balls consisting of individual plants, due to the nature of their environment (Figure A.2). They can be grown under this condition for around 3 weeks. Growth typically starts to retard around 2.5 weeks, and by week 4 the leaves will start to yellow and look translucent. Herein and unless otherwise mentioned, 7-d-old Arabidopsis seedlings grown in liquid culture are used for all experiments.

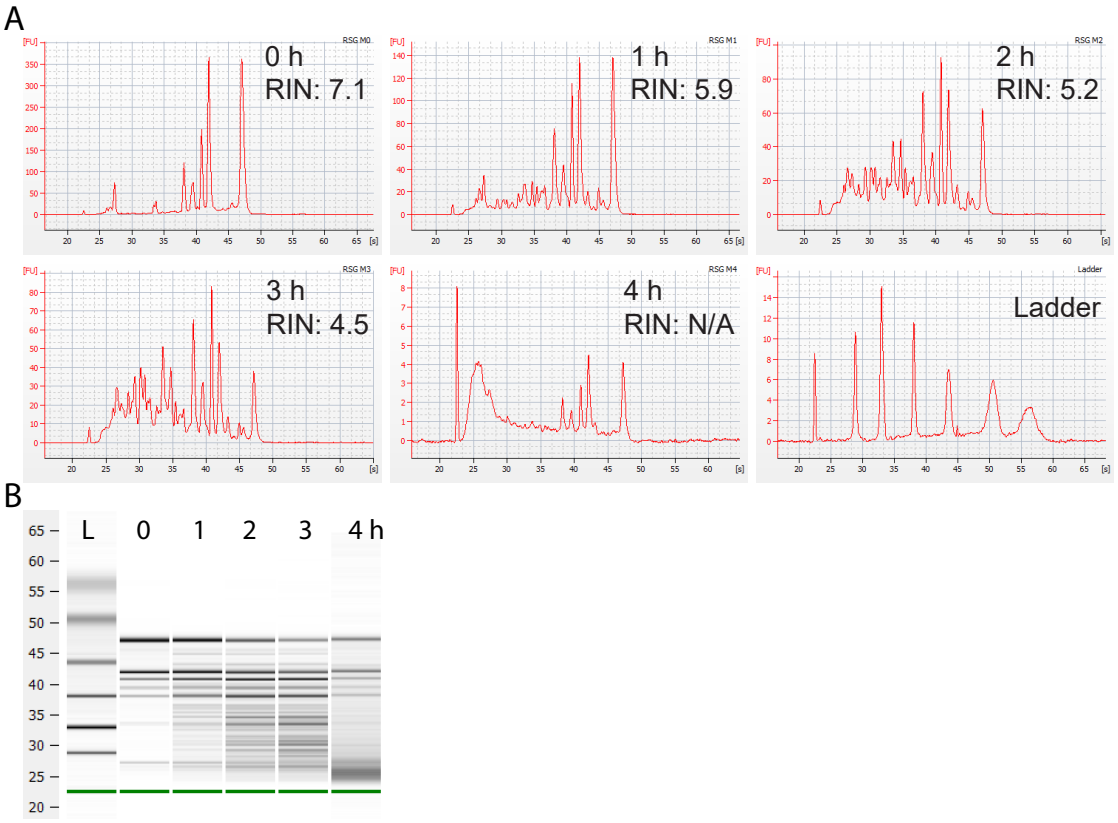

Figure 7: Vacuum infiltration impairs RNA integrity. Quality analysis via Bioanalyzer of total RNA was performed on samples from vacuum infiltrated seedlings in conditions described in Fig. 5, and harvested at the indicated amount of time after infiltration. Electropherograms (A) and gel-like view of corresponding data (B) are depicted. RNA integrity number (RIN) calculated by the Bioanalyzer software with default settings.

4.1.3 Downstream analysis for the half-life assay

The assay begins by taking 7-d-old liquid grown plants, washed with MilliQ water (H_2O), and distributing them among different treatments, containing 150 μg/ml of cordycepin (Figure 8). In this study, wherever H_2O is mentioned, it will refer to MilliQ water. Samples are then taken every hour up to 4 hours. In some cases, a pretreatment is performed, where the plants are incubated in the treatment solution without cordycepin for a designated amount of time. RNA is extracted, RT, and the complementary DNA (cDNA) is diluted and used for quantitative PCR (q-PCR). Several NMD targets were selected for analysis. The *SMG7* transcript is a strong NMD target, displaying several NMD target features, including introns in the 3' UTR, long 3' UTR, as well as an uORF that overlaps with the main ORF (Kesarwani, Lee, Ricca et al., 2019). SMG7 transcript levels are upregulated when NMD was suppressed in *N. benthamiana* leaves (Kerényi et al., 2008) and in *A. thaliana* seedlings (Rayson et al., 2012a). The pre-mRNAs of *PTB2+* (*AT5G53180*), *RS2Z33+* (*AT2G37340*), and *AT2G45670+* are alternatively spliced and include a

PTC, which is a known NMD trigger.

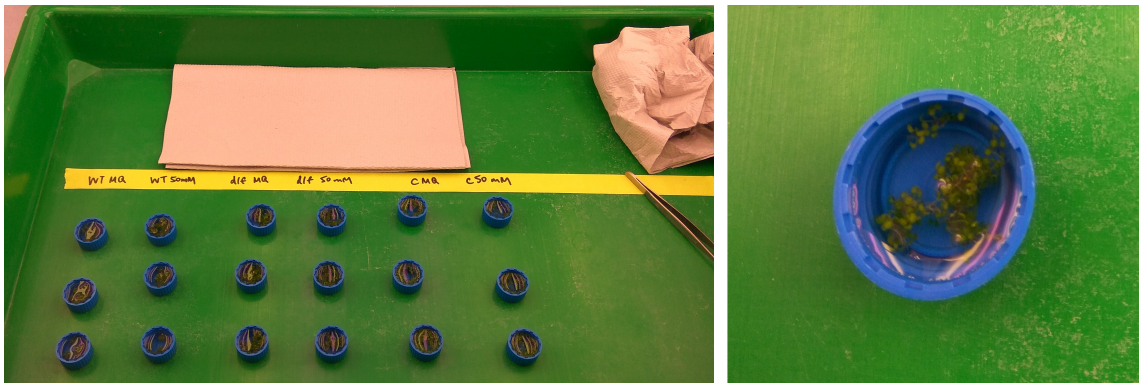

Figure 8: Setup of the half-life assay. Residual growth medium is washed off the seedlings with MilliQ water, and the seedlings are distributed for individual treatments in caps of 15 ml tubes.

4.2 NMD inhibition responds to NaCl stress in a dose dependent manner

As a major modulator of the *A. thaliana* transcriptome (Kalyna et al., 2012; Drechsel et al., 2013), NMD is also involved in biotic stress responses in plants (Jeong et al., 2011; Rayson et al., 2012a,b; Riehs-Kearnan et al., 2012; Gloggnitzer et al., 2014). To address a potential function of this RNA surveillance mechanism in plants under abiotic stress, expression of NMD factors were analyzed in *A. thaliana* plants exposed to salt stress. If not otherwise mentioned, in this study salt will refer specifically to NaCl. NMD factor transcripts and protein levels were found to be upregulated under NaCl stress (Figure B.1; Kesarwani, Wachter, et al., unpublished). To provide direct evidence for NaCl-mediated NMD impairment, the half-life assay was performed on six NMD target transcripts (Figure B.2), three of which are NMD core components: *UPF1*, *UPF2* and *SMG7* (Figure B.2A–C), three AS-PTC+ variants *PTB2+*, *AT2G45670+* and *RS2Z33+* (Figure B.2D–F), and one non-NMD target that is an AS-PTC− variant *RS2Z33−* (Figure B.2G). All NMD target transcripts were stabilized upon 500 mM NaCl treatment (Figure B.2A–F), while the non-NMD target *RS2Z33−* was barely affected by NaCl (Figure B.2G). Examination of the PTC+/PTC− ratio of the AS-NMD target *PTB1* showed a rapid decline over time (Figure B.2H) under control conditions, due to the targeting of the PTC+ variant by NMD. In the NaCl treated samples, PTC+/PTC− ratios remained stable over time, showing stabilization of target transcript, through inhibition of NMD (Figure B.2H).

4.2.1 NMD targets are dose-dependently stabilized upon NaCl

Although this provides evidence that NaCl affects transcript turnover, however the question still remains whether the NMD pathway behaves in a similar way under

NaCl concentrations present in natural or agricultural conditions. To determine an appropriate NaCl concentration that is more physiologically relevant, the decay of the NMD target transcripts *SMG7*, *PTB2+* and *RS2Z33+* were analyzed under a range of NaCl concentrations. Liquid grown *A. thaliana* seedlings were treated with 0, 50, 100, 200, and 500 mM of NaCl, and as a result the stability of these transcripts clearly show a positive correlation with NaCl stress (Figure 9). The half-life analysis was separated into two phases, one early phase from 0–1 h typically with rapid decay, and a later one from 1–4 h typically showing slower decay. In the early phase, NMD transcripts respond strongly to salt treatment, and are stabilized rapidly, displayed by the rate constant (K) changes (Figure 9B). K is solved through graphing $ln[A]_t = ln[A]_0 - Kt$ (natural log of concentration at any given time, equals the natural log of the initial concentration minus Kt, where the $-K$ is the slope, t is time). Since half-life ($t_{1/2}$) — a 1st order reaction — is assumed to be constant, the relationship of half-life to rate constant is $t_{1/2}= ln(2)/K$. Therefore, the higher the number K (unit expressed in reciprocal of time, in this case would be 1/hours), the faster the degradation. If $K \leq 0$, it is assumed that there is no degradation, and the treatment has completely stabilized the target transcript. In the early phase, a transcript increase of *PTB2+* and *RS2Z33+* with 200 mM NaCl (Figure 9) was seen, and could be due to cordycepin not yet completely incorporated, and transcription still partially active. It could also be due to post-transcriptional splicing on existing pre-mRNAs, causing an increase of PTC+ isoforms, or a combination of both. In the later stage, a much milder correlation between transcript stabilization and NaCl concentration can be seen in *SMG7* and *RS2Z33+*, but no obvious correlation is seen in *PTB2+* (Figure 9B), which could be due to the presence of different transcript populations.

4.2.2 The study of NMD using low to moderate NaCl doses

In both phases, 500 mM of NaCl is shown to completely stabilize NMD target transcripts in the decay graphs (Figure 9). However, 500 mM is beyond a natural stress conditions, and if applied directly, likely induces salt shock instead of salt stress (Shavrukov, 2013). To examine NMD target accumulation under different salt concentrations, a co-amplification PCR was performed on *RS2Z33*, which can be alternatively spliced to a PTC+ (NMD target) isoform and a PTC− (non-NMD target) form. Primers were designed to cover the alternatively spliced region, and to capture both splicing isoforms (Stauffer et al., 2010), and were quantified using a Bioanalyzer™. The ratio of *RS2Z33+/−* correlates positively with incubation time, as well as NaCl concentrations, up to 200 mM NaCl (Figure 10A). This cannot be seen for seedlings under 500 mM of NaCl treatment, where NMD targets no longer show accumulation relative to non-NMD targets (Figure 10A). Upon

reverse transcription and quantitative PCR (RT-qPCR) analysis, *RS2Z33+* is seen to accumulate while *RS2Z33−* is unchanged, excluding that NaCl changes the alternative splicing (Figure 10B,C). These data suggest that 500 mM NaCl was toxic to the plants, and it could be speculated that the dysfunction of NMD could be an indicator of cell death at high salt concentrations. Literature suggests that a single application of NaCl levels of over 150 mM in general would cause salt shock (Pritchard et al., 1991; Munns, 2002; Tang et al., 2011; Zhang et al., 2011), and 50–100 mM is sufficient to study expression of genes responsive to salt stress (Roshandel and Flowers, 2009; Shavrukov, 2013). The NMD targets already accumulate significantly upon 50 mM of NaCl (Figure 10B), and the PTC+/− ratio display significance with 100 mM of NaCl in comparison to the control (Figure 10A). Therefore, taken together, 50 or 100 mM of NaCl was used for further experiments, due to observable changes in NMD, under more practical NaCl concentrations that should not cause salt shock.

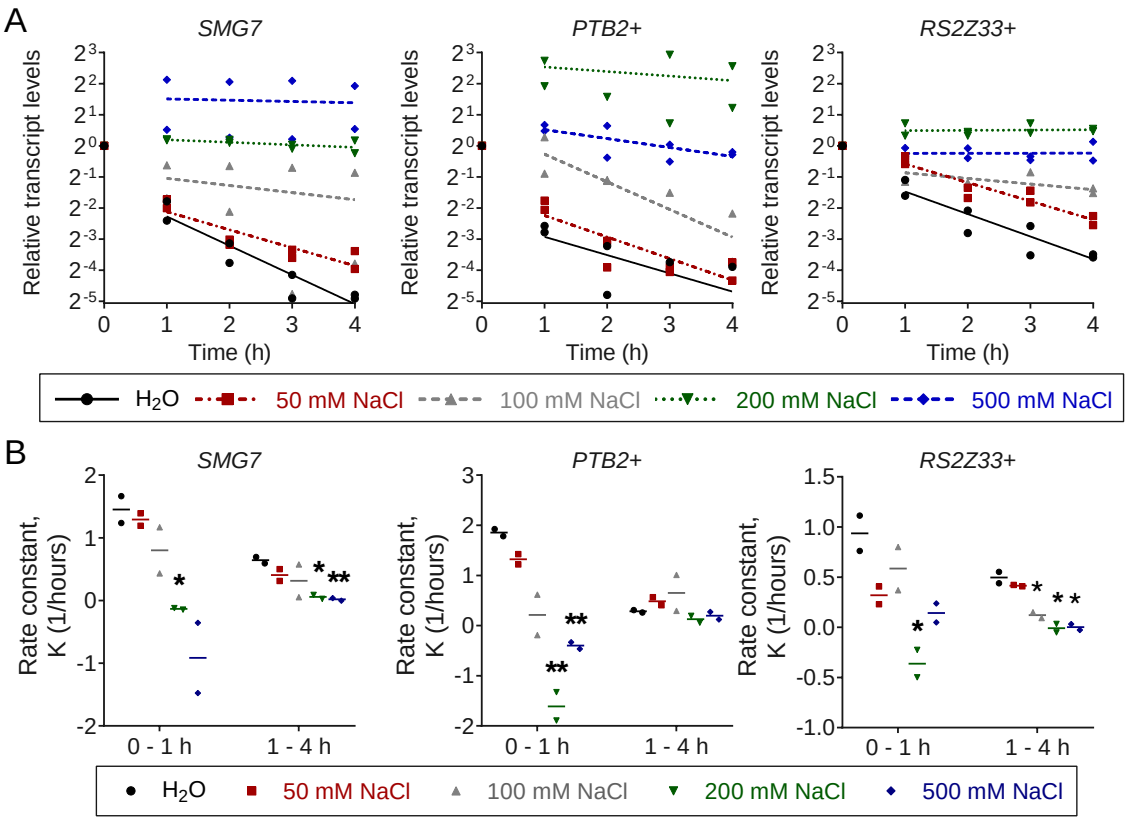

Figure 9: NMD target transcripts are stabilized upon NaCl application dose-dependently (A) Decay graphs of NMD targets *SMG7*, *PTB2+* and *RS2Z33+* under 0, 50, 100, 200, and 500 mM of NaCl treatment. Dots represent individual values ($n = 2$), line represents least squares non-linear regression. (B) Rate constant K of the above transcripts within the 1st hour of transcription inhibition (0–1 h), and from 1st–4th hour after transcription inhibition (1–4 h). K is seen to decrease as NaCl concentration gets higher, and eventually nearing or going below 0 under 200 or 500 mM of NaCl, showing complete stabilization of the target transcripts. *, $P < 0.05$; **, $P < 0.01$ by unpaired t-test compared against H_2O control, line represents mean.

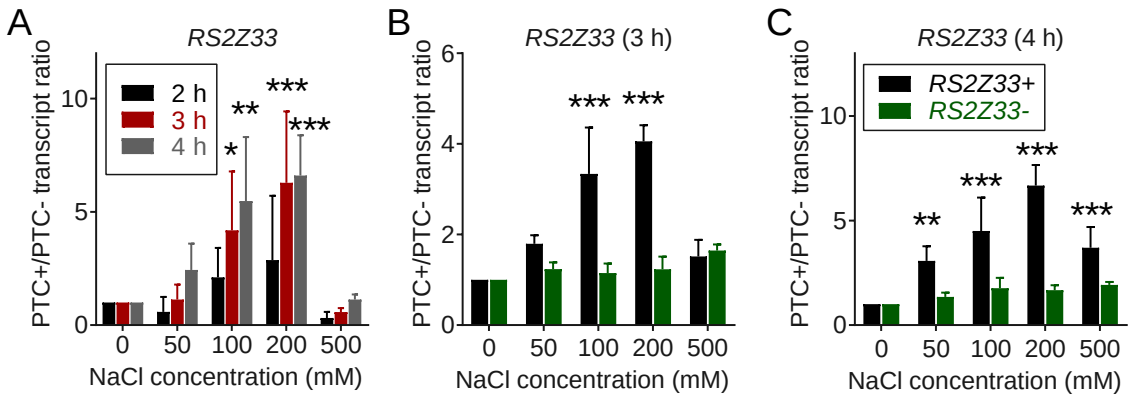

Figure 10: NMD target transcripts accumulate upon NaCl stress, and PTC+/− ratio culled in 500 mM NaCl. (Data collected by Siliya Köster-Hofmann). (A) Bioanalyzer analysis of *RS2Z33* PTC+/PTC− splicing variant ratios ($n = 3$). (B, C) q-PCR analysis of *RS2Z33*+ and *RS2Z33*− steady state levels after 3 h (B) and 4 h (C) of NaCl treatment. Columns represent mean ($n = 3$), error bars represent standard deviation (SD). *, $P < 0.05$; **, $P < 0.01$; ***, $P < 0.001$ by unpaired t-test compared against 0 mM NaCl control.

4.3 Minor osmotic involvement in NaCl-induced inhibition

An osmotic component is present in the early phase of salt stress (Shavrukov, 2013), therefore it was important to identify whether these transcript changes are due to shared or stimulus-specific response. Kreps et al. (2002) have examined transcriptome changes in *A. thaliana* with salt, osmotic and cold stress, and identified many genes that are regulated upon both NaCl and osmotic stress, as well as genes that respond specifically to NaCl, osmotic, or cold stress. Despite thousands of genes analyzed, the NMD specific genes were not among those, therefore it was necessary to investigate the osmotic component of NaCl-mediated NMD inhibition. Under steady state levels, exposure of mannitol shows a much weaker accumulation of NMD target transcripts (Figure C.1, Kesarwani, Wachter, et al., unpublished).

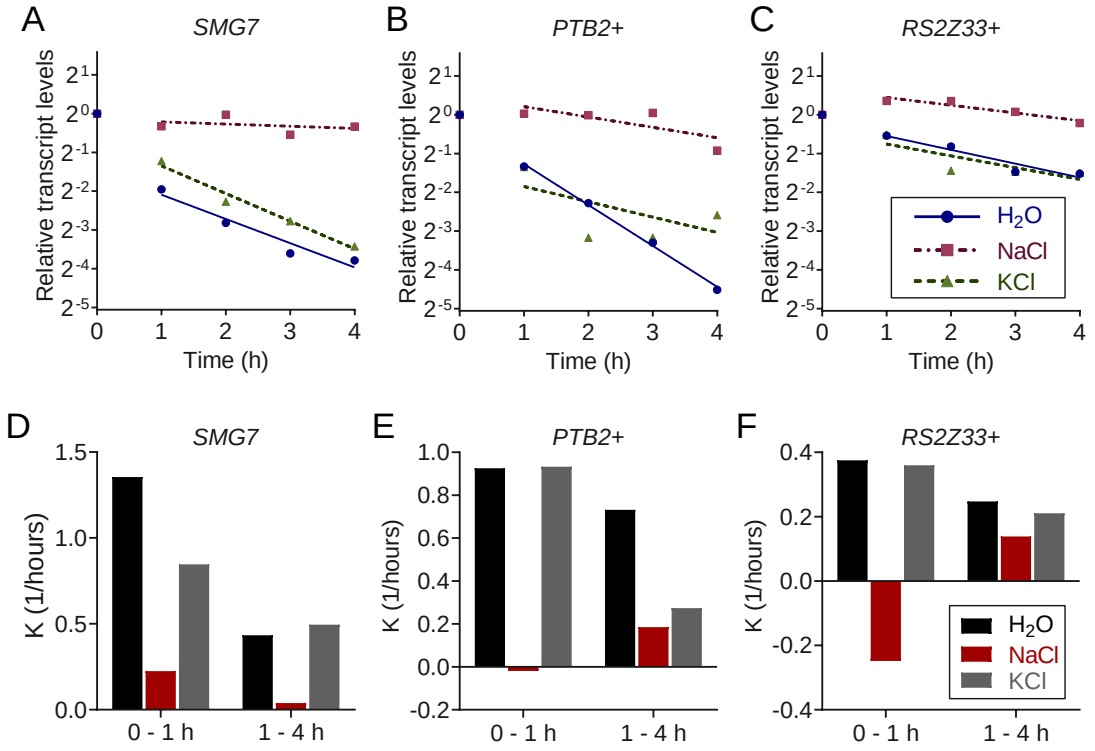

Figure 11: NMD target transcripts are stabilized to a greater degree with NaCl treatment compared to equimolar KCl, in both the 1st hour and hours 1–4. Decay graphs (A–C) and rate constants (D–F) of NMD target transcripts of 7-d-old Arabidopsis seedlings under 100 mM NaCl or 100 mM KCl treatment ($n = 1$). Color key in (C) applies to (A–C), key in (F) applies to (D–F).

To further confirm that NaCl induced NMD inhibition was not purely osmotic, half-life assays were performed to assess the transcript turnover of three NMD target transcripts — *SMG7*, *PTB2+* and *RS2Z33+* — with 100 mM NaCl and 100 mM KCl (Figure 11). NMD targets show much lower decay rates under NaCl treatment compared to KCl, which is especially evident during the 1st hour (Figure 11D–F). In the later phase (1–4 h) the same effect is still present, but to a lesser degree

(Figure 11D-F). To take it even further, the concentration was lowered to 50 mM (Figure 12), and the NaCl treated samples showed significant reduction in the decay rate compared to KCl, in the 1st hour (Figure 12B). Altogether, data argues the NMD inhibition is not caused purely by the osmotic component of salt stress, and could be due to Na^+ ion toxicity.

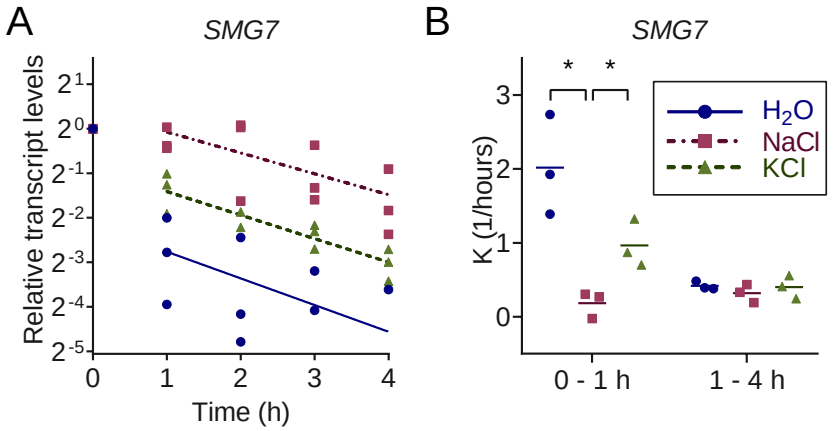

Figure 12: NMD target transcript *SMG7* under 50 mM NaCl and 50 mM KCl. Decay graph (A) and rate constant (B) shows higher stability under NaCl treatment in the 1st hour. Color key in (B) applies to both figures. Dots represent individual values, lines in (A) represent least squares non-linear regression, lines in (B) represent mean ($n = 3$). *, $P < 0.05$, t-test comparing NaCl with H_2O control and KCl.

4.4 Transcript stabilization by NaCl is likely NMD specific

There are many pathways that carry out mRNA decay, some are triggered by particular features (Section 3.3.3), others simply undergo general decay (Section 3.3.1) without additional recognition through special complexes. Decay pathways that recognize specific features, e.g. NMD or miRNA-specific cleavage, target specific mRNA substrates (Kervestin and Jacobson, 2012; Bologna and Voinnet, 2014), and can channel transcripts in decay via general pathways. General decay involves exoribonucleases, which can degrade the bulk of RNA substrates from 3'→5' (exosome) after deadenylation, or 5'→3' (XRNs) following the decapping process (Garneau et al., 2007; Schoenberg and Maquat, 2012; Zhang and Guo, 2017; Sorenson et al., 2018). Before addressing the pathway specificity of NaCl inhibition, it should be noted that under control conditions, non-NMD targets have slower degradation compared to NMD targets (Figure D.1;Kesarwani, Lee, Ricca et al. (2019)). To discuss the question whether the inhibition of RNA decay was NMD specific, or an inhibition of general RNA decay, the decay of six non-NMD targets (Figure 13) were analyzed in parallel with four NMD targets (Figure 14) which act as positive controls. The non-NMD targets used were: *SOS1 (AT2G01980)*, two splice variants

of *SERINE/ARGININE-RICH PROTEIN 30 (SR30) (AT1G09140) — SR30.1*, a productive splice variant, and *SR30.2*, a non-productive splice variant (Hartmann et al., 2018) — *PROTEIN PHOSPHATASE 2A (PP2A) (AT1G10430), WRKY6 (AT1G62300)*, and *RBOHD (AT5G47910)*. Accompanied by NMD targets used as control: *SMG7, PTB2+, RS2Z33+*, and *AT2G45670+* as described previously. Seedlings were treated with 0 or 100 mM of NaCl and RNA decay measurements were taken and analyzed via RT-qPCR. All four NMD target transcripts showed significant stabilization upon NaCl treatment (Figure 14). Two of the non-NMD targets, *SOS1* and *WRKY6*, showed stabilization in the early phase of decay, but not the later phase (Figure 14). A previous report has also observed an increase in steady state levels of *SOS1* upon salt treatment (Shi et al., 2000), and it is reasonable to assume that the stabilization of *SOS1* is due to increased Na^+ stress, and not NMD, as SOS1 is an Na^+/H^+ antiporter, which is essential to maintain low intracellular levels of toxic Na^+ under salt stress (Zhu, 2002; Qiu et al., 2002; Quintero et al., 2002, 2011; Nunez-Ramirez et al., 2012). The curbed degradation of *WRKY6* on the other hand, could be due to indirect consequences which NMD and *WRKY6* have in common (for a more detailed discussion see Section 5.3.1): that downregulated NMD and upregulated *WRKY6* have similar responses in e.g. sensitivity to salt (Fan et al., 2015), biotic and abiotic stress (Riehs-Kearnan et al., 2012; Gloggnitzer et al., 2014; Rigby and Rehwinkel, 2015; Cai et al., 2015; Phukan et al., 2016), and increased salicylic acid (SA) accumulation (Jeong et al., 2011; Choi et al., 2015).

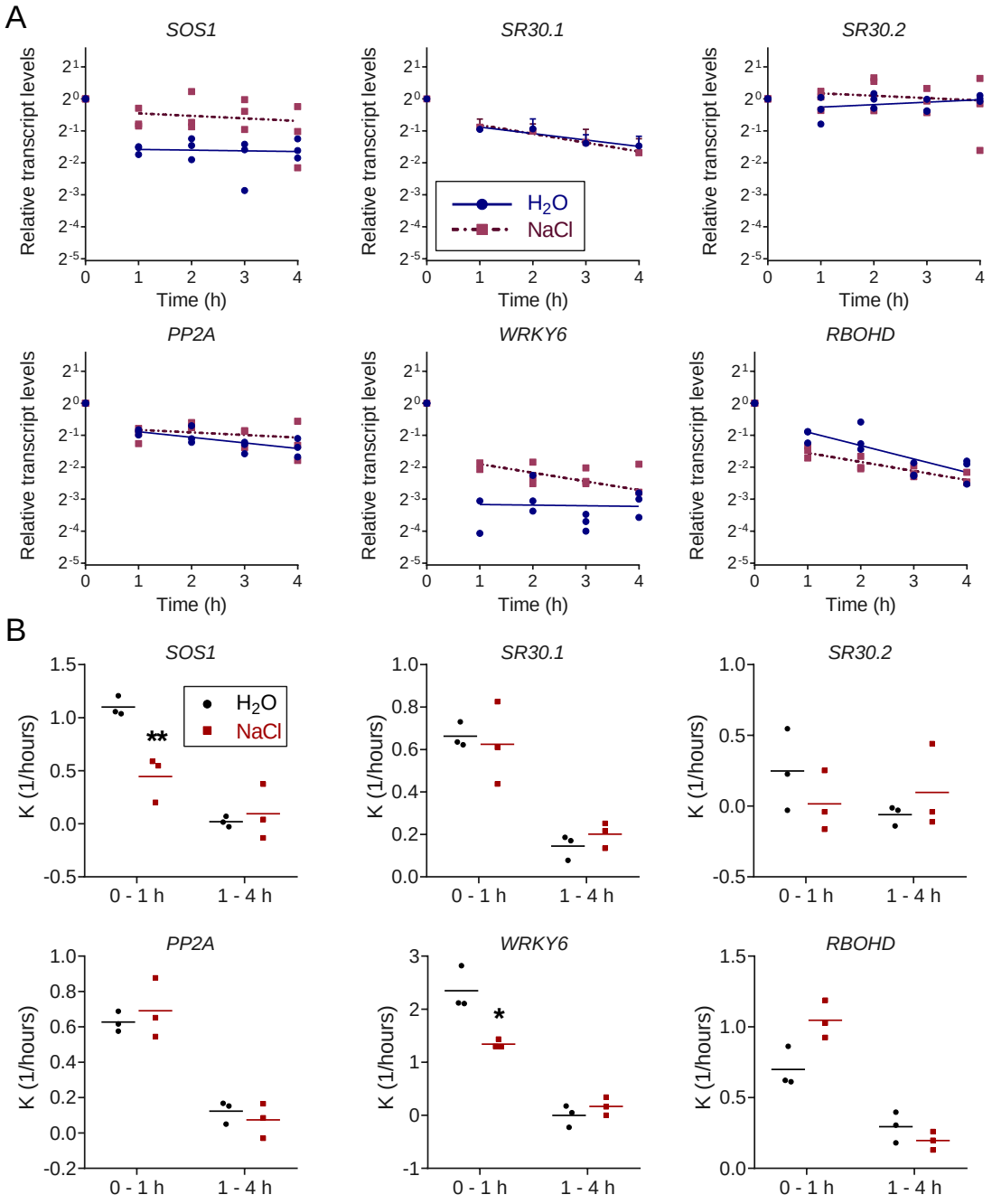

Figure 13: Non-NMD transcripts under NaCl treatment. Decay graphs (A) and rate constant (B) from the RNA stability assay using 7-d-old *A. thaliana* seedlings treated with 100 mM NaCl ($n = 3$). Data generated by RT-qPCR. *, $P < 0.05$; **, $P < 0.01$ by unpaired t-test compared against H_2O control. Dots represent individual values, line in (A) represents least squares non-linear regression; line in (B) represents mean.

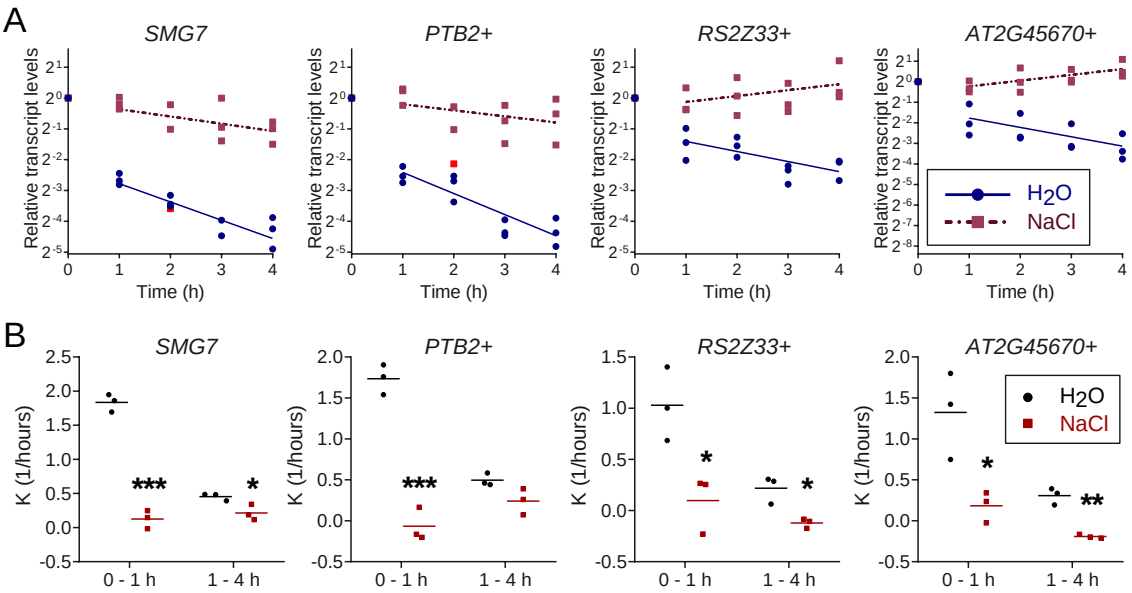

Figure 14: NMD target transcripts under NaCl treatment. Decay graphs (A) and rate constant (B) from the RNA stability assay on 7-d-old *A. thaliana* seedlings treated with 100 mM NaCl ($n = 3$). Data generated by RT-qPCR. *, $P < 0.05$; **, $P < 0.01$; ***, $P < 0.001$, by unpaired t-test compared against H_2O control. Line in (A) represents least squares non-linear regression; line in (B) represents mean.

***SOS1*, *RBOHD* and *RBOHF* are not NMD target transcripts** Steady state transcript levels of *SOS1*, *RBOHD* and *RBOHF* are measured under 4 h of 10 μg/ml CHX treatment, and normalized to 4 h mock-treated *A. thaliana* Col-0 WT plants (Figure 15). Accumulation could be seen for *RBOHD* and *RBOHF* but not for *SOS1*, hinting *RBOHD* and *RBOHF* could be NMD targets. Steady state transcript levels of *SOS1*, *RBOHD* and *RBOHF* are measured in NMD mutants *lba1* and *upf3-1* and normalized to *A. thaliana* Col-0 WT plants. No transcript accumulation can be seen for these three transcripts, further confirming *SOS1* is not an NMD target transcript. While *RBOHD* and *RBOHF* are not NMD target transcripts, they are affected when translation is inhibited, as a secondary effect of CHX treatment.

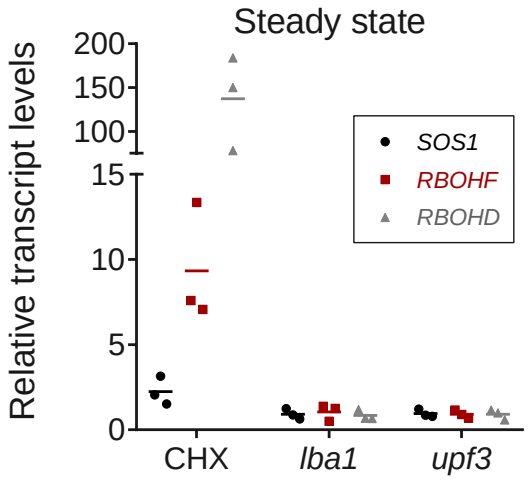

Figure 15: Steady state transcript levels of *SOS1*, *RBOHD* and *RBOHF* do not accumulate in NMD mutants *lba1* and *upf3*, relative to Col-0. *RBOHD* and *RBOHF* accumulate under 4 h 10 μg/ml CHX treatment, normalized to mock treated samples. Data derived from RT-qPCR, dots represent individual values ($n = 3$), lines represent mean.

4.5 NMD target transcripts stabilized in NMD mutants, and further stabilized upon NaCl stress

4.5.1 NMD target transcripts are stabilized in NMD factor mutants

As previously discussed, fast and slow decay rates were observed for NMD targets versus non-NMD targets, respectively. For a more specific scope of the NMD targeting status, transcript decay were analyzed in NMD factor mutants: the UPF1 missense mutant *low-beta-amylase* (*lba1*) (Yoine et al., 2006), and a transfer DNA (T-DNA) insertion mutant *upf3-1* (Hori and Watanabe, 2005). The hypomorphic *smg7-1* T-DNA insertion mutant shows strong growth defects, and is sterile when homozygous (Riehs et al., 2008). Due to these strong phenotypes, the experimental procedures of the half life assay was unsuitable for *smg7-1* mutants, and therefore a separate set of *smg7-1* and Col-0 WT plants were grown on soil for 35 days (Figure E.1), and steady state levels were analyzed without salt (Figure 16).

In total, the decay of eight different transcripts were analyzed. Four core NMD factor transcripts: *UPF1*, *UPF2*, *UPF3* and *SMG7* (Figure 17), and another four

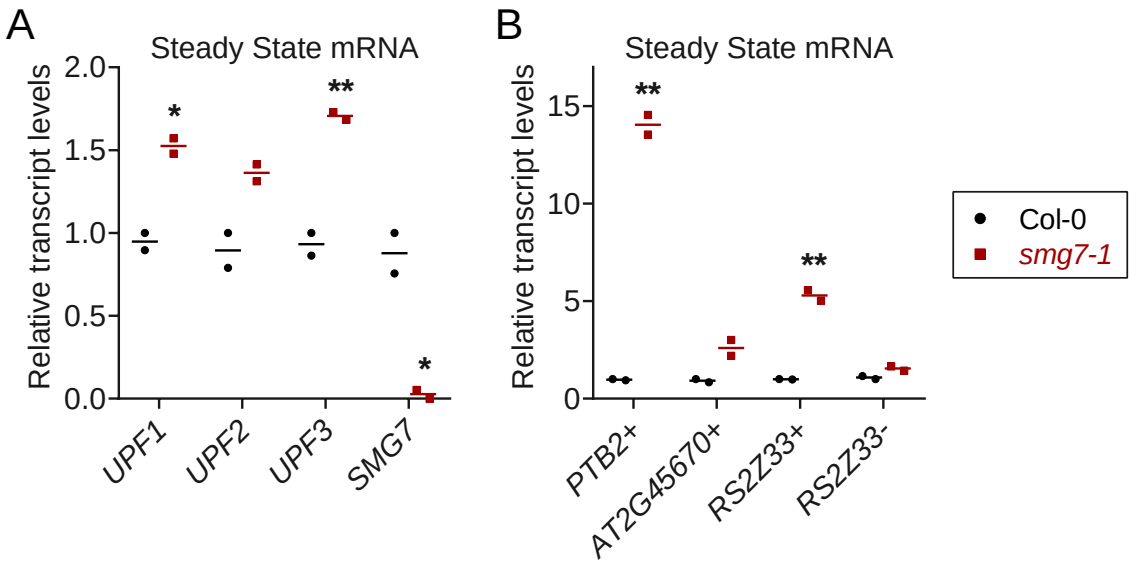

Figure 16: NMD targets accumulate in *smg7-1* mutants. Steady state levels of transcripts from NMD factor genes (A) and other NMD or AS non-NMD targets (B). Transcript levels determined via RT-qPCR from 35-d-old soil-grown plants (Figure E.1). All data normalized to *Actin 7* as reference and expressed to one WT sample. *, $P < 0.05$; **, $P < 0.01$, unpaired t-test comparing WT and mutants ($n = 2$).

AS transcripts that are not core regulators of the NMD machinery: *PTB2+*, *AT2G45670+*, *RS2Z33+* and *RS2Z33–* (Figure 18). Of the eight, *UPF2* and *RS2Z33–* were not NMD targets. The steady state measurements were also analyzed for these eight transcripts, in NMD mutants *smg7-1* (Figure 16), *lba1* and *upf3-1* (Figure 19). Analysis of the steady state levels in *smg7-1* shows significant accumulation of all NMD target transcripts except *AT2G45670+* and *SMG7*, while the non-NMD targets *UPF2* and *RS2Z33–* showed little alterations compared to WT (Figure 16). *SMG7* transcript levels were greatly reduced in the *smg7-1* mutant (Figure 16A), most likely due to the T-DNA insertion in this locus. Of the NMD core factors, only *UPF2* was not stabilized in the *lba1* and *upf3-1* mutants (Figure 17B, E). All other NMD factors show a more pronounced stabilization in the *upf3-1* mutant, with moderate stabilization in *lba1* (Figure 17A, C–D, F–H). A similar pattern was also seen in the other NMD targets, where the transcripts were more stabilized in the *upf3-1* mutant compared to *lba1* (Figure 18A–F). The non-NMD targets on the other hand do not display such tendency (Figure 17B, E, Figure 18G–H). Steady state levels of NMD targets also reflect transcript stabilization in *lba1* and *upf3-1*, where NMD targets show transcript accumulation in the NMD mutants, with higher accumulation in *upf3-1* than *lba1* (Figure 19), with the exception being *UPF3*, where there are significantly lower levels of transcript in the *upf3-1* mutant (Figure 19C). This likely is also due to the T-DNA insertion in this locus, similar as described above for SMG7 in the corresponding mutant (Figure 16A). While all measured

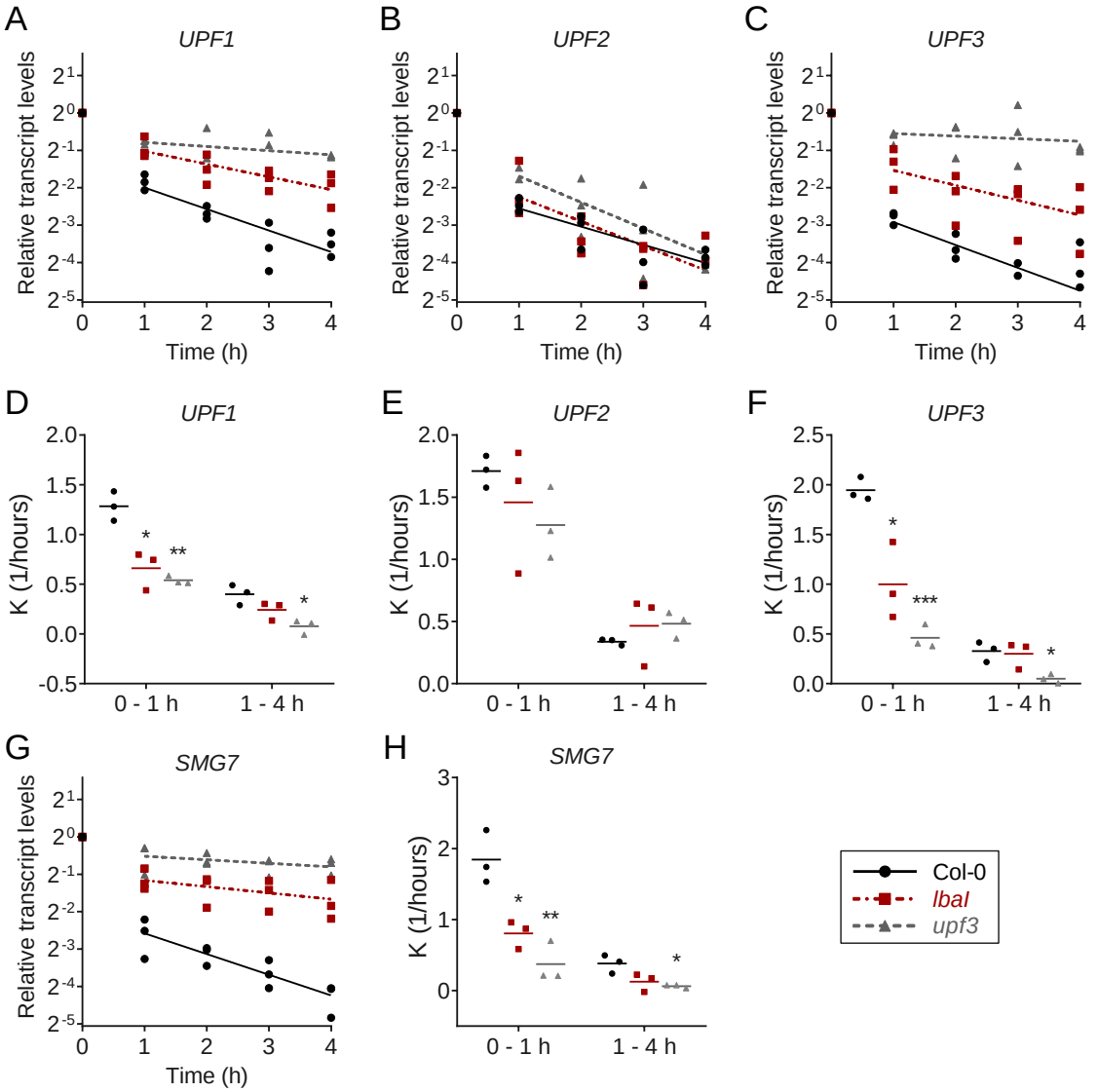

Figure 17: NMD target transcripts stabilize in NMD mutants *lba1* and *upf3-1*. Decay graphs (A–C, G) and rate constants (D–F, H) of NMD core component transcripts in 7-d-old *A. thaliana* seedlings. *, $P < 0.05$; **, $P < 0.01$; ***, $P < 0.001$, unpaired t-test comparing WT and mutants ($n = 3$). Dots represent individual values, lines in (A–C, G) represent least squared non-linear regression, lines in (D–F, H) represent mean.

NMD targets display the aforementioned traits, the non-NMD target *UPF2* do not show higher accumulation in *upf3-1* compared to *lba1* (Figure 19B), and *RS2Z33–* — the AS counterpart of *RS2Z33+* — shows only moderate accumulation in *upf3-1* (Figure 19H). This excludes the level increase seen in *RS2Z33+* is caused by altered AS in favor of the PTC+ isoform of this transcript. Altogether, this assay shows direct evidence that NMD activity is diminished in *lba1* and *upf3-1* mutants, and based on the data, *upf3-1* has higher levels of NMD-impairment than *lba1*, in 7-d-old liquid grown *A. thaliana* seedlings.

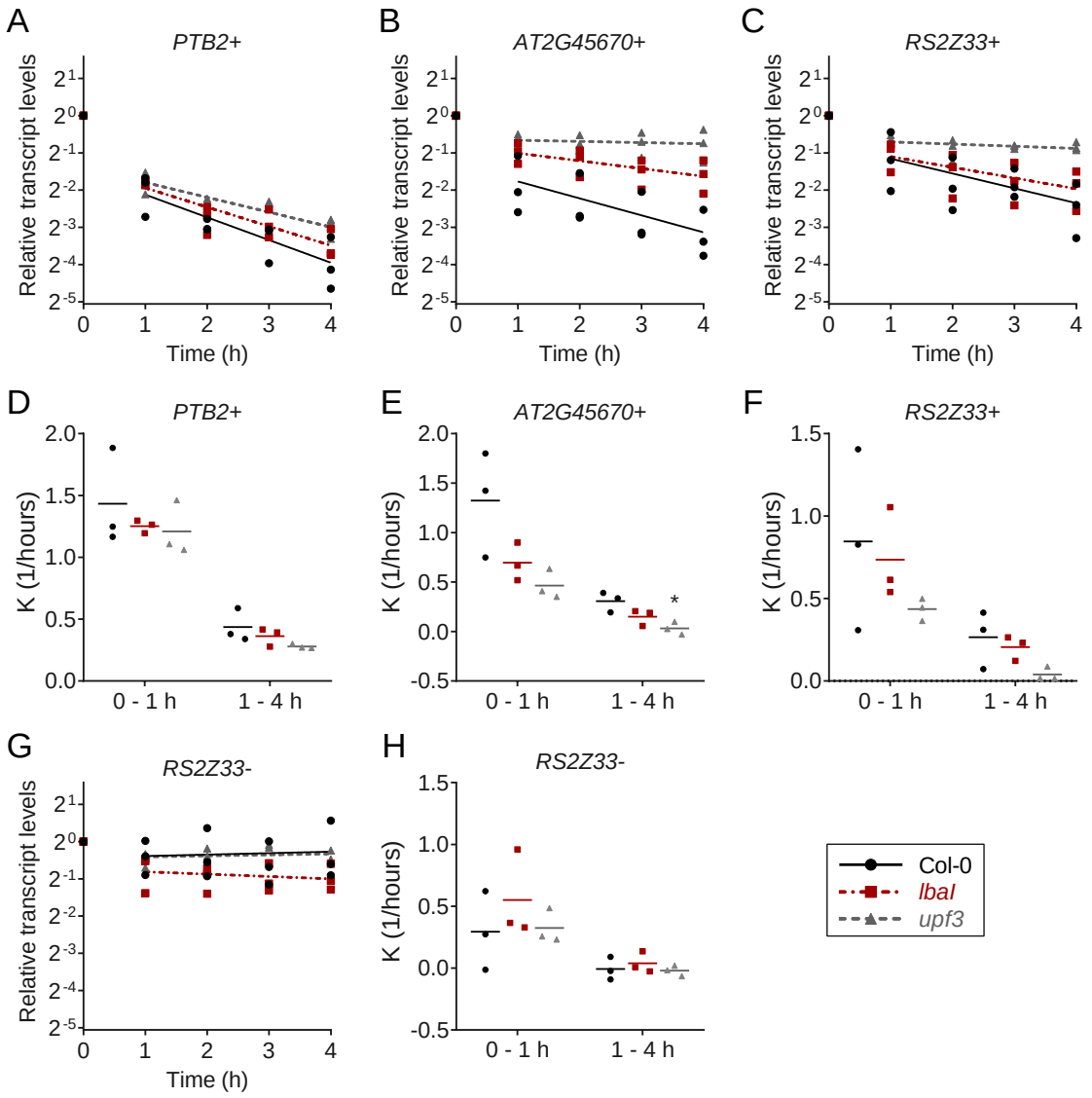

Figure 18: NMD target transcripts stabilize in NMD mutants *lba1* and *upf3-1*. Decay graphs (A–C, G) and rate constants (D–F, H) of NMD target transcripts in 7-d-old *A. thaliana* seedlings. *, $P < 0.05$; unpaired t-test performed comparing WT and mutants ($n = 3$). Dots represent individual values, lines in (A–C, G) represent least squared non-linear regression, lines in (D–F, H) represent mean.

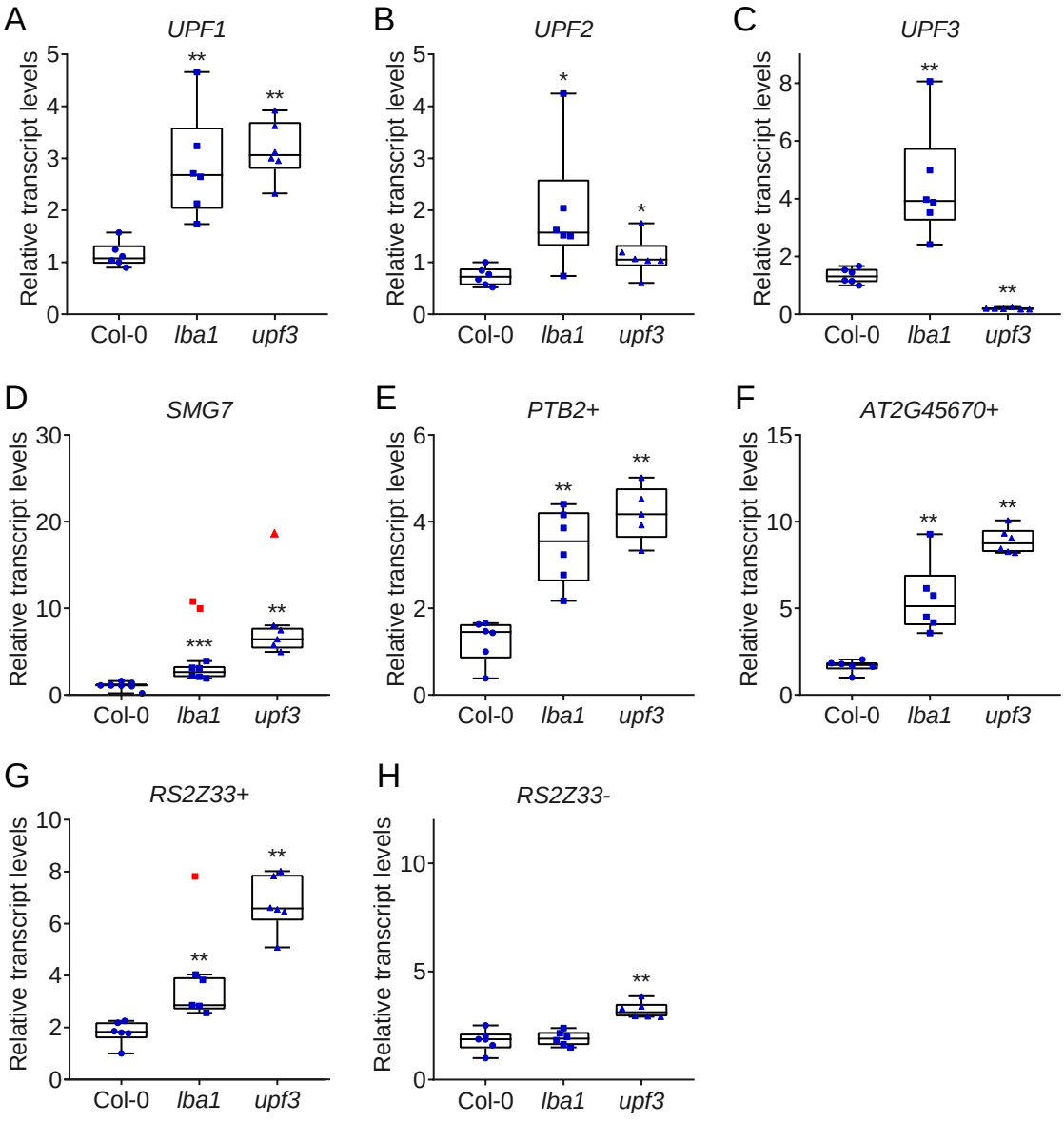

Figure 19: Steady state levels of NMD targets accumulate in NMD mutants. Steady state levels of NMD core transcripts (A–D) and NMD target transcripts (E–G). Non-NMD target transcripts are (B) *UPF2* and (H) *RS2Z33*– (n = 5–8). All data were normalized to one WT sample. Box plot represents first quartile, median, third quartile, whiskers represent min and max. Outliers determined through robust regression and outlier removal (ROUT) ($Q = 5\,\%$), and are plotted in red.

4.5.2 Transcripts stabilize further with NaCl application in NMD mutants

Having established the baseline for NMD target stabilization in NMD mutants, the next interesting thing would be to see the behaviour of these transcripts when salt is added. In all cases, transcripts have stabilized with the addition of NaCl in both mutants, which can be seen in the decay graphs for *lba1* (Figure 20), and *upf3-1* (Figure 21), which was quantified with the rate constants (Figure 22). The stabilization upon salt treatment in the mutants were to a similar degree as in WT.

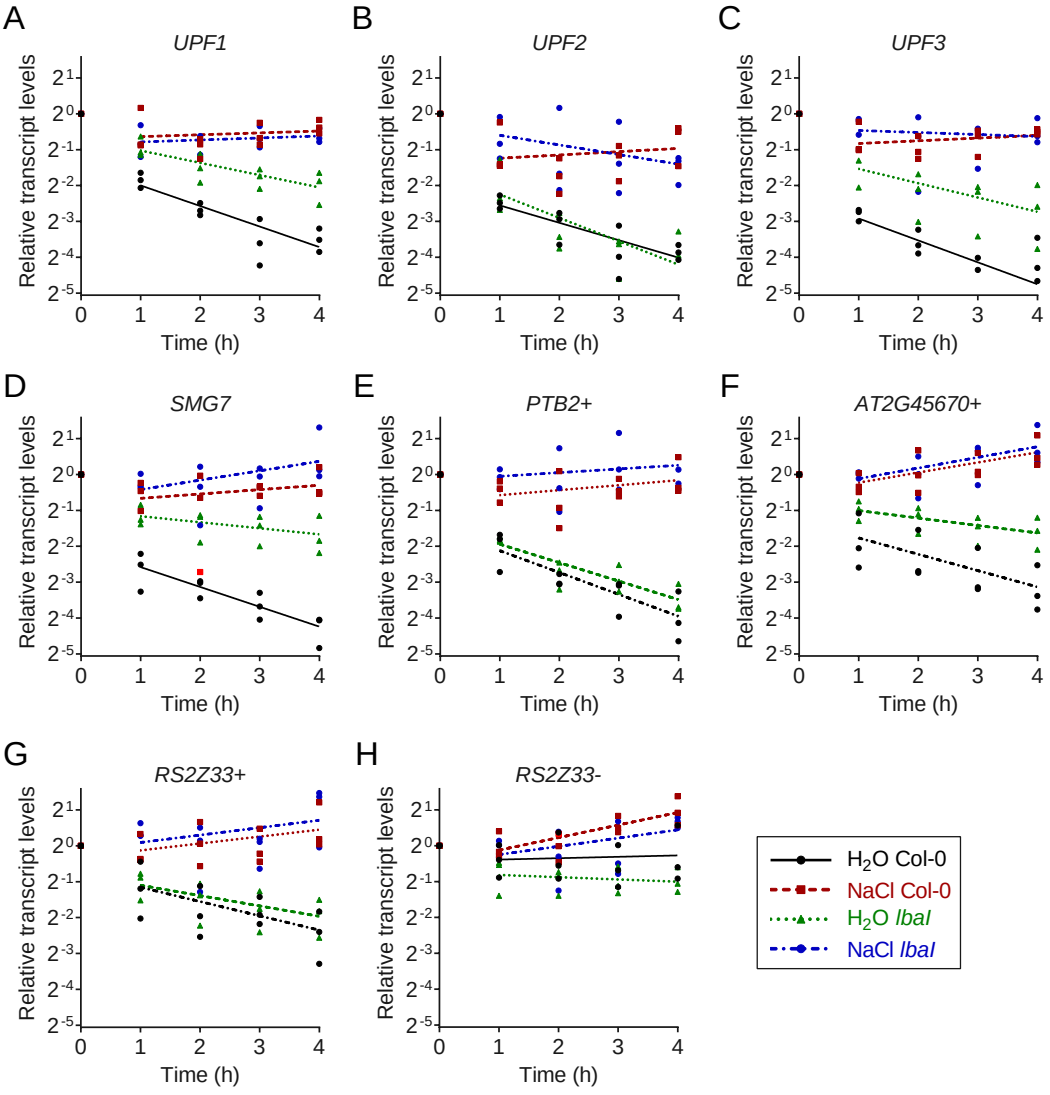

Figure 20: Transcripts stabilize in *lba1* under 100 mM NaCl. NMD core transcripts (A–D) and NMD target transcripts (E–G). Non-NMD target transcripts are (B) *UPF2* and (H) *RS2Z33–* ($n = 3$). Dots represent individual values, lines represent least squared non-linear regression.

In this experiment, it is probable that transcription was not completely blocked, particularly obvious in *AT2G45670+* and *RS2Z33–*, indicated by the positive slope of the regression lines in the decay graphs (Figure 20F, H, Figure 21F, H) and the

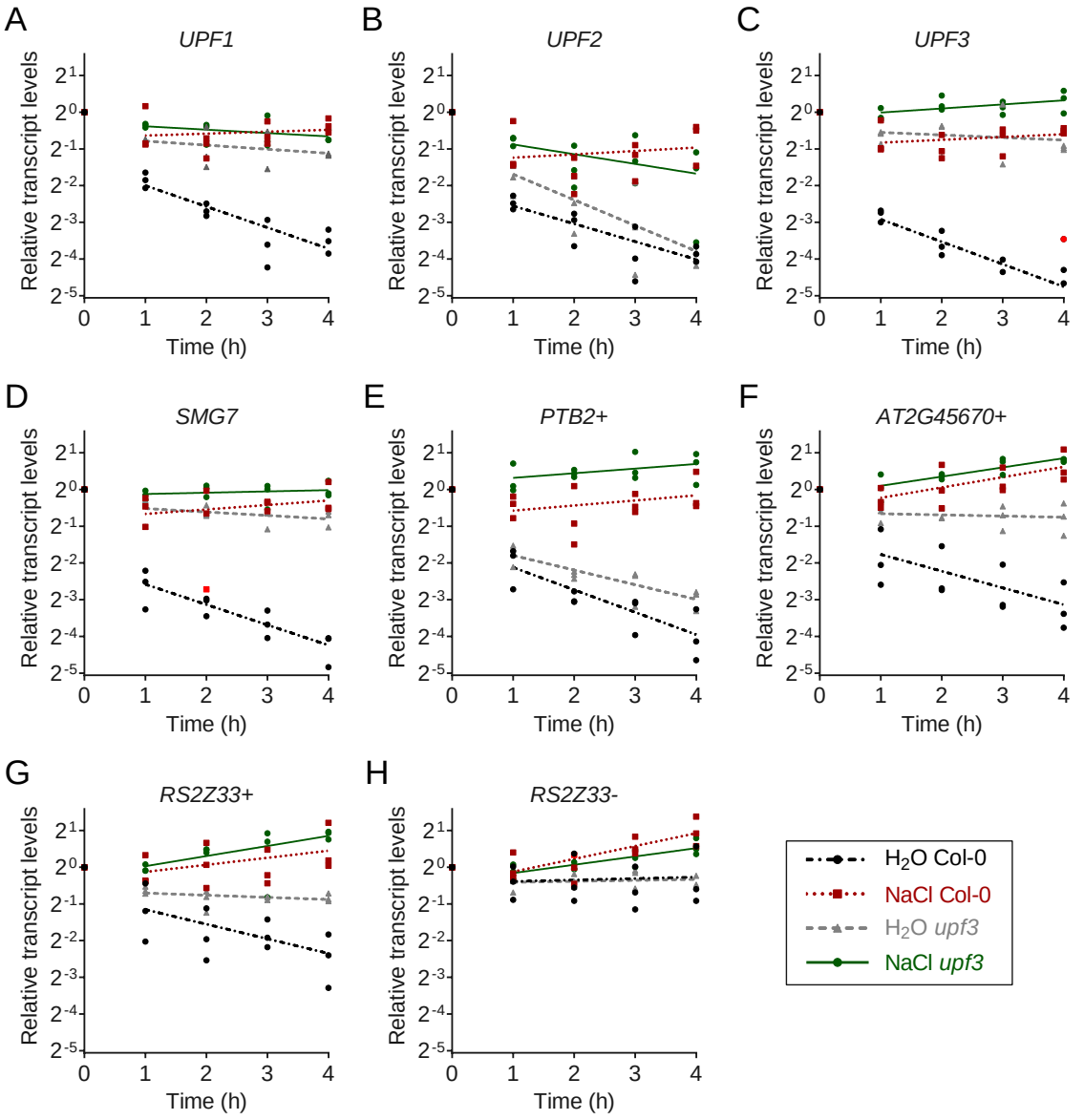

Figure 21: Transcripts stabilize in *upf3-1* under 100 mM NaCl. NMD core transcripts (A–D) and NMD target transcripts (E–G). Non-NMD target transcripts are *UPF2* (B) and *RS2Z33*– (H) ($n = 3$). Dots represent individual values, lines represent least squared non-linear regression.

negative value in rate constants (Figure 19F, H). Due to instances like this, salt and mock controls were performed for each individual half-life assay, and comparisons are done within each independent experiment itself. Reasons for variation could be from plant growth, discrepancy in time of day the experiment was conducted, or deviations between different batches of cordycepin that were used. Taken together, these transcripts which were further stabilized with NaCl treatment could be explained by neither of these mutants are complete knock-outs, and NMD was inhibited to a greater degree upon NaCl stress. In this case, with 100 mM NaCl treatment, the transcripts are already giving almost complete stabilization in the WT, therefore no additional effect can be seen in the mutant. A repeat with lower concentrations of

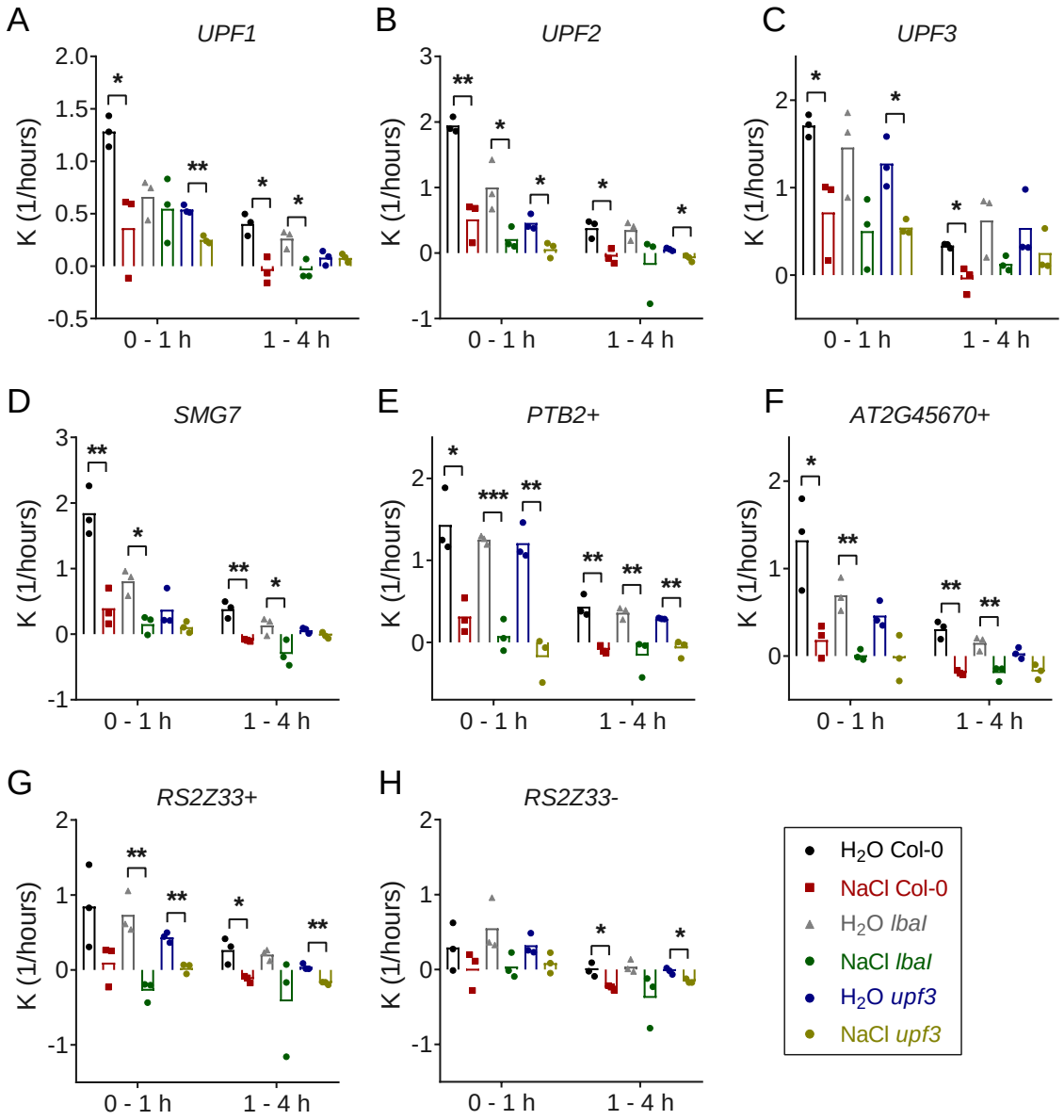

Figure 22: Slowed decay of NMD core transcripts (A–D) and NMD target transcripts (E–G) under 100 mM NaCl in NMD mutants *lba1* and *upf3-1*. Non-NMD target transcripts are *UPF2* (B) and *RS2Z33*– (H). *, $P < 0.05$; **, $P < 0.01$; ***, $P < 0.001$, unpaired t-test comparing NaCl to their respective negative control H_2O ($n = 3$).

NaCl should be performed to observe possible subtle changes in these mutants.

4.6 Translation inhibition is involved in NaCl-mediated NMD inhibition, but not through eIF2aα phosphorylation, nor TOR inhibition

4.6.1 Induction of eIF2α phosphorylation is insufficient for NMD inhibition

It is well documented that NMD is tied tightly to translation, with obstructed ribosomes acting as one of the central elements for recruitment of NMD factors (Carter et al., 1996; Thermann et al., 1998; Maquat et al., 2010; Brogna et al., 2016; Karousis et al., 2016; Raimondeau et al., 2018). In mammalian cells, stress-induced NMD inhibition has been shown to involve the inhibition of translation through phosphorylation of the EUKARYOTIC INITIATION FACTOR 2α (eIF2α) (Gardner, 2010; Karam et al., 2013), and this phosphorylation have also been shown to occur under stress in *A. thaliana* (Lageix et al., 2008; Zhang et al., 2008). In *A. thaliana*, treatment with 100 mM NaCl showed transient increase of phosphorylated eIF2α and using chlorsulfuron — an inducer of eIF2α phosphorylation (Lageix et al., 2008; Zhang et al., 2008) — resulted in a massive accumulation of phosphorylated eIF2α (Wachter et al., unpublished). In order to see if the phosphorylation of eIF2α results in NMD inhibition in *A. thaliana*, the decay pattern of five NMD target transcripts were analyzed under chlorsulfuron treatment (Figure 23). Out of the five transcripts, *SMG7* showed a trend of slight decrease in decay within the 1st hour (Figure 23), albeit not statistically significant (Figure F.1). The other four NMD targets *PTB2+*, *AT2G45670+*, *RS2Z33+* and *UPF3* all showed no stabilization (Figure 23, Figure F.1).

4.6.2 eIF2α phosphorylation is not necessary for salt-mediated NMD inhibition

The kinase GENERAL CONTROL NON-DEREPRESSIBLE 2 (GCN2) is mandatory for the phosphorylation of eIF2α (Lageix et al.; Zhang et al., Wachter et al., unpublished). To examine if eIF2α phosphorylation is required for NMD inhibition, the decay of NMD target transcripts *SMG7*, *RS2Z33+* and *PTB2+* were analyzed in Col-0 WT and *gcn2* mutants. If eIF2α phosphorylation is necessary for NMD inhibition under NaCl stress, then no NMD inhibition would be expected in *gcn2* mutants, when NaCl is applied. In all three transcripts under control conditions, no trends were observed comparing WT and *gcn2* in the steady state level (Figure 24G). Slight tendency for stabilization were seen for the decay patterns in *gcn2* (Figure 24A–C), though not enough to be statistically significant (Figure 24D–E). With the addition of 100 mM NaCl, data shows the same extent of stabilization in *gcn2* and WT (Figure 24A, B, D, E), suggesting that eIF2α phosphorylation is not necessary for NMD inhibition under NaCl stress.

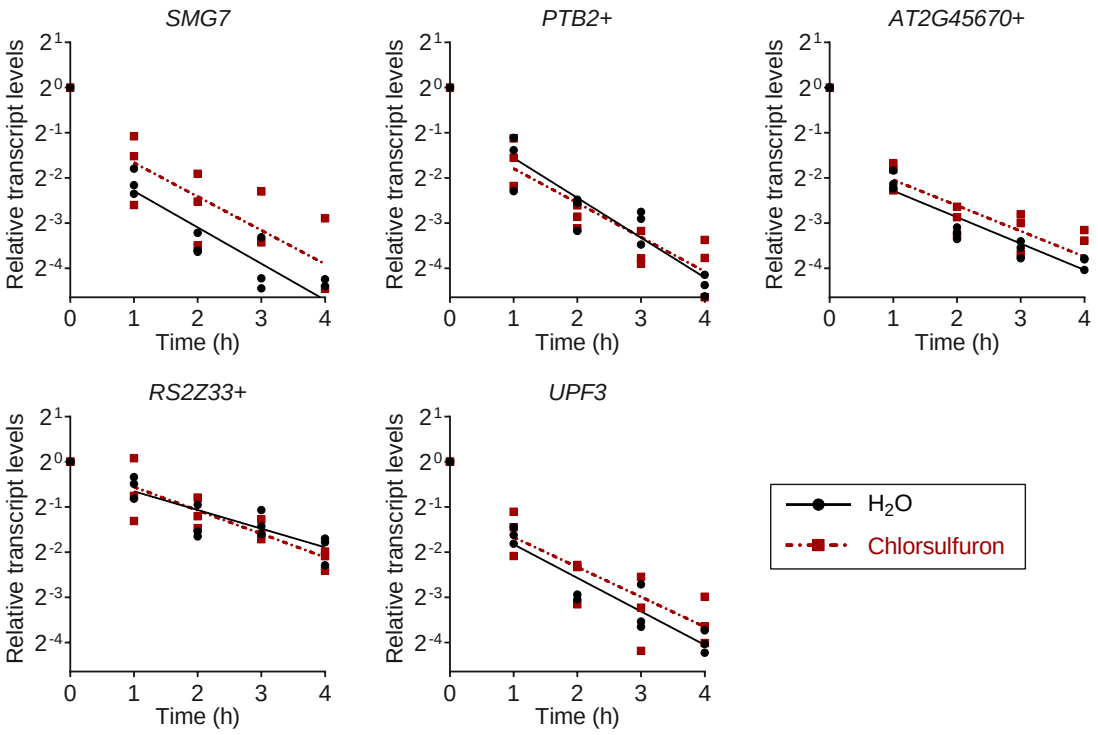

Figure 23: NMD target transcripts not stabilized under chlorsulfuron treatment. Decay patterns of NMD target transcripts in 7-d-old *A. thaliana* seedlings treated with 0 mM or 0.6 μM Chlorsulfuron. Data derived from RT-qPCR. Dots represent individual values, lines represent least squares non-linear regression ($n = 3$). Corresponding rate constant plotted in Figure F.1.

4.6.3 NaCl-mediated NMD inhibition is not dependent on TOR regulated translation

Target of rapamycin (TOR), a Ser/Thr protein kinase, is a major regulator of growth and development in all eukaryotes (Cafferkey et al., 1993; Kunz et al., 1993; De Virgilio and Loewith, 2006). In Arabidopsis, manipulating TOR kinase activity or *TOR* expression levels leads to changes in growth and development (Menand et al., 2002; Deprost et al., 2007; Ren et al., 2011; Xiong and Sheen, 2012; Caldana et al., 2013; Xiong et al., 2013). TOR controls various components of the translation initiation machinery (Ma and Blenis, 2009; Thoreen et al., 2012; Gandin et al., 2016; Sesma et al., 2017), and the inactivation of mTOR during hypoxia reduces the translation of specific mRNAs with 5' terminal oligopyrimidine (TOP) tracts and overall protein biosynthesis (Spriggs et al., 2010; Thoreen et al., 2012).
To investigate if NMD inhibition through NaCl is due to translation being affected in a TOR dependent manner, T-DNA insertion lines of *SULFITE REDUCTASE (SIR)1*, *sir1-1* (Khan et al., 2010; Dong et al., 2017; Speiser et al., 2018) and MUTANT, *SNC1*-ENHANCING (MUSE)6, *muse6* (Xu et al., 2015) were used to analyze NMD target transcript behavior. These mutants have been reported to have decreased

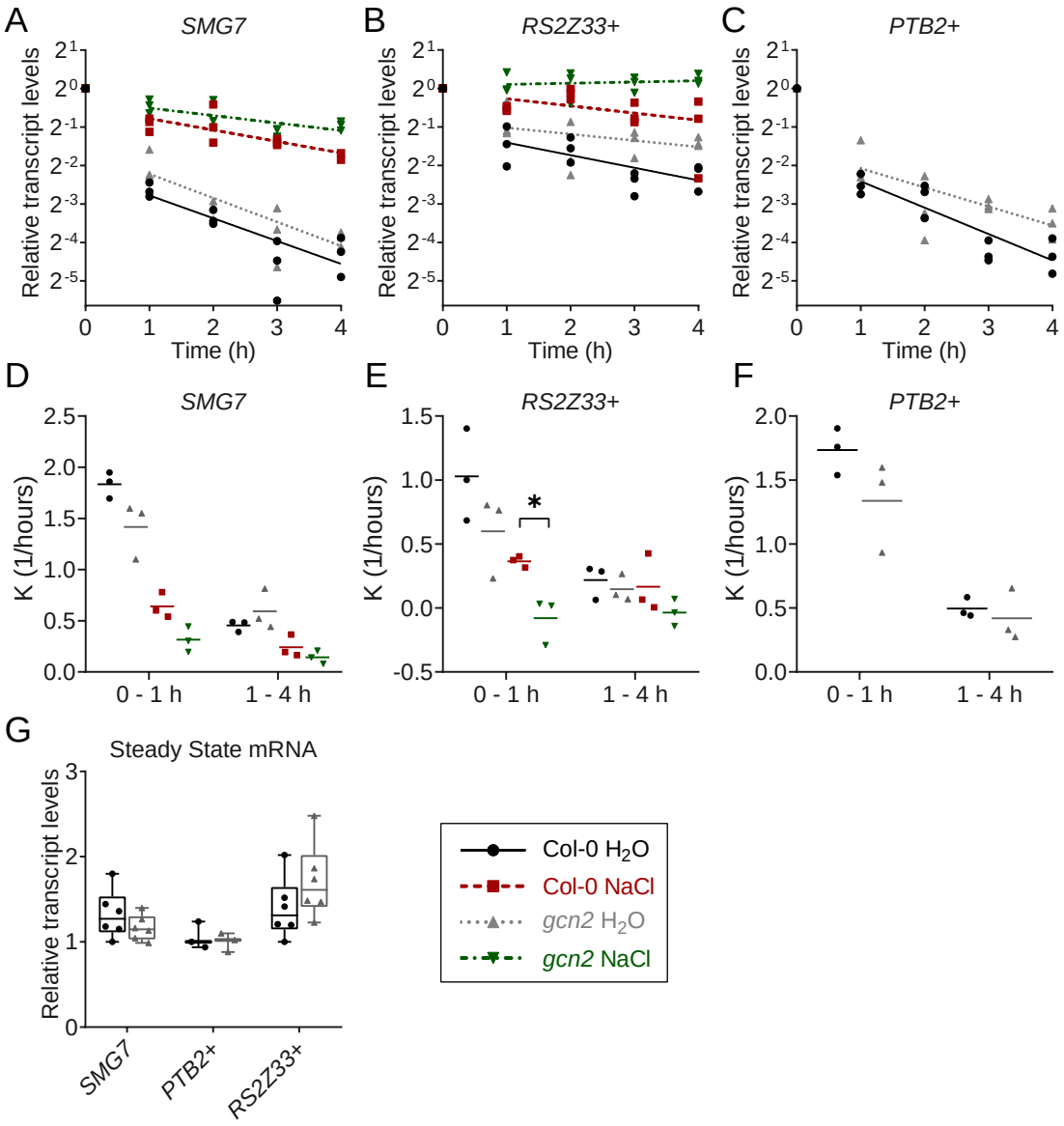

Figure 24: NMD target transcripts are not destabilized in *gcn2* upon 100 mM NaCl. Decay graphs (A–C), rate constant (D–F) and steady state mRNA levels (G) of NMD target transcripts ($n = 3$). Color key applies to all graphs. Data derived from RT-qPCR, dots represent individual values, lines in (A–C) represent least squares non-linear regression, (E–F) represent mean. *, $P < 0.05$, t-test of *gcn2* against WT control. Box plot in (G) represents first quartile, median, third quartile, whiskers represent min and max.

translation, likely due to downregulated ribosome biogenesis (Dong et al., 2017), and decreased TOR activity (Speiser et al., 2018). *muse6-1* has also been reported to be a negative regulator of NOD-LIKE RECEPTOR (NLR)-mediated immunity (Xu et al., 2015). The degradation patterns of NMD target transcripts *SMG7* and *RS2Z33+* were analyzed in WT, *sir1-1* and *muse6* in the Col-0 background, with 0 mM, 50 mM and 100 mM of NaCl treatment (Figure 25). If TOR regulated translation played a major role in NaCl-induced NMD inhibition, the expected outcome would result

in a destabilization of NMD target transcripts under NaCl treatment. Both NMD transcripts showed mild stabilization in *sir1-1* and *muse6* in the control group with no NaCl (Figure 25A,D). This trend was continued in 50 mM and 100 mM NaCl treated groups, while no obvious trend was realized for *RS2Z33+* in 100 mM NaCl. In all cases, no destabilization was observed (Figure 25), indicating downregulated translation through the TOR pathway do not abolish the NaCl-induced transcript stabilization.

Furthermore, the TOR inhibitor AZD8055 was used to look at the relation TOR regulated translation has with NMD. AZD8055 in known to inhibits the phosphorylation of TORC1 as well as TORC2 and downstream proteins. The decay of five NMD targets were analyzed — *SMG7*, *PTB2+*, *AT2G45670+*, *RS2Z33+* and *UPF3* — with or without the TOR inhibitor (Figure 26). Out of the five NMD targets, only *SMG7* displayed a trend of decreased decay (Figure 26), however it was not statistically significant (Figure F.1). All other four transcripts behaved similar to the control treatment (Figure 26, F.1).

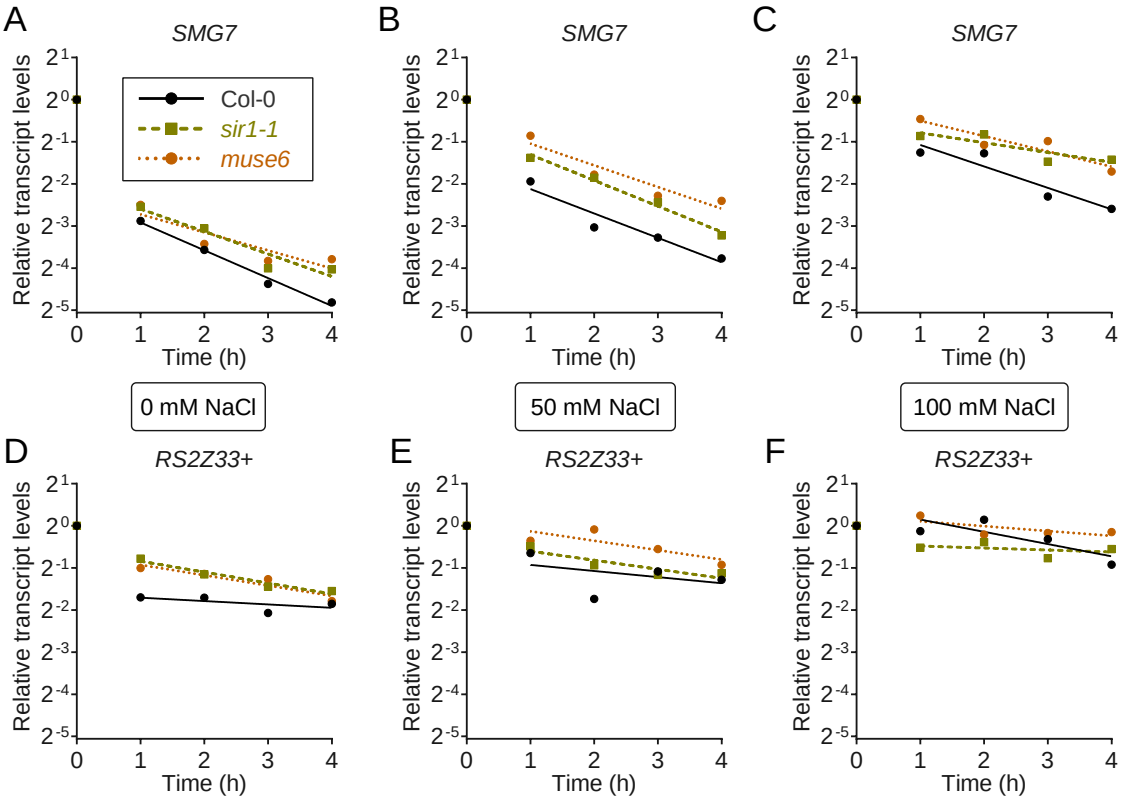

Figure 25: NMD target transcripts are not destabilized upon NaCl treatment in translationally downregulated mutants *sir1-1* and *muse6*. Transcripts *SMG7* and *RS2Z33+* in Col-0 WT, *sir1-1*, and *muse6*, treated with 0 mM (A, D), 50 mM (B, E) and 100 mM (C, F) NaCl ($n = 1$). Color key in (A) applies to all graphs. Dots represent individual values, lines represent least squares non-linear regression.

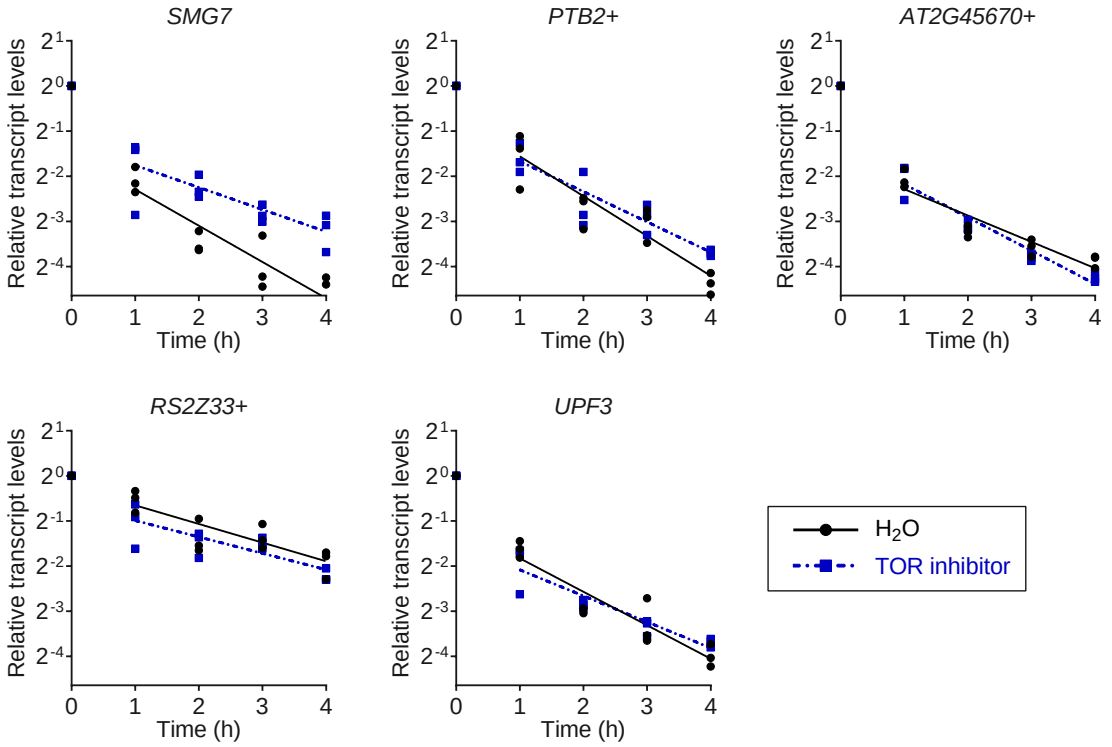

Figure 26: NMD target transcripts do not show increased stability upon TOR inhibition. Decay graphs of 7-d-old *A. thaliana* seedlings treated with 5 μM TOR inhibitor (AZD8055) or H_2O as control. Data derived from RT-qPCR, dots represent individual values ($n = 3$), line represents least squares non-linear regression. Corresponding rate constant (K) shown in Figure F.1.

4.6.4 NMD targets accumulate upon translation inhibition by CHX

Although the data here shows NaCl-induced NMD inhibition is independent of eIF2α phosphorylation and TOR regulation, other modes of translation inhibition cannot be excluded. As supporting evidence for affirmation, four NMD target transcripts (*SMG7*, *PTB2+*, *AT2G45670+*, *RS2Z33+*) and one non-NMD target (*RS2Z33−*) was analyzed in samples treated with the translation inhibitor CHX (Figure 27). Since this experiment was done before the liquid culture was established, it was performed with 10-d-old plate grown seedlings, where the treatment was done with plate flooding, and transcripts were normalized to *eIF4A1 (AT3G13920)*. *A. thaliana* seedlings were pre-treated with mock (flooding with H_2O) and NaCl for 6 h, and under steady state conditions, an accumulation of NMD targets (Figure 27A) was detected compared to mock, consistent with previous data in Section 9. The same plants were then treated with CHX for 4 h, which the NMD targets in mock plants (H_2O followed by addition of CHX) showed an accumulation in all four NMD target transcripts, while the plants pretreated with NaCl (NaCl treatment followed by addition of CHX), showed no further accumulation of NMD target transcripts (Figure 27B). The non-NMD transcript *RS2Z33−* remains unchanged (Figure 27B).

Foremost, this further confirms that NMD targets accumulate upon NaCl, in spite of flooding stress (Figure 27A), and furthermore shows translation inhibition can also cause NMD target accumulation (Figure 27B). On top of that, the NMD targets in NaCl pretreated plants do not further accumulate upon CHX treatment (Figure 27B), showing that inhibition of NMD target transcript decay by CHX could be along the same pathway as NaCl-induced inhibition, or that they act independently, but maximum extent of stabilization has already been reached by NaCl treatment.

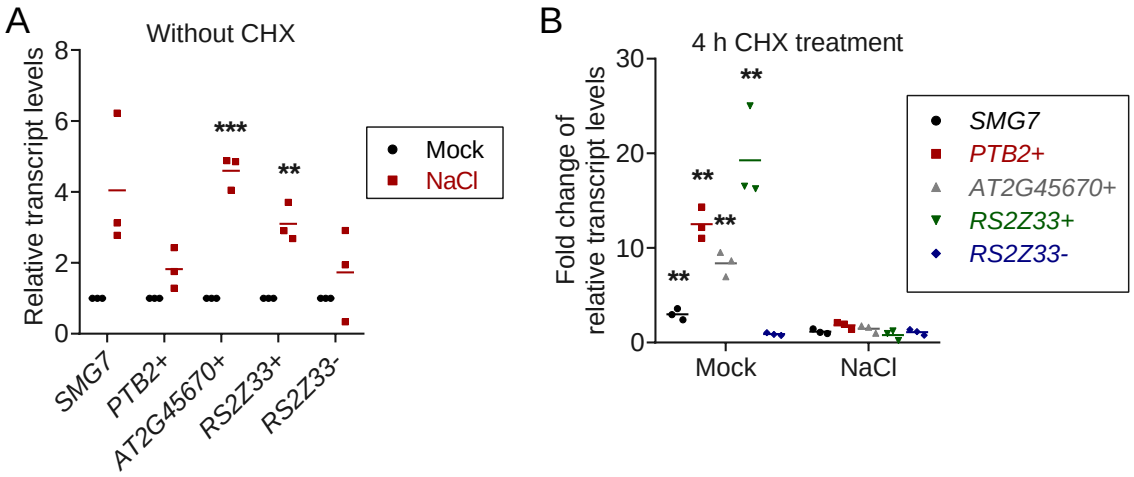

Figure 27: Steady state levels of NMD target transcripts accumulate under NaCl and CHX, but does not further accumulate when treated with CHX under NaCl conditions. (A) 10-d-old plate grown *A. thaliana* seedlings were pre-treated for 6 h with mock or 500 mM NaCl. Data derived from RT-qPCR, genes normalized to *eIF4A1*. **, $P < 0.01$; ***, $P < 0.001$, t-tests performed comparing against mock treated plants. Dots represent individual values ($n = 3$), line represent mean. (B) The same plants from (A) were subsequently treated with 10 μg/ml CHX for 4 h, and fold change of NMD target transcripts were calculated against corresponding samples in (A). t-tests were performed against corresponding samples in (A). Data derived from RT-qPCR, transcripts normalized to *eIF4A1*.

4.7 ABA and downstream SnRK2s do not have major involvement in NMD inhibition under NaCl

The phytohormone ABA is involved in many plant developmental processes, and is a major responder to environmental stresses, including drought and soil salinity (Zhu, 2002). Therefore, the relationship between ABA and NaCl-induced NMD inhibition was examined. NMD factor transcripts *UPF1*, *UPF2*, *UPF3* and *SMG7* were not altered with ABA treatment (Figure G.1A–D, Kesarwani, Wachter, et al., unpublished), while positive control genes *ABI1* (Leung et al., 1997) and *ZINK-FINGER PROTEIN 2* (*AZF2*) (Drechsel et al., 2010) showed a massive induction (Figure G.1A–D, Kesarwani, Wachter, et al., unpublished), showing increased ABA

alone is insufficient for NMD inhibition. To check if ABA is required, the ABA-insensitive mutant *abi2-1* (Leung et al., 1994; Meyer et al., 1994) is compared to the corresponding *A. thaliana* ecotype Landsberg (Ler) WT, which also did not show significant differences (Figure G.1E,F), indicating that ABA is not required for NaCl-induced NMD inhibition.

4.7.1 NMD targets unaffected in *snrk2* mutants

The SnRK 2 family members are plant-specific serine/threonine kinases involved in responses to abiotic stress and ABA-dependent plant development (Anderberg and Walker-Simmons, 1992; Holappa and Walker-Simmons, 1995; Mikolajczyk et al., 2000; Li et al., 2000; Fujii and Zhu, 2009a; Fujita et al., 2009; Nakashima et al., 2009). The SNRK2 family members are divided into three groups based on phylogenetic analysis (Kulik et al., 2011) — subclass I, which consists of kinases not activated by ABA, subclass II, which are weakly or not activated by ABA depending on plant species, and subclass III, which are strongly activated by ABA. Subclass III kinases (SRK2D/SnRK2.2, SRK2E/SnRK2.6 and SRK2I/SnRK2.3 in Arabidopsis) are principal positive regulators of ABA signaling (Park et al., 2009; Ma and Blenis, 2009; Nishimura et al., 2009; Santiago et al., 2009; Miyazono et al., 2009; Umezawa et al., 2009) under osmotic stress (Fujii and Zhu, 2009a; Fujita et al., 2009; Umezawa et al., 2009), and induce stress-responsive genes (Furihata et al., 2006; Fujii and Zhu, 2009a; Yoshida et al., 2015a,b). Subclass I SnRK2s (SRK2A/SnRK2.4, SRK2B/SnRK2.10, SRK2G/SnRK2.1, SRK2H/SnRK2.5 and SRK2J/SnRK2.9) on the other hand, are ABA-unresponsive but are osmotic stress-responsive (Boudsocq et al., 2004; Fujii et al., 2011; McLoughlin et al., 2012; Fujita et al., 2013), and furthermore shown to regulate mRNA decay under osmotic and NaCl stress (Soma et al., 2017). As nomenclature of SnRK2s are somewhat complicated, a concise summary is provided in Table 4.1 for quick reference.

Table 4.1: Subclass, nomenclature, ABA and stress response of SnRK2s

	Nomenclature		ABA	Subclass	Associated stresses
SnRK2	A	2.4	unresponsive	I	Salt[3,6], Osmotic[1,3]
	B	2.10	unresponsive	I	Salt[3,6], Osmotic[2,3]
	G	2.1	unresponsive	I	Salt[3], Osmotic[3]
	H	2.5	unresponsive	I	Salt[3], Osmotic[3]
	J	2.9	unresponsive	I	
	C	2.8	weak response	II	Salt[3], Osmotic[3], Drought[4,5]
	F	2.7	weak response	II	Salt[3], Osmotic[3], Drought[5]
	D	2.2	responsive	III	Salt[3], Osmotic[3]
	E	2.6	responsive	III	Salt[3], Osmotic[3]
	I	2.3	responsive	III	Salt[3], Osmotic[3]

1. Mikolajczyk et al. (2000) 2. Yoshida et al. (2002) 3. Boudsocq et al. (2004) 4. Umezawa et al. (2004)
5. Mizoguchi et al. (2010) 6. McLoughlin et al. (2012)

Seeds of *snrk2abgh* and *snrk2dei* were acquired from Kazuko Yamaguchi-Shinozaki (Soma et al., 2017), and the decay and steady state levels of NMD transcripts *SMG7* and *PTB2+* were measured (Figure 28). Variation in decay pattern was observed, however it was not significant, and showed no general trend. Although both transcripts showed no significantly altered decay in either mutants, under both control and 50 mM NaCl treatment (Figure 28A, B, D, E, G, H), a steady state accumulation can be seen in *snrk2dei*, which are categorized under the ABA-responsive subclass III SnRK2s. As this subclass of SnRK2s are known to directly modulate transcription factors (Yoshida et al., 2002; Furihata et al., 2006; Fujii et al., 2007; Fujii and Zhu, 2009a; Nakashima et al., 2009; Canto and Auwerx, 2010; Kulik et al., 2011; Feng et al., 2014; Sakuraba et al., 2015; Tan et al., 2018), increases in transcription levels would be a likely explanation for the accumulation of *SMG7* and *PTB2+* in steady state conditions.

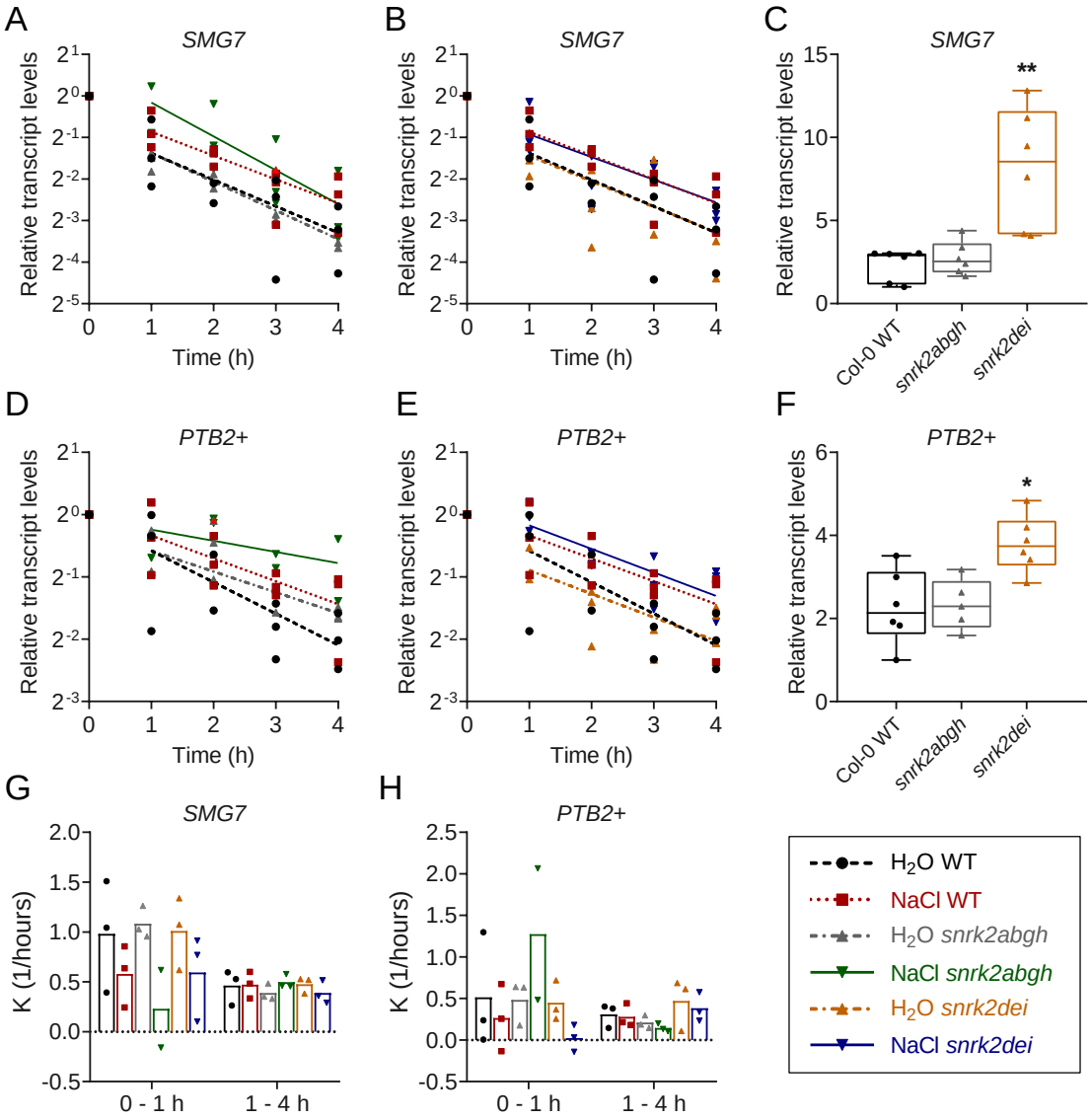

Figure 28: Decay of NMD targets not affected upon NaCl treatment in subclass I and subclass III *snrk2* mutants, but increased steady state levels of NMD targets in ABA-responsive subclass III SnRK2 mutants were observed. (Data collected by Siliya Köster-Hofmann). Decay graphs of NMD targets with or without 50 mM NaCl treatment in *snrk2abgh* quadruple mutants (A, D) and *snrk2dei* triple mutants (B, E). Dots represent individual values ($n = 3$), line represent least squares non-linear regression. Steady state levels of NMD targets in *snrk2abgh* and *snrk2dei* (C, F). Box plot represents first quartile, median, third quartile, whiskers represent min and max. Dots represent individual values ($n = 6$), *, $P < 0.05$; **, $P < 0.01$, Mann-Whitney rank test comparing mutants to WT. (G, H) Rate constants of NMD transcripts with or without NaCl treatment, corresponding to (A, B, D, E). Dots represent individual values, column represents mean.

4.8 Extracellular Reactive Oxygen Species may play a role in NMD inhibition under NaCl

4.8.1 Extracellular H_2O_2 stabilizes NMD targets comparably to NaCl

Despite that ROS, such as O_2^{*-} and H_2O_2, are not only toxic by-products of aerobic metabolism, but are also generated for signaling. ROS signaling is a major responder to many types of stresses, and in the case of salt stress, there is a dramatic increase of ROS such as H_2O_2 (Vaidyanathan et al., 2003; Valderrama et al., 2006; Leshem et al., 2007; Miller et al., 2010; Jiang et al., 2013; Nath et al., 2018). To determine if ROS can also alter the stability of NMD target transcripts, extracellular H_2O_2 was applied in parallel with NaCl. 1 mM and 10 mM of H_2O_2 were tested, and the decay of NMD targets *SMG7* and *PTB2+* were analysed. Both transcripts were stabilized to a greater degree upon 10 mM compared to 1 mM H_2O_2, showing a first indication of a dose-response relationship between extracellular H_2O_2 and NMD inhibition (Figure H.1). Another repeat was performed with only 10 mM H_2O_2, and both NMD target transcripts showed stabilization to a comparable level to NaCl (Figure 29, H.2). In the 0–1 h phase, decay rate constants show significantly decreased decay compared to H_2O control. This shows decreased decay of NMD target transcripts when H_2O_2 was applied extracellularly, and indicates ROS could either act as an intermediate or separate pathway for NMD target stabilization under NaCl.

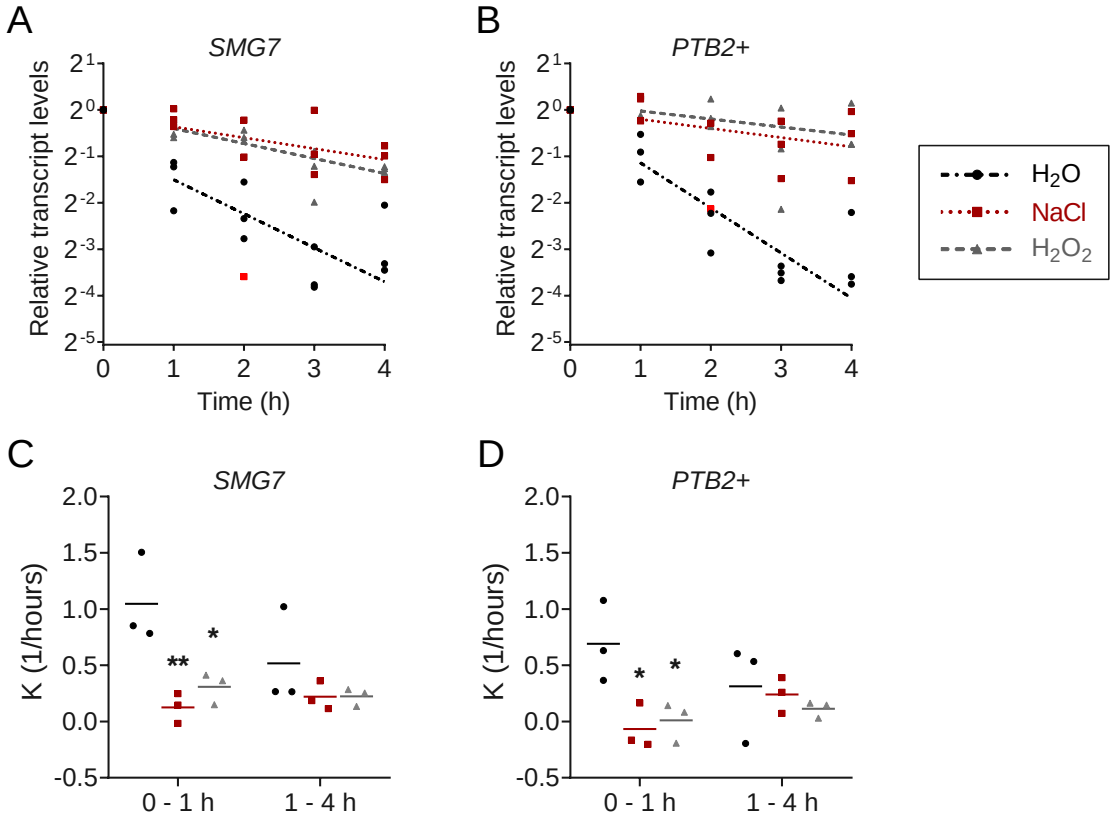

Figure 29: NMD target transcripts stabilize upon H_2O_2. Decay graphs (A–B) and rate constants (C–D) of 7-d-old *A. thaliana* under 100 mM NaCl or 10 mM H_2O_2 treatment. Dots represent individual values, lines represent least squared non-linear regression (A–B) and mean (C–D). *, $P < 0.05$; **, $P < 0.01$, unpaired t-tests performed against negative control H_2O.

4.8.2 ROS generated at the chloroplast is not involved in NMD

Paraquat (or methylviologen; N,N'-dimethyl-4,4'-bipyridinium dichloride) is a rapid-acting, non-selective herbicide (Haley, 1979), and is widely used as a source of O_2^{*-} radicals in the study of photosynthesis (Kurepa et al., 1998). Paraquat is a redox-cycle reagent, accepts electrons from PSI and donates them to O_2, producing O_2^{*-}, inducing membrane damage and cell death (Dodge, 1971; Haley, 1979; Babbs et al., 1989; Fujii et al., 1990; Suntres, 2002; Bonneh-Barkay et al., 2005; Han et al., 2014). O_2^{*-} has a lifetime in the range of milliseconds, and is quickly dismutated by SODs to H_2O_2, staying close to the site of generation. H_2O_2 has a longer lifetime, from milliseconds to seconds (Waszczak et al., 2018), and thus can diffuse from the generation site to fulfil a signaling function. Decay of NMD target transcripts *SMG7* and *RS2Z33+* were measured with or without paraquat, and treated samples showed no changes compared to mock (Figure 30). Mock for this experiment was equimolar sodium phosphate buffer (SPB) pH 7.0 in which the paraquat stock was solved in. This indicates O_2^{*-} stress or H_2O_2 signaling generated from the chloroplast is not involved in NMD inhibition. However, a control to test for paraquat functioning is

missing, and should be performed.

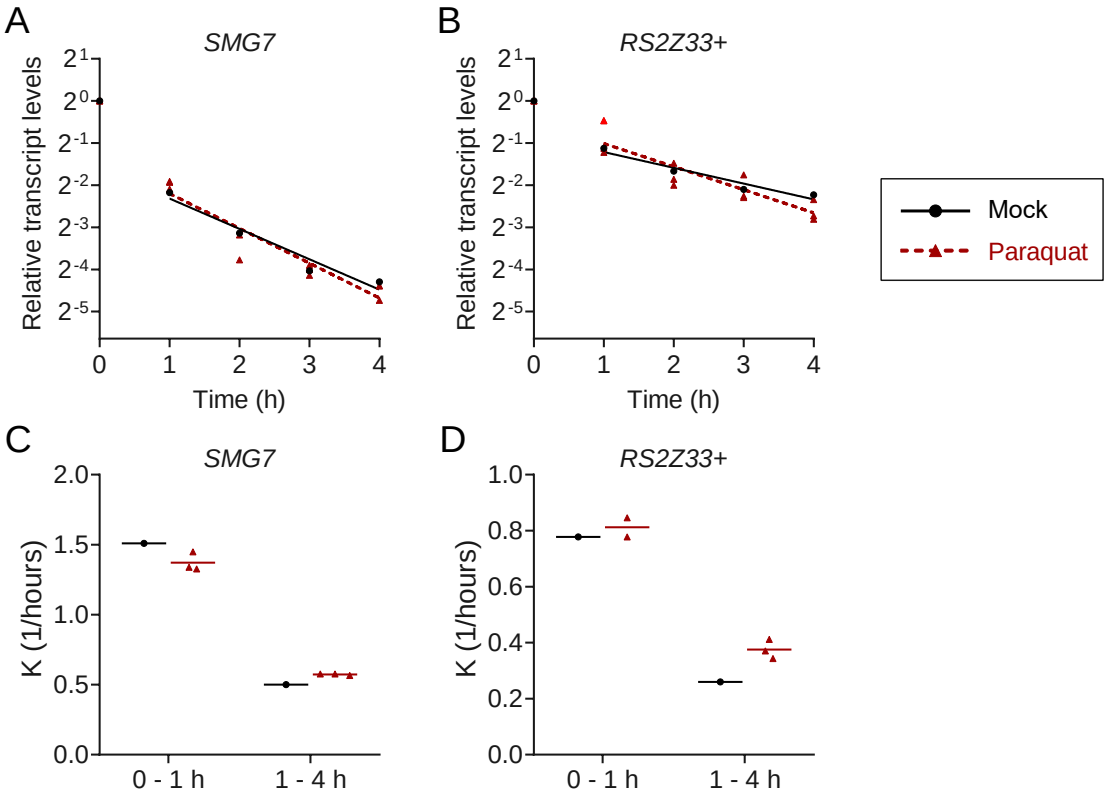

Figure 30: NMD targets not affected by paraquat. Decay graphs (A–B) and rate constants (C–D) treated with 7 mM paraquat ($n = 3$) or under mock ($n = 1$) as control. Paraquat stock was solved in SPB pH 7.0, mock was equimolar SPB in H_2O. Dots represent individual values, lines represent least squares non-linear regression (A–B) and mean (C–D).

4.8.3 NMD targets are not destabilized in *rbohd/f* or *rbohc* mutants under salt exposure

In order to determine whether ROS acts as a signaling pathway for NMD, as H_2O_2 is shown to stabilize NMD targets (Figure 29, Figure H.1), NMD targets were observed with and without NaCl under altered ROS metabolism. This was approached in two ways: through applying ROS scavengers (Supplement H), or performing the half-life assay in mutants impaired in ROS production. Data obtained from the ROS scavenger experiments were rather preliminary due to the limitations of the control sets (Supplement H). Therefore, a more stringent way of testing NMD under salt stress in the absence of ROS would be to directly employ mutants deficient in ROS production to begin with.

One of the enzymatic systems that can actively produce ROS are NOXs. NOX homologues in *A. thaliana* comprise the RBOH protein family. The 10 NOX homologues *RbohA-J*, exhibit different patterns of expression in response to environmental factors (Marino et al., 2012; Kurusu et al., 2015). RBOHD and RBOHF are calcium-

dependent NOX that generates O_2^{*-} (Song et al., 2006) and has been shown to be required for ROS accumulation in plant defence response (Torres et al., 2002), ROS-dependent ABA signaling (Kwak et al., 2003), and are known to be inhibited by diphenyleneiodonium (DPI) (Desikan et al., 2006; Fagard et al., 2007). Expression of *RBOHD* and *RBOHF* are highly induced under salinity stress (Ma et al., 2012), and an *RBOHF* mutant showed strong Na^+ hypersensitivity (Jiang et al., 2012). RBOHC is also a calcium-dependent NOX, and is required for H_2O_2 production under K^+ deficiency (Shin and Schachtman, 2004), affects stress-induced ROS generation, and regulates root hair elongation in a Ca^{2+}-dependent manner (Foreman et al., 2003; Takeda et al., 2008; GB et al., 2009; Kurusu et al., 2015).

Seeds of *rbohd/f* and *rbohc* were acquired from Miguel Torres, and a luminol-based oxidative burst assays were performed (Figure H.6, Wall (2017)), where ROS is massively produced after the detection of pathogen-associated molecular pattern (PAMP)s by receptors such as FLAGELLIN-SENSING 2 (FLS2) (Doke, 1985; Bradley et al., 1992; Jabs et al., 1997). Wall (2017) confirmed *rbohd/f* remains unresponsive to flagellin peptide flg22 (flg22) (Figure H.6A), while a weak response is triggered in *rbohc* (Figure H.6B). Therefore, the half-life assay was performed with 50 mM and 100 mM NaCl on *rbohd/f* double mutants, and NMD target transcripts *SMG7* and *PTB2+* were analyzed (Figure 31). No significant NMD target accumulation were found comparing steady state levels of WT and *rbohd/f* (Figure 31G–H). Under control conditions, *SMG7* show no distinct trends comparing the *rbohd/f* mutant with WT (Figure 31A, C, E). However, *PTB2+* shows significant faster decay within the 1st hour, but not from 1–4 h (Figure 31B, D, F). This shows a similar pattern of *PTB2+* in Section 4.5, where a rapid degradation is seen during the 1st hour followed by a slowed decay (Figure 18A, D), which could be explained by altered AS that affect two separate collections of *PTB2+* mRNAs that undergo alternative degradation pathways. With 100 mM NaCl treatment, the NMD targets were almost completely stabilized in both WT and *rbohd/f* (Figure 31C–F), while with 50 mM of NaCl, both transcripts display slightly faster decay within the 1st hour, albeit not statistically significant (Figure 31A–B, E–F). Due to higher discernibility, 50 mM NaCl was used to proceed with *rbohd/f* and *rbohc* mutants. Steady state levels were analysed in *rbohd/f* and *rbohc*, and no significant accumulation was found in both mutants compared to WT (Figure 32G–H). Results of *rbohd/f* once again did not show significant difference when comparing to WT, under both control or NaCl conditions (Figure 32A–B, E–F). In *rbohc*, however, both under control conditions or NaCl, a faster decay was found within the 1st hour in *SMG7* (Figure 32C, E). This pattern was not present in *PTB2+* (Figure 32D, F). There seems to be a general trend in the 1st hour for *SMG7* in both *rboh* mutants, where under control conditions a faster decay was seen when compared to WT, but this effect was not sustained

when NaCl was added. This could be caused by interference of actin by the lack of RBOH (Eggenberger et al., 2017), as oxidative stress can cause the glutathionylation of a critical cysteine residue (C374) in *A. thaliana* and disrupt actin remodeling (Dixon et al., 2005). Under normal conditions, RBOH provides a base supply of O_2^{*-} that is available for signaling triggered by endogenous auxin. In combination with phospholipase D (PLD) activity, this results in a homeostasis of capped and uncapped cortical actin filaments with dynamic turnover (Chang et al., 2015). Therefore, a disruption in RBOH, could very well also affect actin dynamics in the cell. However, the relationship between actin and ROS has not been shown on a transcript level, and the possible influence of altered RBOH production on actin is pure speculation at this point. With everything combined, it is still open-ended if or how directly ROS influences NMD activity under salt stress, nevertheless ROS may play a minor role or act on a different pathway that influences NMD target transcripts.

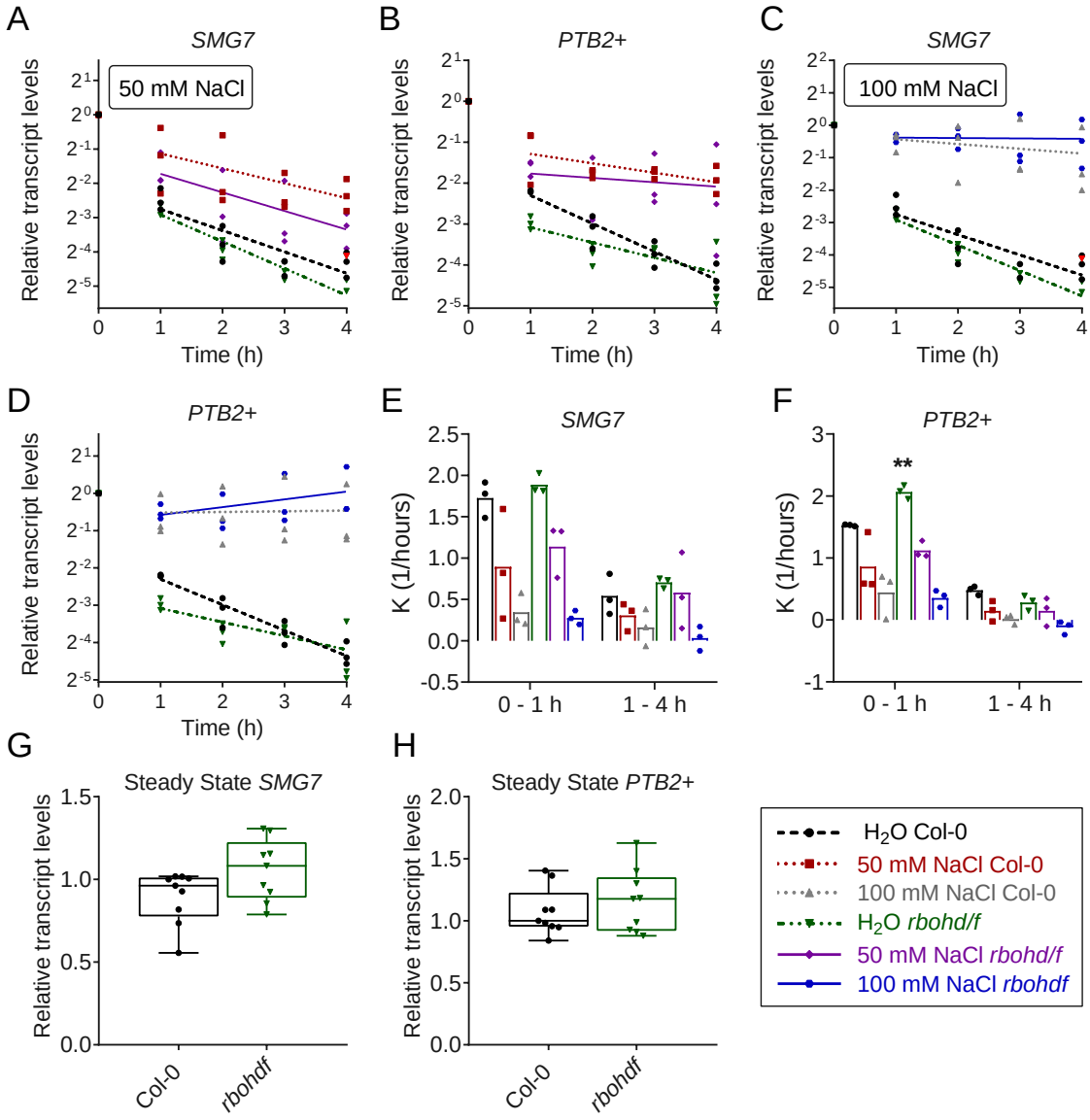

Figure 31: NMD targets under NaCl stress are not significantly destabilized in *rbohd/f*. Decay graphs of NMD targets under 50 mM (A–B) and 100 mM NaCl (C–D) in Col-0 WT and *rbohd/f* mutants ($n = 3$). Rate constants in (E) corresponds to (A, C), and (F) corresponds to (B, D). Steady state levels (G–H) of Col-0 WT and *rbohd/f* mutants ($n = 9$), box plot represents first quartile, median, third quartile, whiskers represent min and max. Dots represent individual values, lines in (A–D) represent least square non-linear regression, columns in (E–F) represent mean.

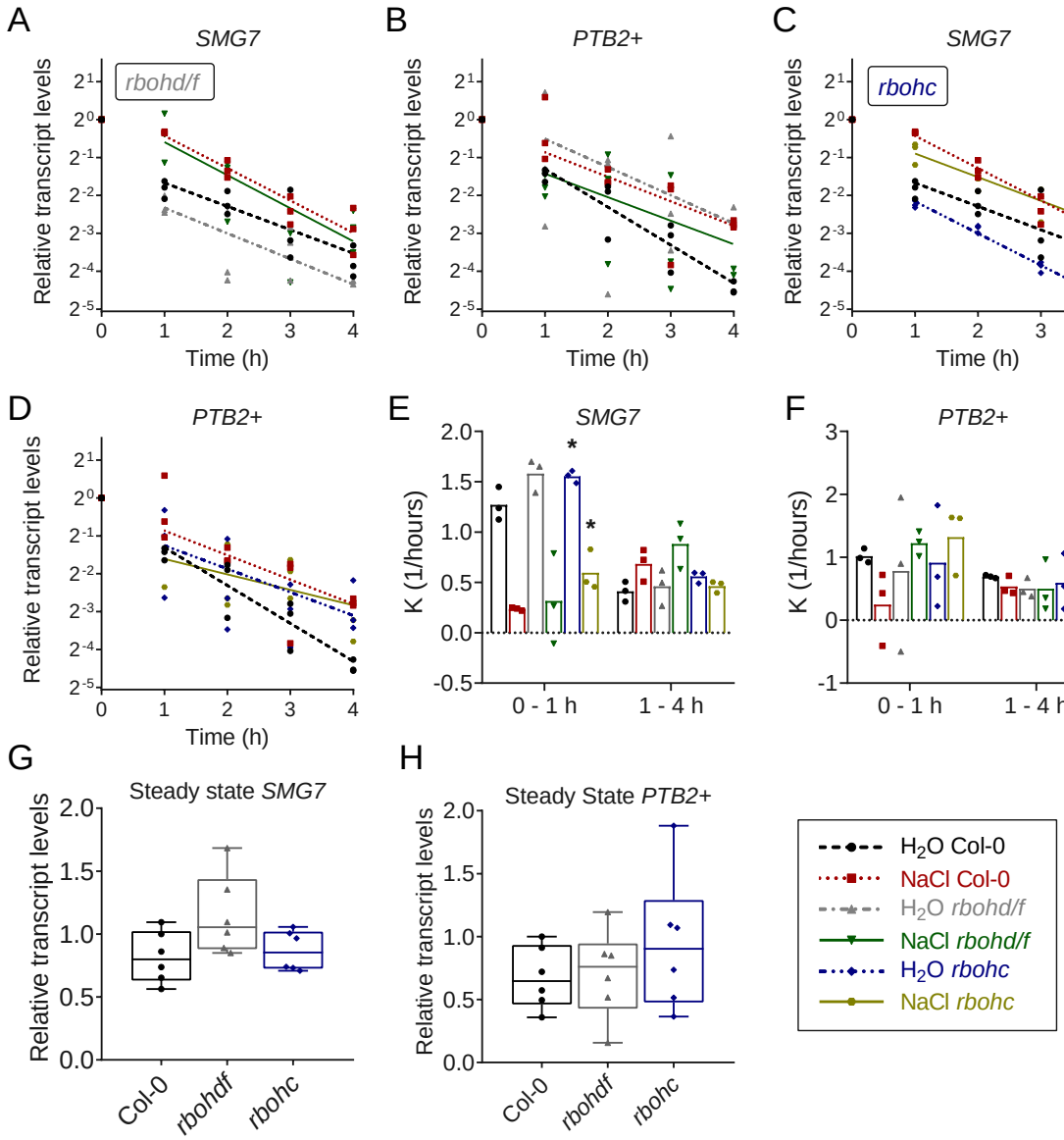

Figure 32: NMD target transcript *SMG7* shows faster decay in *rbohc* mutants, in both H_2O and NaCl treatment. Decay graphs of *rbohd/f* ($n = 3$) (A–B) or *rbohc* ($n = 3$) (C–D) under 50 mM NaCl. Rate constants of *SMG7* (E) and *PTB2+* (F) corresponding to graphs (A, C) and (B, D) respectively. Steady state levels of *SMG7* (G) and *PTB2+* (H) ($n = 9$). Dots represent individual values, lines in (A–D) represent least squared non-linear regression, columns in (E–F) represent mean. Lines in box plot (G–H) represents first quartile, median, third quartile, whiskers represent min and max.

4.9 NMD inhibition by NaCl is rapid and reversible

To understand whether the inhibition of NMD is caused by a signaling cascade triggered by NaCl, or if sustained NaCl treatment was needed, a salt spike experiment was performed. Two NMD target transcripts *SMG7* and *PTB2+* were analyzed, with slight modifications to the half life assay. Before cordycepin treatment, 7-d-old *A. thaliana* were "spiked" with 100 mM of NaCl for 5, 10, or 60 minutes. The negative control remained in H_2O, while the positive control remained under constant salt treatment (Figure 33A). NMD transcripts of all "spiked" samples show no stabilization compared to the negative control (Figure 33B, D, E, G), while NMD transcripts remains stabilized in the positive control. Steady state levels show strong accumulation of NMD targets after 60 min of incubation, with no prominent changes after 5 or 10 min of incubation, except for *SMG7* showing slight accumulation after 5 min, which could be due to statistical noise (Figure 33C, F). This shows that the NMD inhibition must be under continuous NaCl stress, and is not triggered and sustained by a signaling cascade.

As the salt spike experiment indicated, constant NaCl stress is required for NMD inhibition. In order to have a closer look at how quickly NMD inhibition can be activated or reversed, a salt timing experiment was performed. 7-d-old *A. thaliana* seedlings were incubated in H_2O or 100 mM NaCl, and switched into or out of NaCl treatment 2 h after cordycepin was added. One set was pretreated for 60 min to see if there are any priming effects, since previous reports indicate improved salt tolerance after a period of priming (Sivritepe et al., 2003; Yan et al., 2015). The negative control remained in H_2O, and the positive control remained under 100 mM NaCl treatment (Figure 34A). NMD targets *SMG7* and *PTB2+* were analyzed. Starting from time window 1–2 h, samples that were under NaCl treatment remain stable and have low degradation rates (Figure 34B–E, maroon squares and green inverted triangle), while samples without salt treatment showed faster degradation (Figure 34B–E, black circles, grey triangles and blue diamonds). After switching samples into or out of salt treatment, in the time window 2–4 h, the samples under NaCl treatment show similar stability (Figure 34B–E, maroon squares, grey triangles, blue diamonds), while samples that were moved out of salt treatment regained degradation, on a comparable level to the negative control (Figure 34B–E, black circles, green inverted triangles). In both time windows — before or after the switch — the 60 min pre-treated samples (Figure 34 blue diamonds) showed degradation when in H_2O, and stabilization when under NaCl stress, indicating that pre-treatment has no substantial priming effect on NMD inhibition. Based on the data from both the salt spike (Figure 33) and salt timing (Figure 34) experiment, shows NaCl stress inhibits NMD in a fast and reversible manner.

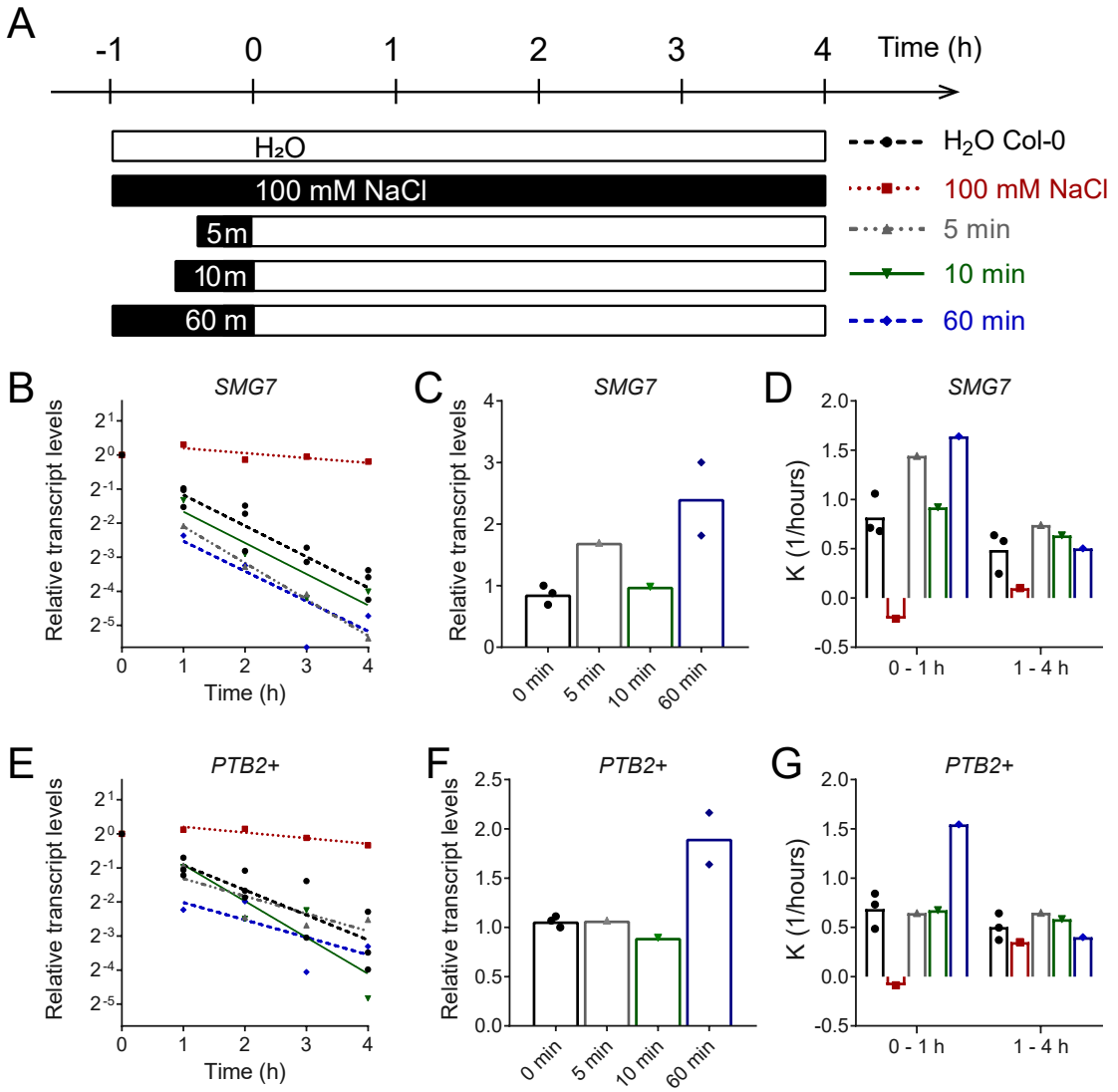

Figure 33: Sustained NMD inhibition requires constant salt environment. (A) Experimental scheme. Time at 0 h represents the time point when cordycepin was added. Black represents 100 mM NaCl treatment, white represents H_2O control. 7-d-old *A. thaliana* seedlings were pre-treated with 100 mM NaCl for 5, 10 or 60 min before transcription was inhibited. The negative control sample was not treated by NaCl, and the positive control was under constant NaCl treatment. Decay graphs (B, E), steady state levels (measured at $t = 0$ h) (C, F) and rate constants (D, G) of NMD targets under negative ($n = 3$) or positive ($n = 1$) control conditions, or pretreated with 100 mM NaCl for 5 min ($n = 1$), 10 min ($n = 1$) or 60 min ($n = 1$). Dots represent individual values, lines in (B, E) represent least squares non-linear regression. Columns in (C, D, F, G) represent mean.

4.9.1 Phosphorylation likely plays a role in NMD inhibition under NaCl stress

Given the quick reaction time and reversibility of NMD inhibition, it is probable that phosphorylation signaling is involved. Therefore, a cell-permeable kinase inhibitor from *Nonomuraea longicatena* (K252a) (Kase et al., 1987; Hashimoto et al., 1991; Raychaudhuri et al., 2004; Pan et al., 2007) was used. The decay of NMD

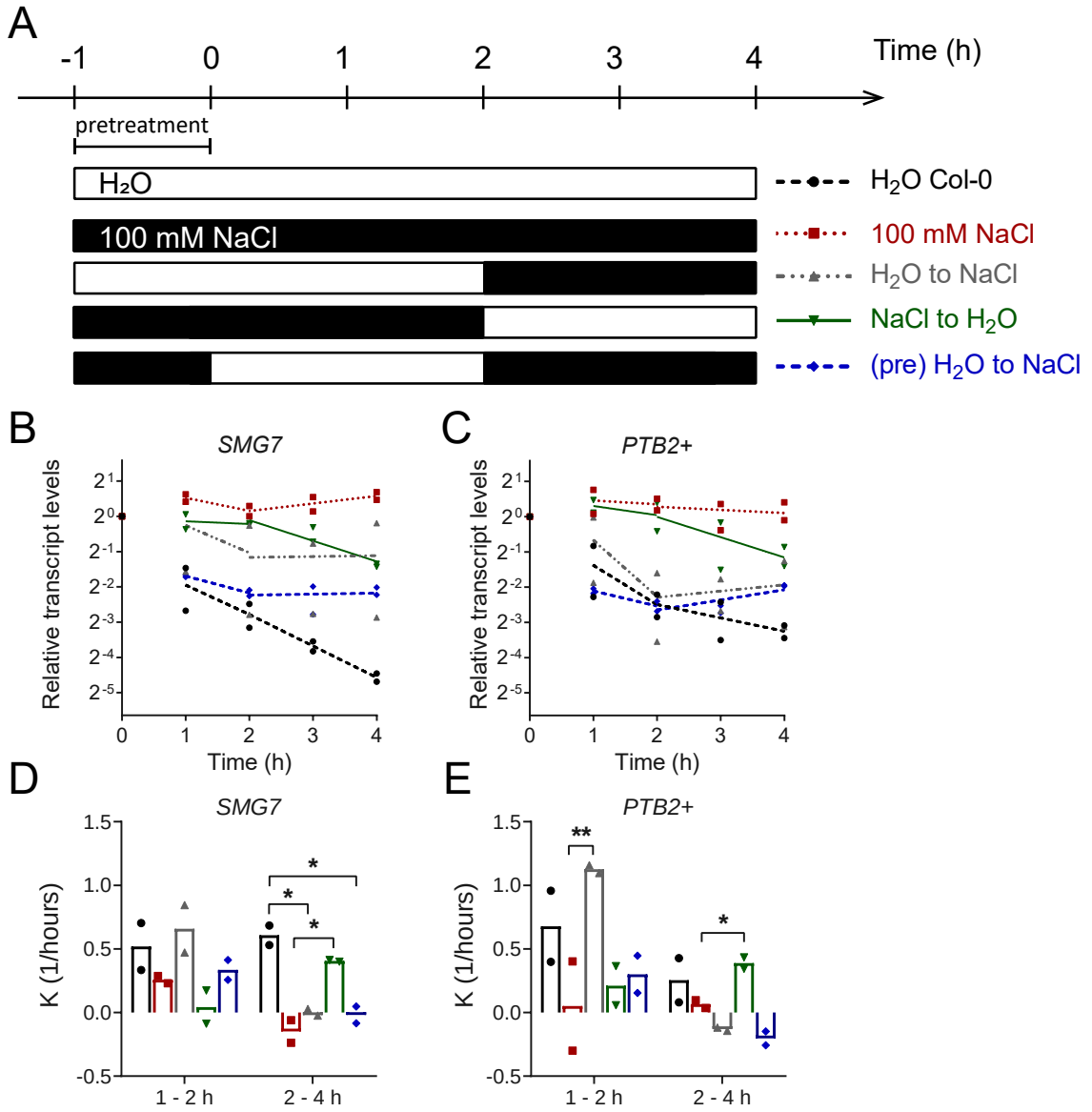

Figure 34: NMD inhibition responds in a rapid and reversible manner. (Data collection and analysis were combined efforts of Caroline Wall and myself.) (A) Experimental scheme. Time at 0 h represents the timepoint when cordycepin was added. Black represents 100 mM NaCl treatment, white represents H_2O treatment. Samples ($n = 2$) were switched into or out of 100 mM NaCl at the 2 h timepoint, indicated by the black or white bars. Decay graphs (B–C) and rate constants (D–E) are separately calculated and plotted from 1–2 h, and 2–4 h. Dots in (B–C) represent individual values, lines represent least squares non-linear regression. Dots and columns in (D–E) represent a single K value corresponding to the decay graphs. *, $P < 0.05$; **, $P < 0.01$, by unpaired t-test against H_2O negative control and 100 mM NaCl positive control.

transcripts *SMG7* and *PTB2+* were measured with and without K252a treatment, under control or NaCl stress conditions. The K252a stock was dissolved in DMSO, therefore the mock control for this experiment is equimolar DMSO in H_2O. During the early phase of decay from 0–1 h, K252a shows a trend of stabilizing *SMG7* under

both mock and NaCl conditions, which becomes prominent in the decay phase from 1–4 h (Figure 35A, C). For *PTB2+* in decay phase 0–1 h, K252a is seen to reverse the stabilization caused by NaCl, however this occurrence disappears during phase 1–4 h, and an opposite trend, where enhancement of transcript stability by K252a under salt is seen instead (Figure 35B, D). On a similar vein, a phosphatase inhibitor was also used to examine phosphorylation signaling in NaCl-mediated NMD inhibition. Okadiac acid (OA) is a eukaryotic protein phosphatase inhibitor, known to remove phosphate from serine and threonine residues (Cohen et al., 1990). Like K252a, samples were treated with OA under mock or NaCl conditions, and the decay of NMD target transcripts *SMG7* and *PTB2+* were measured. For *SMG7*, there were no obvious trends compared between the samples with or without OA, in the early decay phase 0–1 h (Figure 36A, C). For *PTB2+*, however, a stronger decay was shown in OA applied samples, although this was not seen when salt was applied (Figure 36B, D). During the 1–4 h phase, OA is shown to inhibit the decay of both NMD targets, while comparing mock and OA samples, but this trend disappears again when a low concentration of NaCl is applied (Figure 36). There are similarities and differences of NMD target transcript behaviour under K252a or OA, and the treatment of kinase inhibitors and phosphatase inhibitors do not derive to opposite results. First, when looking at *SMG7*, a NMD target not subject to alternative splicing, seems to have consistent behaviour between K252a and OA in the later phase of decay. *PTB2+* on the other hand, is a product of alternative splicing. During the early phase both K252a and OA seems to stabilize *PTB2+*, and upon salt exposure, K252a is seen to exaggerate the decay, while there is no difference in stability under OA. In the later phase with *SMG7*, K252a and OA behave similarly, stabilizing whether salt stress is present or not. However, this is not the case with *PTB2+*, where stability remains nearly unchanged. This indicates that phosphorylation could be playing a role in NMD targets affected by alternative splicing under NaCl stress conditions. This result could also be due to the wide spectrum of targets K252a and OA affect. For a more definitive description, specific kinase or phosphatase inhibitors should be employed, for example, OA has no effect on the Mg- or Mn-dependent protein phosphatase family, or tyrosine phosphatases. However, OA has different phosphatase inhibition profiles, where the half maximal inhibitory concentration (IC_{50}) for PP2A ranges from 0.1 – 100 nM, while for PP2C the $IC_{50} > 10,000$ nM (Hescheler et al., 1988; Haystead et al., 1989; Holmes et al., 1990; Honkanen et al., 1990; Huang and Honkanen, 1998; Prickett and Brautigan, 2006; Swingle et al., 2007). By employing a combination of different types and concentrations of various kinase or phosphatase, one can narrow down the scope of which processes are involved.

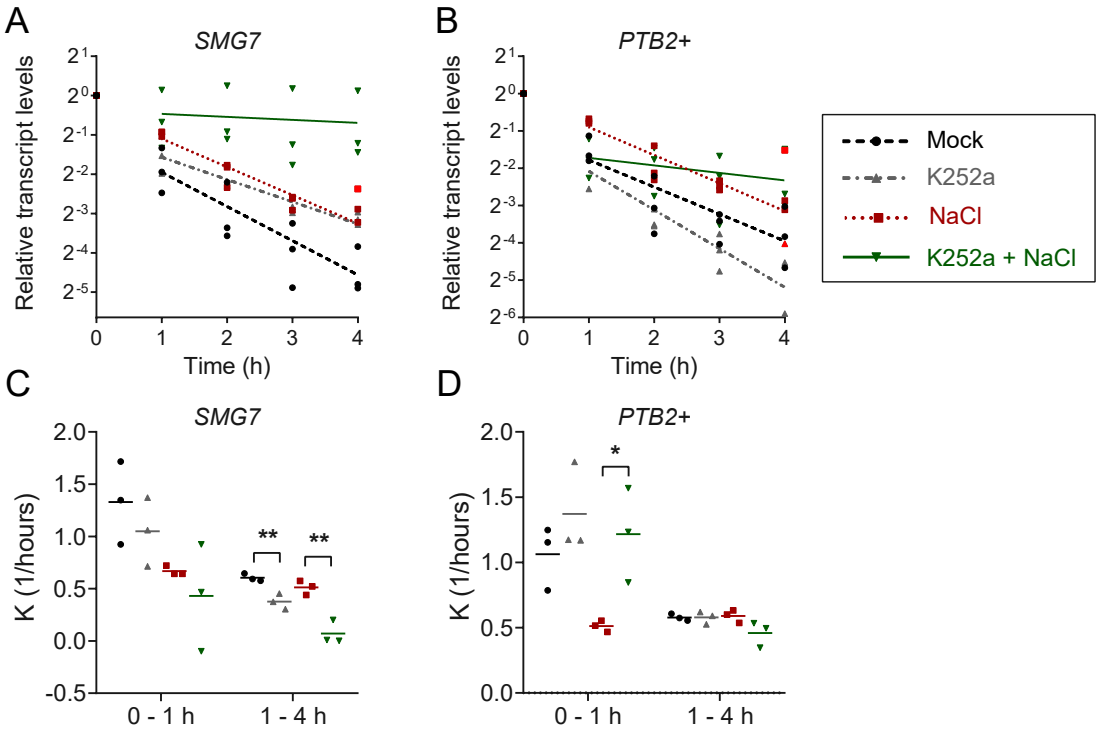

Figure 35: Kinase inhibitor K252a stabilizes NMD targets under both control and NaCl treatment. Decay graphs (A–B) and rate constants (C–D) of 7-d-old *A. thaliana* seedlings treated with 4 μM K252a with or without 50 mM NaCl, with mock as negative control, and 50 mM NaCl treatment as positive control ($n = 3$). Dots represent individual values, lines in (A–B) represent least squared non-linear regression, lines in (C–D) represent mean. Unpaired t-tests were performed against their respective controls, i.e. K252a is compared to mock, and K252a + 50 mM NaCl is compared to 50 mM NaCl treatment. *, $P < 0.05$; **, $P < 0.01$, by unpaired t-test comparing K252a to Mock, under control or NaCl conditions. Outliers determined through ROUT (Motulsky and Brown, 2006) ($Q = 5\,\%$), and are plotted in red.

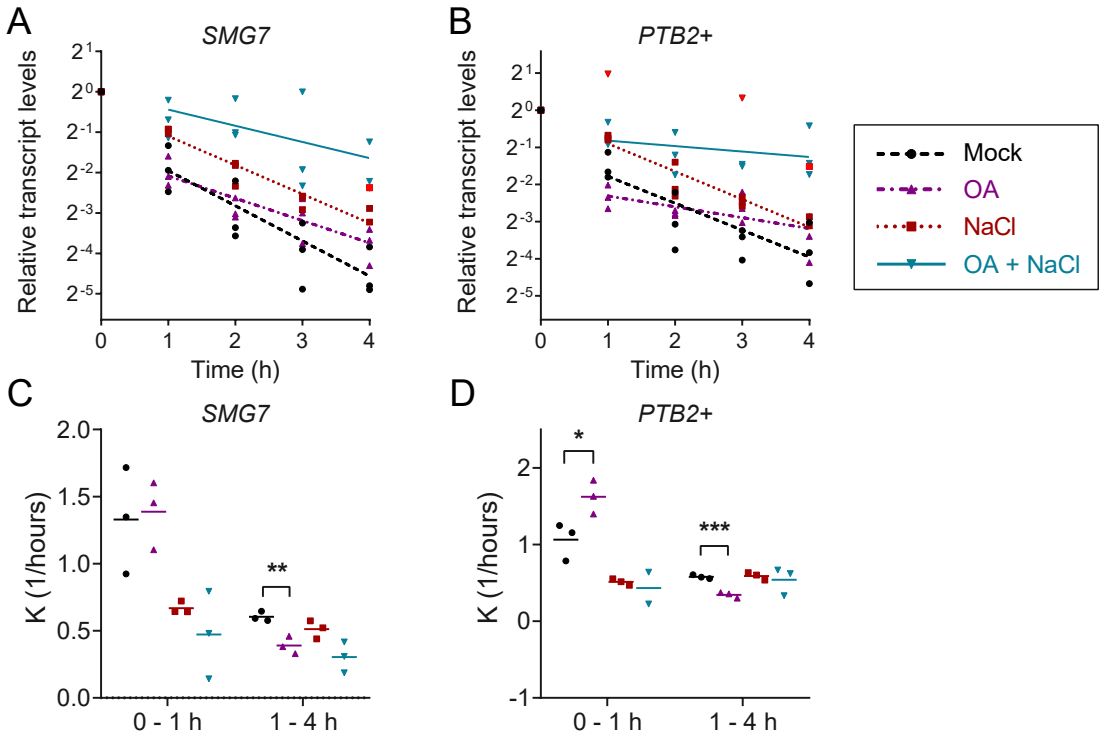

Figure 36: Phosphatase inhibitor Okadaic Acid (OA) stabilizes NMD targets under both control and NaCl treatment. Decay graphs (A–B) and rate constants (C–D) of 7-d-old *A. thaliana* seedlings treated with 1 μM OA with or without 50 mM NaCl, with mock as negative control, and 50 mM NaCl treatment as positive control($n = 3$). Dots represent individual values, lines in (A–B) represent least squared non-linear regression, lines in (C–D) represent mean. Unpaired t-tests were performed against their respective controls, i.e. OA is compared to mock, and OA+50 mM NaCl is compared to 50 mM NaCl treatment. Outliers determined through ROUT ($Q = 5\,\%$), and are plotted in red.

4.10 Increases in cytosolic calcium causes NMD target stabilization, blocked Ca^{2+} channels may increase NMD sensitivity to NaCl

Apart from being an essential plant nutrient (Sanders et al., 2002; White and Broadley, 2003), Ca^{2+} is one of the most important secondary messengers in response to stimuli (Liese and Romeis, 2013; Valmonte et al., 2014; Simeunovic et al., 2016). Under abiotic stress, cytosolic calcium ($[Ca^{2+}]_{cyt}$) rises rapidly and dramatically in plants, almost without exception (White and Broadley, 2003). Both ROS (discussed in Section 4.8) and Na^+ stress are known to trigger $[Ca^{2+}]_{cyt}$ influx (Pei et al., 2000; Guan et al., 2013a), and affect a plethora of downstream processes (Figure 37). Recently, an Arabidopsis CPK, AtCPK1, was shown to enhance salt or drought tolerance, possibly through regulation of ROS signaling (Huang et al., 2018). It has even been shown that plants lacking nuclear-localized calcium-binding protein SHORT ROOT IN SALT MEDIUM 1 (RSA1) are hypersensitive to NaCl, but not general osmotic stress (Guan et al., 2013a), in line with the finding that NMD inhibition through NaCl is at least partially ionic stress specific (Section 4.3). In humans, intracellular calcium have been found to regulate NMD (Nickless et al., 2014). However, the role of Ca^{2+} signaling in the context of NMD inhibition under NaCl in plants have not yet been scrutinized.

Considering Ca^{2+} is such an important signaling component, plant have a variety of ways to regulate Ca^{2+} and maintain homeostasis. This means $[Ca^{2+}]_{cyt}$ levels cannot be increased by simply adding extracellular Ca^{2+}, for example $CaCl_2$. Therefore, to avoid using NaCl or H_2O_2 (in Section 4.8, H_2O_2 was shown to stabilize NMD target transcripts), extracellular ATP was used in order to trigger a Ca^{2+} spike (Song et al., 2006; Shang et al., 2009). The decay of two NMD target transcripts *SMG7* and *PTB2+* were analysed with 1 mM ATP, using H_2O as negative control and 100 mM NaCl as positive control. Both NMD targets were stabilized to a comparable degree with ATP treatment and NaCl (Figure 38, I.1). This stabilization has striking similarities to the stabilization seen with 10 mM H_2O_2 (Figure 29, H.2). Tied in with the results of Section 4.7 and Section 4.8.1 — where NMD targets were unaffected by ABA, but stabilized by H_2O_2 — it can be extrapolated that the ROS produced by ABA stimulation is not enough to cause NMD target stabilization, but rather the downstream $[Ca^{2+}]_{cyt}$ influx caused by extracellular H_2O_2 could be the main reason for NMD inhibition.

To further investigate the role of Ca^{2+} signaling in NMD inhibition under NaCl, a calcium channel blocker was employed. The Ca^{2+} channel blocker lanthanum (III) chloride ($LaCl_3$) has been shown to inhibit the transient elevation of $[Ca^{2+}]_{cyt}$ triggered by H_2O_2 in *Nicotiana tabacum* (Price et al., 1994). Rentel and Knight (2004)

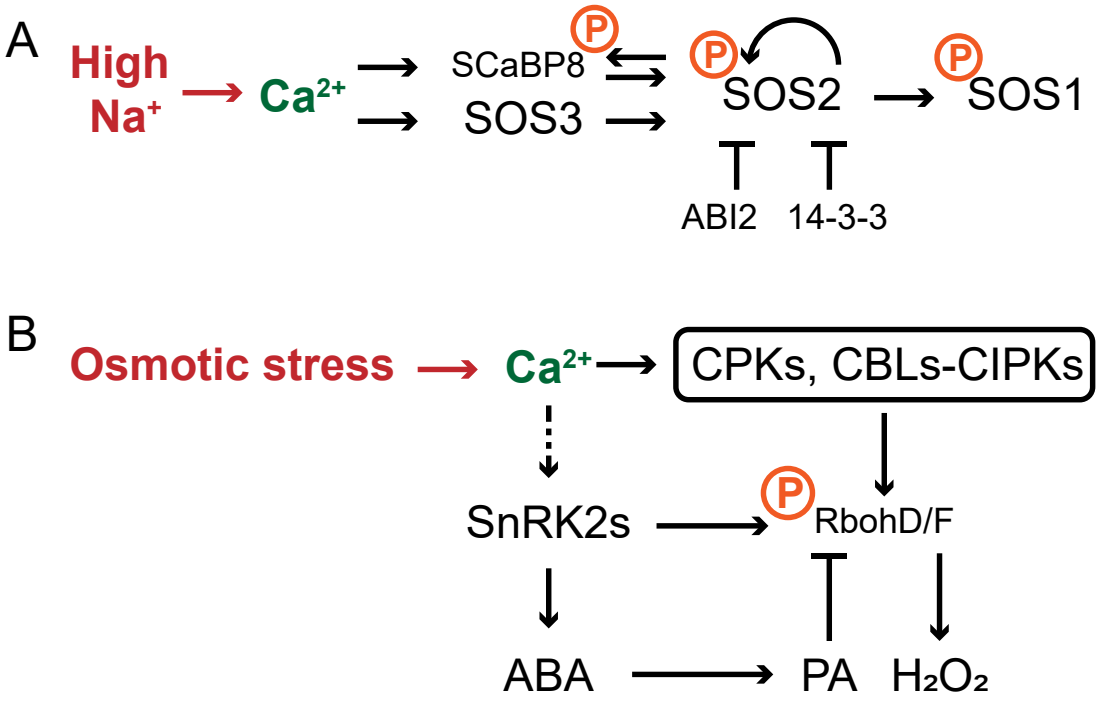

Figure 37: Simplified stress-triggered Ca^{2+} signaling modules. Ionic stress by Na^+ (A) triggers the SOS signaling pathway. Calcium binding proteins SOS3 and SCaBP8 (also known as CBL10) activate the protein kinase SOS2. SOS2 phosphorylates itself (Fujii and Zhu, 2009b), SCaBP8 (Lin et al., 2009b), and SOS1, an Na^+/H^+ antiporter (Qiu et al., 2002; Quintero et al., 2002). Osmotic stress (B) may activate CPKs and CBLs–CIPKs, which activates SnRK2s (Section 4.7.1) that leads to ABA accumulation (Section 4.7). Activated SnRK2s phosphorylate RbohD/F, and ABA induces second messengers phosphatidic acid (PA) which regulates proteins like Rbohs. Arrows indicate activation, bars indicate inhibition, dashed lines indicate postulated regulation. The orange P in a circle denotes phosphorylation. Scheme adapted from Kulik et al. (2011); Zhu (2016).

have found that H_2O_2 trigger a biphasic $[Ca^{2+}]_{cyt}$ influx in *A. thaliana* seedlings. A quick, rapid, early phase located in the cotyledons, leaves and hypocotyl, and a prolonged later phase located exclusively in the lower root sections. These two peaks are independent of each other, and $LaCl_3$ was able to inhibit the early peak, with variable results in the second peak, but was mainly able to delay and decrease the magnitude. The decay of two NMD targets, *SMG7* and *PTB2+* were analyzed in the presence of $LaCl_3$ with or without NaCl. Under $LaCl_3$ treatment alone, the decay patterns from 1–4 h in the NMD targets show similarities to NaCl treatment (Figure I.2), indicating blocked Ca^{2+} channels alone may already inhibit NMD. When NaCl is added, both transcripts are even more so stabilized (Figure I.2), indicating that blocked Ca^{2+} may enhance NaCl sensitivity of NMD in *A. thaliana*. For an even closer look at the ties between NaCl sensitivity and calcium signaling, the SOS pathway is examined. The SOS pathway is a calcium-dependent protein kinase

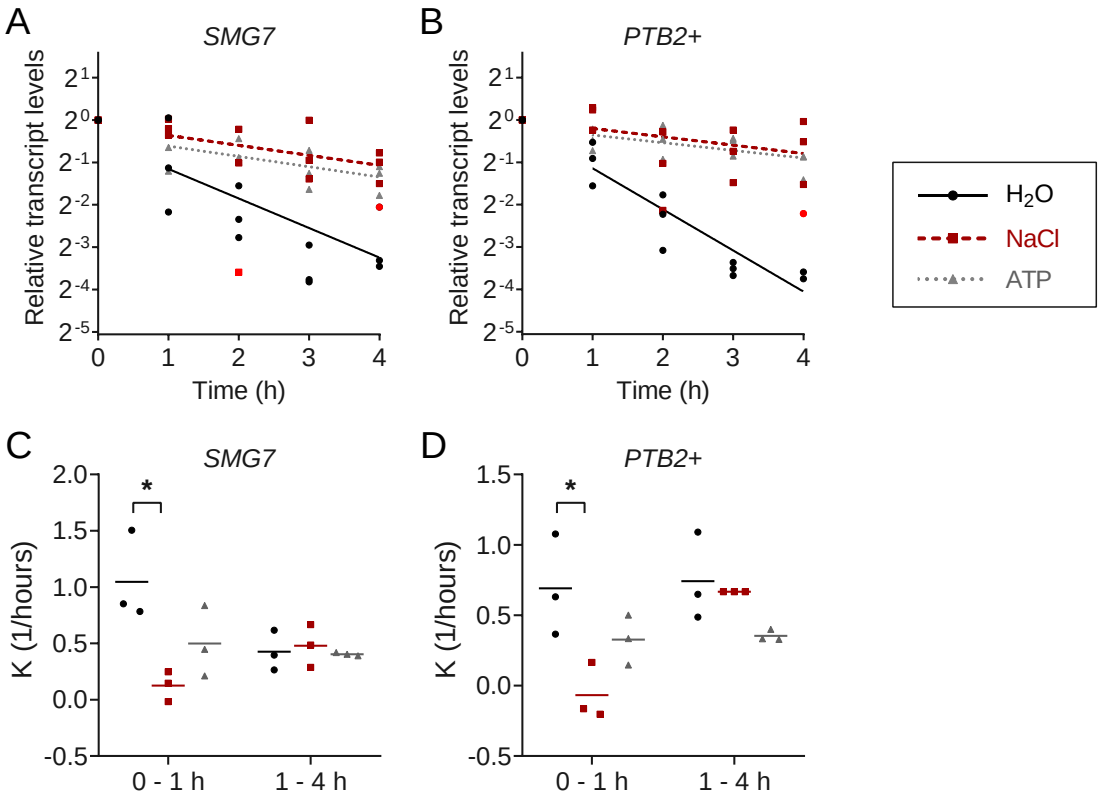

Figure 38: NMD target transcripts stabilized upon ATP treatment, to a comparable level with NaCl. Decay graphs (A–B) and rate constants (C–D) of 7-d-old liquid grown *A. thaliana* seedlings treated with H_2O, 100 mM NaCl, or 1 mM of ATP ($n = 3$). Dots represent individual values, lines in (A–B) represent least squared non-linear regression, lines in (C–D) represent mean. *, $P < 0.05$, unpaired t-tests were performed against their respective controls. Outliers determined through ROUT ($Q = 1\,\%$), and are plotted in red.

pathway for salt stress signaling and Na^+ tolerance (Zhu, 2002), and is further discussed in Section 4.11.

4.11 NMD targets are hyperstabilized in *sos1-1* and *sos2-2* mutants under NaCl treatment, but not via inhibition of dephosphorylation of UPF1

4.11.1 NMD targets are hyperstabilized in *sos1-1*, *sos2-2*, but not *sos3-1*

A general signal transduction starts with signal perception by sensors, followed by a Ca^{2+} surge, along with production of other secondary messengers like ROS or ABA, which could also regulate signal transduction independently. These signaling components may feedback and trigger iterations of Ca^{2+} increase, which initiates a protein phosphorylation cascade, and in turn activates transcription factors that regulate stress-responsive genes (Figure 39).

In the previous sections, ABA (Section 4.7) involvement was ruled out, while ROS (Section 4.8) seemed only to play a partial role in NMD inhibition under NaCl stress. NMD target transcripts respond to manipulation of Ca^{2+}, through either stimulating $[Ca^{2+}]_{cyt}$ influx or using Ca^{2+} channel blockers (Section 4.10). Downstream of the signaling transduction pathway comes phosphoprotein cascades, in which Section 4.9.1 shows prospect that phosphorylation plays a role in NMD inhibition upon NaCl stress. Several well-known players include SnRK2s, CPKs, and serine/threonine phosphatases like SOS2. Subclass I and II of SnRK2s, however, do not seem to have major involvement in NMD inhibition (Section 4.7.1). This leaves other components that respond to salt stress, including CPKs and SOS2. In this section, components of the SOS signaling pathway, will be looked at in-depth regarding NMD inhibition.

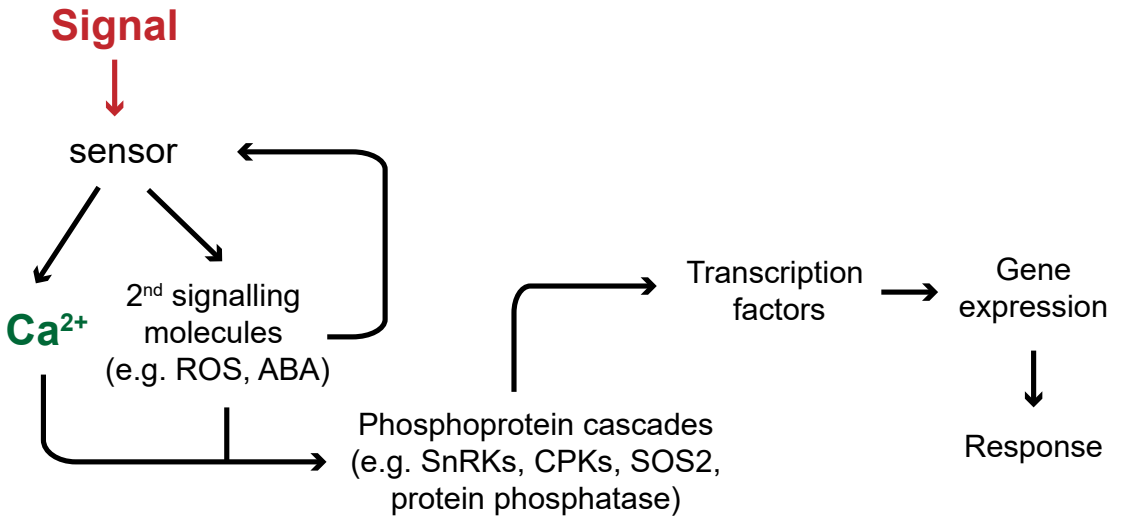

Figure 39: General signal transduction for stress in plants. Stress signals triggers receptor-mediated Ca^{2+} influx and generate secondary signaling molecules, which stimulate a secondary increase in transient Ca^{2+}. The Ca^{2+} transients from different sources may have different biological significance with different outputs. Secondary signaling molecules such as ROS or ABA may also regulate signal transduction independently without Ca^{2+}. Intracellular phosphoprotein cascades then transduce and amplify the information. Major plant protein kinases are serine/threonine kinases, for example SOS2, which plays a central role in the SOS pathway, SnRKs as described in Section 4.7.1, or CPKs, which respond rapidly to drought and salt stress, but not to temperature or ABA (Urao et al., 1994). Transcription factors are then triggered, gene expression is modified, and subsequently a response is elicited as output. Scheme adapted from Xiong and Zhu (2001); Xiong et al. (2002); Kulik et al. (2011).

One of the ways plants deal with Na^+ toxicity and maintain ionic homeostasis, is through the SOS signaling pathway (Clarkson and Hanson, 1980; Tester and Davenport, 2003; Zhu, 2000; Ji et al., 2013). The SOS signaling pathway was originally discovered through the role of CBLs in salt tolerance (Xiong et al., 2002; Shi et al., 2005), and three major genes were identified: *SOS1* (Wu et al., 1996),

SOS2 (Zhu et al., 1998) and *SOS3* (Liu and Zhu, 1997). The *sos* mutants have increased sensitivity to NaCl, and were identified through the root bending assay, where root growth was inhibited under NaCl but not mannitol or KCl, excluding the involvement of osmotic stress (Wu et al., 1996; Zhu et al., 1998). Similarly, NMD inhibition was weaker under equimolar mannitol or KCl compared to NaCl, also showing ionic specificity (Section 4.3). It should also be noted that both *SOS2* and *SOS3* are PTC-containing AS NMD targets, and shows significant transcript increase in NMD mutants *upf1-5*, *upf3-1*, as well as under translation inhibition with CHX (Kalyna et al., 2012).

To test the interrelation between NMD under salt sensitive plants, three *sos* mutants were acquired through the Nottingham Arabidopsis Stock Centre (NASC), *sos1-1* (N3862), *sos2-2* (N3863) and *sos3-1* (N3864) and genotyped (Wall, 2017). The decay of NMD target transcripts *SMG7* and *PTB2+* were analysed in these *sos* mutants with or without NaCl. These mutants were in the Columbia 5 (Col-5) background, and therefore *A. thaliana* Col-5 were used as WT control. In both transcripts, *sos1-1* and *sos2-2* showed hyperstabilization under NaCl treatment compared to WT (Figure 40A–B, D–E, G–H), while *sos3-1* showed the same degree of stabilization compared to WT under NaCl (Figure 40C, F–H). This hyperstabilization can be seen in the 1st hour, and continues to be amplified during 1–4 h. Statistical significance was found in the rate constants comparing *sos* mutant and WT under 50 mM NaCl treatment, for *SMG7* in *sos1-1* during the phase 1–4 h, *sos2-2* during both phases 0–1 h and 1–4 h (Figure 40G), and *PTB2+* in *sos1-1* during both phases as well (Figure 40H). The steady state levels of *SMG7* and *PTB2+* were also analysed in the *sos* mutants, and no noteworthy accumulation can be seen compared to WT (Figure 41). Combined with the transcript decay data (Figure 40), we can conclude the NMD machinery is functional in the *sos* mutants, and NMD inhibition under NaCl stress is connected to SOS1 and SOS2, but not SOS3. This raises the question, whether the hyperstabilization of NMD targets in *sos1-1* and *sos2-2* is a result of a more effective NaCl stress, or due to impaired signaling. Even though all three *sos* mutants show hypersensitivity to salt (growth > 20 more sensitive to inhibition by NaCl (Wu et al., 1996)), *sos1* mutants seem to be the most sensitive (Ji et al., 2013).

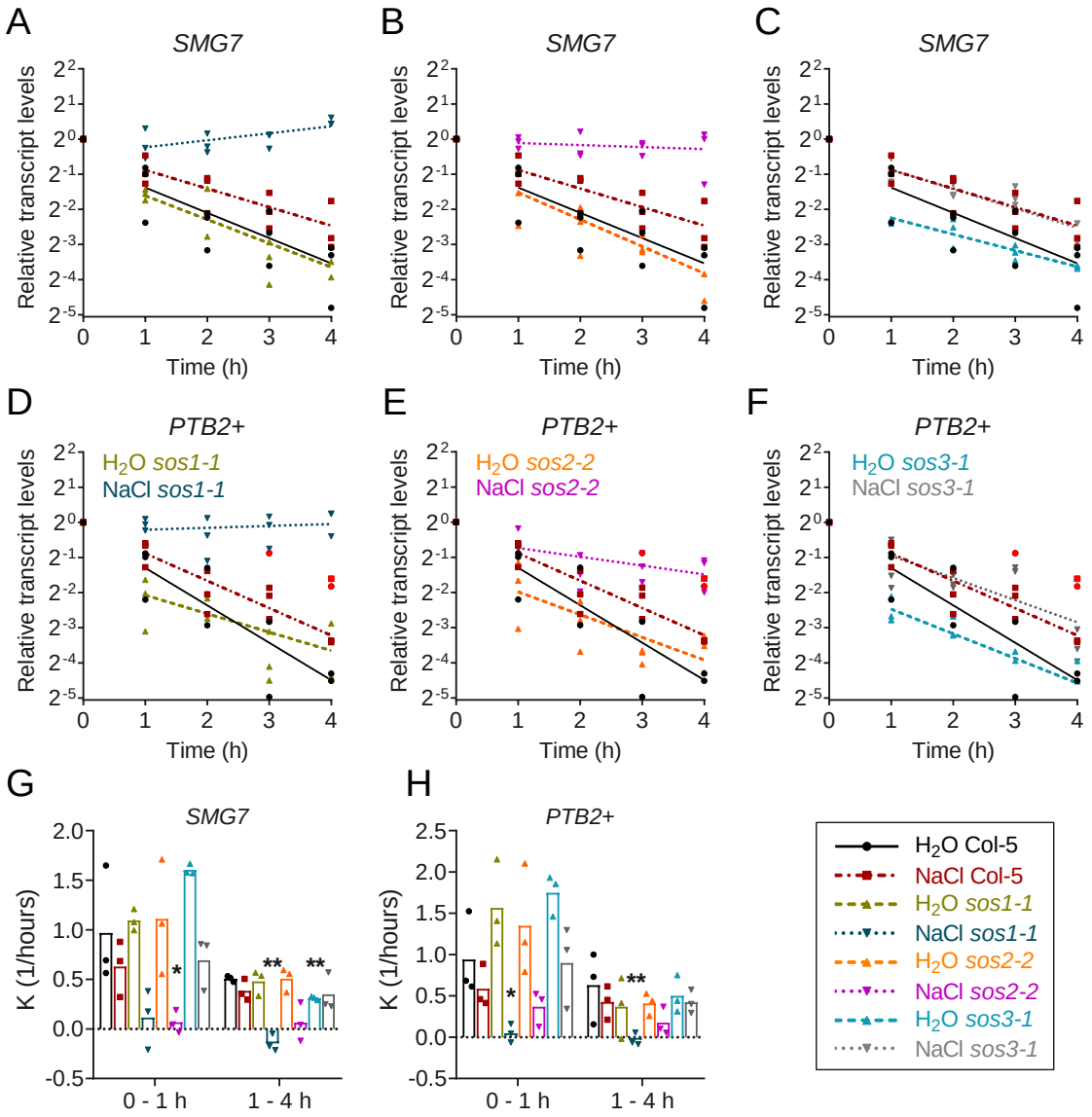

Figure 40: Hyperstabilization in response to NaCl in *sos1-1* and *sos2-2* but not *sos3-1*. Decay graphs (A–F) of *sos1-1* (A, D), *sos2-2* (B, E), *sos3-1* (C, F) of 7-d-old *A. thaliana* seedlings treated with or without 50 mM NaCl, with Col-5 WT control ($n = 3$). Rate constants (G–H) of (A–F) ($n = 3$), unpaired t-tests performed on mutants compared to WT, i.e non-treated mutants to H_2O Col-5 WT, NaCl-treated mutants to NaCl-treated Col-5. *, $P < 0.05$; **, $P < 0.01$. Dots represent individual values, lines represent least squared non-linear regression (A–F), columns represent mean value (G–H). Outliers determined through ROUT ($Q = 5\,\%$) and plotted in red.

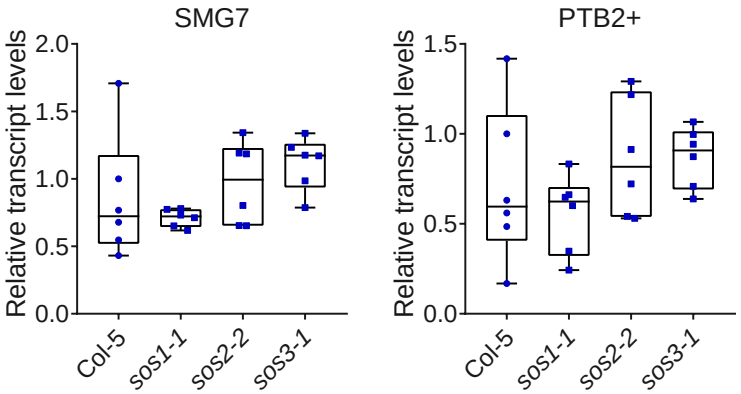

Figure 41: NMD target transcripts do not accumulate in *sos* mutants under steady state conditions under control conditions (no salt treatment). Steady state levels of *SMG7* (left) and *PTB2+* (right) ($n = 6$). All values normalized to one WT sample. Box plot represents first quartile, median, third quartile, whiskers represent min and max. Dots represent individual values. *, $P < 0.05$; **, $P < 0.01$; Mann-Whitney rank test comparing mutants to WT.

4.11.2 UPF1 phosphorylation unchanged under NaCl in *sos1-1* or *sos2-2*

As described above, SOS3 was ruled out of playing a major part in NMD inhibition under NaCl, which leaves SOS1 and SOS2 under scrutiny. The *A. thaliana* SOS1 is an Na^+/H^+ antiporter localized at the PM, and is essential for plant salt tolerance (Shi et al., 2000; Qiu et al., 2002; Zhu, 2002). SOS2 is a serine/threonin protein kinase and belongs to the CIPK family (Liu et al., 2000), and has many interaction partners (Table 4.2). Under NaCl stress, the binding of Ca^{2+} and SOS3 causes a change in shape and properties, which allows the dimerization of SOS2 and SOS3, which then phosphorylates SOS1 at the PM (Shi, 2007; Sánchez-Barrena et al., 2013). SOS2 can also activate the vacuolar Ca^{2+}/H^+ antiporter CAX1, implying CAX1 could regulate $[Ca^{2+}]_{cyt}$ signaling during salt stress (Cheng et al., 2004; Shi, 2007). SOS2 may also affect activities of other transporters such as HKT1, which is involved in Na^+ uptake (Laurie et al., 2002; Rus et al., 2001), and sodium/hydrogen exchanger 1 (NHX1) which removes $[Ca^{2+}]_{cyt}$ into the vacuole (Apse et al., 1999; Maathuis, 2008). Among the many interaction partners of SOS2, 14-3-3 proteins are one of them (Zhou et al., 2014; Tan et al., 2016). SMG7 is an NMD core factor, has a 14-3-3 like domain, which is also conserved for SMG5 and SMG6 (Fukuhara et al., 2005). SMG7 is involved in the dephosphorylation of UPF1 (Yamashita, 2013), and recently been shown in plants for the first time (Figure 42, Kesarwani, Lee, Ricca et al. (2019)).

NMD activity is dependent on the phosphorylation and dephosphorylation of UPF1, where the 14-3-3-like domain of SMG7 binds to the phosphorylated sites of UPF1 and is essential for the decay of the targeted RNA (Fukuhara et al., 2005; Riese et al., 2007; Kerényi et al., 2008; Rayson et al., 2012a; Okada-Katsuhata et al., 2012; Jonas et al., 2013; Lloyd and Davies, 2013; Merai et al., 2013). Therefore, changes to the phosphorylation status of UPF1 was monitored in the *sos* mutants with or without NaCl. A Phos-tag™ gel was used to separate phosphorylated protein extracts from the non-phosphorylated counterparts. Leaves of 35-d soil-grown *A. thaliana* Col-0 WT and *smg7-1* plants were taken as control, and 7-d liquid-grown whole seedlings of *A. thaliana* Col-5 WT, *sos1-1* and *sos2-2* were treated for 4 h with 0, 50 or 100 mM of NaCl. The expected size for UPF1 is 136.9 kilo Dalton (kDa), which is congruent with the uppermost band, and hyperphosphorylation of UPF1 can be seen in *smg7-1* as a smear (Figure 42). Several bands of smaller sizes were detected as well, which could be processing or modification products, as discussed in Kesarwani, Lee, Ricca et al. (2019). Compared with liquid-grown seedlings, no hyperphosphorylation of UPF1 is observed, in WT, *sos1-1*, *sos2-2*, treated or untreated. SMG7 is expected at 117 kDa. While the Col-0 soil-grown sample shows the correct size, in the liquid-grown samples, only processing or degradation products are seen, with almost no signal in *sos2-2* plants. This first hints at lower amounts of SMG7 in *sos2-2*, but normal *SMG7*

Table 4.2: Interaction partners of SOS2 in *A. thaliana*

Gene	Identifier	Interaction	Data Source
ABI1	AT4G26080	Physical	BioGRID interaction data set
ABI2	AT5G57050	Physical	BioGRID, IntAct interaction data set
AT1G30860		Physical	BioGRID, IntAct interaction data set
AT2G41090		Physical	BioGRID interaction data set
CAM1	AT5G37780	Physical	BioGRID interaction data set
CAM4	AT1G66410	Physical	BioGRID interaction data set
CAM6	AT5G21274	Physical	BioGRID interaction data set
CAM7	AT3G43810	Physical	BioGRID interaction data set
CAM8	AT4G14640	Physical	BioGRID interaction data set
CAM9	AT3G51920	Physical	BioGRID interaction data set
CAT2	AT4G35090	Physical	BioGRID, IntAct interaction data set
CAT3	AT1G20620	Physical	BioGRID, IntAct interaction data set
CAX1	AT2G38170	Physical	BioGRID interaction data set
CBL1	AT4G17615	Physical	BioGRID, IntAct interaction data set
CBL2	AT5G55990	Physical	BioGRID, IntAct interaction data set
CBL3	AT4G26570	Physical	BioGRID, IntAct interaction data set
CBL5	AT4G01420	Physical	BioGRID, IntAct interaction data set
CBL7	AT4G26560	Physical	BioGRID, IntAct interaction data set
CBL8	AT1G64480	Physical	BioGRID interaction data set
CBL9	AT5G47100	Physical	BioGRID, IntAct interaction data set
CBL10	AT4G33000	Physical	BioGRID, IntAct interaction data set
CCB1	AT3G26710	Physical	BioGRID interaction data set
DET3	AT1G12840	Physical	BioGRID, IntAct interaction data set
EIN3	AT3G20770	Physical	Quan et al. (2017)
ESE1	AT3G23220	Genetic	Quan et al. (2017)
GDU4	AT2G24762	Physical	BioGRID interaction data set
GI	AT1G22770	Physical	BioGRID interaction data set
HAI2	AT1G07430	Physical	BioGRID interaction data set
IAA11	AT4G28640	Physical	BioGRID, IntAct interaction data set
NDPK2	AT5G63310	Physical, Genetic	Verslues et al. (2007)
PDE331	AT2G01190	Physical	BioGRID, IntAct interaction data set
PKP-ALPHA	AT3G22960	Physical	BioGRID, IntAct interaction data set
SOS1	AT2G01980	Physical	BioGRID interaction data set
SOS3	AT5G24270	Physical	BioGRID, IntAct interaction data set
TCH3	AT2G41100	Physical	BioGRID interaction data set
TUF	AT4G11150	Physical	BioGRID, IntAct interaction data set
VAB1	AT1G76030	Physical	BioGRID, IntAct interaction data set
VAB2	AT4G38510	Physical	BioGRID, IntAct interaction data set
VAB3	AT1G20260	Physical	BioGRID, IntAct interaction data set
VHA-A	AT1G78900	Physical	BioGRID, IntAct interaction data set
VMA10	AT3G01390	Physical	BioGRID, IntAct interaction data set
For details visit:	https://thebiogrid.org https://www.ebi.ac.uk/intact		

transcript levels (Figure 41), and normal decay patterns (Figure 40B, G). Tubulin is expected at 50 kDa, and surprisingly, phosphorylation of Tubulin can be seen under NaCl treatment in liquid-grown seedlings. With α-Tubulin, a shift is visible with 100 mM NaCl in Col-5 WT and *sos2-2*, but a shift can already be seen in *sos1-1* mutants with 50 mM NaCl. This shows Tubulin in *sos1-1* plants are more readily phosphorylated compared to *sos2-2* or WT plants under salt. The same blot was used for all three antibodies.

An immunoblot was performed with a standard sodium dodecyl sulfate polyacrylamide gel electrophoresis (SDS-PAGE) gel with the same samples and amounts of total protein for comparison (Figure 43). Immunoblot analysis of UPF1 for the soil-grown plants were weak relative to liquid-grown seedlings, most likely due to difference in age and material of samples. This is also seen for the Tubulin blot, which is meant as control. Blotting with α-SMG7 shows bands of the expected size as well as degradation products, and shows equally strong signals in the *sos2-2* mutants as well. This argues against changes in total SMG7 levels *sos2-2* mutants. Band intensity in the control samples of 35-d soil grown (Col-0) are generally weaker compared to 7-d liquid grown (Col-5) for α-UPF1 and α-Tubulin blots, while with the α-SMG7 blot, a different band pattern is observed (Figure 42, 43). The 35-d soil grown sample shows a stronger band at the expected size, with some degradation products visible, while the 7-d liquid grown sample shows more processing or degradation products, with less intensity at the expected 117 kDa. An explanation for this, as well as the weaker signal of SMG7 in the Phos-gel (Figure 42) could be attributed to sample harvested at different growth stages in plants, as well as different tissue samples as well, where leaves were sampled in soil-grown plants, and whole seedlings were sampled in the liquid-grown plants. There is also the unlikely possibility that SMG7 in the Col-5 ecotype differs from Col-0.

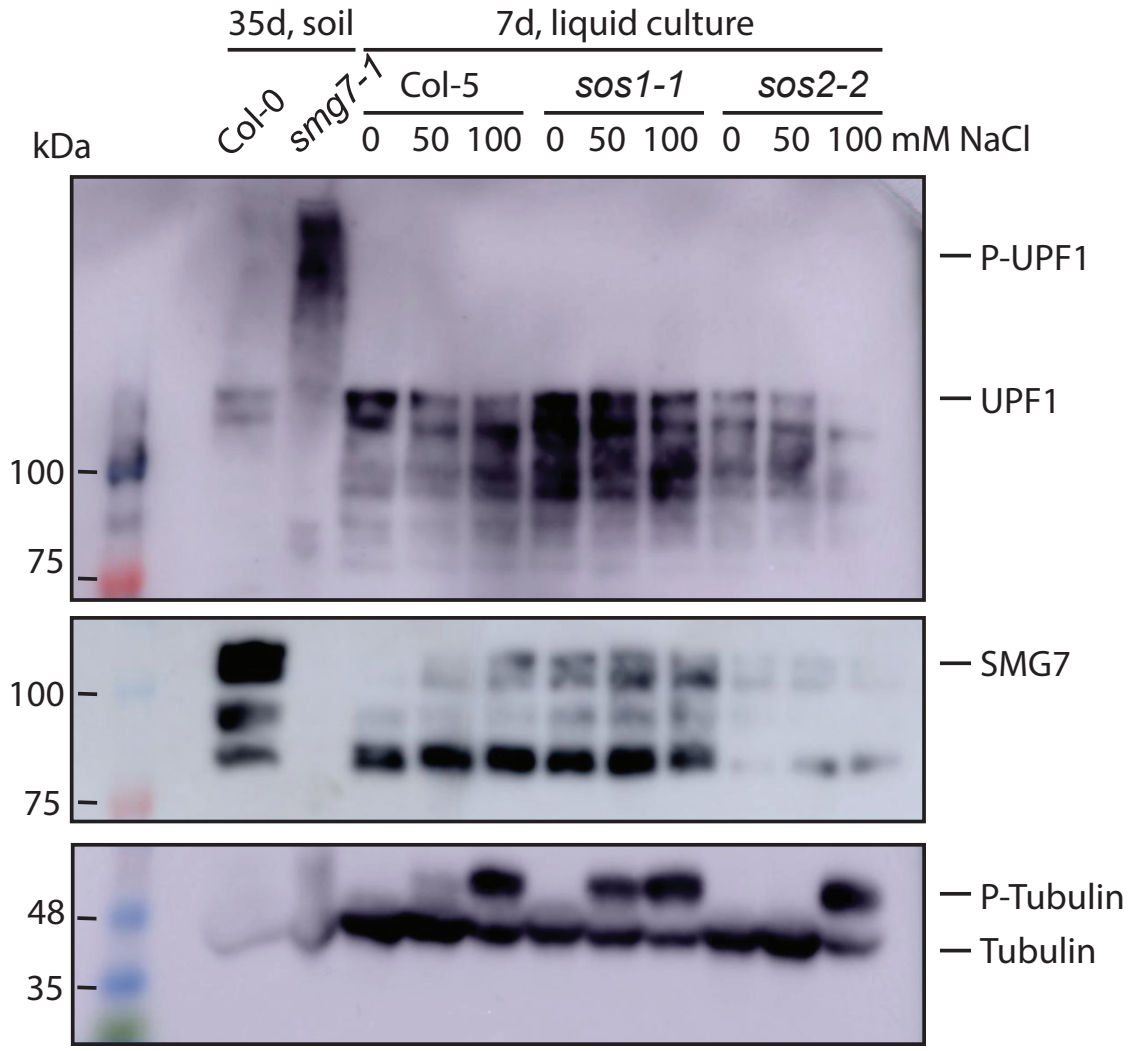

Figure 42: UPF1 not phosphorylated in WT, *sos1-1*, *sos2-2*, with or without NaCl. An immunoblot of Phos-tag™ gel separation of α-UPF1 (top), α-SMG7 (middle) and α-Tubulin (bottom) proteins in 35-day soil grown *A. thaliana* Col-0 and *smg7-1* plants (60 μg total protein per lane), and 7-day liquid cultured *A. thaliana* Col-5 WT, *sos1-1* and *sos2-2*, which were treated with 0, 50, or 100 mM NaCl for 4 h (20 μg total protein per lane). Samples were extracted using a native extraction buffer. Immunosignals were derived from the same membrane by subsequent detection with the three respective antibodies. "P-" represents phosphorylated versions of indicated protein.

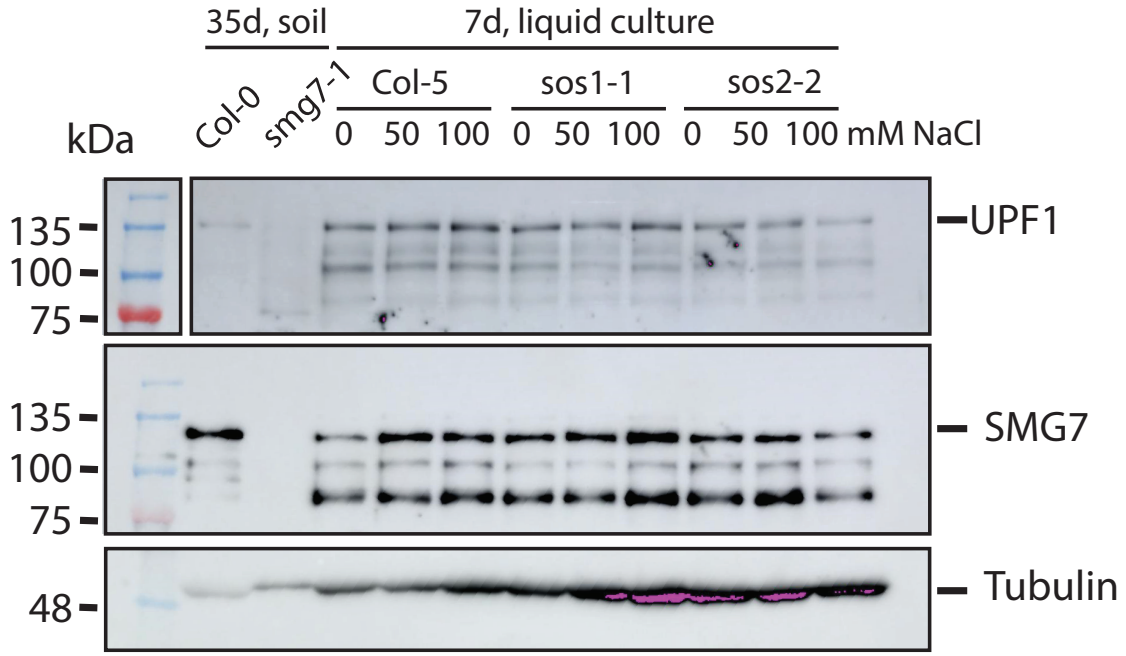

Figure 43: SMG7 proteins present in *sos2-2*. Immunoblot analysis using standard SDS-PAGE separation of α-UPF1 (top), α-SMG7 (middle) and α-Tubulin (bottom) proteins in 35-day soil grown *A. thaliana* Col-0 and *smg7-1* plants (60 μg total protein per lane), and 7-day liquid cultured *A. thaliana* Col-5 WT, *sos1-1* and *sos2-2*, which were treated with 0, 50, or 100 mM NaCl for 4 h (20 μg total protein per lane). Samples were extracted using a native extraction buffer (the same samples that were run in parallel with Figure 42). Immunosignals were derived from the same membrane by subsequent detection with the three respective antibodies.

4.12 Processing bodies and stress granules are involved in mRNA decay

Stress granules are aggregates of proteins and untranslated mRNAs, which are formed in response to stress, and can protect the RNA from degradation (Protter and Parker, 2016). In plants, stress granules can be induced by hypoxia, heat, salt, oxidative stress, and various other stresses (Nover et al., 1983; Weber et al., 2008; Pomeranz et al., 2010; Sorenson and Bailey-Serres, 2014; Yan et al., 2014; Gutierrez-Beltran et al., 2015; Lokdarshi et al., 2016). In yeast, stress granules formed from heat shock can vanish after cells are returned to non-shock temperatures (Parsell et al., 1994; Cherkasov et al., 2013), and shows near-complete reversibility of aggregation (Wallace et al., 2015). Recently, several P-body and stress granule associated proteins, were identified as UPF1 interacting proteins — DCP5, eIF4G, and DEAD-box ATP-dependent RNA helicase 14 (RH14) — are shown to have decreased steady state level of NMD targets in their T-DNA mutants in *A. thaliana* (Chicois et al., 2018), indicating that they are negative regulators of NMD. Given these connections, to see if the stabilization of NMD transcripts during salt stress was caused by the protection RNA due to the formation of stress granules, *dcp5-1*, *eif4g* and *rh14* were used to study the decay of NMD targets (*SMG7*, *PTB2+*, *AT2G45670+*, *RS2Z33+*) and non-NMD target (*RS2Z33−*) transcripts.

4.12.1 The stability of several transcripts are increased in *dcp5-1*

Arabidopsis DCP5 is an Sm-like (LSM) domain-containing RNA-binding protein (RBP), and is required for decapping and the formation of P-bodies (Xu and Chua, 2009). Under steady state conditions, in 7-d-old liquid grown *A. thaliana* seedlings, *dcp5-1* show lower amounts of NMD target accumulation under steady state levels compared to WT (Figure 44A–D), consistent with the study by Chicois et al. (2018). The non-NMD target *RS2Z33−*, however, also shows lower amounts of transcript accumulation (Figure 44E), indicating it is not necessarily NMD specific. The decay graphs show slower decay of *SMG7*, *PTB2+* and *RS2Z33+* in *dcp5-1* during the 1st hour under control conditions as a general trend (Figure 45), with the 0–1 h stabilization in *PTB2+* (Figure J.1B) being the only one that was statistically significant. Since *dcp5-1* is a knockdown mutant with residual decapping activity (Xu and Chua, 2009), the moderately slowed decay can be attributed to the disrupted decapping mechanism, partially protecting these transcripts from degradation, or the extent of impairment in the mutant is not sufficient to result in a change of these transcripts. *AT2G45670+* and *RS2Z33−* show barely any difference between *dcp5-1* and WT control (Figure 45C, E), which could indicate these transcripts are not direct targets of DCP5. Since all the tested NMD targets show decay, compared to the non-NMD target that remains unperturbed (Figure 45), indicates at least an overall

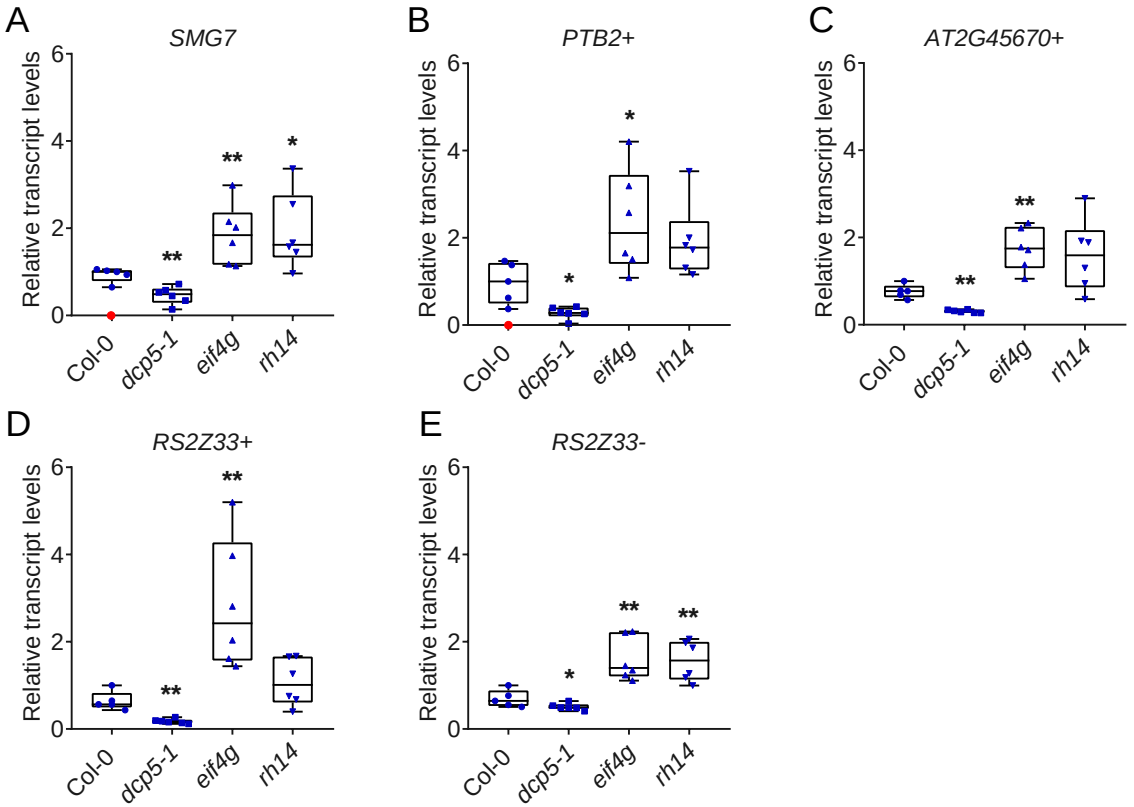

Figure 44: Steady state transcript levels in *dcp5-1*, *eif4g*, and *rh14*. Reduction of NMD target transcripts (A–D) and non-NMD target (E) in *dcp5-1*. Accumulation of NMD target and non-target transcripts in *eif4g*, and accumulation of *SMG7* (A) and *RS2Z33–* (E) in *rh14*. All values normalized to one WT sample. Box plot represents first quartile, median, third quartile, whiskers represent min and max. Dots represent individual values. *, $P < 0.05$; **, $P < 0.01$; Mann-Whitney rank test comparing mutants to WT. Outliers determined through ROUT ($Q = 5\,\%$), and plotted in red. Data derived from RT-qPCR.

functional NMD system in *dcp5-1* mutants. This also holds true in *eif4g* (Figure 46) and *rh14* (Figure 47) mutants. Under NaCl stress, all tested transcripts in *dcp5-1* show minimal difference to WT. In the case of *PTB2+* and *RS2Z33+* however, since transcript levels in *dcp5-1* under control conditions were elevated (Figure 45B, D), there was little stabilization seen for these transcripts under NaCl stress in *dcp5-1*. In particular, NaCl showed weak effects during the 1–4 h phase. These transcripts that are partially protected from degradation through decapping and do not further stabilize when NMD is inhibited, suggesting the decapping handicap is sufficient for protection of these transcripts.

4.12.2 NMD targets stabilize slightly in *eif4g*

The methylated ^{7}mG mRNA cap structure is a binding site for eIF4F. Higher plants encode a second eIF4F complex, eIFiso4F, which comprises of small cap-binding subunit eIF4E (eIFiso4E) and a larger scaffolding protein eIF4G (eIFiso4G)

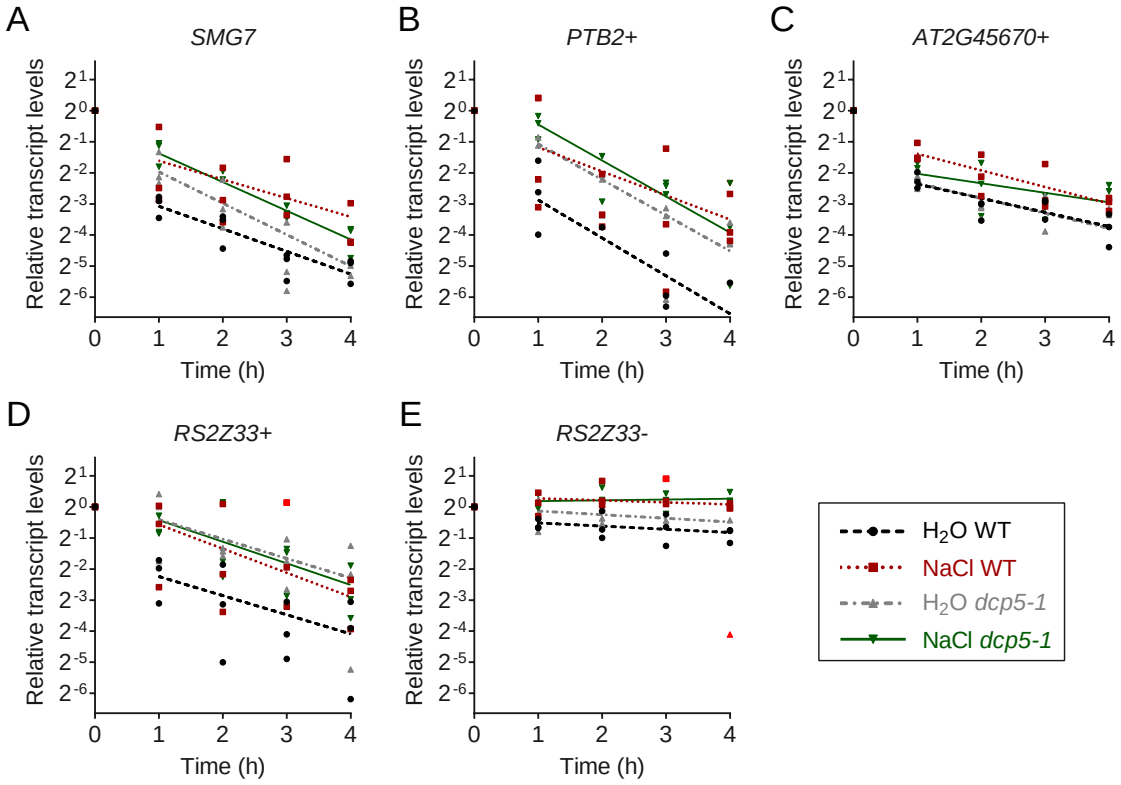

Figure 45: Several transcripts are stabilized in *dcp5-1* mutants. Several NMD target stabilize to a similar degree as NaCl treatment in *dcp5-1* and NaCl-treated *dcp5-1* samples do not stabilize further. (Data collected by Siliya Köster-Hofmann). Decay graphs of NMD target transcripts (A–D) and non-target transcript (E) in *dcp5-1* and Col-0 WT, with or without 50 mM NaCl treatment. Dots represent individual values, lines represent least squared linear regression. Outliers determined through ROUT ($Q = 5\,\%$) and plotted in red.

(Browning et al., 1992; Browning, 1996), which serves to circularize mRNA, leading to the assembly of the 80S ribosome (Aitken and Lorsch, 2012). In *A. thaliana*, eIFiso4G mutants have reduced tolerance to salinity (Lellis et al., 2010), and eIF4G have been co-purified with NMD core factor UPF1 (Chicois et al., 2018).

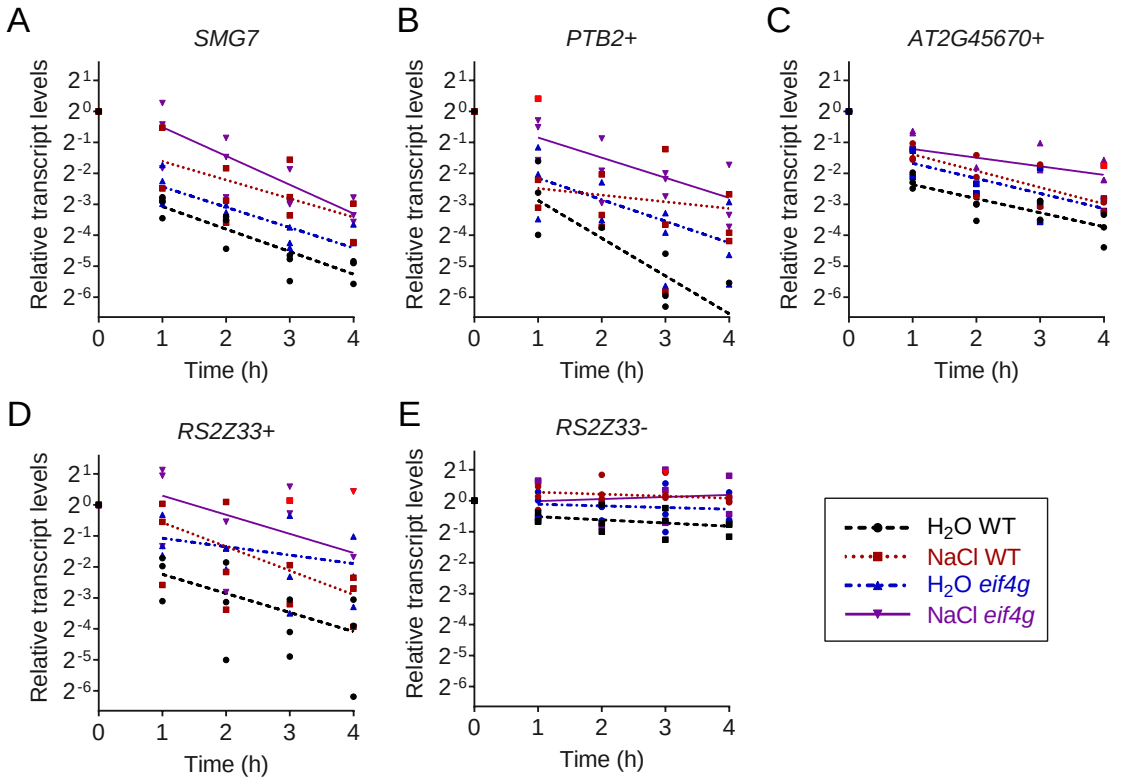

Figure 46: NMD targets stabilize slightly in *eif4g*. Both H_2O control as well as NaCl treated samples in *eif4g* stabilize slightly compared to their respective controls in WT. (Data collected by Siliya Köster-Hofmann). Decay graphs of NMD target transcripts (A–D) and a non-target (E) in *A. thaliana* Col-0 WT and *eif4g*, with or without 50 mM NaCl treatment. Dots represent individual values, lines represent least squared linear regression. Outliers determined through ROUT ($Q = 5\,\%$) and plotted in red.

In *eif4g*, steady state accumulation is seen for all measured transcripts, even the non-NMD target *RS2Z33–* (Figure 44). This again could indicate the transcript accumulation in *eif4g* is not NMD specific. Under control conditions, the decay graphs of these transcripts show slight stabilization of NMD targets in *eif4g* mutants compared to WT (Figure 46), more so with *PTB2+* and *RS2Z33+* compared to *SMG7* or *AT2G45670+*. This could be due to impaired translation, as translation inhibition is shown to be strongly tied to NMD (Section 4.6). Upon NaCl treatment, *eif4g* shows further stabilization of NMD target transcripts (Figure 46), indicating the mechanism of NMD inhibition by NaCl stacks with the mode of transcript decay inhibition by *eif4g*, and eIF4G acts on a different pathway for transcript decay.

4.12.3 The stability of several transcripts are increased in *rh14*

Previous reports show DEAD-box RNA helicases and RBPs contribute to biotic and abiotic stresses in plants (Gong et al., 2005; Li et al., 2008; Germain et al., 2010; Guan et al., 2013b). RH14, also known as ARABIDOPSIS THALIANA DEAD BOX RNA HELICASE 1 (AtDRH1), is associated with the nucleoporin (NUP) complex and required for mRNA export (Du et al., 2016). RH14 is also known to be involved in NMD, pre-mRNA splicing, and ribosome biogenesis (Bond et al., 2001; Guan et al., 2013a; Chicois et al., 2018). Under steady state levels in *rh14*, only statistical significant accumulation was seen for one of the NMD targets *SMG7*, and *RS2Z33–* (Figure 44). In the decay graphs, under control conditions *rh14* showed stabilization in three of the NMD target transcripts during the 1st hour — *SMG7*, *PTB2+* and *RS2Z33+* (Figure 47A, B, D). The stabilization of these transcripts were not statistically significant (Figure J.1). There was little difference in the decay patterns of *AT2G45670+* (Figure 47C, E), indicating that only some NMD target transcripts are affected by RH14. Upon NaCl treatment, only *SMG7* showed slight stabilization (Figure 47A), while *PTB2+*, *AT2G45670+*, *RS2Z33+* and *RS2Z33–* did not show substantial changes (Figure 47B–E), indicating salt does not further stabilize transcripts in *rh14*. This could be due to the impaired nuclear export functions, causing a retention of mRNAs in the nucleus, making it inaccessible the NMD machinery.

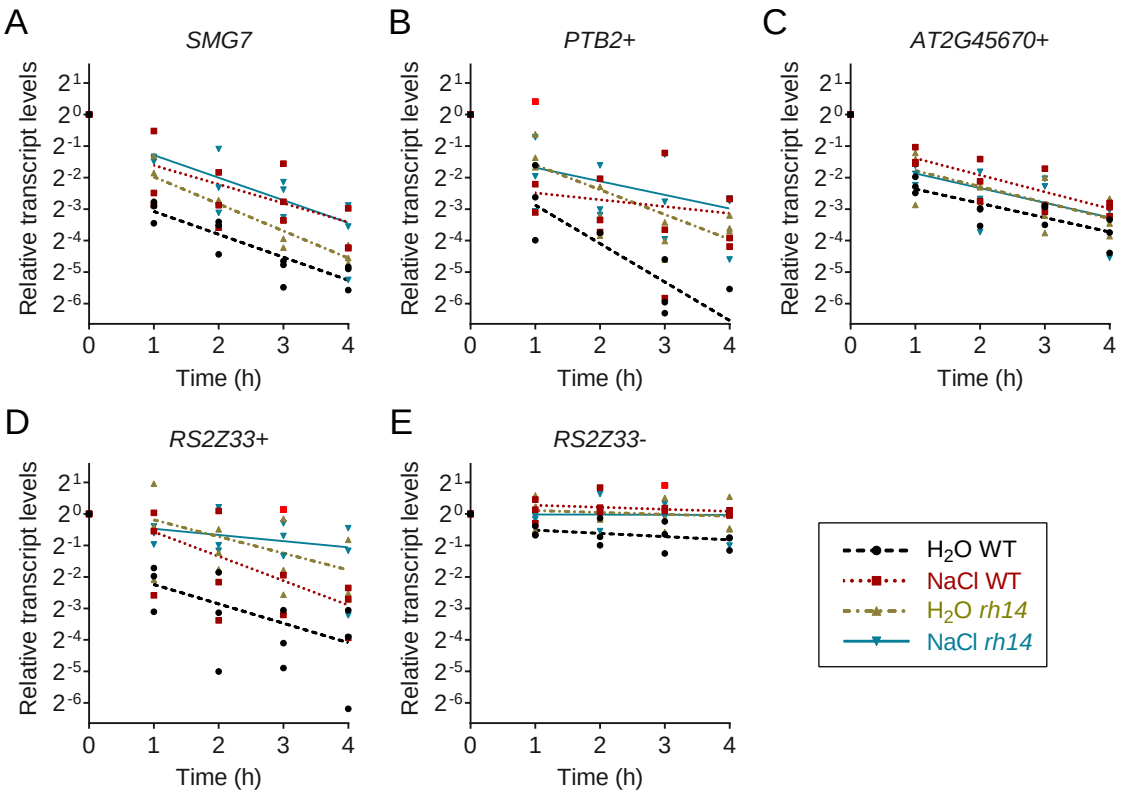

Figure 47: Several NMD targets stabilize in *rh14*. NaCl-treated *rh14* samples do not stabilize further. (Data collected by Siliya Köster-Hofmann). Decay graphs of NMD target transcripts (A–D) and non-NMD target transcript (E) in *rh14* and Col-0 WT, with or without 50 mM NaCl treatment. Dots represent individual values, lines represent least squared linear regression. Outliers determined through ROUT ($Q = 5\,\%$) and plotted in red.

4.12.4 Accelerated mRNA decay in *VCS*-knockdown line no.2

One major cytoplasmic RNA degradation pathway is through mRNA decapping. Decapping of mRNA is carried out by the DCP2-DCP1 heterodimer (Coller and Parker, 2004; Parker, 2012), and in plants, the scaffolding protein VCS is required (Deyholos et al., 2003; Xu et al., 2006; Goeres et al., 2007). VCS contributes to decay of 68 % of the transcriptome, especially of short-lived RNAs (Sorenson et al., 2018), and have been found to regulate mRNA decay under osmotic stress conditions, through phosphorylation by SnRK2s that are localized to P-bodies (Soma et al., 2017). To test the relationship between VCS and NMD, two *VCS*-artificial microRNA (amiRNA) knockdown lines: *VCS*-knockdown line no. 2 (*VCS*-ami no. 2) and *VCS*-knockdown line no. 4 (*VCS*-ami no. 4), and the WT provided by Soma et al. (2017) were used to analyze two NMD target transcripts, *SMG7* and *PTB2+*. Steady state levels show a significant accumulation of both NMD target transcripts in *VCS*-ami no. 2, and a lesser accumulation albeit not statistically significant in *VCS*-ami no. 4 (Figure 48C, F). The decay of *SMG7* and *PTB2+* were also analyzed in these samples, with or without 50 mM of NaCl. Under H_2O control conditions, in both transcripts, *VCS*-ami no. 2 showed a faster decay within the 1st hour, and decayed at a similar rate to WT from 1–4 h (Figure 48A, D, G–H), with *SMG7* showing a stronger decay compared to *PTB2+*. On the other hand, in contrast with *VCS*-ami no. 2, *VCS*-ami no. 4 showed similar decay to the WT in the 1st hour, but had stronger decay from 1–4 h (Figure 48B, E, G–H), also more prominent in *SMG7*. With the addition of NaCl, NMD transcripts in both *VCS*-ami lines stabilized to a similar degree of WT without NaCl treatment, and did not stabilize to the degree of WT with NaCl treatment. These results suggests that a lack of VCS contributes to accelerated mRNA decay, and NMD target transcripts are stabilized in *VCS*-ami lines upon salt stress. The NaCl response observed in the knockdown lines suggests that VCS is not involved in NaCl-mediated NMD impairment.

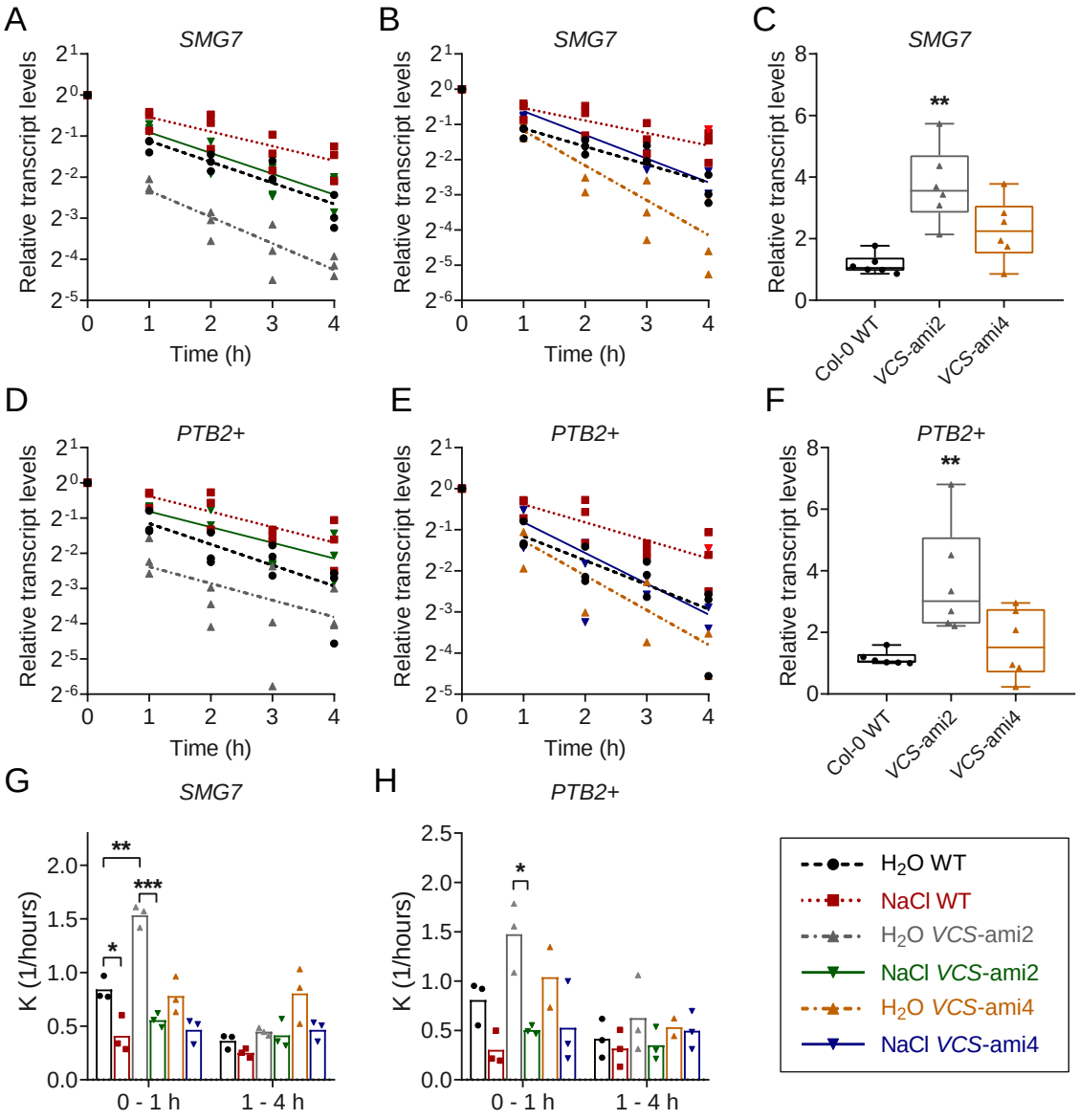

Figure 48: Decay in *VCS*-ami lines are altered in control conditions. (Data collected by Siliya Köster-Hofmann). Decay graphs of NMD targets with or without 50 mM NaCl treatment in *VCS*-ami no. 2 (A, D) and *VCS*-ami no. 4 (B, E). Dots represent individual values ($n = 3$), line represent least squares non-linear regression. Steady state levels of NMD targets in *VCS*-ami no. 2 (C) and *VCS*-ami no. 4 (F). All values normalized to one WT sample. Box plots represent first quartile, median, third quartile, whiskers represent min and max. Dots represent individual values. *, $P < 0.05$; **, $P < 0.01$, Mann-Whitney rank test comparing mutants to WT ($n = 6$). (G, H) Rate constants of NMD transcripts with or without NaCl treatment, corresponding to (A, B, D, E). Dots represent individual values, column represents mean. *, $P < 0.05$; **, $P < 0.01$, ***, $P < 0.001$, unpaired t-tests performed on the NaCl treated amiRNA lines against their respective controls ($n = 3$).

4.13 Other stresses

4.13.1 ER stress is unlikely to be the cause of NMD inhibition under NaCl

Driven by interest, it was compelling to test other types of stresses, and if it can cause NMD impairment as well. The lumen of the ER is an oxidative environment, and is crucial for formation of the proper folding of proteins, as well as the formation of disulfide bonds. Stress in the ER can be triggered by 1,4-Dithiothreitol (DTT), a reducing agent that disrupts disulfide bonds. This results in a massive aggregation of unfolded or misfolded proteins, and is shown to induce autophagy (Ron and Walter, 2007; Liu et al., 2012; Pérez-Martín et al., 2014). In mammalian systems, NMD is shown to be inhibited by ER stress (Karam et al., 2015; Goetz and Wilkinson, 2017; Li et al., 2017b), and forms a cross-inhibition loop with UPR (Introduction 3.5.4).

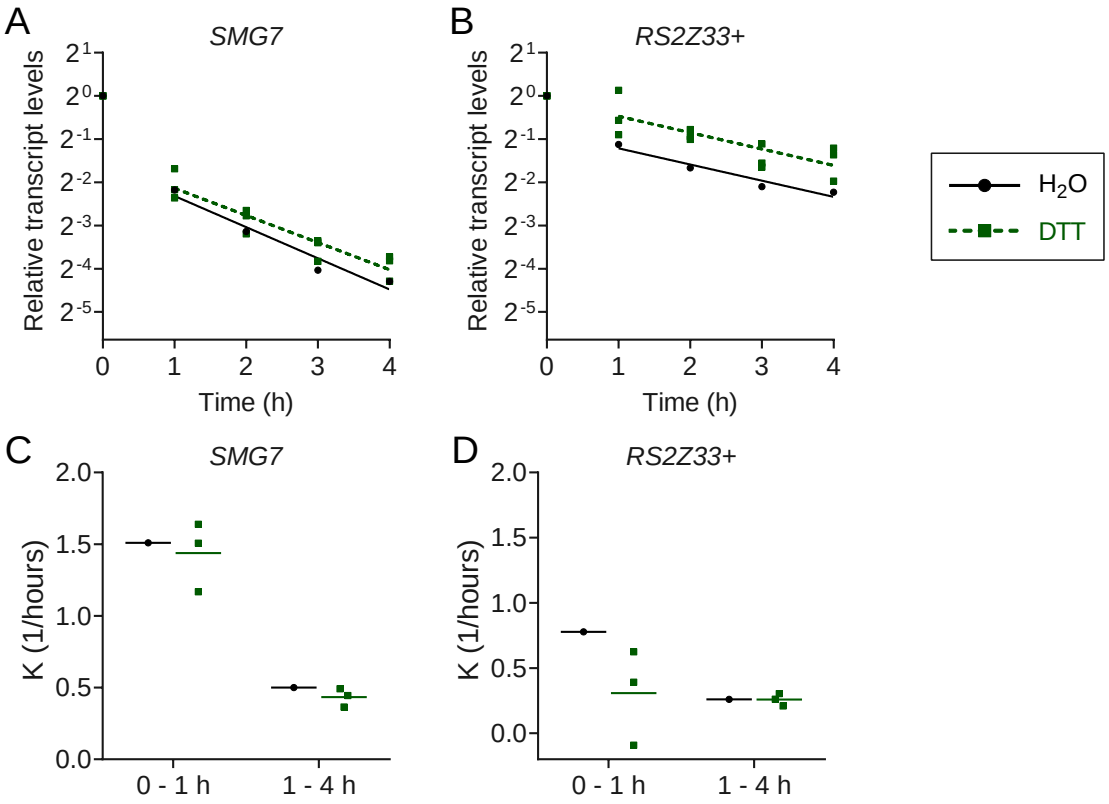

Figure 49: Turnover of NMD targets is not affected by DTT. Decay graphs (A–B) and rate constants (C–D) for samples from 7-d-old *A. thaliana* seedlings treated with 1.6 mM DTT ($n = 3$) or under H_2O ($n = 1$) as control. Dots represent individual values, lines represent least squares non-linear regression (A–B) and mean (C–D).

To test the relationship of ER stress and NMD in plants, the decay of two NMD target transcripts *SMG7* and *RS2Z33+* were analyzed in the presence or absence of DTT (Figure 49). Samples treated with DTT show little change compared to H_2O control, with only *RS2Z33+* showing slightly slower degradation during the 1st hour (Figure 49B, D). This slight change could be from attenuated mRNA translation

in response to ER stress, caused by increased protein-kinase activity of protein kinase RNA-like endoplasmic reticulum kinase (PERK), which phosphorylates eIF2α and inhibits translation (Harding et al., 1999). This result shows similar decay patterns to Figure 23, and further confirms the result in Section 4.6.1 and 4.6.2, where phosphorylation of eIF2α does not seem to play a dominant role in NMD inhibition under NaCl.

4.13.2 Heat affects NMD target transcripts and some non-NMD target transcripts

Like many other abiotic stresses, heat has a complex impact on cell function. It is known to affect membrane-associated processes due to alterations in permeability and fluidity (Alfonso et al., 2001; Sangwan et al., 2002), changes or loss of enzyme function from protein denaturation (Vierling, 1991; Kampinga et al., 1995), and promote programmed cell death (Swidzinski et al., 2002; Vacca et al., 2004). Recent studies in *A. thaliana* has not only revealed networks involving many transcriptional regulators during heat shock (Ohama et al., 2017), but also epigenetic modifications (Lämke et al., 2016). Ca^{2+} and ROS are triggered as initial signaling factors that respond to heat shock (Dat et al., 1998a,b; Gong et al., 1998; Larkindale and Knight, 2002; Sangwan et al., 2002; Swidzinski et al., 2002; Liu et al., 2005; Suzuki and Mittler, 2005; Volkov et al., 2006; Suri and Dhindsa, 2007; Saidi et al., 2009; Baxter et al., 2014). When heat shock occurs, increase in PM fluidity causes Ca^{2+} influx into the cytosol (Sangwan et al., 2002; Saidi et al., 2009), and ROS are generated, mainly in the chloroplasts (Mittler, 2002), but are also actively generated by NOXs, RBOHB and RBOHD (Königshofer et al., 2008; Wang et al., 2014). To study the effect of heat on NMD, the decay of three NMD targets *SMG7*, *PTB2+*, *RS2Z33+* and two non-NMD targets *RBOHD* and *PP2A* were analyzed. 7-d-old liquid grown *A. thaliana* Col-0 seedlings were placed in 38 °C for heat treatment, or remained under 22 °C growth temperature as control. All NMD target transcripts and *RBOHD* showed stabilized pattern under heat treatment (Figure 50A–D, F–I), while *PP2A* did not show visible changes (Figure 50E). Only *SMG7* showed statistical significance of decreased rate constants (Figure 50F). Interestingly, at 30 °C, the NMD target *SMG7* show significantly faster degradation (Figure 51), and *RS2Z33+* also shows a slight trend of destabilization, in contrast to strong stabilization of some transcripts in plants at 38 °C. This could likely be from the temperature threshold of stress granule formation at 34 °C, discussed in Section 5.9.

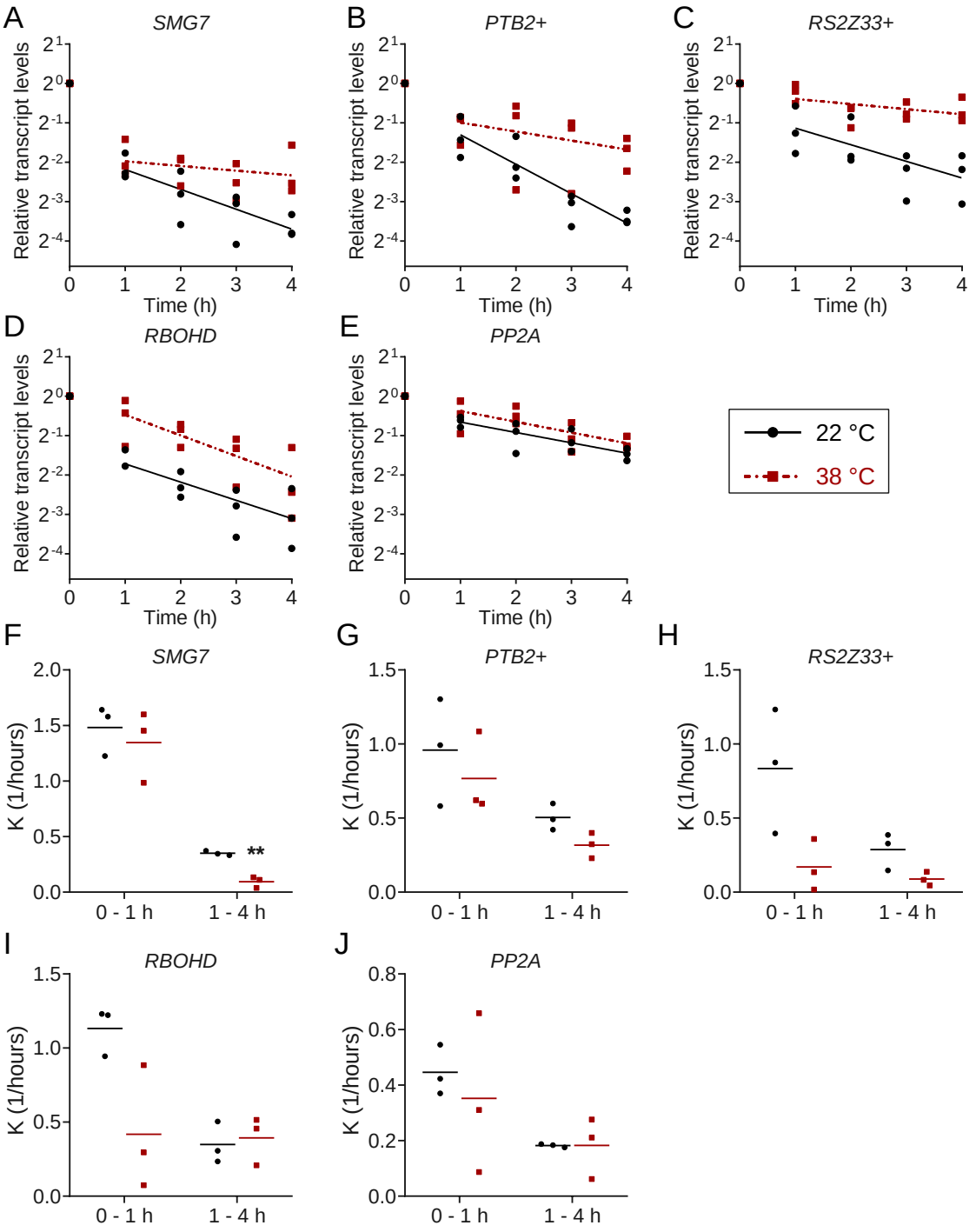

Figure 50: High heat affects NMD target transcript and some non-NMD target transcripts (data collected by Siliya Köster-Hofmann). Decay graphs (A–E) and rate constants (F–J) of NMD targets (A–C, F–H) and non-NMD targets (D–E, I–J) of 7-d-old *A. thaliana* seedlings under growth temperature (22 °C) or heat treatment (38 °C). Dots represent individual values ($n = 3$), lines represent least squares non-linear regression (A–E) and mean (F–J). **, $P < 0.05$, unpaired t-test of heat treated samples against control.

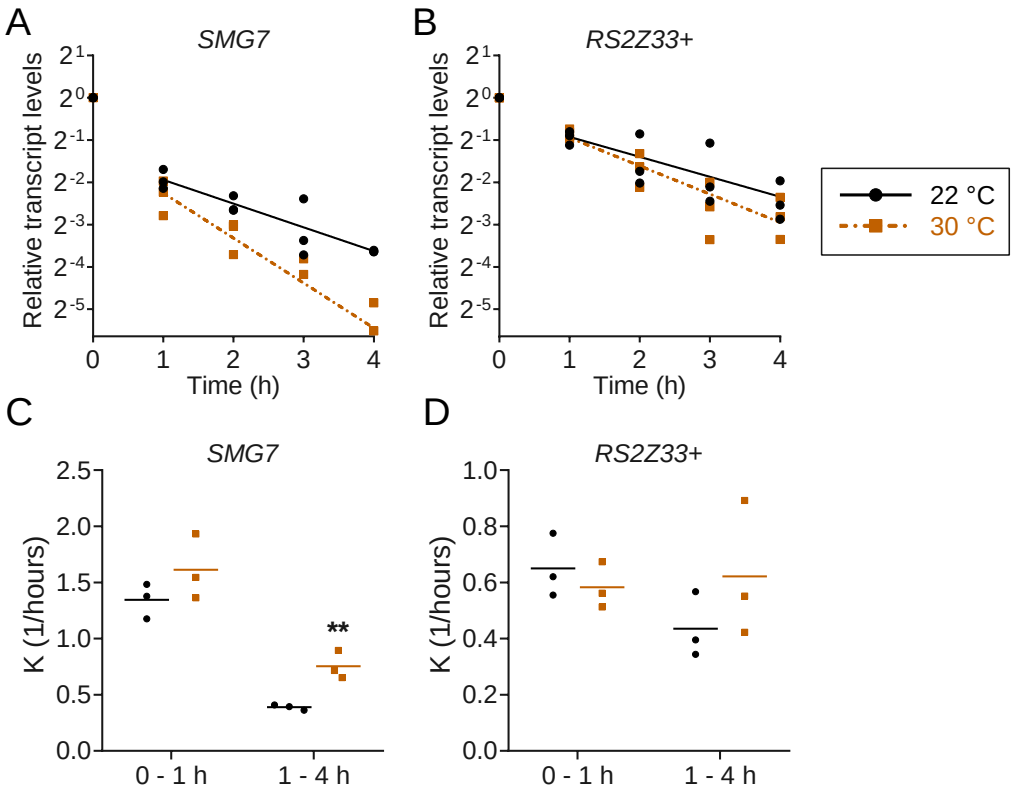

Figure 51: Moderate heat destabilizes NMD targets (data collected by Siliya Köster-Hofmann). Decay graphs (A–B) and rate constants (C–D) of NMD targets *SMG7* and *RS2Z33+* in 7-d-old *A. thaliana* seedlings under growth temperature (22 °C) or heat treatment (30 °C). Dots represent individual values ($n = 3$), lines represent least squares non-linear regression (A–E) and mean (F–J). **, $P < 0.05$, unpaired t-test of heat treated samples against control.

5 Discussion and Outlook

5.1 Experimental design

There are various ways to measure the decay of mRNA (Table 5.1), most of which are well established in yeast or mammalian cells. Common methods include transcription inhibition either using chemicals or through inducible promoters (Chen et al., 2008). Other recent methods include metabolic labeling with 4-thiouridine (4sU), also known as s4U or 4tU (Rädle et al., 2013; Russo et al., 2017; Chan et al., 2018), and variations of the nucleoside analogs 5-bromouridine (5BrU) (Tani et al., 2012; Tani and Akimitsu, 2012; Paulsen et al., 2014; Maekawa et al., 2015) and 5-ethynyluridine (5EU) (Abe et al., 2012). Isotope labeling such as [^{3}H]-adenine or [^{32}P]-phosphate (Hynes and Phillips, 1976; Herrick et al., 1990) have also been used in the past but have since lost popularity, mostly due to cellular damage (e.g. DNA double-strand breaks) caused by radiation. Each method has their own advantages and disadvantages, and half-lives obtained from one method should not be compared side-by-side with another, as it could differ (Wada and Becskei, 2017).

Table 5.1: Comparisons of mRNA half-life measurement methods

Method	Advantages	Disadvantages
Transcription inhibition	Measures global, endogenous transcripts. Relative simplicity in preparation and downstream processing steps (speed). Cost effective.	Cellular stress and toxicity could influence decay rate, and affects downstream pathways.
Inducible promoters	Less invasive and avoids toxiticy issues. Tight and rapid genetic switch.	Cannot be used with endogenous mRNAs, yields measurements of single transcript. Artificial promoters could influence decay rate.
Metabolic labeling (non-radioactive)	Less invasive, less interference with ongoing expression pathways. Can measure endogenous mRNAs, and can be used to assess downstream translation elements.	Laborious, requires extra pull-down steps. Higher sample-to-sample variations. Variable uptake, and impact on cell physiology between each nucleobase derivative. Can trigger nucleolar stress response, which can interfere with RNA stability measurements. More expensive.

Chen et al. (2008); Russo et al. (2017); Wada and Becskei (2017); Chan et al. (2018)

This study (Results 4.1) uses cordycepin as a transcription inhibitor, a classic method for mRNA decay measurement. Common downsides to global transcription inhibition is the relative higher cellular stress that accompanies the treatment, as transcription inhibition is toxic to cells, and in turn affect decay rates. However, all currently known methods of RNA half-life measurements affect decay rates to some degree (Table 5.1). The choice of transcription inhibitor was made from several

pilot tests (Results 4.1), and suits the needs of this study well (Figure 5, A.1). The advantage is the ability to measure endogenous mRNAs, relative speed, cost effectiveness of this method due to simpler preparation, and downstream processing. From a practical standpoint, this means less areas to troubleshoot if unexpected problems arise, compared to the metabolic labeling method. Furthermore, due to the global nature of affected transcripts, the samples have relatively higher flexibility when it comes to future analysis, compared to the singular output from inducible promoters. All in all, each method has their own individual value, and should be considered when addressing different issues when it comes to experimental design.

5.2 Dose-response relationship between NaCl stress and NMD

In Section 4.2, to find a concentration of NaCl that elicits an NMD inhibitory response, liquid cultured samples were treated with different concentrations of salt. A positive correlation of transcript stabilization to NaCl concentration was found, showing that NMD can be fine-tuned by different degrees of stress, opposed to a binary on-off mechanism. From a physiological perspective, having precise and tunable control makes sense for biological systems that need to respond to complex signals quickly and continuously.

In Figure 9, 200 mM of NaCl stabilizes the transcripts more compared to 500 mM NaCl, giving a negative rate constant in the 1st hour. In a perfect system, the minimum value of rate constant (K) should be greater than zero ($K > 0$), as $K = 0$ would indicate no degradation is taking place. However, several cases in this study (Figure 9, 14, 20, 21, 31, 40), mRNA levels show an increase upon addition of the transcription inhibitor. For instance, in Figure 9, the increase occurs during 0–1 h, and ceases to rise in the 1–4 h phase. These rises in transcript levels during the 1st hour indicate possible ongoing transcription, and could be due to delayed integration of the transcription inhibitor, or other processes that regulate transcription, such as chromatin accessibility.

Early and late phases of decay After data collection, rate constants K are calculated individually for two phases: an early phase defined as 0–1 h, and a later phase defined as 1–4 h. Conventionally, although half-lives ($t_{1/2}$) are the standard measurement for mRNA degradation, due to reasons described in Section 5.2, where in some situations salt causes complete stabilization, plus the imperfect integration of transcription inhibitors or other factors, results in a negative value for half-life (increased transcript levels). This makes for invalid direct comparisons, since a negative half-life can be interpreted as having no degradation ($t_{1/2} = \infty$), low half-lives depict very unstable transcript, and long half-lives show again more stable transcripts. Therefore, instead of half-lives, rate constants (K) are calculated, as high K correlates to fast degradation

rates and can be compared linearly. Furthermore, using half-lives only allows U-tests, while t-tests can be performed with rate constants.

In WT samples under control conditions, it is characteristic of NMD transcripts to display massive degradation during the 1st hour, followed by a milder decay in the following hours (e.g. Figure 9), both of which are gradually stabilized under increasing salt stress. In some cases, under higher concentrations of salt treatment, there is an increase of RNA levels in the 1st hour (discussed in Section 5.2). This shows the complexity of ongoing mRNA decay, quite likely with more than one mechanism acting in different phases. Distinct transcript pools may be affected in different ways as well. Although the bulk of degradation occurs in the cytoplasm (Introduction 3.3.1, 3.3.3), possibly some transcripts are differentially accessible than others, perhaps due to localization (e.g. cytoplasmic granules, Introduction 3.3.2), speed of transcription or translation (e.g. codon optimality, Introduction 3.4), susceptibility to other degradation pathways, on-going AS events, or a combination of those factors can all affect the rate of degradation. Possible mechanisms could act additively, contributing to faster decay, or in an inhibitory manner which slows down the decay. Speculations include localization of NMD targets to P-bodies or stress granules, or activity of different nucleases affected by the transcription inhibitor or treatment. Results of comparison of NMD vs. non-NMD transcripts in Results Section 4.4 suggests, NMD is still the main pathway affected by salt treatment, as NMD targets are stabilized with salt and non-targets in general are unchanged (exceptions discussed in Section 5.3.1). Therefore, to simplify the analysis, a single exponential function for one phase decay was employed (Material and Methods 6.4). For future work, if one or more major degradation pathways that are overlapping with NMD is discovered, the total decay rate should be calculated as the sum of decay routes, that the sum of the two amplitudes (A) equals one. For example, in the case of two processes, where t is time and K_1 and K_2 are the rate constants of each process:

$$f(t) = (1 - A) \cdot e^{-K_1 \cdot t} + A \cdot e^{-K_2 \cdot t} \quad (1)$$

5.3 NaCl specifically induces NMD inhibition

5.3.1 Salt stress specifically inhibits degradation of NMD targets

In Results 4.4, the stability of four NMD targets and six non-NMD targets were analysed with and without NaCl. All four NMD targets stabilized upon salt application, with significant decreases in K in both early and late phases, except for *PTB2+*, which only showed significance in the early phase (Figure 14). Out of six non-NMD targets, all transcripts except *SOS1* and *WRKY6* showed no changes (Figure 13). Although *SOS1* is not an NMD target transcript (Figure 15), it has been

reported to accumulate under salt stress (Shi et al., 2003), and thus the weakened decay is not unexpected. It should be noted that the K value is only significantly decreased during the early phase (Figure 13B). Although in plants there is a group of *WRKY* genes identified to be salt-responsive (Fan et al., 2015), *WRKY6* behaves differently even in the same genus. It is downregulated in *Gossypium hirsutum* and upregulated in *Gossypium aridum*, indicating some orthologous *WRKY* genes may have similar functions, while some may not. What is known about WRKY6 transcription factor (TF) in Arabidopsis is that it activates ABA signaling during seed germination and early seedling development (Huang et al., 2016), and like NMD, ABA is a major responder to stress. Apart from this connection, many members of the *WRKY* gene family in plants respond to biotic and abiotic stresses (Phukan et al., 2016). *WRKY6* is known to be upregulated and provide tolerance towards heat and humidity stress, as well as upon *Ralstonia solanacearum* infection, and regulate resistance to *R. solanacearum* in *Capsicum annuum* (Cai et al., 2015; Phukan et al., 2016). In *Oryza sativa* , not only *OsWRKY6* positively regulates defense response as well as increase salicylic acid (SA) accumulation upon overexpression, it regulates a SA-inducible promoter *OsPR10a* expression (Choi et al., 2015). NMD is also known to regulate innate immunity in Arabidopsis, through inhibition under stress (Riehs-Kearnan et al., 2012; Gloggnitzer et al., 2014; Rigby and Rehwinkel, 2015). NMD mutants *lba1* and *upf3* show SA accumulation (Jeong et al., 2011), similar to the upregulation of WRKY6 under stress. So although *WRKY6* is not a direct NMD target, it could be influenced indirectly when NMD is affected due to the commonalities in plant biotic and abiotic stress, as listed above. However, there is no other direct evidence except the data in this study, that indicates the induction in *WRKY6* is due to reduced transcript decay, rather than transcriptional induction.

5.3.2 NMD inhibition is partially specific to Na^+ ionic stress

In Results 4.3, NaCl significantly stabilized NMD target transcripts compared to equimolar KCl during the early phase (Figure 12), showing an Na^+ ionic component to the stress specificity, and at the same time ruling out Cl^-. When comparing KCl to the H_2O control, some stabilization is seen in the early phase, albeit not significant (Figure 12). This could be from stress of elevated cation levels, or could indicate that osmotic stress also plays a minor role, where NaCl-treated samples shows higher accumulation of NMD target transcripts compared to mannitol-treated samples, and the non-NMD target did not (Figure C.1). Under osmotic stress, SnRK2 protein kinases and its phosphorylation target VCS have been shown to modulate mRNA decay (Soma et al., 2017). In Results 4.7.1, the relationship between *snrk* mutants and NMD are investigated under NaCl stress, and no strong inhibition of decay in NMD target transcripts were measured in comparison to the WT (Figure 28),

indicating only minor correlation between NaCl and NMD inhibition through the SnRK2 network, if at all. As subclass III SnRK2s are major positive regulators of ABA signaling, this result is in line with data from Section 4.7, where ABA is neither sufficient nor required for NMD inhibition (Figure G.1). Assuming the mechanism for NMD inhibition through NaCl is ion specific, and is separate from osmotic stress, then the SOS pathway would be an important pathway to study. When comparing growth of the *sos* mutants, they were found hypersensitive to Na^+ and Li^+, but not K^+, Cs^+, Mg^{2+}, Ca^{2+}, Cl^-, NO_3^- or SO_4^- (Wu et al., 1996; Liu and Zhu, 1997; Zhu et al., 1998; Zhu, 2000), in line with the result of transcript stabilization upon NaCl but not KCl. To further investigate if NaCl inhibition of NMD is through the SOS pathway, Li^+ stress can be used as a positive control, where a similar stabilization to NaCl would be expected.

5.4 The Salt Overly Sensitive pathway

NMD targets are found to be hyperstabilized in *sos1-1* and *sos2-2* (Results 4.11, Figure 40). In Results 4.9, Figure 33, 34 show that NMD inhibition by NaCl is rapid, and reversible, giving first indication that phosphorylation might be involved. Results 4.9.1 furthermore show, NMD inhibition under NaCl is affected by kinase and phosphatase inhibitors (Figure 35, 36). The kinase and phosphatase inhibitor used were not specific enough to zone in on any specific pathways, however due to the points in Section 5.3.1 and 5.3.2 discussed, SOS2 (Section 3.5.1, 4.11, Table 4.2) would be a good candidate for further investigation. If a connection is found between SOS2 and any of the NMD core factors, this would provide a direct connection between Na^+-activated stress pathway and NMD. The NMD machinery hinges on the phosphorylation and dephosphorylation of UPF1, however no hyperphosphorylation of UPF1 is seen in *sos2-2* mutants (Figure 42). One straightforward interpretation is simply the NaCl inhibitory effects on NMD is not due to phosphorylation of UPF1. Yet, it is possible that there is still catalytic activity in *sos2-2*, since the mutation in *sos2-2* only abolishes the regulatory domain (Liu et al., 2000). Although both the regulatory and kinase domain activity are required for Na^+ tolerance, this does not exclude the possibility of SOS2 kinase activity with NMD components. Instead, as a follow-up on this experiment, *sos2* mutants *sos2-5*, *sos2-6*, *sos2-7* or *sos2-8* should be used instead, as they are predicted to disrupt the kinase catalytic domain (Liu et al., 2000).

SMG7 is involved in the dephosphorylation of UPF1. Given the data so far, there is potential that SMG7 and SOS2 are interacting, and that this interaction is changed under NaCl stress. This can either be a direct or indirect connection, since it is known that SOS2 no longer self-inhibits under NaCl, and the catalytic

domain is free to perform kinase activities (Guo et al., 2004). SMG7 is a 14-3-3-like adaptor (Fukuhara et al., 2005), and SOS2 is known to interact with 14-3-3 proteins (Zhou et al., 2014; Yang et al., 2019). Recent evidence shows salt stress promotes interaction between 14-3-3 proteins and PKS5, that represses kinase activity and releasing inhibition of SOS2 (Yang et al., 2019). The calcium signatures generated by salt stress modulates 14-3-3-dependent regulation of SOS2 and PKS5 kinase activity (Yang et al., 2019), pointing to the involvement of calcium signaling as a probable upstream component.

5.5 Ca^{2+} signatures are likely involved in NaCl-induced NMD inhibition

SOS3/SOS2 confers plant salt tolerance as a CBL-CIPK signaling pathway, and furthermore SOS1 has also been shown to be regulated by RSA1, a nuclear-localized calcium-binding protein, through a transcription factor (Guan et al., 2013a). In mammalian cells, intracellular Ca^{2+} is a key regulator of NMD, dependent on the binding and inhibition of Na^+/K^+-ATPase on the PM (Nickless et al., 2014). Even though some calcium transduction systems are very different between animals and plants, a comparative analysis reports that Ca^{2+} elements with basic functions in cell response, e.g. Ca^{2+}-ATPase, Ca^{2+}/Na^+ (K^+) ion exchangers are basically conserved between plants and animals (Nagata et al., 2004). This further demonstrates a probability that Ca^{2+} signaling could also regulate NMD in plants.

In this study, using external ATP to stimulate Ca^{2+} influx reveals NMD target transcripts in *A. thaliana* are stabilized to a comparable degree as those put under salt stress (Figure 38, I.1), and calcium channel blocker $LaCl_3$-treated samples seems to show hyperstabilization of NMD targets under salt (Figure I.2). However, more biological replicates are needed for Figure I.2 for statistical conclusion. These findings indicate that manipulation of Ca^{2+} signaling can influence NMD targets under NaCl. It should be noted, that $LaCl_3$ is not a specific inhibitor, and is suggested to act on PM calcium channels (Knight et al., 1996). This means the role of intracellular Ca^{2+} stores, and other Ca^{2+} transport proteins (Introduction 3.5.3), could be interesting to pursue to further investigate the inhibition of NMD, or mRNA decay in general. Furthermore, although under salt treatment $LaCl_3$ substantially decreases the initial $[Ca^{2+}]_{cyt}$ spike, it does not completely inhibit the $[Ca^{2+}]_{cyt}$-spike, and in addition shifts the amplitude of $[Ca^{2+}]_{cyt}$ concentration post-spike, compared to untreated samples (Knight et al., 1997). CDPKs are also responders to stress in plants. Interestingly, *AtCDPK1* and *AtCDPK2* expression was rapidly induced by drought and salt, but not by cold, heat or ABA (Urao et al., 1994). This shares some similarities with salt-inhibited NMD — particularly, a quick response to salt (Results 4.9), and no

involvement of ABA (Results 4.7). Since CDPKs are demonstrated to cross-regulate 14-3-3 proteins (Ormancey et al., 2017), it can be speculated that downstream of the initial salt-induced calcium signature, CDPKs can play a part in the network that influences NMD.

Calcium-dependent phosphorylation Another speculation would be phosphorylation of SMG7 instead of UPF1 under NaCl. The 14-3-3-like domain of AtSMG7 is predicted to have 10 phosphorylation sites with a phosphorylation potential score over 0.9 (Table I.1. NetPhos 3.1b: http://www.cbs.dtu.dk/services/NetPhos/, Blom et al. (1999)), and AtSMG7 has been already experimentally confirmed to have at least one phosphorylation site at S602 (Wang et al., 2013; Rayapuram et al., 2014; Roitinger et al., 2015; Rayapuram et al., 2018). Interestingly enough, AtSMG7^{S602} is not phosphorylated through PAMP-triggered events (Rayapuram et al., 2014), consistent with our findings where flg22 failed to trigger NMD inhibition (Wall, 2017). However, this result is contradictory to findings in Gloggnitzer et al. (2014), where flg22 was able to stabilize NMD targets in 14-d-old soil grown *A. thaliana* leaves. Additionally, there are several studies showing phosphorylation of 14-3-3 proteins in plants by CDPKs (Swatek et al., 2014; Chen et al., 2017b; Ormancey et al., 2017), and in rice, 14-3-3 proteins are phosphorylated in response to salt (Chen et al., 2017b). In Arabidopsis, salt-induced calcium signatures are perceived by 14-3-3 and SOS3/SCaPB8 proteins, which then regulate cytosolic Na^+ homeostasis (Yang et al., 2019). This suggests a possibility that SMG7 could either be an intended target, or simply caught in the crossfire of salt-induced signal transduction, and in turn affect the efficiency of NMD.

To test this theory, differential phosphorylation of SMG7 with and without salt stress should first be identified. The critical phosphorylation sites can be distinguished through mass spectrometry, so the phosphorylation status of SMG7 can first be confirmed under salt stress. Further experiments can be done using phosphomimetics. If SMG7 at a constant phosphorylated state (e.g. SMG7^{S602D}) can mimic the characteristics of salt-induced NMD response (dose-responsive, ABA-unresponsive etc.), and a phosphorylation disabled SMG7^{S602A} cannot, then it would be a direct link that the phosphorylation status of SMG7 affects NMD activity. In parallel, the Phos-tag immunoblot should be optimized. Notably, in Figure 42, very faint and almost no band could be seen for α-SMG7. Apart from it simply being an artifact, an explanation could possibly be that phosphorylated forms of SMG7 are abundant in *sos2-2*, however is not visible on the immunoblot due to different extraction conditions needed for extracting phosphorylated SMG7 compared to UPF1. For example, the phosphorylated UPF1 can only be visualized on the Phos-tag gel when boiling temperature and time is 95 °C for 5 m (data not shown), while other proteins need a much lower boiling temperature with longer duration. The protocol for extracting

phosphorylated forms of SMG7 should be optimized, and the immunoblot should be repeated.

5.6 Apoplastic ROS as initiator of Ca^{2+} signaling

In order for long-distance cell-to-cell signal transduction, Ca^{2+}-signaling alone is not sufficient. While Ca^{2+} in the cytosol is tightly regulated, and therefore is a good stage for Ca^{2+} signal transduction, the plasma membrane and the apoplast make for poor platforms. Ca^{2+} cannot journey for long under the hydrophilic characteristics of the plasma membrane, and high levels of Ca^{2+} in the apoplast makes it unsuitable for transduction of specific Ca^{2+} signatures. ROS however, can be constantly produced and scavenged in the apoplast. As the plant perceives (salt) stress, NOXs are quickly activated and produce O_2^{*-} on the apoplastic side of the PM. O_2^{*-} are then dismutated to H_2O_2 and diffuse to neighboring cells, which are sensed by Ca^{2+} channels on the PM, leading to an increased $[Ca^{2+}]_{cyt}$ concentration. Cell-to-cell signal transduction continues with Ca^{2+} binding to the EF-hands of RBOHD, and multiple CDPKs, CBLs and calcium-dependent components are activated in orchestra (including the SOS pathway). ROS accumulates in the apoplast of the neighboring cell, further triggering ROS and Ca^{2+} sensors, and information is propelled forward (Waszczak et al., 2018).

With respect to Results 4.8, the application of extracellular H_2O_2 stabilizes NMD target transcripts similar to NaCl (Results 4.8.1, Figure 29, H.2), and also has a dose-response relationship (Figure H.1), similar to that seen with NaCl (Results 4.2, Figure 9). However, in *rbohd/f* (and *rbohc*) mutants, NMD targets were not destabilized (Figure 31). This shows RBOHD/F and RBOHC are not crucial for the interaction with NMD components, and hints that NMD inhibition through Ca^{2+} signaling is independent of NOXs, as Ca^{2+}-signaling can be triggered separately from ROS (Results 4.10, Figure 39). Furthermore, paraquat induced ROS at the chloroplast seemed to not affect NMD target transcripts (Figure 30), showing not all ROS causes NMD inhibition. These results reinforces the model described in the above paragraph, and suggests the NMD machinery is affected by the downstream signaling from apoplastic ROS, but not dependent on RBOHD/F. This ties into Ca^{2+} signaling, as discussed in Section 5.5, whether ROS-triggered or not, that NMD inhibition could be caused through Ca^{2+}-activated components that affect 14-3-3 proteins.

5.7 NMD inhibition is involved with interference of translation elongation, but not translation initiation

The degradation of mRNA is tightly tied to the translation machinery (Introduction 3.4). In mammals, NMD inhibition under stress involves the phosphorylation of eIF2α, which results in translation inhibition (Wek et al., 2006; Gardner, 2010; Karam et al., 2013). However, results in Section 4.6 seems to suggest induction of eIF2α phosphorylation itself does not seem to be sufficient for NMD inhibition in *A. thaliana* (Figure 23). In plants, TOR is involved in the translation initiation of mRNAs with uORFs in the 5' UTR (Schepetilnikov and Ryabova, 2018), which happens to be an NMD triggering feature. All tested NMD target transcripts do not show altered decay upon TOR inhibition (Figure 26, F.1), with the exception of *SMG7* showing slight but not significant stabilization, indicating that TOR is not involved in the degradation of these mRNAs. As TOR has recently been shown to phosphorylate PYL ABA receptors for stress regulation (Wang et al., 2018), this supports data in Results 4.7, downstream of TOR, where ABA and SnRK2s also do not have major involvement in NMD inhibition under NaCl. Both TOR and eIF2α are involved in translation initiation, which do not seem to play a big role in NMD inhibition. CHX however, impedes translation elongation through interference with tRNA translocation. The results from Section 4.6.4 (Figure 27) shows translation inhibition through CHX is involved in NMD inhibition under NaCl. This indicates either the mRNA stability has already reached saturation with NaCl, and can no longer be further stabilized, or translation inhibition acts as an independent pathway for mRNA decay. To further explore the relationship between translation, NMD, and NaCl, the use of metabolic labeling methods could be worth the extra effort. Metabolic labeling (Section 5.1) such as 4sU has been reported to be less invasive compared to global transcription inhibition, and can be used to determine mRNA stability in relation to translation (Chan et al., 2018). It also has the advantage of also being able to monitor both transcription as well as degradation rates, and has already been established in Arabidopsis (Sidaway-Lee et al., 2014; Sugliani et al., 2016).

5.8 P-bodies and stress granules

DCP5, eIF4G and RH14 are P-body and stress granule associated proteins that were recently identified as UPF1 interacting proteins. It was observed in this study, that the commonalities in the *dcp5-1*, *eif4g* and *rh14* mutants are that NMD target transcripts are stabilized in the early phase under control conditions (Results 4.12, Figure 45, 46, 47). This could be due to disrupted interactions with UPF1, leading

to slower degradation of NMD transcripts. Alternatively, the stability of these transcripts could also be changed due to alterations in decapping in the case of *dcp5-1*, or impaired translation in *eif4g*, or impaired nuclear export functions in *rh14*. Although stress granules have been shown to regulate *A. thaliana* growth under stress (Yan et al., 2014), Hamada et al. (2018) found, that 200mM NaCl solution can cause stress granule formation but not 150 mM NaCl, for *A. thaliana* seedlings immersed in liquid solution. In this study, with the exception for Section 4.2 and Figure B.2, all test conditions were done in with either 50 or 100 mM NaCl, therefore it is unlikely that the formation of stress granules could be the main reason for transcript stabilization under salt. P-bodies, however, are not ruled out. P-bodies are strongly associated with stress granules: they are also mRNA-ribonucleoprotein (mRNP) aggregates, formed through LLPS, and can interact with stress granules. Despite this, they are generally associated with degradation, consisting of multiple decapping components, deadenylases, NMD components, and a 5'→3' exonuclease (Table 3.1). NMD target transcripts are also known to localize to P-bodies (Chantarachot and Bailey-Serres, 2018). With this in mind, it could make sense to speculate NMD targets could be partially degraded in P-bodies in some conditions.

5.9 Heat-induced stress granule formation may protect NMD target transcripts from degradation

Heat stress is known to pause translation elongation in mouse, humans, as well as plants (Shalgi et al., 2013; Merret et al., 2015). Merret et al. (2015) shows in *A. thaliana*, heat-induced ribosomal pausing triggers XRN4-mediated mRNA decay. The stabilization patterns (Figure 50) could indicate disruption of the translation machinery through high heat (38 °C), as NMD targets accumulate under inhibition of translation elongation through CHX (Figure 27B), as well as *RBOHD* under CHX treatment (Figure 15). Another possibility could be from stress granules, which are formed at a temperature threshold of 34 °C (Hamada et al., 2018) in *A. thaliana* in liquid culture, and could be the reason for transcript stabilization under heat treatment. This would explain the seemingly opposite results for plants treated with 30 °C, where decay was accelerated instead. Under higher temperatures, cellular biochemical reactions tend to be faster, therefore resulting in faster decay than the control group at 22 °C (Figure 51). As the temperature continues to rise, stress granules are formed, and therefore certain transcripts are protected from decay (Figure 50). It would be interesting to see if these affected transcripts are commonly found in P-bodies, as it is known that P-bodies share some similar factors with stress granules, and they can interact with each other as well (Section 3.3.2). Notably, at least for two of the NMD targets, *SMG7* and *PTB2+*, the heat-induced stabilization

is seen mainly in the later phase from 1–4 h, while NaCl has a major effect in the 1st hour. Coincidentally, SMG7 and PTB2 proteins are known to localize to P-bodies in plants (Stauffer et al., 2010; Merai et al., 2013), which contain degradation enzymes (Introduction 3.3.2). It could be speculated that under heat stress, a partial pool of these transcripts (*SMG7* and *PTB2* in this case) are preferentially directed to locations of these interacting LLPS compartments, possibly contributing to the nucleation of these granules (due to on-site translation), fulfill their function locally and then degraded. Although there is no direct evidence, and is pure speculation, this could be a first glimpse at the difference between cytosolic degradation and degradation in P-bodies.

5.10 Concluding Remarks

The starting point for this study was an observation of altered splice ratios and steady-state accumulation of NMD-regulated genes under salt stress (Kesarwani, 2014). Behind a seemingly simple phenomenon, lies a complex network of pathways. This study explored a wide range of components related to abiotic stress signaling, in attempt to dissect the mechanism connecting salt stress to NMD, a dominant player in specialized degradation pathways. The first and arguably the most important part of this study was the establishment of a reliable method for measuring specialized mRNA decay, without destroying cellular integrity, which causes mass global transcript degradation, which leads to inaccurate measurements, and is especially significant when studying specific degradation pathways. Thereafter, foundational aspects of salt induced NMD inhibition was demonstrated as being 1. dose-dependent, 2. seemed specific to the NMD pathway, and 3. involves an ion-specific (Na^+) component.

With the current evidence obtained, the following mechanism is proposed as the most likely (Figure 52): Phosphorylation of SMG7, possibly by SOS2, due to specific calcium signatures triggered by NaCl. Phosphorylation is a likely component at play, considering the rapid and reversible nature of salt-induced NMD inhibition, as well as hyperstabilization of NMD targets under kinase or phosphatase inhibitors under salt (Results 4.9). From Results 4.10, it is clear that stimulation of Ca^{2+}-influx mimics the effects of NaCl very accurately (Figure 38, I.1). What leaves to be desired is a more conclusive experiment with Ca^{2+} channel blockers, and to take it further, Ca^{2+} pumps and antiporters should be considered as well. The idea of phosphorylation of SMG7 started out with the results of the Phos-tag gel, where SMG7 in *sos2-2* cannot be visualized (Figure 42), but is present in WT and *sos1-1*, as well as in all WT and mutants on the western blot (Figure 43). This hints at possibly non-optimal extraction conditions that destroys phosphorylated forms of SMG7, which is present in *sos2-2*. It should be noted that the mutation in *sos2-2*

abolishes the regulatory domain, not the catalytic domain of the protein. Although both domains are necessary for salt tolerance, it is possible that the catalytic domain is still sufficient for phosphorylation of NMD components. Phosphorylation from Ca^{2+}-dependent signatures is based on 1. recent literature where 14-3-3-proteins are phosphorylated in a calcium-dependent manner under salt stress (Yang et al., 2019), 2. and cross-regulation of CDPK and 14-3-3 proteins (Ormancey et al., 2017). 3. The SOS pathway is a calcium-dependent pathway, with SOS2 (CIPK24/SnRK3.11) acting as a central Ser/Thr protein kinase, which interacts with many proteins (Table 4.2), including 14-3-3 proteins. 4. SMG7 possesses a 14-3-3-like domain, and 5. has already been experimentally shown to have at least one phosphorylation site (S602). 6. This theory compliments the results found in Results 4.8, where H_2O_2 is sufficient to induce transcript stabilization, but NOXs are not necessarily involved in NMD (Discussion 5.6). The next steps to proceed would be mass spectrometry to identify differentially phosphorylated sites, followed by phosphomimetics. In parallel, the kinase activity of *sos2-2* can be tested, and extraction conditions of phosphorylated forms of SMG7 should be optimized, or a phospho-specific antibody can be developed. Subsequently, Phos-gels should be repeated, with *sos2-2* and a *sos2* mutant where the mutation is located in the kinase domain (Discussion 5.4).

In a more global context, so far, not a lot is known about the specific mechanism which controls NMD under stress in plants. However, NMD feedback regulation was shown to manage steady state levels of NMD targets in animals and plants (Huang et al., 2011; Degtiar et al., 2015). For example, NMD is attenuated upon amino acid deprivation in yeast (Mendell et al., 2004), and under hypoxic environments in mammalian cells (Gardner, 2008). In plants, *UPF3* levels affect the sensitivity of *A. thaliana* plants to NaCl, and salt stress can induce *UPF3* expression (Vexler et al., 2016). UPF3 is an NMD core factor, and apart from *UPF3*, transcripts of some NMD core factors are also under NMD regulation. For example, plant *UPF1*, *UPF3* and *SMG7* transcripts have NMD triggering features and are targets of NMD (Kerényi et al., 2008; Lloyd and Davies, 2013; Nyikó et al., 2013; Rayson et al., 2012a; Degtiar et al., 2015; Vexler et al., 2016; Kesarwani, Lee, Ricca et al., 2019). In mammals, *UPF1*, *UPF2*, *UPF3B*, *SMG1*, *SMG5*, *SMG6* and *SMG7* showed increased steady state levels and half-lives upon NMD impairment (Huang et al., 2011; Yepiskoposyan et al., 2011), and disrupting this feedback control can affect growth in mammalian cells (Huang et al., 2011), and stress tolerance in *A. thaliana* (Vexler et al., 2016). It has been proposed that NMD has evolved for defense against RNA pathogens and later repurposed for endogenous transcript regulation (Hamid and Makeyev, 2016). For example, NMD is known shown to restrict mammalian RNA virus replication (Balistreri et al., 2014; Wada et al., 2018), and has also been shown in mammals to be inhibited upon virus infection (Wada et al., 2018). In plants, NMD is also

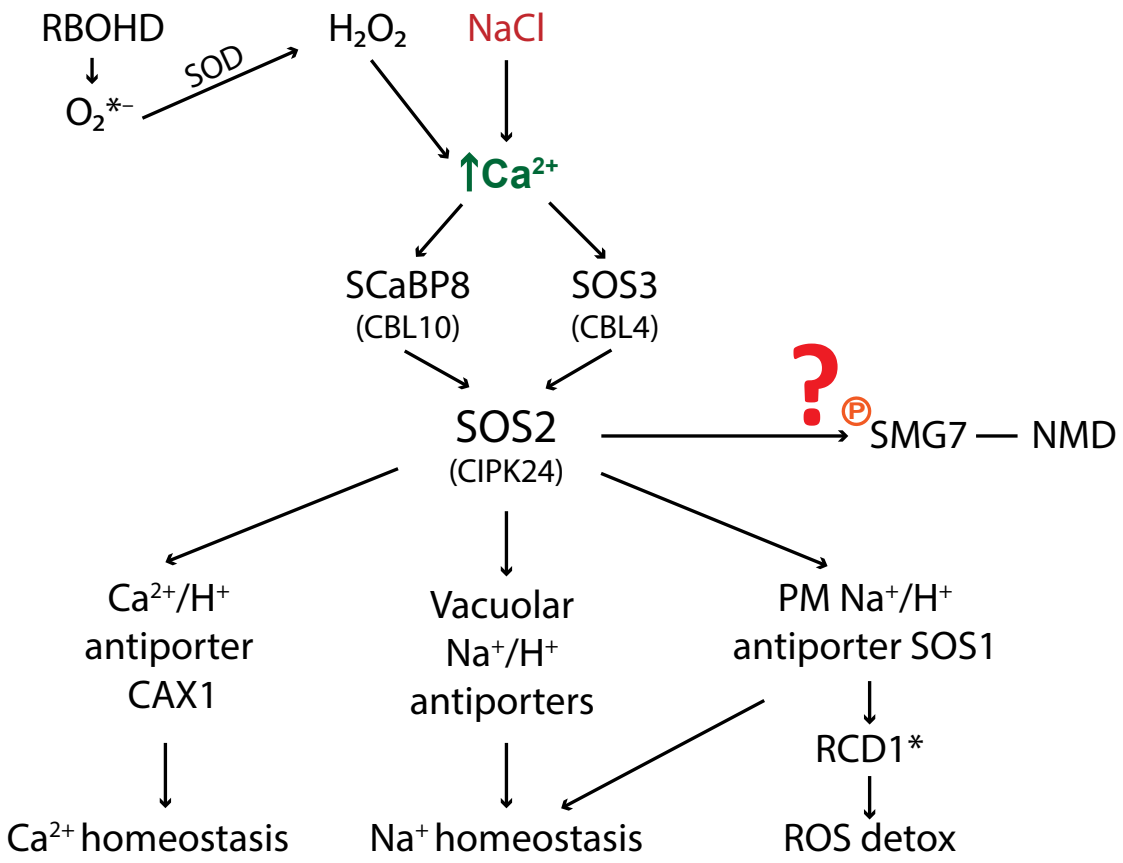

Figure 52: Proposed model of salt-induced NMD inhibition. $[Ca^{2+}]_{cyt}$ signaling induced by NaCl or H_2O_2 triggers the SOS pathway. SOS3 and SCaBP8 binds to SOS2, which can activate Ca^{2+}/H^+ antiporters to regulate Ca^{2+} homeostasis, and Na^+/H^+ antiporters at the vacuole or plasma membrane (PM) to regulate Na^+ homeostasis. SOS2 possibly interacts with the 14-3-3-like domain of SMG7 and alters its phorphorylation status, and in turn affects NMD efficiency. H_2O_2 can be produced at the PM when superoxide dismutase (SOD) dismutates O_2^{*-} produced by RBOHD (Introduction 3.5.2). The apoplastic H_2O_2 can then trigger cytosolic Ca^{2+} signaling. Other stresses that also elicit similar Ca^{2+} signatures may also trigger similar NMD responses. The orange-red question mark indicates the next step that needs to be investigated. Orange "P" denotes possible phosphorylation. * SOS1 interacts with RADICAL-INDUCED CELL DEATH (RCD)1 to confer oxidative stress tolerance in *Arabidopsis* (Katiyar-Agarwal et al., 2006).

inhibited upon pathogen infection (Jeong et al., 2011; Gloggnitzer et al., 2014). NMD mutants show a constitutive immune response and elevated pathogen resistance in *A. thaliana* (Jeong et al., 2011; Rayson et al., 2012b,a; Riehs-Kearnan et al., 2012). NMD has also been shown to control the turnover of numerous TNL transcripts, which encode for immune receptors (Gloggnitzer et al., 2014). At least in one case, the *Turnip crinkle virus* has evolved to evade NMD by having an unstructured region immediately downstream of the coat protein stop codon, and this is suspected that it might be a prevalent strategy for protecting transcripts that otherwise would

be NMD-sensitive (May et al., 2018), further displaying the complexity between NMD and immunity. There could be several physiological implications of NMD inhibition. In plants, NMD has been reported to compete for RNA substrates with post-transcriptional gene silencing, which is triggered through the production of dsRNA, that goes through siRNA-directed ARGONAUTE-mediated endonucleolytic cleavage (Moreno et al., 2013). Therefore, restriction of the NMD pathway may be necessary for certain functions in post-transcriptional gene silencing. In the recent years, more and more physiological mRNAs are being reported as under NMD regulation (Drechsel et al., 2013; Lykke-Andersen and Jensen, 2015; Nasif et al., 2018), and NMD has a positive correlation with the "strength" of NMD-triggering features in that particular transcript. For example, in plants, a reporter construct with a longer 3'-UTR is more efficiently degraded (Kertész et al., 2006; Hori and Watanabe, 2007), or in mammals, UPF1 preferentially associates with longer 3'-UTR lengths, enhanced binding to PTC-containing mRNAs, and further enhanced binding along a 3'-UTR in the presence of an EJC (Kurosaki and Maquat, 2013). This tunable control of transcript turnover argues for its potential in precise control over gene expression. Taken together, profound evidence indicates that NMD acts as a dampener under normal circumstances, constantly turning over stress responsive transcripts (such as TNLs) that are constitutively expressed. Once exogenous stress is perceived, NMD is diminished to varying degrees, and the plant can quickly respond to environmental changes in a controlled manner. It is important to gain a deeper insight on how this machinery is regulated, in order to dissect the significance of NMD in the complete picture of physiology and cellular stress.

6 Materials and Methods

6.1 Plant associated Methods

Seed sterilization *A. thaliana* seedlings were surface sterilized with 3.75 % NaOCl and 0.01 % Triton X-100, vortexed for 3 min, and incubated for an additional of 2 min. Seeds were briefly spun down and washed with sterile ultrapure water of Type 1 laboratory use Milli-Q water (defined by ISO 3696) from the Millipore Corporation (MilliQ) water 3–4 times or until water turns clear.

Liquid culture 0.03 g of sterilized seeds are pipetted into 100 mL of autoclaved half strength Murashige and Skoog medium without sucrose (Duchefa M0222; ½ MS, 2.2 g in 1 L) in 500 mL Erlenmeyer flasks. Flasks were placed in 4°C darkness overnight for stratification, and grown under constant aeration through shaking at approximately 100 rpm, in 8 h dark, 16 h light cycles, at 22°C. 100–250 mL Erlenmeyer flasks can also be used, but shaking speed should be adjusted to roughly 110 rpm. 50 mL flasks are not recommended, but when used, seed amount and medium volume should be halved, and shaking speed increased to roughly 115 rpm.

Hydroponics *A. thaliana* were grown on ½ MS with 2 % sucrose and 0.8 % plant agar (Duchefa P1001) on plates for two weeks and moved to a hydroponic system (0.5 mM KH_2PO_4, 0.5 mM $MgSO_4$, 0.125 mM K_2SO_4, 25 μM KCl, 15 μM H_2BO_3, 2.5 μM $MnSO_4$, 0.5 μM $ZnSO_4$, 0.5 μM $CuSO_4$, 0.5 μM $NaMo_4$, 0.125 mM $CaCl_2$, 0.5 mM KNO_3, 0.05 mM Na-Fe-EDTA, adjusted to pH 5.8 with KOH). Seedlings were balanced in holes with 4 mm diameter, with only the roots submerged in hydroponic medium. Medium was exchanged daily, and supplemented with 100 mM or 200 mM for 24 or 48 h before samples were taken.

Suspension culture Cell culture performed by Dr. Caterina Brancato from Central Facilities in Zentrum für Molekularbiologie der Pflanzen (ZMBP), Tübingen, Germany. 10 mL of old culture of *A. thaliana* Col-0 cells* were grown in 50 mL Medium "*MSCol*" (4.3 g/L MS salts, 1 mg/L Nicotin acid, 1 mg/L Pyridoxin-HCl, 10 mg/L Thiamin-HCl, 100 mg/L myo-Inositol, 30 g/L Sucrose, adjusted to pH 5.8, with 1 mg/L 2,4-D added after autoclave. Stored in 4°C darkness). Put on shaker at 120 rpm in 250–300 mL sterile flasks. *Cell culture from Prof. Dr. Karen Schumacher, ZMBP — Plant Physiology, Tübingen, Germany.

Soil Seeds were sown on water-saturated soil and placed in 4 °C darkness overnight for stratification with a plastic dome to retain moisture, and moved to the long-day growth chamber, with 8 h dark and 16 h light cycles, at 22 °C. Plastic dome was removed after 3 days and plants were alternately treated with nematodes or Confidor periodically for pest control.

6.2 Biochemical Methods

Antibody Purification The UPF1 antibody were purified from raw serum (rabbit, 23404) by affinity purification using recombinant protein (construct 980, N-terminal half of UPF1, detects UPF1 and degradation products) separated on an SDS-PAGE gel, blotted on a nitrocellulose membrane. Raw serum were diluted 1:1 in 2 % milk in Tris buffered saline (TBS) (20 mM Tris, 150 mM NaCl, pH 7.5), and bound to the antigen at 4 °C for 1 h. Subsequently, nitrocellulose strips were washed three times for 10 min with 2 % milk-TBS, followed by short washing steps with TBS and water. Antibodies were eluted in two steps by a pH shift. Strips were eluted for 3 min in elution buffer 1 (5 mM Gly and 0.5 M NaCl, pH 2.8) on ice with robust shaking. After the first elution, the supernatant was neutralized immediately with Tris, pH 8.0, to a final concentration of 90 mM Tris. The elution was repeated with elution buffer 2 (5 mM Gly and 0.5 M NaCl, pH 2.2) on ice with robust shaking, then elution fractions were combined and supplemented with 0.1 % bovine serum albumin (BSA). Finally, all elution fractions were concentrated using Pierce™ Protein Concentrators (ThermoFisher 88516).

Protein Extraction Buffers used for proteins to be run in the Phos-tag gels cannot contain the chelating agent ethylenediaminetetraacetic acid (EDTA), therefore, all chemicals should be EDTA free. Proteins extracted using 300 μl native extraction buffer (50 mM Tris-HCl pH 7.9, 120 mM NaCl, 2 mM $MgCl_2$, 0.1 % Triton X-100, 10 % Glycerol, 1 mM β-Mercaptoethanol (β-Me), 2 mM phenylmethylsulfonyl fluoride (PMSF), 1x cOmplete ULTRA EDTA-free Protease inhibitor (Roche 05892791001), 1x Phos-STOP Phosphatase inhibitor EDTA-free (Roche 04906837001)) to 100 mg plant material. Sample concentration were determined via standard bradford analysis, and were boiled in sample buffer (0.125 mol/L Tris-HCl pH 6.8, 20 % (w/v) Glycerol, 4 % (w/v) Sodium-Dodecyl-Sulfate (SDS), 10 % (vol) β-Me, 0.002 % Bromphenolblue) at 95 °C for 5 min. Samples were loaded freshly and ran on Phos-tag and a standard SDS-PAGE gel.

Phos-tag Gels 60 μg of total protein of 35-d soil-grown *A. thaliana* or 20 μg total protein of 7-d liquid grown seedlings were separated on Zn^{2+}-Phos-tag™ SuperSep Pre-cast gels (Wako 192-17401). The WIDE-VIEW™ Prestained Protein Size Marker (Wako 230-02461) was used. Proteins that were phosphorylated runs slower than un-phosphorylated proteins, causing separation. The samples were run in 4 °C at 100 V for 5 min, and the voltage was turned down to max. 40 V with fixed current 10 mA and run for 24 h. Gel was incubated in transfer buffer (48 mM Tris-Base, 39 mM Glycine, 0.0375 % SDS, 20 % (vol) ethanol (EtOH)) supplemented with 10 mM EDTA for 10 m, and washed with transfer buffer without EDTA 3x for 10 min before blotting onto a polyvinylidenfluorid (PVDF) membrane. Membranes were detected

using Ultra sensitive HRP substrate (TaKaRa T7104A). Membrane was stripped (in 0.1 L: 20 mL 10 % SDS, 12.5 mL 0.5 M Tris HCL pH 6.8, 67.5 mL H_2O, 0.8 mL β-Me) at 50 °C for 45 min before incubation with α-SMG7. Secondary antibody α-Rabbit (Sigma A6154).

Western Blots Same amount of total protein as the Phos-tag gels were loaded on a standard SDS-PAGE gel and run at 100 to 200 Volts (V) until finished in room temperature. Gel transferred to a PVDF membrane. Blots handled in the same manner as Phos-tag gels described above.

6.3 Molecular Methods

RNA Extraction Total RNA was extracted from approximately 100 mg of plant tissue using the Universal RNA Purification kit (Roboklon E3598), including on-column DNaseI (Thermo Fisher EN0521) treatment performed according to the manufacturer's instructions. RNA was eluted in 40 μl RNase free water and stored at −20 °C.

Reverse Transcription All RNA was transcribed using Superscript II (Thermo Fisher 18064014) except for the following: Figure A.3 as indicated, and AMV Reverse Transcriptase Native (Roboklon E1372) was used for Figure B.1, Figure C.1, and Figure G.1. In Figure A.3 Protoscript II is from New England BioLabs (Cat. No. M3068). All reverse transcriptase were used according to the manufacture's instructions. For all half-life assays, after RNA extraction, all RNA samples were measured on a Nanodrop™ machine and adjusted to equal amounts before performing reverse transcription to ensure Ct values from qPCR would fall in range of the relative standard curve (described below).

Quantitative PCR Quantitative PCR (qPCR) was performed with the Biorad CFX384 realtime PCR system, with MESA GREEN qPCR Mastermix Plus (Eurogentec). Serial dilutions of the templates were conducted to determine primer efficiency and plot a standard curve each time. Data were analyzed by interpolation between cycle threshold (Ct) values and the relative standard curve, and expression was normalized relative to *Actin7* (AT5G09810) transcript levels if not otherwise mentioned. Three technical replicates were performed for each biological replicate, outliers were defined as 0.5 Ct above or below minimum or maximum value, respectively. For example, if the Ct values for three technical replicates read 28.89, 28.91, and 28.43, 28.43 would be removed as the outlier and the average of 28.89 and 28.91 would be used for further calculations, described in Section 6.4.

Co-amplification PCR Co-amplification PCR is performed with one set of primers which could amplify alternatively spliced regions of the same gene. A cDNA tem-

plate was used and products of two different sizes can be separated on standard electrophoresis gels, or quantified using a Bioanalyzer^{TM}.

Bioanalyzer The Bioanalyzer^{TM} (Agilent, http://www.chem.agilent.com) was used to check RNA quality or quantify co-amplified PCR products.

6.4 Computational Analysis

Primer efficiency, Interpolation Primer efficiency and interpolation for qPCR analysis were calculated in Microsoft Excel using the following functions:
Slope:

$$\text{slope} = \frac{\Delta\overline{\text{Ct}}}{\Delta \log \text{cDNA}} \tag{2}$$

Axis intercept:

$$\text{Intercept} = \Delta\overline{\text{Ct}} - \text{slope} \cdot \Delta \log \text{cDNA} \tag{3}$$

Primer efficiency:

$$\text{Efficiency} = 10^{\text{slope}^{-1}} - 1 \tag{4}$$

Interpolation of relative cDNA amounts:

$$f(x) = 10^{(\overline{\text{Ct}_x} - \text{intercept/slope})} \tag{5}$$

Normalization to reference gene:

$$f(x) = \frac{\text{Interpolated cDNA amounts of Gene of interest}}{\text{Interpolated cDNA amounts of Reference gene}} \tag{6}$$

- **Ct** represent cycle threshold, and is the number of cycles required for the fluorescent signal to cross the threshold and exceeds background level. Ct levels are inversely proportional to the amount of target nucleic acid in the sample. $\overline{\text{Ct}}$ is the mean of the three technical replicates performed.
- **cDNA** would be theoretical relative cDNA amounts, as each step of the dilution series would theoretically yield half the amount of cDNA of the step before.
- **Primer efficiency** is a percentage of how efficient that specific primer pair is. An ideal efficiency would be 100 %, meaning that specific primer pair doubles the amount of target sequence per cycle. If the efficiency is higher than 100 %, the primer pair has higher efficiency and amplifies the target sequence more than once, and vice versa. As a result, if the primer efficiency is exactly 100 %, the Ct value would increase by 1 per serial dilution.

GraphPad Prism Values from qPCR are input into GraphPad Prism version 8.0.1 for Windows, GraphPad Software, Sandiego, California USA, www.graphpad.com.
Least squares non-linear regression equation (one phase decay) as follows:

$$Y = (Y_0 - \text{Plateau}) \cdot e^{(-K \cdot X)} + \text{Plateau} \tag{7}$$

- Y_0 is the Y value when X (time) is zero. It is expressed in the same units as Y.
- *Plateau* is the Y value at infinite times, expressed in the same units as Y. This parameter is restricted to 0. The $Y_0 - \text{Plateau}$ is described as amplitude (A) in Section 5.2.
- K is the rate constant, expressed in reciprocal of the X axis time units. If X is in hours, then K is expressed in inverse hours.
- *Span* is the difference between Y_0 and Plateau, expressed in the same units as the Y values.

Half-life ($t_{1/2}$) is in the time units of the X axis and calculated as such:

$$t_{1/2} = \frac{ln(2)}{K} \tag{8}$$

Unpaired t-tests for K values uses fewer assumptions and analyses each row (0–1 h and 1–4 h) individually, and reports the corresponding two-tailed P value. Statistical significance defined with $\alpha = 0.05$.
Mann-Whitney rank test for relative transcript levels in steady state conditions. More power to detect a shift in the median, but less power to detect differences in the shape of the distributions. Unpaired nonparametric test, P value is two-tailed, definition of statistical significance: $P < 0.05$.

6.5 Oligonucleotides

Table 6.1: List of Primers used for co-amplification PCR

Gene name	Identifier	Primer code	Primer sequence (5'→3')
PTB1	*AT3G01150*	AWHD46	CTCAGGCCAAACTCAGTTCC
		AWHD47	TGCACAAATCCAAAAGCAGA
RS2Z33	*AT2G37340*	AWTU483	TTAGGGCTTCCGTGTTTCG
		AWTU484	TCGCTTCATATCCACATCTCG

Table 6.2: List of Primers used for RT-qPCR

Gene name	Identifier	Primer code	Primer sequence (5'→3')
Actin7	*AT5G09810*	BL008	GGATGCTTGTGATGATGCTGTTTT
		BL009	GCTGCATTGTCACCCGATAC
UPF1	*AT5G47010*	BL001	CGACTTTGCTACACAGGCC
		BL002	ACGAGAATAACCGCCTTGAGA
UPF2	*AT2G39260*	AK136	AACTGAAGGCCTTACTTCAGGA
		AK137	GATCCTTCAAAAACACTCATCG
UPF3	*AT1G33980*	AK138	AGAGGCGTACAAGAAACAAGG
		AK139	TTCCTGCTGAAGATAGTGGTTG
SMG7	*AT5G19400*	BL004	ATTCTTTTTACCCGAACAAGCCT
		BL005	GCTGAGCCCAAAGAAATCACC
AT2G45670+	*AT2G45670*	AWTU496	TGCTGTGCATGAAATAAAGGGATGT
		AWTU495	TCGTGGTTCCTTCGGGGAAT
RS2Z33+	*AT2G37340*	AWTU493	CGCCTTGGCGATTCTGTTTGTAG
		AWTU492	GGGATCACCAAATTCAACGAAAGC
RS2Z33-	*AT2G37340*	AWTU491	TACGGAAGAGTGCGAGATGTGG
		AWTU492	GGGATCACCAAATTCAACGAAAGC
PTB2+	*AT5G53180*	AWHD95	TTCAGTGGCAGCCTAATGC
		AWHD96	TCCATCGAGGGCAAGTTT
SOS1	*AT2G01980*	BL030	CAGCTTCAGAGATCATTTCGT
		BL031	AACCATGCTGCCGAAAAT
RBOHF	*AT1G64060*	BL036	TGGTGATTGGACTCAAGAACTC
		BL037	AAACTTTTCTTTGTTGTTTCGTCG
RBOHD	*AT5G47910*	BL038	GTGGATGTTGTGTCGGG
		BL039	CTCCTATTCTTTTGCCGGGA
PP2A	*AT1G13320*	DNA28	GGTAATAACTGCATCTAAAGACAGAGTTCC
		DNA29	CCACAACCGCTTGGTCG

Table 6.3: List of Primers used for genotyping

Gene name	Identifier	Primer code	Primer sequence (5'→3')
dSpm transposon	dSpm1	BL040	CTTATTTCAGTAAGAGTGTGGGGTTTTGG
dSpm transposon	dSpm11	BL041	GGTGCAGCAAAACCCACACTTTTACTTC
AtRBOHC	*AT5G51060*	BL042	TAGCTTCTCCATGTGACCGCG
		BL043	ATCTAAAGCTAGATGCCTTAGC
AtRBOHD	*AT5G47910*	BL044	GTCGCCAAAGGAGGCGCCGA
		BL045	GGATACTGATCATAGGCGTGGCTCCA
AtRBOHF	*AT1G64060*	BL046	CTTCCGATATCCTTCAACCAACTC
		BL047	CGAAGAAGATCTGGAGACGAGA
SALK line	SALK_ LBb1.3	BL067	ATTTTGCCGATTTCGGAAC
eIF4g	*AT3G60240*	BL061	GAACGCACCAGAGTGCTTATC
		BL062	AGGTTCATGTTGATCAATGCC
RH14	*AT3G01540*	BL063	ATATCGTGGTTGCAACTCCTG
		BL064	TACCTCTGCCACCATAACCAG
DCP5	*AT1G26100*	BL065	CCATCAGCAGAGGATGAAGAG
	AT1G26110	BL066	GTCCCAAAATTCAAGGCCTAG

6.6 Chemical usage, handling and storage

Table 6.4: Chemical data, handling and storage used in this study

Common Name	Product number	Stock Solvent	End conc.	Storage
Actinomycin D	Sigma A4262	20 mg/ml in DMSO	100 μg/ml	−20 °C
Cordycepin	Sigma C3394	1 mg/ml in H_2O	150 μg/ml	Used freshly
Cycloheximide	Sigma C7698	5 mg/ml in H_2O	10 μg/ml	−20 °C
DF	Sigma D9533	0.1 M in H_2O	1 mM	Used freshly
DMTU	Sigma D188700	1.5 M in MeOH	15 mM	−20 °C
DPI	Sigma D2926	12.5 M in DMSO	250 μM	−20 °C
K252a	Sigma K1639	1 mM in DMSO	4 μM	−20 °C
$LaCl_3$	Sigma 262072	1 M in H_2O	1 mM	n.a.
Okadiac Acid	Sigma O7760	0.1 mM in H_2O	1 μM	−20 °C
Paraquat	Sigma 36541	1 M in SPB pH 7.0	7 μM	4 °C

n.a.: Not applicable, chemical used only once, no storage was involved.

References

Abbasi, F. M. and Komatsu, S., 2004. A proteomic approach to analyze salt-responsive proteins in rice leaf sheath. *Proteomics*, 4:2072–81.

Abe, K., Ishigami, T., Shyu, A.-B., Ohno, S., Umemura, S., and Yamashita, A., 2012. Analysis of interferon-beta mRNA stability control after poly(I:C) stimulation using RNA metabolic labeling by ethynyluridine. *Biochemical and biophysical research communications*, 428:44–9.

Advani, V. M., Belew, A. T., and Dinman, J. D., 2013. Yeast telomere maintenance is globally controlled by programmed ribosomal frameshifting and the nonsense-mediated mRNA decay pathway. *Translation (Austin, Tex.)*, 1:e24418.

Aitken, C. E. and Lorsch, J. R., 2012. A mechanistic overview of translation initiation in eukaryotes. *Nature structural & molecular biology*, 19:568–76.

Alfonso, M., Yruela, I., Almarcegui, S., Torrado, E., Perez, M. A., and Picorel, R., 2001. Unusual tolerance to high temperatures in a new herbicide-resistant D1 mutant from *Glycine max* (L.) Merr. cell cultures deficient in fatty acid desaturation. *Planta*, 212:573–82.

Anderberg, R. J. and Walker-Simmons, M. K., 1992. Isolation of a wheat cDNA clone for an abscisic acid-inducible transcript with homology to protein kinases. *Proceedings of the National Academy of Sciences of the United States of America*, 89:10183–7.

Anderson, J. T., 2005. RNA Turnover: Unexpected Consequences of Being Tailed. *Current Biology*, 15(16):R635–R638. ISSN 0960-9822.

Apse, M. P., Aharon, G. S., Snedden, W. A., and Blumwald, E., 1999. Salt tolerance conferred by overexpression of a vacuolar Na+/H+ antiport in Arabidopsis. *Science (New York, N.Y.)*, 285:1256–8.

Asada, K., 2006. Production and scavenging of reactive oxygen species in chloroplasts and their functions. *Plant physiology*, 141(16760493):391–396. ISSN 1532-2548.

Asano, T., Hayashi, N., Kikuchi, S., and Ohsugi, R., 2012. CDPK-mediated abiotic stress signaling. *Plant signaling & behavior*, 7(22751324):817–821. ISSN 1559-2316.

Ayoubi, T. A. and Van De Ven, W. J., 1996. Regulation of gene expression by alternative promoters. *FASEB journal : official publication of the Federation of American Societies for Experimental Biology*, 10:453–60.

Babbs, C. F., Pham, J. A., and Coolbaugh, R. C., 1989. Lethal hydroxyl radical production in paraquat-treated plants. *Plant physiology*, 90:1267–70.

Balistreri, G., Horvath, P., Schweingruber, C., Zünd, D., McInerney, G., Merits, A., Mühlemann, O., Azzalin, C., and Helenius, A., 2014. The Host Nonsense-Mediated mRNA Decay Pathway Restricts Mammalian RNA Virus Replication. *Cell Host & Microbe*, 16(3):403–411. ISSN 1931-3128. doi:10.1016/j.chom.2014.08.007.

Banani, S. F., Lee, H. O., Hyman, A. A., and Rosen, M. K., 2017. Biomolecular condensates: organizers of cellular biochemistry. *Nature reviews. Molecular cell biology*, 18:285–298.

Banerjee, A. K., 1980. 5'-terminal cap structure in eucaryotic messenger ribonucleic acids. *Microbiological reviews*, 44(6247631):175–205. ISSN 0146-0749.

Barbas, J. A., Chaix, J. C., Steinmetz, M., and Goridis, C., 1988. Differential splicing and alternative polyadenylation generates distinct NCAM transcripts and proteins in the mouse. *The EMBO journal*, 7(3396534):625–632. ISSN 1460-2075.

Baxter, A., Mittler, R., and Suzuki, N., 2014. ROS as key players in plant stress signalling. *Journal of Experimental Botany*, 65(5):1229–1240. ISSN 0022-0957.

Bazzini, A. A., Del Viso, F., Moreno-Mateos, M. A., Johnstone, T. G., Vejnar, C. E., Qin, Y., Yao, J., Khokha, M. K., and Giraldez, A. J., 2016. Codon identity regulates mRNA stability and translation efficiency during the maternal-to-zygotic transition. *The EMBO journal*, 35:2087–2103.

Belew, A. T., Advani, V. M., and Dinman, J. D., 2011. Endogenous ribosomal frameshift signals operate as mRNA destabilizing elements through at least two molecular pathways in yeast. *Nucleic acids research*, 39:2799–808.

Belew, A. T., Hepler, N. L., Jacobs, J. L., and Dinman, J. D., 2008. PRFdb: A database of computationally predicted eukaryotic programmed -1 ribosomal frameshift signals. *BMC Genomics*, 9(1):339. ISSN 1471-2164.

Belew, A. T., Meskauskas, A., Musalgaonkar, S., Advani, V. M., Sulima, S. O., Kasprzak, W. K., Shapiro, B. A., and Dinman, J. D., 2014. Ribosomal frameshifting in the CCR5 mRNA is regulated by miRNAs and the NMD pathway. *Nature*, 512(25043019):265–269. ISSN 0028-0836.

Ben Rejeb, K., Lefebvre-De Vos, D., Le Disquet, I., Leprince, A.-S., Bordenave, M., Maldiney, R., Jdey, A., Abdelly, C., and Savoure, A., 2015. Hydrogen peroxide produced by NADPH oxidases increases proline accumulation during salt or mannitol stress in Arabidopsis thaliana. *The New phytologist*, 208:1138–48.

Berberich, T. and Kusano, T., 1997. Cycloheximide induces a subset of low temperature-inducible genes in maize. *Molecular & general genetics : MGG*, 254:275–83.

Berget, S. M., 1995. Exon recognition in vertebrate splicing. *The Journal of biological chemistry*, 270:2411–4.

Bernstein, P. and Ross, J., 1989. Poly(A), poly(A) binding protein and the regulation of mRNA stability. *Trends in Biochemical Sciences*, 14(9):373 – 377. ISSN 0968-0004. doi:https://doi.org/10.1016/0968-0004(89)90011-X.

Bhattacharya, A., Czaplinski, K., Trifillis, P., He, F., Jacobson, A., and Peltz, S. W., 2000. Characterization of the biochemical properties of the human Upf1 gene product that is involved in nonsense-mediated mRNA decay. *RNA (New York, N.Y.)*, 6:1226–35.

Bienroth, S., Keller, W., and Wahle, E., 1993. Assembly of a processive messenger RNA polyadenylation complex. *The EMBO journal*, 12(8440247):585–594. ISSN 1460-2075.

Black, D. L., 2003. Mechanisms of Alternative Pre-Messenger RNA Splicing. *Annu. Rev. Biochem.*, 72(1):291–336. ISSN 0066-4154. doi:10.1146/annurev.biochem.72.121801.161720.

Blatt, M. R., 2000. Ca2+ signalling and control of guard-cell volume in stomatal movements. *Current Opinion in Plant Biology*, 3(3):196–204. ISSN 1369-5266.

Blom, N., Gammeltoft, S., and Brunak, S., 1999. Sequence and structure-based prediction of eukaryotic protein phosphorylation sites. *Journal of molecular biology*, 294:1351–62.

Bologna, N. G. and Voinnet, O., 2014. The Diversity, Biogenesis, and Activities of Endogenous Silencing Small RNAs in Arabidopsis. *Annu. Rev. Plant Biol.*, 65(1):473–503. ISSN 1543-5008. doi:10.1146/annurev-arplant-050213-035728.

Bond, A. T., Mangus, D. A., He, F., and Jacobson, A., 2001. Absence of Dbp2p alters both nonsense-mediated mRNA decay and rRNA processing. *Molecular and cellular biology*, 21:7366–79.

Bonneh-Barkay, D., Reaney, S. H., Langston, W. J., and Di Monte, D. A., 2005. Redox cycling of the herbicide paraquat in microglial cultures. *Brain research. Molecular brain research*, 134:52–6.

Botella, J. R., Arteca, J. M., Somodevilla, M., and Arteca, R. N., 1996. Calcium-dependent protein kinase gene expression in response to physical and chemical stimuli in mungbean (Vigna radiata). *Plant molecular biology*, 30:1129–37.

Boudsocq, M., Barbier-Brygoo, H., and Lauriere, C., 2004. Identification of nine sucrose nonfermenting 1-related protein kinases 2 activated by hyperosmotic and saline stresses in *Arabidopsis thaliana*. *The Journal of biological chemistry*, 279:41758–66.

Bradley, D. J., Kjellbom, P., and Lamb, C. J., 1992. Elicitor- and wound-induced oxidative cross-linking of a proline-rich plant cell wall protein: A novel, rapid defense response. *Cell*, 70(1):21–30. ISSN 0092-8674.

Brandman, O. and Hegde, R. S., 2016. Ribosome-associated protein quality control. *Nature structural & molecular biology*, 23:7–15.

Brannan, K., Kim, H., Erickson, B., Glover-Cutter, K., Kim, S., Fong, N., Kiemele, L., Hansen, K., Davis, R., Lykke-Andersen, J., and Bentley, D. L., 2012. mRNA decapping factors and the exonuclease Xrn2 function in widespread premature termination of RNA polymerase II transcription. *Molecular cell*, 46:311–24.

Breckenridge, D. G., Germain, M., Mathai, J. P., Nguyen, M., and Shore, G. C., 2003. Regulation of apoptosis by endoplasmic reticulum pathways. *Oncogene*, 22:8608–18.

Brogna, S., McLeod, T., and Petric, M., 2016. The Meaning of NMD: Translate or Perish. *Trends in genetics : TIG*, 32:395–407.

Browning, K. S., 1996. The plant translational apparatus. *Plant molecular biology*, 32:107–44.

Browning, K. S., Webster, C., Roberts, J. K., and Ravel, J. M., 1992. Identification of an isozyme form of protein synthesis initiation factor 4F in plants. *The Journal of biological chemistry*, 267:10096–100.

Brunkard, J. O. and Baker, B., 2018. A Two-Headed Monster to Avert Disaster: HBS1/SKI7 Is Alternatively Spliced to Build Eukaryotic RNA Surveillance Complexes. *Frontiers in plant science*, 9(30258456):1333–1333. ISSN 1664-462X.

Burge, C. B., Tuschl, T., Sharp, P. A., Burge, C. B., Tuschl, T., and Sharp, P. A., 1999. Splicing of Precursors to mRNAs by the Spliceosomes. *2354 Nucleic Acids Research*.

Böhmer, M. and Schroeder, J. I., 2011. Quantitative transcriptomic analysis of abscisic acid-induced and reactive oxygen species-dependent expression changes and proteomic profiling in Arabidopsis suspension cells. *The Plant journal : for cell and molecular biology*, 67(21426425):105–118. ISSN 0960-7412.

Cafferkey, R., Young, P. R., McLaughlin, M. M., Bergsma, D. J., Koltin, Y., Sathe, G. M., Faucette, L., Eng, W. K., Johnson, R. K., and Livi, G. P., 1993. Dominant missense mutations in a novel yeast protein related to mammalian phosphatidylinositol 3-kinase and VPS34 abrogate rapamycin cytotoxicity. *Molecular and cellular biology*, 13:6012–23.

Cai, H., Yang, S., Yan, Y., Xiao, Z., Cheng, J., Wu, J., Qiu, A., Lai, Y., Mou, S., Guan, D., Huang, R., and He, S., 2015. CaWRKY6 transcriptionally activates CaWRKY40, regulates Ralstonia solanacearum resistance, and confers high-temperature and high-humidity tolerance in pepper. *Journal of experimental botany*, 66:3163–74.

Caldana, C., Li, Y., Leisse, A., Zhang, Y., Bartholomaeus, L., Fernie, A. R., Willmitzer, L., and Giavalisco, P., 2013. Systemic analysis of inducible target of rapamycin mutants reveal a general metabolic switch controlling growth in Arabidopsis thaliana. *The Plant journal : for cell and molecular biology*, 73:897–909.

Canto, C. and Auwerx, J., 2010. AMP-activated protein kinase and its downstream transcriptional pathways. *Cellular and molecular life sciences : CMLS*, 67:3407–23.

Carocho, M. and Ferreira, I. C. F. R., 2013. A review on antioxidants, prooxidants and related controversy: Natural and synthetic compounds, screening and analysis methodologies and future perspectives. *Food and Chemical Toxicology*, 51:15–25. ISSN 0278-6915.

Carter, M. S., Doskow, J., Morris, P., Li, S., Nhim, R. P., Sandstedt, S., and Wilkinson, M. F., 1995. A regulatory mechanism that detects premature nonsense codons in T-cell receptor transcripts in vivo is reversed by protein synthesis inhibitors in vitro. *The Journal of biological chemistry*, 270:28995–9003.

Carter, M. S., Li, S., and Wilkinson, M. F., 1996. A splicing-dependent regulatory mechanism that detects translation signals. *The EMBO journal*, 15:5965–75.

Causier, B., Li, Z., De Smet, R., Lloyd, J. P. B., Van de Peer, Y., and Davies, B., 2017. Conservation of Nonsense-Mediated mRNA Decay Complex Components Throughout Eukaryotic Evolution. *Scientific reports*, 7:16692.

Cerana, M., Bonza, M. C., Harris, R., Sanders, D., and De Michelis, M. I., 2006. Abscisic acid stimulates the expression of two isoforms of plasma membrane Ca2+-ATPase in *Arabidopsis thaliana* seedlings. *Plant biology (Stuttgart, Germany)*, 8:572–8.

Chan, L. Y., Mugler, C. F., Heinrich, S., Vallotton, P., Weis, K., Hinnebusch, A. G., Manley, J. L., and Parker, R., 2018. Non-invasive measurement of mRNA decay reveals translation initiation as the major determinant of mRNA stability. *eLife*, 7:e32536. ISSN 2050-084X.

Chang, X., Riemann, M., Liu, Q., and Nick, P., 2015. Actin as deathly switch? How auxin can suppress cell-death related defence. *PloS one*, 10(25933033):e0125498–e0125498. ISSN 1932-6203.

Chantarachot, T. and Bailey-Serres, J., 2018. Polysomes, Stress Granules, and Processing Bodies: A Dynamic Triumvirate Controlling Cytoplasmic mRNA Fate and Function. *Plant Physiol.*, 176(1):254.

Chapman, J. M., Muhlemann, J. K., Gayomba, S. R., and Muday, G. K., 2019. RBOH-Dependent ROS Synthesis and ROS Scavenging by Plant Specialized Metabolites To Modulate Plant Development and Stress Responses. *Chemical research in toxicology*, 32:370–396.

Chehab, E. W., Patharkar, O. R., Hegeman, A. D., Taybi, T., and Cushman, J. C., 2004. Autophosphorylation and subcellular localization dynamics of a salt- and water deficit-induced calcium-dependent protein kinase from ice plant. *Plant physiology*, 135:1430–46.

Chekanova, J. A., Gregory, B. D., Reverdatto, S. V., Chen, H., Kumar, R., Hooker, T., Yazaki, J., Li, P., Skiba, N., Peng, Q., Alonso, J., Brukhin, V., Grossniklaus, U., Ecker, J. R., and Belostotsky, D. A., 2007. Genome-Wide High-Resolution Mapping of Exosome Substrates Reveals Hidden Features in the Arabidopsis Transcriptome. *Cell*, 131(7):1340–1353. ISSN 0092-8674.

Chen, C.-Y. A., Ezzeddine, N., and Shyu, A.-B., 2008. Messenger RNA half-life measurements in mammalian cells. *Methods in enzymology*, 448:335–57.

Chen, T., Cui, P., Chen, H., Ali, S., Zhang, S., and Xiong, L., 2013. A KH-domain RNA-binding protein interacts with FIERY2/CTD phosphatase-like 1 and splicing factors and is important for pre-mRNA splicing in Arabidopsis. *PLoS genetics*, 9:e1003875.

Chen, W., Jia, Q., Song, Y., Fu, H., Wei, G., and Ni, T., 2017a. Alternative Polyadenylation: Methods, Findings, and Impacts. *Genomics, proteomics & bioinformatics*, 15(29031844):287–300. ISSN 1672-0229.

Chen, X.-J., Zhang, X.-H., Hu, L.-D., Zhang, J.-Q., Jiang, Y., Yang, Y., and Yan, Y.-B., 2016. DsCaf1 is involved in environmental stress response of Dunaliella salina. *International journal of biological macromolecules*, 82:369–74.

Chen, Y., Zhou, X., Chang, S., Chu, Z., Wang, H., Han, S., and Wang, Y., 2017b. Calcium-dependent protein kinase 21 phosphorylates 14-3-3 proteins in response to ABA signaling and salt stress in rice. *Biochemical and biophysical research communications*, 493:1450–1456.

Cheng, N.-H., Pittman, J. K., Barkla, B. J., Shigaki, T., and Hirschi, K. D., 2003. The Arabidopsis cax1 mutant exhibits impaired ion homeostasis, development, and hormonal responses and reveals interplay among vacuolar transporters. *The Plant cell*, 15(12566577):347–364. ISSN 1532-298X.

Cheng, N.-h., Pittman, J. K., Shigaki, T., and Hirschi, K. D., 2002. Characterization of CAX4, an Arabidopsis H(+)/cation antiporter. *Plant physiology*, 128(11950973):1245–1254. ISSN 1532-2548.

Cheng, N.-H., Pittman, J. K., Zhu, J.-K., and Hirschi, K. D., 2004. The Protein Kinase SOS2 Activates the Arabidopsis H+/Ca2+ Antiporter CAX1 to Integrate Calcium Transport and Salt Tolerance. *Journal of Biological Chemistry*, 279(4):2922–2926.

Cheng, Z. and Menees, T. M., 2011. RNA splicing and debranching viewed through analysis of RNA lariats. *Molecular Genetics and Genomics*, 286(5):395–410. ISSN 1617-4623.

Cherkasov, V., Hofmann, S., Druffel-Augustin, S., Mogk, A., Tyedmers, J., Stoecklin, G., and Bukau, B., 2013. Coordination of translational control and protein homeostasis during severe heat stress. *Current biology : CB*, 23:2452–62.

Chiba, Y., Johnson, M., Lidder, P., Vogel, J., van Erp, H., and Green, P., 2004. AtPARN is an essential poly(A) ribonuclease in Arabidopsis. *Gene*.

Chicois, C., Scheer, H., Garcia, S., Zuber, H., Mutterer, J., Chicher, J., Hammann, P., Gagliardi, D., and Garcia, D., 2018. The UPF1 interactome reveals interaction networks between RNA degradation and translation repression factors in Arabidopsis. *The Plant journal : for cell and molecular biology*, 96:119–132.

Choi, C., Hwang, S.-H., Fang, I. R., Kwon, S. I., Park, S. R., Ahn, I., Kim, J. B., and Hwang, D.-J., 2015. Molecular characterization of Oryza sativa WRKY6, which binds to W-box-like element 1 of the Oryza sativa pathogenesis-related (PR) 10a promoter and confers reduced susceptibility to pathogens. *The New phytologist*, 208:846–59.

Chou, W.-L., Chung, Y.-L., Fang, J.-C., and Lu, C.-A., 2017. Novel interaction between CCR4 and CAF1 in rice CCR4-NOT deadenylase complex. *Plant molecular biology*, 93:79–96.

Chou, W.-L., Huang, L.-F., Fang, J.-C., Yeh, C.-H., Hong, C.-Y., Wu, S.-J., and Lu, C.-A., 2014. Divergence of the expression and subcellular localization of CCR4-associated factor 1 (CAF1) deadenylase proteins in Oryza sativa. *Plant molecular biology*, 85:443–58.

Chung, J.-S., Zhu, J.-K., Bressan, R. A., Hasegawa, P. M., and Shi, H., 2008. Reactive oxygen species mediate Na+-induced SOS1 mRNA stability in Arabidopsis. *The Plant journal : for cell and molecular biology*, 53:554–65.

Chung, W. S., Lee, S. H., Kim, J. C., Heo, W. D., Kim, M. C., Park, C. Y., Park, H. C., Lim, C. O., Kim, W. B., Harper, J. F., and Cho, M. J., 2000. Identification of a calmodulin-regulated soybean Ca(2+)-ATPase (SCA1) that is located in the plasma membrane. *The Plant cell*, 12(10948258):1393–1407. ISSN 1532-298X.

Clancy, S., 2008. RNA Splicing: Introns, Exons and Spliceosome. *Nature Education*.

Clarkson, D. T. and Hanson, J. B., 1980. The Mineral Nutrition of Higher Plants. *Annu. Rev. Plant. Physiol.*, 31(1):239–298. ISSN 0066-4294. doi:10.1146/annurev.pp.31.060180.001323.

Cohen, P., Holmes, C. F., and Tsukitani, Y., 1990. Okadaic acid: a new probe for the study of cellular regulation. *Trends in biochemical sciences*, 15:98–102.

Collart, M. A., 2016. The Ccr4-Not complex is a key regulator of eukaryotic gene expression. *Wiley interdisciplinary reviews. RNA*, 7:438–54.

Coller, J. and Parker, R., 2004. Eukaryotic mRNA decapping. *Annual review of biochemistry*, 73:861–90.

Coller, J. M., Gray, N. K., and Wickens, M. P., 1998. mRNA stabilization by poly(A) binding protein is independent of poly(A) and requires translation. *Genes & development*, 12(9784497):3226–3235. ISSN 0890-9369.

Cooper, G. M. and Hausman, R. E., 2007. *The Cell: A Molecular Approach. 4th Edition*.

Corvelo, A., Hallegger, M., Smith, C. W. J., and Eyras, E., 2010. Genome-wide association between branch point properties and alternative splicing. *PLoS computational biology*, 6(21124863):e1001016–e1001016. ISSN 1553-734X.

Cougot, N., Babajko, S., and Séraphin, B., 2004. Cytoplasmic foci are sites of mRNA decay in human cells. *J Cell Biol*, 165(1):31.

Czaplinski, K., Weng, Y., Hagan, K. W., and Peltz, S. W., 1995. Purification and characterization of the Upf1 protein: a factor involved in translation and mRNA degradation. *RNA (New York, N.Y.)*, 1:610–23.

Dai, Y., Li, W., and An, L., 2016. NMD mechanism and the functions of Upf proteins in plant. *Plant Cell Reports*, 35(1):5–15. ISSN 1432-203X.

Daszkowska-Golec, A., Skubacz, A., Marzec, M., Slota, M., Kurowska, M., Gajecka, M., Gajewska, P., Plociniczak, T., Sitko, K., Pacak, A., Szweykowska-Kulinska, Z., and Szarejko, I., 2017. Mutation in HvCBP20 (Cap Binding Protein 20) Adapts Barley to Drought Stress at Phenotypic and Transcriptomic Levels. *Frontiers in plant science*, 8:942.

Dat, J. F., Foyer, C. H., and Scott, I. M., 1998a. Changes in Salicylic Acid and Antioxidants during Induced Thermotolerance in Mustard Seedlings. *Plant Physiol.*, 118(4):1455.

Dat, J. F., Lopez-Delgado, H., Foyer, C. H., and Scott, I. M., 1998b. Parallel Changes in H2O2 and Catalase during Thermotolerance Induced by Salicylic Acid or Heat Acclimation in Mustard Seedlings. *Plant Physiol.*, 116(4):1351.

Day, I. S., Reddy, V. S., Shad Ali, G., and Reddy, A. S. N., 2002. Analysis of EF-hand-containing proteins in Arabidopsis. *Genome biology*, 3(12372144):RESEARCH0056–RESEARCH0056. ISSN 1465-6906.

De Virgilio, C. and Loewith, R., 2006. The TOR signalling network from yeast to man. *The international journal of biochemistry & cell biology*, 38:1476–81.

Decker, C. J. and Parker, R., 2012. P-bodies and stress granules: possible roles in the control of translation and mRNA degradation. *Cold Spring Harbor perspectives in biology*, 4:a012286.

Degtiar, E., Fridman, A., Gottlieb, D., Vexler, K., Berezin, I., Farhi, R., Golani, L., and Shaul, O., 2015. The feedback control of UPF3 is crucial for RNA surveillance in plants. *Nucleic acids research*, 43(25820429):4219–4235. ISSN 0305-1048.

Deng, X., Gu, L., Liu, C., Lu, T., Lu, F., Lu, Z., Cui, P., Pei, Y., Wang, B., Hu, S., and Cao, X., 2010. Arginine methylation mediated by the Arabidopsis homolog of PRMT5 is essential for proper pre-mRNA splicing. *Proceedings of the National Academy of Sciences of the United States of America*, 107:19114–9.

Deprost, D., Yao, L., Sormani, R., Moreau, M., Leterreux, G., Nicolai, M., Bedu, M., Robaglia, C., and Meyer, C., 2007. The Arabidopsis TOR kinase links plant growth, yield, stress resistance and mRNA translation. *EMBO reports*, 8:864–70.

Desikan, R., Last, K., Harrett-Williams, R., Tagliavia, C., Harter, K., Hooley, R., Hancock, J. T., and Neill, S. J., 2006. Ethylene-induced stomatal closure in Arabidopsis occurs via AtrbohF-mediated hydrogen peroxide synthesis. *The Plant journal : for cell and molecular biology*, 47:907–16.

Deyholos, M. K., Cavaness, G. F., Hall, B., King, E., Punwani, J., Van Norman, J., and Sieburth, L. E., 2003. VARICOSE, a WD-domain protein, is required for leaf blade development. *Development*, 130(26):6577.

DeYoung, B. J. and Innes, R. W., 2006. Plant NBS-LRR proteins in pathogen sensing and host defense. *Nature immunology*, 7(17110940):1243–1249. ISSN 1529-2916.

Dinesh-Kumar, S. P. and Baker, B. J., 2000. Alternatively spliced N resistance gene transcripts: their possible role in tobacco mosaic virus resistance. *Proceedings of the National Academy of Sciences of the United States of America*, 97:1908–13.

Ding, F., Cui, P., Wang, Z., Zhang, S., Ali, S., and Xiong, L., 2014. Genome-wide analysis of alternative splicing of pre-mRNA under salt stress in Arabidopsis. *BMC genomics*, 15:431.

Dixon, D. P., Skipsey, M., Grundy, N. M., and Edwards, R., 2005. Stress-induced protein S-glutathionylation in Arabidopsis. *Plant physiology*, 138:2233–44.

Dodge, A. D., 1971. The mode of action of the bipyridylium herbicides, paraquat and diquat. *Endeavour*, 30:130–5.

Doke, N., 1985. NADPH-dependent O2- generation in membrane fractions isolated from wounded potato tubers inoculated with *Phytophthora infestans*. *Physiological Plant Pathology*, 27(3):311–322. ISSN 0048-4059.

Doma, M. K. and Parker, R., 2006. Endonucleolytic cleavage of eukaryotic mRNAs with stalls in translation elongation. *Nature*, 440(7083):561–564. ISSN 1476-4687.

Dong, Y., Silbermann, M., Speiser, A., Forieri, I., Linster, E., Poschet, G., Allboje Samami, A., Wanatabe, M., Sticht, C., Teleman, A. A., Deragon, J.-M., Saito,

K., Hell, R., and Wirtz, M., 2017. Sulfur availability regulates plant growth via glucose-TOR signaling. *Nature communications*, 8(29079776):1174–1174. ISSN 2041-1723.

Doyle, M., Jaskiewicz, L., Filipowicz, W., Guo, F., and Tamanoi, F., 2012. Chapter One - Dicer Proteins and Their Role in Gene Silencing Pathways. In *The Enzymes*, volume 32. Academic Press, pp. 1–35.

Drechsel, G., Kahles, A., Kesarwani, A. K., Stauffer, E., Behr, J., Drewe, P., Rätsch, G., and Wachter, A., 2013. Nonsense-Mediated Decay of Alternative Precursor mRNA Splicing Variants Is a Major Determinant of the *Arabidopsis* Steady State Transcriptome. *Plant Cell*, 25(10):3726.

Drechsel, G., Raab, S., and Hoth, S., 2010. Arabidopsis zinc-finger protein 2 is a negative regulator of ABA signaling during seed germination. *Journal of plant physiology*, 167:1418–21.

Du, J., Gao, Y., Zhan, Y., Zhang, S., Wu, Y., Xiao, Y., Zou, B., He, K., Gou, X., Li, G., Lin, H., and Li, J., 2016. Nucleocytoplasmic trafficking is essential for BAK1- and BKK1-mediated cell-death control. *The Plant journal : for cell and molecular biology*, 85:520–31.

Dubiella, U., Seybold, H., Durian, G., Komander, E., Lassig, R., Witte, C.-P., Schulze, W. X., and Romeis, T., 2013. Calcium-dependent protein kinase/NADPH oxidase activation circuit is required for rapid defense signal propagation. *Proceedings of the National Academy of Sciences of the United States of America*, 110(23650383):8744–8749. ISSN 0027-8424.

Egawa, C., Kobayashi, F., Ishibashi, M., Nakamura, T., Nakamura, C., and Takumi, S., 2006. Differential regulation of transcript accumulation and alternative splicing of a DREB2 homolog under abiotic stress conditions in common wheat. *Genes & genetic systems*, 81:77–91.

Eggenberger, K., Sanyal, P., Hundt, S., Wadhwani, P., Ulrich, A. S., and Nick, P., 2017. Challenge Integrity: The Cell-Penetrating Peptide BP100 Interferes with the Auxin-Actin Oscillator. *Plant & cell physiology*, 58:71–85.

Estavillo, G. M., Crisp, P. A., Pornsiriwong, W., Wirtz, M., Collinge, D., Carrie, C., Giraud, E., Whelan, J., David, P., Javot, H., Brearley, C., Hell, R., Marin, E., and Pogson, B. J., 2011. Evidence for a SAL1-PAP chloroplast retrograde pathway that functions in drought and high light signaling in Arabidopsis. *The Plant cell*, 23:3992–4012.

Evans, D. E. and Williams, L. E., 1998. P-type calcium ATPases in higher plants - biochemical, molecular and functional properties. *Biochimica et biophysica acta*, 1376:1–25.

Fagard, M., Dellagi, A., Roux, C., Perino, C., Rigault, M., Boucher, V., Shevchik, V. E., and Expert, D., 2007. Arabidopsis thaliana expresses multiple lines of defense to counterattack Erwinia chrysanthemi. *Molecular plant-microbe interactions : MPMI*, 20:794–805.

Fan, X., Guo, Q., Xu, P., Gong, Y., Shu, H., Yang, Y., Ni, W., Zhang, X., and Shen, X., 2015. Transcriptome-wide identification of salt-responsive members of the WRKY gene family in Gossypium aridum. *PloS one*, 10(25951083):e0126148–e0126148. ISSN 1932-6203.

Farrell, R. E., 2010. Chapter 15 - Quantification of Specific mRNAs by Nuclease Protection. In *RNA Methodologies (Fourth Edition)*. Academic Press, San Diego, pp. 321–339.

Feng, C.-Z., Chen, Y., Wang, C., Kong, Y.-H., Wu, W.-H., and Chen, Y.-F., 2014. Arabidopsis RAV1 transcription factor, phosphorylated by SnRK2 kinases, regulates the expression of ABI3, ABI4, and ABI5 during seed germination and early seedling development. *The Plant journal : for cell and molecular biology*, 80:654–68.

Feng, J., Li, J., Gao, Z., Lu, Y., Yu, J., Zheng, Q., Yan, S., Zhang, W., He, H., Ma, L., and Zhu, Z., 2015. SKIP Confers Osmotic Tolerance during Salt Stress by Controlling Alternative Gene Splicing in *Arabidopsis*. *Molecular Plant*, 8(7):1038–1052. ISSN 1674-2052. doi:10.1016/j.molp.2015.01.011.

Fica, S. M., Tuttle, N., Novak, T., Li, N.-S., Lu, J., Koodathingal, P., Dai, Q., Staley, J. P., and Piccirilli, J. A., 2013. RNA catalyses nuclear pre-mRNA splicing. *Nature*, 503:229.

Filichkin, S. A., Cumbie, J. S., Dharmawardhana, P., Jaiswal, P., Chang, J. H., Palusa, S. G., Reddy, A. S. N., Megraw, M., and Mockler, T. C., 2015. Environmental stresses modulate abundance and timing of alternatively spliced circadian transcripts in Arabidopsis. *Molecular plant*, 8:207–27.

Filichkin, S. A., Priest, H. D., Givan, S. A., Shen, R., Bryant, D. W., Fox, S. E., Wong, W.-K., and Mockler, T. C., 2010. Genome-wide mapping of alternative splicing in Arabidopsis thaliana. *Genome research*, 20(19858364):45–58. ISSN 1088-9051.

Flowers, T. J. and Colmer, T. D., 2008. Salinity tolerance in halophytes. *New Phytologist*, 179(4):945–963. ISSN 0028-646X. doi:10.1111/j.1469-8137.2008.02531.x.

Foreman, J., Demidchik, V., Bothwell, J. H. F., Mylona, P., Miedema, H., Torres, M. A., Linstead, P., Costa, S., Brownlee, C., Jones, J. D. G., Davies, J. M., and Dolan, L., 2003. Reactive oxygen species produced by NADPH oxidase regulate plant cell growth. *Nature*, 422:442–6.

Foyer, N. G., Christine H, 2016. Stress-triggered redox signalling: what's in pROSpect? *Plant, Cell & Environment*, 39(5):951–964. ISSN 1365-3040. doi:10.1111/pce.12621. PCE-15-0311.R1.

Frischmeyer, P. A., van Hoof, A., O'Donnell, K., Guerrerio, A. L., Parker, R., and Dietz, H. C., 2002. An mRNA surveillance mechanism that eliminates transcripts lacking termination codons. *Science (New York, N.Y.)*, 295:2258–61.

Fujii, H., Verslues, P. E., and Zhu, J.-K., 2007. Identification of two protein kinases required for abscisic acid regulation of seed germination, root growth, and gene expression in Arabidopsis. *The Plant cell*, 19:485–94.

Fujii, H., Verslues, P. E., and Zhu, J.-K., 2011. Arabidopsis decuple mutant reveals the importance of SnRK2 kinases in osmotic stress responses in vivo. *Proceedings of the National Academy of Sciences of the United States of America*, 108:1717–22.

Fujii, H. and Zhu, J.-K., 2009a. Arabidopsis mutant deficient in 3 abscisic acid-activated protein kinases reveals critical roles in growth, reproduction, and stress. *Proceedings of the National Academy of Sciences of the United States of America*, 106:8380–5.

Fujii, H. and Zhu, J.-K., 2009b. An autophosphorylation site of the protein kinase SOS2 is important for salt tolerance in Arabidopsis. *Molecular plant*, 2:183–90.

Fujii, T., Yokoyama, E.-i., Inoue, K., and Sakurai, H., 1990. The sites of electron donation of Photosystem I to methyl viologen. *Biochimica et Biophysica Acta (BBA) - Bioenergetics*, 1015(1):41–48. ISSN 0005-2728.

Fujita, Y., Nakashima, K., Yoshida, T., Katagiri, T., Kidokoro, S., Kanamori, N., Umezawa, T., Fujita, M., Maruyama, K., Ishiyama, K., Kobayashi, M., Nakasone, S., Yamada, K., Ito, T., Shinozaki, K., and Yamaguchi-Shinozaki, K., 2009. Three SnRK2 protein kinases are the main positive regulators of abscisic acid signaling in response to water stress in Arabidopsis. *Plant & cell physiology*, 50:2123–32.

Fujita, Y., Yoshida, T., and Yamaguchi-Shinozaki, K., 2013. Pivotal role of the AREB/ABF-SnRK2 pathway in ABRE-mediated transcription in response to osmotic stress in plants. *Physiologia plantarum*, 147:15–27.

Fukuhara, N., Ebert, J., Unterholzner, L., Lindner, D., Izaurralde, E., and Conti, E., 2005. SMG7 is a 14-3-3-like adaptor in the nonsense-mediated mRNA decay pathway. *Molecular cell*, 17:537–47.

Furihata, T., Maruyama, K., Fujita, Y., Umezawa, T., Yoshida, R., Shinozaki, K., and Yamaguchi-Shinozaki, K., 2006. Abscisic acid-dependent multisite phosphorylation regulates the activity of a transcription activator AREB1. *Proceedings of the National Academy of Sciences of the United States of America*, 103:1988–93.

Gandin, V., Masvidal, L., Hulea, L., Gravel, S.-P., Cargnello, M., McLaughlan, S., Cai, Y., Balanathan, P., Morita, M., Rajakumar, A., Furic, L., Pollak, M., Porco, J. A. J., St-Pierre, J., Pelletier, J., Larsson, O., and Topisirovic, I., 2016. nanoCAGE reveals 5' UTR features that define specific modes of translation of functionally related MTOR-sensitive mRNAs. *Genome research*, 26:636–48.

Gao, J.-P., Chao, D.-Y., and Lin, H.-X., 2007. Understanding Abiotic Stress Tolerance Mechanisms: Recent Studies on Stress Response in Rice. *Journal of Integrative Plant Biology*, 49(6):742–750. ISSN 1672-9072. doi:10.1111/j.1744-7909.2007.00495.x.

Garciadeblas, B., Benito, B., and Rodríguez-Navarro, A., 2001. Plant cells express several stress calcium ATPases but apparently no sodium ATPase. *Plant and Soil*, 235(2):181–192. ISSN 1573-5036.

Gardner, L. B., 2008. Hypoxic inhibition of nonsense-mediated RNA decay regulates gene expression and the integrated stress response. *Molecular and cellular biology*, 28(18362164):3729–3741. ISSN 0270-7306.

Gardner, L. B., 2010. Nonsense-mediated RNA decay regulation by cellular stress: implications for tumorigenesis. *Molecular cancer research : MCR*, 8(20179151):295–308. ISSN 1541-7786.

Garneau, N. L., Wilusz, J., and Wilusz, C. J., 2007. The highways and byways of mRNA decay. *Nature reviews. Molecular cell biology*, 8:113–26.

Garzia, A., Jafarnejad, S. M., Meyer, C., Chapat, C., Gogakos, T., Morozov, P., Amiri, M., Shapiro, M., Molina, H., Tuschl, T., and Sonenberg, N., 2017. The E3 ubiquitin ligase and RNA-binding protein ZNF598 orchestrates ribosome quality control of premature polyadenylated mRNAs. *Nature Communications*, 8:16056.

GB, M., TN, B., MH, W., and S., G., 2009. Ca2+ regulates reactive oxygen species production and pH during mechanosensing in Arabidopsis roots. *Plant Cell*, 21:2341–2356.

Geisler, M., Frangne, N., Gomès, E., Martinoia, E., and Palmgren, M. G., 2000. The ACA4 gene of Arabidopsis encodes a vacuolar membrane calcium pump that improves salt tolerance in yeast. *Plant physiology*, 124:1814–27.

Gendreau, E., Corbineau, F., Hoang, H. H., El-Maarouf-Bouteau, H., Leymarie, J., Meimoun, P., Chazoule, V., Bailly, C., and Vitkauskaité, G., 2017. Role of Reactive Oxygen Species in the Regulation of Arabidopsis Seed Dormancy. *pcp*, 53(1):96–106. ISSN 0032-0781.

Germain, H., Qu, N., Cheng, Y. T., Lee, E., Huang, Y., Dong, O. X., Gannon, P., Huang, S., Ding, P., Li, Y., Sack, F., Zhang, Y., and Li, X., 2010. MOS11: a new component in the mRNA export pathway. *PLoS genetics*, 6:e1001250.

Gilroy, S., Białasek, M., Suzuki, N., Górecka, M., Devireddy, A. R., Karpiński, S., and Mittler, R., 2016a. ROS, Calcium, and Electric Signals: Key Mediators of Rapid Systemic Signaling in Plants. *Plant Physiology*, 171(3):1606–1615. doi: 10.1104/pp.16.00434.

Gilroy, S., Suzuki, N., Miller, G., Choi, W.-G., Toyota, M., Devireddy, A. R., and Mittler, R., 2016b. A tidal wave of signals: calcium and ROS at the forefront of rapid systemic signaling. *Trends in Plant Science*, 19(10):623–630. ISSN 1360-1385. doi:10.1016/j.tplants.2014.06.013.

Gloggnitzer, J., Akimcheva, S., Srinivasan, A., Kusenda, B., Riehs, N., Stampfl, H., Bautor, J., Dekrout, B., Jonak, C., Jiménez-Gómez, J. M., Parker, J. E., and Riha, K., 2014. Nonsense-Mediated mRNA Decay Modulates Immune Receptor Levels to Regulate Plant Antibacterial Defense. *Cell Host & Microbe*, 16(3):376 – 390. ISSN 1931-3128. doi:https://doi.org/10.1016/j.chom.2014.08.010.

Goeres, D. C., Van Norman, J. M., Zhang, W., Fauver, N. A., Spencer, M. L., and Sieburth, L. E., 2007. Components of the *Arabidopsis* mRNA Decapping Complex Are Required for Early Seedling Development. *Plant Cell*, 19(5):1549.

Goetz, A. E. and Wilkinson, M., 2017. Stress and the nonsense-mediated RNA decay pathway. *Cellular and molecular life sciences : CMLS*, 74(28503708):3509–3531. ISSN 1420-682X.

Gong, M., Li, Y.-J., and Chen, S.-Z., 1998. Abscisic acid-induced thermotolerance in maize seedlings is mediated by calcium and associated with antioxidant systems. *Journal of Plant Physiology*, 153(3):488–496. ISSN 0176-1617.

Gong, Z., Dong, C.-H., Lee, H., Zhu, J., Xiong, L., Gong, D., Stevenson, B., and Zhu, J.-K., 2005. A DEAD box RNA helicase is essential for mRNA export and important for development and stress responses in Arabidopsis. *The Plant cell*, 17:256–67.

Grabov, A. and Blatt, M. R., 1998. Membrane voltage initiates Ca2+ waves and potentiates Ca2+ increases with abscisic acid in stomatal guard cells. *Proceedings of the National Academy of Sciences of the United States of America*, 95(9539815):4778–4783. ISSN 1091-6490.

Graveley, B. R., Hertel, K. J., and Maniatis, T., 2001. The role of U2AF35 and U2AF65 in enhancer-dependent splicing. *RNA (New York, N.Y.)*, 7:806–18.

Guan, Q., Wu, J., Yue, X., Zhang, Y., and Zhu, J., 2013a. A Nuclear Calcium-Sensing Pathway Is Critical for Gene Regulation and Salt Stress Tolerance in Arabidopsis. *PLOS Genetics*, 9(8):e1003755. doi:10.1371/journal.pgen.1003755.

Guan, Q., Wu, J., Zhang, Y., Jiang, C., Liu, R., Chai, C., and Zhu, J., 2013b. A DEAD box RNA helicase is critical for pre-mRNA splicing, cold-responsive gene regulation, and cold tolerance in Arabidopsis. *The Plant cell*, 25:342–56.

Gudipati, R., Villa, T., Boulay, J., and Libri, D., 2008. Phosphorylation of the RNA polymerase II C-terminal domain dictates transcription termination choice. *Nat. Struct. Mol. Biol.*

Guhaniyogi, J. and Brewer, G., 2001. Regulation of mRNA stability in mammalian cells. *Gene*, 265(1):11–23. ISSN 0378-1119.

Guo, Y., Halfter, U., Ishitani, M., and Zhu, J. K., 2001. Molecular characterization of functional domains in the protein kinase SOS2 that is required for plant salt tolerance. *The Plant cell*, 13(11402167):1383–1400. ISSN 1532-298X.

Guo, Y., Qiu, Q.-S., Quintero, F. J., Pardo, J. M., Ohta, M., Zhang, C., Schumaker, K. S., and Zhu, J.-K., 2004. Transgenic evaluation of activated mutant alleles of SOS2 reveals a critical requirement for its kinase activity and C-terminal regulatory domain for salt tolerance in Arabidopsis thaliana. *The Plant cell*, 16(14742879):435–449. ISSN 1532-298X.

Guth, S. and Valcárcel, J., 2000. Kinetic Role for Mammalian SF1/BBP in Spliceosome Assembly and Function after Polypyrimidine Tract Recognition by U2AF. *Journal of Biological Chemistry*.

Gutierrez, R. A., Ewing, R. M., Cherry, J. M., and Green, P. J., 2002. Identification of unstable transcripts in Arabidopsis by cDNA microarray analysis: rapid

decay is associated with a group of touch- and specific clock-controlled genes. *Proceedings of the National Academy of Sciences of the United States of America*, 99(12167669):11513–11518. ISSN 1091-6490.

Gutierrez-Beltran, E., Moschou, P. N., Smertenko, A. P., and Bozhkov, P. V., 2015. Tudor staphylococcal nuclease links formation of stress granules and processing bodies with mRNA catabolism in Arabidopsis. *The Plant cell*, 27:926–43.

Gy, I., Gasciolli, V., Lauressergues, D., Morel, J.-B., Gombert, J., Proux, F., Proux, C., Vaucheret, H., and Mallory, A. C., 2007. Arabidopsis FIERY1, XRN2, and XRN3 are endogenous RNA silencing suppressors. *The Plant cell*, 19:3451–61.

Halbach, F., Reichelt, P., Rode, M., and Conti, E., 2013. The yeast ski complex: crystal structure and RNA channeling to the exosome complex. *Cell*, 154:814–26.

Haley, T. J., 1979. Review of the toxicology of paraquat (1,1'-dimethyl-4,4'-bipyridinium chloride). *Clinical toxicology*, 14:1–46.

Halfter, U., Ishitani, M., and Zhu, J.-K., 2000. The *Arabidopsis* SOS2 protein kinase physically interacts with and is activated by the calcium-binding protein SOS3. *Proc Natl Acad Sci USA*, 97(7):3735.

Hamada, T., Yako, M., Minegishi, M., Sato, M., Kamei, Y., Yanagawa, Y., Toyooka, K., Watanabe, Y., and Hara-Nishimura, I., 2018. Stress granule formation is induced by a threshold temperature rather than a temperature difference in Arabidopsis. *J. Cell Sci.*:jcs.216051.

Hamid, F. M. and Makeyev, E. V., 2016. Exaptive origins of regulated mRNA decay in eukaryotes. *BioEssays*, 38(9):830–838. ISSN 0265-9247. doi:10.1002/bies.201600100.

Han, H.-J., Peng, R.-H., Zhu, B., Fu, X.-Y., Zhao, W., Shi, B., and Yao, Q.-H., 2014. Gene expression profiles of Arabidopsis under the stress of methyl viologen: a microarray analysis. *Molecular biology reports*, 41:7089–102.

Harding, H. P., Zhang, Y., and Ron, D., 1999. Protein translation and folding are coupled by an endoplasmic-reticulum-resident kinase. *Nature*, 397:271–4.

Harigaya, Y. and Parker, R., 2016. Analysis of the association between codon optimality and mRNA stability in Schizosaccharomyces pombe. *BMC genomics*, 17:895.

Harmon, A. C., Gribskov, M., Gubrium, E., and Harper, J. F., 2001. The CDPK superfamily of protein kinases. *New Phytologist*, 151(1):175–183. ISSN 0028-646X. doi:10.1046/j.1469-8137.2001.00171.x.

Harrold, S., Genovese, C., Kobrin, B., Morrison, S. L., and Milcarek, C., 1991. A comparison of apparent mRNA half-life using kinetic labeling techniques vs decay following administration of transcriptional inhibitors. *Analytical Biochemistry*, 198(1):19 – 29. ISSN 0003-2697. doi:https://doi.org/10.1016/0003-2697(91)90500-S.

Hartmann, L., Wiessner, T., and Wachter, A., 2018. Subcellular Compartmentation of Alternatively Spliced Transcripts Defines *SERINE/ARGININE-RICH PROTEIN30* Expression. *Plant physiology*, 176:2886–2903.

Hashimoto, Y., Nakayama, T., Teramoto, T., Kato, H., Watanabe, T., Kinoshita, M., Tsukamoto, K., Tokunaga, K., Kurokawa, K., and Nakanishi, S., 1991. Potent and preferential inhibition of Ca2+/calmodulin-dependent protein kinase II by K252a and its derivative, KT5926. *Biochemical and biophysical research communications*, 181:423–9.

Haystead, T. A., Sim, A. T., Carling, D., Honnor, R. C., Tsukitani, Y., Cohen, P., and Hardie, D. G., 1989. Effects of the tumour promoter okadaic acid on intracellular protein phosphorylation and metabolism. *Nature*, 337:78–81.

He, F. and Jacobson, A., 2015. Nonsense-Mediated mRNA Decay: Degradation of Defective Transcripts Is Only Part of the Story. *Annual review of genetics*, 49(26436458):339–366. ISSN 0066-4197.

Herrick, D., Parker, R., and Jacobson, A., 1990. Identification and comparison of stable and unstable mRNAs in Saccharomyces cerevisiae. *Molecular and cellular biology*, 10:2269–84.

Hescheler, J., Mieskes, G., Rüegg, J. C., Takai, A., and Trautwein, W., 1988. Effects of a protein phosphatase inhibitor, okadaic acid, on membrane currents of isolated guinea-pig cardiac myocytes. *Pflügers Archiv*, 412(3):248–252. ISSN 1432-2013.

Hetz, C., Bernasconi, P., Fisher, J., Lee, A.-H., Bassik, M. C., Antonsson, B., Brandt, G. S., Iwakoshi, N. N., Schinzel, A., Glimcher, L. H., and Korsmeyer, S. J., 2006. Proapoptotic BAX and BAK Modulate the Unfolded Protein Response by a Direct Interaction with IRE1α. *Science*, 312(5773):572.

Holappa, L. D. and Walker-Simmons, M. K., 1995. The Wheat Abscisic Acid-Responsive Protein Kinase mRNA, PKABA1, Is Up-Regulated by Dehydration, Cold Temperature, and Osmotic Stress. *Plant physiology*, 108:1203–1210.

Holmes, C. F. B., Luu, H. A., Carrier, F., and Schmitz, F. J., 1990. Inhibition of protein phosphatases-1 and -2A with acanthifolicin. *FEBS Letters*, 270(1-2):216–218. ISSN 0014-5793. doi:10.1016/0014-5793(90)81271-o.

Honkanen, R. E., Zwiller, J., Moore, R. E., Daily, S. L., Khatra, B. S., Dukelow, M., and Boynton, A. L., 1990. Characterization of microcystin-LR, a potent inhibitor of type 1 and type 2A protein phosphatases. *The Journal of biological chemistry*, 265:19401–4.

Hori, K. and Watanabe, Y., 2005. UPF3 suppresses aberrant spliced mRNA in Arabidopsis. *The Plant journal : for cell and molecular biology*, 43:530–40.

Hori, K. and Watanabe, Y., 2007. Context analysis of termination codons in mRNA that are recognized by plant NMD. *Plant & cell physiology*, 48:1072–8.

Houseley, J. and Tollervey, D., 2009. The Many Pathways of RNA Degradation. *Cell*, 136(4):763–776. ISSN 0092-8674. doi:10.1016/j.cell.2009.01.019.

Hrabak, E. M., Chan, C. W. M., Gribskov, M., Harper, J. F., Choi, J. H., Halford, N., Kudla, J., Luan, S., Nimmo, H. G., Sussman, M. R., Thomas, M., Walker-Simmons, K., Zhu, J.-K., and Harmon, A. C., 2003. The Arabidopsis CDPK-SnRK Superfamily of Protein Kinases. *Plant Physiol.*, 132(2):666.

Hu, W., Sweet, T. J., Chamnongpol, S., Baker, K. E., and Coller, J., 2009. Co-translational mRNA decay in *Saccharomyces cerevisiae*. *Nature*, 461:225–9.

Huang, D., Ou, B., and Prior, R. L., 2005. The Chemistry behind Antioxidant Capacity Assays. *J. Agric. Food Chem.*, 53(6):1841–1856. ISSN 0021-8561. doi: 10.1021/jf030723c.

Huang, K., Peng, L., Liu, Y., Yao, R., Liu, Z., Li, X., Yang, Y., and Wang, J., 2018. Arabidopsis calcium-dependent protein kinase AtCPK1 plays a positive role in salt/drought-stress response. *Biochemical and biophysical research communications*, 498:92–98.

Huang, L., Lou, C.-H., Chan, W., Shum, E. Y., Shao, A., Stone, E., Karam, R., Song, H.-W., and Wilkinson, M. F., 2011. RNA homeostasis governed by cell type-specific and branched feedback loops acting on NMD. *Molecular cell*, 43:950–61.

Huang, X. and Honkanen, R. E., 1998. Molecular cloning, expression, and characterization of a novel human serine/threonine protein phosphatase, PP7, that is homologous to Drosophila retinal degeneration C gene product (rdgC). *The Journal of biological chemistry*, 273:1462–8.

Huang, Y., Feng, C.-Z., Ye, Q., Wu, W.-H., and Chen, Y.-F., 2016. Arabidopsis WRKY6 Transcription Factor Acts as a Positive Regulator of Abscisic Acid Signaling during Seed Germination and Early Seedling Development. *PLOS Genetics*, 12(2):e1005833. doi:10.1371/journal.pgen.1005833.

Hugouvieux, V., Kwak, J. M., and Schroeder, J. I., 2001. An mRNA cap binding protein, ABH1, modulates early abscisic acid signal transduction in Arabidopsis. *Cell*, 106:477–87.

Hull, R., 2014. Chapter 9 - Virus-Plant Interactions: RNA Silencing. In *Plant Virology (Fifth Edition)*. Academic Press, Boston, pp. 477–530.

Hunt, A. G., Xu, R., Addepalli, B., Rao, S., Forbes, K. P., Meeks, L. R., Xing, D., Mo, M., Zhao, H., Bandyopadhyay, A., Dampanaboina, L., Marion, A., Von Lanken, C., and Li, Q. Q., 2008. Arabidopsis mRNA polyadenylation machinery: comprehensive analysis of protein-protein interactions and gene expression profiling. *BMC genomics*, 9(18479511):220–220. ISSN 1471-2164.

Huntzinger, E., Kashima, I., Fauser, M., Saulière, J., and Izaurralde, E., 2008. SMG6 is the catalytic endonuclease that cleaves mRNAs containing nonsense codons in metazoan. *RNA (New York, N.Y.)*, 14(18974281):2609–2617. ISSN 1355-8382.

Hynes, N. E. and Phillips, S. L., 1976. Turnover of polyadenylate-containing ribonucleic acid in Saccharomyces cerevisiae. *Journal of bacteriology*, 125:595–600.

Inada, T., 2013. Quality control systems for aberrant mRNAs induced by aberrant translation elongation and termination. *Biochimica et biophysica acta*, 1829:634–42.

Ishitani, M., Liu, J., Halfter, U., Kim, C.-S., Shi, W., and Zhu, J.-K., 2000. SOS3 Function in Plant Salt Tolerance Requires N-Myristoylation and Calcium Binding. *Plant Cell*, 12(9):1667.

Isken, O. and Maquat, L. E., 2007. Quality control of eukaryotic mRNA: safeguarding cells from abnormal mRNA function. *Genes & development*, 21:1833–56.

Jabs, T., Tschöpe, M., Colling, C., Hahlbrock, K., and Scheel, D., 1997. Elicitor-stimulated ion fluxes and O2- from the oxidative burst are essential components in triggering defense gene activation and phytoalexin synthesis in parsley. *Proc Natl Acad Sci USA*, 94(9):4800.

Jackson, R. J., Hellen, C. U. T., and Pestova, T. V., 2012. Termination and post-termination events in eukaryotic translation. *Advances in protein chemistry and structural biology*, 86:45–93.

Janke, R., Kong, J., Braberg, H., Cantin, G., Yates, r., John R, Krogan, N. J., and Heyer, W.-D., 2016. Nonsense-mediated decay regulates key components of homologous recombination. *Nucleic acids research*, 44(27001511):5218–5230. ISSN 0305-1048.

Januszyk, K. and Lima, C. D., 2014. The eukaryotic RNA exosome. *Current Opinion in Structural Biology*, 24:132–140. ISSN 0959-440X.

Jeacock, L., Faria, J., and Horn, D., 2018. Codon usage bias controls mRNA and protein abundance in trypanosomatids. *eLife*, 7.

Jeong, H.-J., Kim, Y. J., Kim, S. H., Kim, Y.-H., Lee, I.-J., Kim, Y. K., and Shin, J. S., 2011. Nonsense-mediated mRNA decay factors, UPF1 and UPF3, contribute to plant defense. *Plant & cell physiology*, 52:2147–56.

Ji, H., Pardo, J. M., Batelli, G., Van Oosten, M. J., Bressan, R. A., and Li, X., 2013. The Salt Overly Sensitive (SOS) Pathway: Established and Emerging Roles. *Molecular Plant*, 6(2):275–286. ISSN 1674-2052.

Jiang, C., Belfield, E. J., Mithani, A., Visscher, A., Ragoussis, J., Mott, R., Smith, J. A. C., and Harberd, N. P., 2012. ROS-mediated vascular homeostatic control of root-to-shoot soil Na delivery in Arabidopsis. *The EMBO journal*, 31:4359–70.

Jiang, Z., Zhu, S., Ye, R., Xue, Y., Chen, A., An, L., and Pei, Z.-M., 2013. Relationship between NaCl- and H2O2-Induced Cytosolic Ca2+ Increases in Response to Stress in Arabidopsis. *PLOS ONE*, 8(10):e76130. doi:10.1371/journal.pone.0076130.

Jonas, S., Weichenrieder, O., and Izaurralde, E., 2013. An unusual arrangement of two 14-3-3-like domains in the SMG5-SMG7 heterodimer is required for efficient nonsense-mediated mRNA decay. *Genes & Development*, 27(2):211–225.

Jones, M. A., Williams, B. A., McNicol, J., Simpson, C. G., Brown, J. W. S., and Harmer, S. L., 2012. Mutation of Arabidopsis spliceosomal timekeeper locus1 causes circadian clock defects. *The Plant cell*, 24:4066–82.

Juszkiewicz, S. and Hegde, R. S., 2017. Initiation of Quality Control during Poly(A) Translation Requires Site-Specific Ribosome Ubiquitination. *Molecular Cell*, 65(4):743–750.e4. ISSN 1097-2765.

Kadota, Y., Shirasu, K., and Zipfel, C., 2015. Regulation of the NADPH Oxidase RBOHD During Plant Immunity. *Plant & cell physiology*, 56:1472–80.

Kalyna, M., Simpson, C. G., Syed, N. H., Lewandowska, D., Marquez, Y., Kusenda, B., Marshall, J., Fuller, J., Cardle, L., McNicol, J., Dinh, H. Q., Barta, A., and Brown, J. W. S., 2012. Alternative splicing and nonsense-mediated decay modulate expression of important regulatory genes in Arabidopsis. *Nucleic Acids Research*, 40(6):2454–2469. ISSN 0305-1048. doi:10.1093/nar/gkr932.

Kampinga, H. H., Brunsting, J. F., Stege, G. J., Burgman, P. W., and Konings, A. W., 1995. Thermal protein denaturation and protein aggregation in cells made thermotolerant by various chemicals: role of heat shock proteins. *Experimental cell research*, 219:536–46.

Karam, R., Lou, C.-H., Kroeger, H., Huang, L., Lin, J. H., and Wilkinson, M. F., 2015. The unfolded protein response is shaped by the NMD pathway. *EMBO reports*, 16(25807986):599–609. ISSN 1469-221X.

Karam, R., Wengrod, J., Gardner, L. B., and Wilkinson, M. F., 2013. Regulation of nonsense-mediated mRNA decay: implications for physiology and disease. *Biochimica et biophysica acta*, 1829(23500037):624–633. ISSN 0006-3002.

Karousis, E. D. and Muhlemann, O., 2019. Nonsense-Mediated mRNA Decay Begins Where Translation Ends. *Cold Spring Harbor perspectives in biology*, 11.

Karousis, E. D., Nasif, S., and Muhlemann, O., 2016. Nonsense-mediated mRNA decay: novel mechanistic insights and biological impact. *Wiley interdisciplinary reviews. RNA*, 7:661–82.

Kase, H., Iwahashi, K., Nakanishi, S., Matsuda, Y., Yamada, K., Takahashi, M., Murakata, C., Sato, A., and Kaneko, M., 1987. K-252 compounds, novel and potent inhibitors of protein kinase C and cyclic nucleotide-dependent protein kinases. *Biochemical and biophysical research communications*, 142:436–40.

Kastenmayer, J. P. and Green, P. J., 2000. Novel features of the XRN-family in Arabidopsis: Evidence that AtXRN4, one of several orthologs of nuclear Xrn2p/Rat1p, functions in the cytoplasm. *Proc Natl Acad Sci USA*, 97(25):13985.

Katiyar-Agarwal, S., Zhu, J., Kim, K., Agarwal, M., Fu, X., Huang, A., and Zhu, J.-K., 2006. The plasma membrane Na+/H+ antiporter SOS1 interacts with RCD1 and functions in oxidative stress tolerance in Arabidopsis. *Proceedings of the National Academy of Sciences of the United States of America*, 103:18816–21.

Keller, T., Damude, H. G., Werner, D., Doerner, P., Dixon, R. A., and Lamb, C., 1998. A plant homolog of the neutrophil NADPH oxidase gp91phox subunit gene encodes a plasma membrane protein with Ca2+ binding motifs. *The Plant cell*, 10:255–66.

Kerenyi, F., Wawer, I., Sikorski, P. J., Kufel, J., and Silhavy, D., 2013. Phosphorylation of the N- and C-terminal UPF1 domains plays a critical role in plant nonsense-mediated mRNA decay. *The Plant journal : for cell and molecular biology*, 76:836–48.

Kertész, S., Kerényi, Z., Mérai, Z., Bartos, I., Pálfy, T., Barta, E., and Silhavy, D., 2006. Both introns and long 3'-UTRs operate as cis-acting elements to trigger nonsense-mediated decay in plants. *Nucleic acids research*, 34(17088291):6147–6157. ISSN 0305-1048.

Kervestin, S. and Jacobson, A., 2012. NMD: a multifaceted response to premature translational termination. *Nature reviews. Molecular cell biology*, 13(23072888):700–712. ISSN 1471-0072.

Kerényi, Z., Mérai, Z., Hiripi, L., Benkovics, A., Gyula, P., Lacomme, C., Barta, E., Nagy, F., and Silhavy, D., 2008. Inter-kingdom conservation of mechanism of nonsense-mediated mRNA decay. *EMBO J*, 27(11):1585.

Kesarwani, A. K., 2014. Nonsense-Mediated Decay: Transcriptome-Wide Analysis, Feedback Control and Salt Stress Regulation.

Kesarwani, Lee, Ricca, Kesarwani, A., Lee, H.-C., Ricca, G. P., Sullivan, G., Faiss, N., Wagner, G., Wunderling, A., and Wachter, A., 2019. Multifactorial and Species-Specific Feedback Regulation of the RNA Surveillance Pathway Nonsense-Mediated Decay in Plants. *Plant Cell and Physiology*.

Ketteler, R., 2012. On programmed ribosomal frameshifting: the alternative proteomes. *Frontiers in genetics*, 3(23181069):242–242. ISSN 1664-8021.

Khan, M. S., Haas, F. H., Allboje Samami, A., Moghaddas Gholami, A., Bauer, A., Fellenberg, K., Reichelt, M., Hänsch, R., Mendel, R. R., Meyer, A. J., Wirtz, M., and Hell, R., 2010. Sulfite Reductase Defines a Newly Discovered Bottleneck for Assimilatory Sulfate Reduction and Is Essential for Growth and Development in *Arabidopsis thaliana*. *Plant Cell*, 22(4):1216.

Kim, J. S., Jung, H. J., Lee, H. J., Kim, K. A., Goh, C.-H., Woo, Y., Oh, S. H., Han, Y. S., and Kang, H., 2008. Glycine-rich RNA-binding protein 7 affects abiotic stress responses by regulating stomata opening and closing in Arabidopsis thaliana. *The Plant journal : for cell and molecular biology*, 55:455–66.

Kim, Y.-O., Pan, S., Jung, C.-H., and Kang, H., 2007. A zinc finger-containing glycine-rich RNA-binding protein, atRZ-1a, has a negative impact on seed germination and seedling growth of Arabidopsis thaliana under salt or drought stress conditions. *Plant & cell physiology*, 48:1170–81.

Kimura, S., Waszczak, C., Hunter, K., and Wrzaczek, M., 2017. Bound by Fate: The Role of Reactive Oxygen Species in Receptor-Like Kinase Signaling. *Plant Cell*, 29(4):638.

Klepikova, A. V., Kasianov, A. S., Gerasimov, E. S., Logacheva, M. D., and Penin, A. A., 2016. A high resolution map of the Arabidopsis thaliana developmental transcriptome based on RNA-seq profiling. *The Plant journal : for cell and molecular biology*, 88:1058–1070.

Klinge, S., Voigts-Hoffmann, F., Leibundgut, M., Arpagaus, S., and Ban, N., 2011. Crystal structure of the eukaryotic 60S ribosomal subunit in complex with initiation factor 6. *Science (New York, N.Y.)*, 334:941–8.

Knight, H., Trewavas, A. J., and Knight, M. R., 1996. Cold calcium signaling in Arabidopsis involves two cellular pools and a change in calcium signature after acclimation. *The Plant cell*, 8:489–503.

Knight, H., Trewavas, A. J., and Knight, M. R., 1997. Calcium signalling in Arabidopsis thaliana responding to drought and salinity. *The Plant journal : for cell and molecular biology*, 12:1067–78.

Kong, X., Ma, L., Yang, L., Chen, Q., Xiang, N., Yang, Y., and Hu, X., 2014. Quantitative proteomics analysis reveals that the nuclear cap-binding complex proteins arabidopsis CBP20 and CBP80 modulate the salt stress response. *Journal of proteome research*, 13:2495–510.

Kreps, J. A., Wu, Y., Chang, H.-S., Zhu, T., Wang, X., and Harper, J. F., 2002. Transcriptome changes for Arabidopsis in response to salt, osmotic, and cold stress. *Plant physiology*, 130(12481097):2129–2141. ISSN 1532-2548.

Kretsinger, R. H. and Nockolds, C. E., 1973. Carp muscle calcium-binding protein. II. Structure determination and general description. *The Journal of biological chemistry*, 248:3313–26.

Kulik, A., Wawer, I., Krzywińska, E., Bucholc, M., and Dobrowolska, G., 2011. SnRK2 protein kinases–key regulators of plant response to abiotic stresses. *Omics : a journal of integrative biology*, 15(22136638):859–872. ISSN 1536-2310.

Kunz, J., Henriquez, R., Schneider, U., Deuter-Reinhard, M., Movva, N. R., and Hall, M. N., 1993. Target of rapamycin in yeast, TOR2, is an essential phosphatidylinositol kinase homolog required for G1 progression. *Cell*, 73:585–96.

Kurepa, J., Smalle, J., Va, M., Montagu, N., and Inzé, D., 1998. Oxidative stress tolerance and longevity in Arabidopsis: the late-flowering mutant gigantea is tolerant to paraquat. *The Plant Journal*, 14(6):759–764. ISSN 0960-7412. doi: 10.1046/j.1365-313x.1998.00168.x.

Kurihara, Y., 2017. Activity and roles of Arabidopsis thaliana XRN family exoribonucleases in noncoding RNA pathways. *Journal of Plant Research*, 130(1):25–31. ISSN 1618-0860.

Kurihara, Y., Matsui, A., Hanada, K., Kawashima, M., Ishida, J., Morosawa, T., Tanaka, M., Kaminuma, E., Mochizuki, Y., Matsushima, A., Toyoda, T., Shinozaki, K., and Seki, M., 2009. Genome-wide suppression of aberrant mRNA-like noncoding RNAs by NMD in Arabidopsis. *Proceedings of the National Academy of Sciences of the United States of America*, 106:2453–8.

Kurihara, Y., Schmitz, R. J., Nery, J. R., Schultz, M. D., Okubo-Kurihara, E., Morosawa, T., Tanaka, M., Toyoda, T., Seki, M., and Ecker, J. R., 2012. Surveillance of 3' Noncoding Transcripts Requires FIERY1 and XRN3 in Arabidopsis. *G3 (Bethesda, Md.)*, 2:487–98.

Kurosaki, T. and Maquat, L. E., 2013. Rules that govern UPF1 binding to mRNA 3' UTRs. *Proceedings of the National Academy of Sciences of the United States of America*, 110(23404710):3357–3362. ISSN 0027-8424.

Kurusu, T., Kuchitsu, K., and Tada, Y., 2015. Plant signaling networks involving Ca(2+) and Rboh/Nox-mediated ROS production under salinity stress. *Frontiers in plant science*, 6(26113854):427–427. ISSN 1664-462X.

Kwak, J. M., Mori, I. C., Pei, Z.-M., Leonhardt, N., Torres, M. A., Dangl, J. L., Bloom, R. E., Bodde, S., Jones, J. D. G., and Schroeder, J. I., 2003. NADPH oxidase AtrbohD and AtrbohF genes function in ROS-dependent ABA signaling in Arabidopsis. *The EMBO journal*, 22(12773379):2623–2633. ISSN 1460-2075.

Königshofer, H., Tromballa, H.-W., and Loppert, H.-G., 2008. Early events in signalling high-temperature stress in tobacco BY2 cells involve alterations in membrane fluidity and enhanced hydrogen peroxide production. *Plant, cell & environment*, 31:1771–80.

Labno, A., Tomecki, R., and Dziembowski, A., 2016. Cytoplasmic RNA decay pathways - Enzymes and mechanisms. *Biochimica et biophysica acta*, 1863:3125–3147.

Lageix, S., Lanet, E., Pouch-Pélissier, M.-N., Espagnol, M.-C., Robaglia, C., Deragon, J.-M., and Pélissier, T., 2008. Arabidopsis eIF2alpha kinase GCN2 is essential for growth in stress conditions and is activated by wounding. *BMC plant biology*, 8(19108716):134–134. ISSN 1471-2229.

Lange, H. and Gagliardi, D., 2010. The Exosome and 3–5- RNA Degradation in Plants. In Jensen, T. H., editor, *RNA Exosome*. Springer US, New York, NY, pp. 50–62.

Larkindale, J. and Knight, M. R., 2002. Protection against Heat Stress-Induced Oxidative Damage in Arabidopsis Involves Calcium, Abscisic Acid, Ethylene, and Salicylic Acid. *Plant Physiol.*, 128(2):682.

Larkindale, J. and Vierling, E., 2008. Core genome responses involved in acclimation to high temperature. *Plant physiology*, 146:748–61.

Laurie, S., Feeney, K. A., Maathuis, F. J. M., Heard, P. J., Brown, S. J., and Leigh, R. A., 2002. A role for HKT1 in sodium uptake by wheat roots. *The Plant journal : for cell and molecular biology*, 32:139–49.

Le Hir, H., Izaurralde, E., Maquat, L. E., and Moore, M. J., 2000. The spliceosome deposits multiple proteins 20-24 nucleotides upstream of mRNA exon-exon junctions. *The EMBO journal*, 19:6860–9.

Lee, J. H., Ryu, H.-S., Chung, K. S., Pose, D., Kim, S., Schmid, M., and Ahn, J. H., 2013. Regulation of temperature-responsive flowering by MADS-box transcription factor repressors. *Science (New York, N.Y.)*, 342:628–32.

Lellis, A. D., Allen, M. L., Aertker, A. W., Tran, J. K., Hillis, D. M., Harbin, C. R., Caldwell, C., Gallie, D. R., and Browning, K. S., 2010. Deletion of the eIFiso4G subunit of the Arabidopsis eIFiso4F translation initiation complex impairs health and viability. *Plant molecular biology*, 74(20694742):249–263. ISSN 0167-4412.

Leshem, Y., Seri, L., and Levine, A., 2007. Induction of phosphatidylinositol 3-kinase-mediated endocytosis by salt stress leads to intracellular production of reactive oxygen species and salt tolerance. *The Plant journal : for cell and molecular biology*, 51:185–97.

Leung, J., Bouvier-Durand, M., Morris, P. C., Guerrier, D., Chefdor, F., and Giraudat, J., 1994. Arabidopsis ABA response gene ABI1: features of a calcium-modulated protein phosphatase. *Science (New York, N.Y.)*, 264:1448–52.

Leung, J., Merlot, S., and Giraudat, J., 1997. The Arabidopsis ABSCISIC ACID-INSENSITIVE2 (ABI2) and ABI1 genes encode homologous protein phosphatases 2C involved in abscisic acid signal transduction. *The Plant cell*, 9:759–71.

Levine, A., Tenhaken, R., Dixon, R., and Lamb, C., 1994. H2O2 from the oxidative burst orchestrates the plant hypersensitive disease resistance response. *Cell*, 79:583–93.

Lewin, B., Krebs, J., Kilpatrick, S. T., and Goldstein, E. S., 2011. *Lewin's GENES X.* v. 10. Jones & Bartlett Learning.

Li, D., Liu, H., Zhang, H., Wang, X., and Song, F., 2008. OsBIRH1, a DEAD-box RNA helicase with functions in modulating defence responses against pathogen infection and oxidative stress. *Journal of experimental botany*, 59:2133–46.

Li, J., Wang, X. Q., Watson, M. B., and Assmann, S. M., 2000. Regulation of abscisic acid-induced stomatal closure and anion channels by guard cell AAPK kinase. *Science (New York, N.Y.)*, 287:300–3.

Li, Q. Q., Liu, Z., Lu, W., and Liu, M., 2017a. Interplay between Alternative Splicing and Alternative Polyadenylation Defines the Expression Outcome of the Plant Unique OXIDATIVE TOLERANT-6 Gene. *Scientific Reports*, 7(1):2052. ISSN 2045-2322.

Li, Z., Vuong, J. K., Zhang, M., Stork, C., and Zheng, S., 2017b. Inhibition of nonsense-mediated RNA decay by ER stress. *RNA (New York, N.Y.)*, 23(27940503):378–394. ISSN 1355-8382.

Liang, W., Li, C., Liu, F., Jiang, H., Li, S., Sun, J., Wu, X., and Li, C., 2009. The Arabidopsis homologs of CCR4-associated factor 1 show mRNA deadenylation activity and play a role in plant defence responses. *Cell research*, 19:307–16.

Liese, A. and Romeis, T., 2013. Biochemical regulation of in vivo function of plant calcium-dependent protein kinases (CDPK). *Biochimica et biophysica acta*, 1833:1582–9.

Lin, F., Zhang, Y., and Jiang, M.-Y., 2009a. Alternative splicing and differential expression of two transcripts of nicotine adenine dinucleotide phosphate oxidase B gene from Zea mays. *Journal of integrative plant biology*, 51:287–98.

Lin, H., Yang, Y., Quan, R., Mendoza, I., Wu, Y., Du, W., Zhao, S., Schumaker, K. S., Pardo, J. M., and Guo, Y., 2009b. Phosphorylation of SOS3-LIKE CALCIUM BINDING PROTEIN8 by SOS2 protein kinase stabilizes their protein complex and regulates salt tolerance in Arabidopsis. *The Plant cell*, 21:1607–19.

Lin, J. H., Li, H., Yasumura, D., Cohen, H. R., Zhang, C., Panning, B., Shokat, K. M., LaVail, M. M., and Walter, P., 2007. IRE1 Signaling Affects Cell Fate During the Unfolded Protein Response. *Science*, 318(5852):944.

Lisbona, F., Rojas-Rivera, D., Thielen, P., Zamorano, S., Todd, D., Martinon, F., Glavic, A., Kress, C., Lin, J. H., Walter, P., Reed, J. C., Glimcher, L. H., and

Hetz, C., 2009. BAX inhibitor-1 is a negative regulator of the ER stress sensor IRE1alpha. *Molecular cell*, 33:679–91.

Liu, B., Han, Y., and Qian, S.-B., 2013a. Cotranslational response to proteotoxic stress by elongation pausing of ribosomes. *Molecular cell*, 49:453–63.

Liu, B. and Qian, S.-B., 2014. Translational reprogramming in cellular stress response. *Wiley interdisciplinary reviews. RNA*, 5:301–15.

Liu, H.-T., Sun, D.-Y., and Zhou, R.-G., 2005. Ca2+ and AtCaM3 are involved in the expression of heat shock protein gene in Arabidopsis. *Plant, Cell & Environment*, 28(10):1276–1284. ISSN 0140-7791. doi:10.1111/j.1365-3040.2005.01365.x.

Liu, J., Ishitani, M., Halfter, U., Kim, C. S., and Zhu, J. K., 2000. The Arabidopsis thaliana SOS2 gene encodes a protein kinase that is required for salt tolerance. *Proceedings of the National Academy of Sciences of the United States of America*, 97(10725382):3730–3734. ISSN 1091-6490.

Liu, J., Sun, N., Liu, M., Liu, J., Du, B., Wang, X., and Qi, X., 2013b. An autoregulatory loop controlling Arabidopsis HsfA2 expression: role of heat shock-induced alternative splicing. *Plant physiology*, 162:512–21.

Liu, J. and Zhu, J.-K., 1997. An *Arabidopsis* mutant that requires increased calcium for potassium nutrition and salt-tolerance. *Proc Natl Acad Sci USA*, 94(26):14960.

Liu, J. and Zhu, J.-K., 1998. A Calcium Sensor Homolog Required for Plant Salt Tolerance. *Science*, 280(5371):1943.

Liu, N., Dai, Q., Zheng, G., He, C., Parisien, M., and Pan, T., 2015. N(6)-methyladenosine-dependent RNA structural switches regulate RNA-protein interactions. *Nature*, 518(25719671):560–564. ISSN 0028-0836.

Liu, Y., Burgos, J. S., Deng, Y., Srivastava, R., Howell, S. H., and Bassham, D. C., 2012. Degradation of the Endoplasmic Reticulum by Autophagy during Endoplasmic Reticulum Stress in *Arabidopsis*. *Plant Cell*, 24(11):4635.

Lloyd, J. P. B. and Davies, B., 2013. SMG1 is an ancient nonsense-mediated mRNA decay effector. *The Plant journal : for cell and molecular biology*, 76:800–10.

Lokdarshi, A., Conner, W. C., McClintock, C., Li, T., and Roberts, D. M., 2016. Arabidopsis CML38, a Calcium Sensor That Localizes to Ribonucleoprotein Complexes under Hypoxia Stress. *Plant Physiol.*, 170(2):1046.

Luo, Y., Na, Z., and Slavoff, S. A., 2018. P-Bodies: Composition, Properties, and Functions. *Biochemistry*, 57(29381060):2424–2431. ISSN 0006-2960.

Lykke-Andersen, S. and Jensen, T. H., 2015. Nonsense-mediated mRNA decay: an intricate machinery that shapes transcriptomes. *Nature reviews. Molecular cell biology*, 16:665–77.

Lämke, J., Brzezinka, K., Altmann, S., and Bäurle, I., 2016. A hit-and-run heat shock factor governs sustained histone methylation and transcriptional stress memory. *EMBO J*, 35(2):162.

Ma, L., Zhang, H., Sun, L., Jiao, Y., Zhang, G., Miao, C., and Hao, F., 2012. NADPH oxidase AtrbohD and AtrbohF function in ROS-dependent regulation of Na(+)/K(+)homeostasis in Arabidopsis under salt stress. *Journal of experimental botany*, 63:305–17.

Ma, X. M. and Blenis, J., 2009. Molecular mechanisms of mTOR-mediated translational control. *Nature reviews. Molecular cell biology*, 10:307–18.

Maathuis, F. J., 2008. *Root signaling in reponse to Drough and Salinity*. Springer.

Maathuis, F. J. M., 2006. cGMP modulates gene transcription and cation transport in Arabidopsis roots. *The Plant journal : for cell and molecular biology*, 45:700–11.

Maekawa, S., Imamachi, N., Irie, T., Tani, H., Matsumoto, K., Mizutani, R., Imamura, K., Kakeda, M., Yada, T., Sugano, S., Suzuki, Y., and Akimitsu, N., 2015. Analysis of RNA decay factor mediated RNA stability contributions on RNA abundance. *BMC genomics*, 16(25879614):154–154. ISSN 1471-2164.

Makino, D. L., Halbach, F., and Conti, E., 2013. The RNA exosome and proteasome: common principles of degradation control. *Nature Reviews Molecular Cell Biology*, 14:654.

Maldonado-Bonilla, L. D., 2014. Composition and function of P bodies in Arabidopsis thaliana. *Frontiers in plant science*, 5(24860588):201–201. ISSN 1664-462X.

Maquat, L. E., 2002. Skiing Toward Nonstop mRNA Decay. *Science*, 295(5563):2221.

Maquat, L. E., Tarn, W.-Y., and Isken, O., 2010. The pioneer round of translation: features and functions. *Cell*, 142(20691898):368–374. ISSN 0092-8674.

Marcotrigiano, J., Gingras, A.-C., Sonenberg, N., and Burley, S. K., 1997. Cocrystal Structure of the Messenger RNA 5- Cap-Binding Protein (eIF4E) Bound to 7-methyl-GDP. *Cell*, 89(6):951–961. ISSN 0092-8674.

Marin, K., Suzuki, I., Yamaguchi, K., Ribbeck, K., Yamamoto, H., Kanesaki, Y., Hagemann, M., and Murata, N., 2003. Identification of histidine kinases that act

as sensors in the perception of salt stress in Synechocystis sp. PCC 6803. *Proc Natl Acad Sci USA*, 100(15):9061.

Marino, D., Dunand, C., Puppo, A., and Pauly, N., 2012. A burst of plant NADPH oxidases. *Trends in plant science*, 17:9–15.

Marquez, Y., Brown, J. W. S., Simpson, C., Barta, A., and Kalyna, M., 2012. Transcriptome survey reveals increased complexity of the alternative splicing landscape in Arabidopsis. *Genome research*, 22:1184–95.

Matera, A. G. and Wang, Z., 2014. A day in the life of the spliceosome. *Nature Reviews Molecular Cell Biology*, 15:108.

Matlin, A. J., Clark, F., and Smith, C. W. J., 2005. Understanding alternative splicing: towards a cellular code. *Nature Reviews Molecular Cell Biology*, 6:386.

Matsukura, S., Mizoi, J., Yoshida, T., Todaka, D., Ito, Y., Maruyama, K., Shinozaki, K., and Yamaguchi-Shinozaki, K., 2010. Comprehensive analysis of rice DREB2-type genes that encode transcription factors involved in the expression of abiotic stress-responsive genes. *Molecular genetics and genomics : MGG*, 283:185–96.

Matsuo, Y., Ikeuchi, K., Saeki, Y., Iwasaki, S., Schmidt, C., Udagawa, T., Sato, F., Tsuchiya, H., Becker, T., Tanaka, K., Ingolia, N. T., Beckmann, R., and Inada, T., 2017. Ubiquitination of stalled ribosome triggers ribosome-associated quality control. *Nature Communications*, 8(1):159. ISSN 2041-1723.

Mattila, H., Khorobrykh, S., Havurinne, V., and Tyystjarvi, E., 2015. Reactive oxygen species: Reactions and detection from photosynthetic tissues. *Journal of photochemistry and photobiology. B, Biology*, 152:176–214.

May, J. P., Yuan, X., Sawicki, E., and Simon, A. E., 2018. RNA virus evasion of nonsense-mediated decay. *PLOS Pathogens*, 14(11):e1007459. doi:10.1371/journal.ppat.1007459.

Mazel, A., Leshem, Y., Tiwari, B. S., and Levine, A., 2004. Induction of salt and osmotic stress tolerance by overexpression of an intracellular vesicle trafficking protein AtRab7 (AtRabG3e). *Plant physiology*, 134:118–28.

McLoughlin, F., Galvan-Ampudia, C. S., Julkowska, M. M., Caarls, L., van der Does, D., Lauriere, C., Munnik, T., Haring, M. A., and Testerink, C., 2012. The Snf1-related protein kinases SnRK2.4 and SnRK2.10 are involved in maintenance of root system architecture during salt stress. *The Plant journal : for cell and molecular biology*, 72:436–49.

Menand, B., Desnos, T., Nussaume, L., Berger, F., Bouchez, D., Meyer, C., and Robaglia, C., 2002. Expression and disruption of the Arabidopsis TOR (target of rapamycin) gene. *Proceedings of the National Academy of Sciences of the United States of America*, 99(11983923):6422–6427. ISSN 1091-6490.

Mendell, J. T., Sharifi, N. A., Meyers, J. L., Martinez-Murillo, F., and Dietz, H. C., 2004. Nonsense surveillance regulates expression of diverse classes of mammalian transcripts and mutes genomic noise. *Nature genetics*, 36:1073–8.

Mendoza, I., Rubio, F., Rodriguez-Navarro, A., and Pardo, J. M., 1994. The protein phosphatase calcineurin is essential for NaCl tolerance of Saccharomyces cerevisiae. *The Journal of biological chemistry*, 269:8792–6.

Merai, Z., Benkovics, A. H., Nyiko, T., Debreczeny, M., Hiripi, L., Kerenyi, Z., Kondorosi, E., and Silhavy, D., 2013. The late steps of plant nonsense-mediated mRNA decay. *The Plant journal : for cell and molecular biology*, 73:50–62.

Merret, R., Descombin, J., Juan, Y., Favory, J., Carpentier, M., and Chaparro, C., 2013. XRN4 and LARP1 are required for a heat-triggered mRNA decay pathway involved in plant acclimation and survival during thermal stress. *Cell Rep.*

Merret, R., Nagarajan, V. K., Carpentier, M.-C., Park, S., Favory, J.-J., Descombin, J., Picart, C., Charng, Y.-Y., Green, P. J., Deragon, J.-M., and Bousquet-Antonelli, C., 2015. Heat-induced ribosome pausing triggers mRNA co-translational decay in Arabidopsis thaliana. *Nucleic acids research*, 43(25845591):4121–4132. ISSN 0305-1048.

Meyer, K., Leube, M. P., and Grill, E., 1994. A protein phosphatase 2C involved in ABA signal transduction in *Arabidopsis thaliana*. *Science (New York, N.Y.)*, 264:1452–5.

Mikolajczyk, M., Awotunde, O. S., Muszynska, G., Klessig, D. F., and Dobrowolska, G., 2000. Osmotic stress induces rapid activation of a salicylic acid-induced protein kinase and a homolog of protein kinase ASK1 in tobacco cells. *The Plant cell*, 12:165–78.

Miller, G., Schlauch, K., Tam, R., Cortes, D., Torres, M. A., Shulaev, V., Dangl, J. L., and Mittler, R., 2009. The plant NADPH oxidase RBOHD mediates rapid systemic signaling in response to diverse stimuli. *Science signaling*, 2:ra45.

Miller, G., Suzuki, N., Ciftci-Yilmaz, S., and Mittler, R., 2010. Reactive oxygen species homeostasis and signalling during drought and salinity stresses. *Plant, cell & environment*, 33:453–67.

Mishima, Y. and Tomari, Y., 2016. Codon Usage and 3' UTR Length Determine Maternal mRNA Stability in Zebrafish. *Molecular cell*, 61:874–85.

Mittler, R., 2002. Oxidative stress, antioxidants and stress tolerance. *Trends in Plant Science*, 7(9):405–410. ISSN 1360-1385.

Mittler, R., 2006. Abiotic stress, the field environment and stress combination. *Trends in Plant Science*, 11(1):15–19. ISSN 1360-1385. doi:10.1016/j.tplants.2005.11.002.

Mittler, R., Vanderauwera, S., Gollery, M., and Van Breusegem, F., 2004. Reactive oxygen gene network of plants. *Trends in plant science*, 9:490–8.

Miyazono, K.-I., Miyakawa, T., Sawano, Y., Kubota, K., Kang, H.-J., Asano, A., Miyauchi, Y., Takahashi, M., Zhi, Y., Fujita, Y., Yoshida, T., Kodaira, K.-S., Yamaguchi-Shinozaki, K., and Tanokura, M., 2009. Structural basis of abscisic acid signalling. *Nature*, 462:609–14.

Mizoguchi, M., Umezawa, T., Nakashima, K., Kidokoro, S., Takasaki, H., Fujita, Y., Yamaguchi-Shinozaki, K., and Shinozaki, K., 2010. Two closely related subclass II SnRK2 protein kinases cooperatively regulate drought-inducible gene expression. *Plant & cell physiology*, 51:842–7.

Monroy, A. F. and Dhindsa, R. S., 1995. Low-temperature signal transduction: induction of cold acclimation-specific genes of alfalfa by calcium at 25 degrees C. *The Plant cell*, 7:321–31.

Monshausen, G. B., Bibikova, T. N., Messerli, M. A., Shi, C., and Gilroy, S., 2007. Oscillations in extracellular pH and reactive oxygen species modulate tip growth of Arabidopsis root hairs. *Proc Natl Acad Sci USA*, 104(52):20996.

Moore, M. J., 2005. From birth to death: the complex lives of eukaryotic mRNAs. *Science (New York, N.Y.)*, 309:1514–8.

Moreno, A. B., Martínez de Alba, A. E., Bardou, F., Crespi, M. D., Vaucheret, H., Maizel, A., and Mallory, A. C., 2013. Cytoplasmic and nuclear quality control and turnover of single-stranded RNA modulate post-transcriptional gene silencing in plants. *Nucleic acids research*, 41(23482394):4699–4708. ISSN 0305-1048.

Motulsky, H. J. and Brown, R. E., 2006. Detecting outliers when fitting data with nonlinear regression - a new method based on robust nonlinear regression and the false discovery rate. *BMC Bioinformatics*, 7(1):123. ISSN 1471-2105.

Mugridge, J. S., Coller, J., and Gross, J. D., 2018. Structural and molecular mechanisms for the control of eukaryotic 5–3- mRNA decay. *Nature Structural & Molecular Biology*, 25(12):1077–1085. ISSN 1545-9985.

Munns, R., 2002. Comparative physiology of salt and water stress. *Plant, Cell & Environment*, 25(2):239–250. ISSN 0140-7791. doi:10.1046/j.0016-8025.2001.00808.x.

Munns, R. and Tester, M., 2008. Mechanisms of salinity tolerance. *Annual review of plant biology*, 59:651–81.

Munoz, A. and Castellano, M. M., 2012. Regulation of Translation Initiation under Abiotic Stress Conditions in Plants: Is It a Conserved or Not so Conserved Process among Eukaryotes? *Comparative and functional genomics*, 2012:406357.

Murata, Y., Pei, Z. M., Mori, I. C., and Schroeder, J., 2001. Abscisic acid activation of plasma membrane Ca(2+) channels in guard cells requires cytosolic NAD(P)H and is differentially disrupted upstream and downstream of reactive oxygen species production in abi1-1 and abi2-1 protein phosphatase 2C mutants. *The Plant cell*, 13:2513–23.

Mäser, P., Eckelman, B., Vaidyanathan, R., Horie, T., Fairbairn, D. J., Kubo, M., Yamagami, M., Yamaguchi, K., Nishimura, M., Uozumi, N., Robertson, W., Sussman, M. R., and Schroeder, J. I., 2002. Altered shoot/root Na+ distribution and bifurcating salt sensitivity in Arabidopsis by genetic disruption of the Na+ transporter AtHKT1. *FEBS Letters*, 531(2):157–161. ISSN 0014-5793.

Nagarajan, V. K., Jones, C. I., Newbury, S. F., and Green, P. J., 2013. XRN 5'–>3' exoribonucleases: structure, mechanisms and functions. *Biochimica et biophysica acta*, 1829:590–603.

Nagata, T., Iizumi, S., Satoh, K., Ooka, H., Kawai, J., Carninci, P., Hayashizaki, Y., Otomo, Y., Murakami, K., Matsubara, K., and Kikuchi, S., 2004. Comparative Analysis of Plant and Animal Calcium Signal Transduction Element Using Plant Full-Length cDNA Data. *mbe*, 21(10):1855–1870. ISSN 0737-4038.

Nakamura, T., Liu, Y., Hirata, D., Namba, H., Harada, S., Hirokawa, T., and Miyakawa, T., 1993. Protein phosphatase type 2B (calcineurin)-mediated, FK506-sensitive regulation of intracellular ions in yeast is an important determinant for adaptation to high salt stress conditions. *The EMBO journal*, 12:4063–71.

Nakashima, K., Fujita, Y., Kanamori, N., Katagiri, T., Umezawa, T., Kidokoro, S., Maruyama, K., Yoshida, T., Ishiyama, K., Kobayashi, M., Shinozaki, K.,

and Yamaguchi-Shinozaki, K., 2009. Three Arabidopsis SnRK2 protein kinases, SRK2D/SnRK2.2, SRK2E/SnRK2.6/OST1 and SRK2I/SnRK2.3, involved in ABA signaling are essential for the control of seed development and dormancy. *Plant & cell physiology*, 50:1345–63.

Narsai, R., Howell, K. A., Millar, A. H., O'Toole, N., Small, I., and Whelan, J., 2007. Genome-wide analysis of mRNA decay rates and their determinants in Arabidopsis thaliana. *The Plant cell*, 19(18024567):3418–3436. ISSN 1532-298X.

Nasif, S., Contu, L., and Mühlemann, O., 2018. Beyond quality control: The role of nonsense-mediated mRNA decay (NMD) in regulating gene expression. *Seminars in Cell & Developmental Biology*, 75:78–87. ISSN 1084-9521.

Nath, M., Bhatt, D., Jain, A., Saxena, S. C., Saifi, S. K., Yadav, S., Negi, M., Prasad, R., and Tuteja, N., 2018. Salt stress triggers augmented levels of Na+, Ca2+ and ROS and alter stress-responsive gene expression in roots of CBL9 and CIPK23 knockout mutants of *Arabidopsis thaliana*. *Environmental and Experimental Botany*. ISSN 0098-8472.

Neto, A., de, A. D., Prisco, J. T., Enéas-Filho, J., Lacerda, C. F. d., Silva, J. V., Costa, P. H. A. d., and Gomes-Filho, E., 2004. Effects of salt stress on plant growth, stomatal response and solute accumulation of different maize genotypes. *Brazilian Journal of Plant Physiology*, 16:31–38. ISSN 1677-0420.

Newby, M. I. and Greenbaum, N. L., 2002. Sculpting of the spliceosomal branch site recognition motif by a conserved pseudouridine. *Nature Structural Biology*, 9:958.

Nguyen, A. H., Matsui, A., Tanaka, M., Mizunashi, K., Nakaminami, K., Hayashi, M., Iida, K., Toyoda, T., Nguyen, D. V., and Seki, M., 2015. Loss of Arabidopsis 5'-3' Exoribonuclease AtXRN4 Function Enhances Heat Stress Tolerance of Plants Subjected to Severe Heat Stress. *Plant & cell physiology*, 56:1762–72.

Nickless, A., Jackson, E., Marasa, J., Nugent, P., Mercer, R. W., Piwnica-Worms, D., and You, Z., 2014. Intracellular calcium regulates nonsense-mediated mRNA decay. *Nature medicine*, 20:961–6.

Nishimura, N., Hitomi, K., Arvai, A. S., Rambo, R. P., Hitomi, C., Cutler, S. R., Schroeder, J. I., and Getzoff, E. D., 2009. Structural mechanism of abscisic acid binding and signaling by dimeric PYR1. *Science (New York, N.Y.)*, 326:1373–9.

Niu, Y. and Xiang, Y., 2018. An Overview of Biomembrane Functions in Plant Responses to High-Temperature Stress. doi:10.3389/fpls.2018.00915.

Noctor, G., Mhamdi, A., and Foyer, C. H., 2016. Oxidative stress and antioxidative systems: recipes for successful data collection and interpretation. *Plant, cell & environment*, 39:1140–60.

Noensie, E. N. and Dietz, H. C., 2001. A strategy for disease gene identification through nonsense-mediated mRNA decay inhibition. *Nature biotechnology*, 19:434–9.

Nover, L., Scharf, K. D., and Neumann, D., 1983. Formation of cytoplasmic heat shock granules in tomato cell cultures and leaves. *Molecular and cellular biology*, 3:1648–55.

Nunez-Ramirez, R., Sanchez-Barrena, M. J., Villalta, I., Vega, J. F., Pardo, J. M., Quintero, F. J., Martinez-Salazar, J., and Albert, A., 2012. Structural insights on the plant salt-overly-sensitive 1 (SOS1) Na(+)/H(+) antiporter. *Journal of molecular biology*, 424:283–94.

Nyikó, T., Kerényi, F., Szabadkai, L., Benkovics, A. H., Major, P., Sonkoly, B., Mérai, Z., Barta, E., Niemiec, E., Kufel, J., and Silhavy, D., 2013. Plant nonsense-mediated mRNA decay is controlled by different autoregulatory circuits and can be induced by an EJC-like complex. *Nucleic acids research*, 41(23666629):6715–6728. ISSN 0305-1048.

Ohama, N., Sato, H., Shinozaki, K., and Yamaguchi-Shinozaki, K., 2017. Transcriptional Regulatory Network of Plant Heat Stress Response. *Trends in Plant Science*, 22(1):53–65. ISSN 1360-1385. doi:10.1016/j.tplants.2016.08.015.

Ohnishi, T., Yamashita, A., Kashima, I., Schell, T., Anders, K. R., Grimson, A., Hachiya, T., Hentze, M. W., Anderson, P., and Ohno, S., 2003. Phosphorylation of hUPF1 induces formation of mRNA surveillance complexes containing hSMG-5 and hSMG-7. *Molecular cell*, 12:1187–200.

Ohta, M., Guo, Y., Halfter, U., and Zhu, J.-K., 2003. A novel domain in the protein kinase SOS2 mediates interaction with the protein phosphatase 2C ABI2. *Proceedings of the National Academy of Sciences of the United States of America*, 100:11771–6.

Okada-Katsuhata, Y., Yamashita, A., Kutsuzawa, K., Izumi, N., Hirahara, F., and Ohno, S., 2012. N- and C-terminal Upf1 phosphorylations create binding platforms for SMG-6 and SMG-5:SMG-7 during NMD. *Nucleic Acid Research*, 40(3):1251–1266. ISSN 0305-1048.

Ormancey, M., Thuleau, P., Mazars, C., and Cotelle, V., 2017. CDPKs and 14-3-3 Proteins: Emerging Duo in Signaling. *Trends in Plant Science*, 22(3):263–272. ISSN 1360-1385. doi:10.1016/j.tplants.2016.11.007.

Pace, C. N., Heinemann, U., Hahn, U., and Saenger, W., 1991. Ribonuclease T1: Structure, Function, and Stability. *Angew. Chem. Int. Ed. Engl.*, 30(4):343–360. ISSN 0570-0833. doi:10.1002/anie.199103433.

Palma, K., Zhao, Q., Cheng, Y. T., Bi, D., Monaghan, J., Cheng, W., Zhang, Y., and Li, X., 2007. Regulation of plant innate immunity by three proteins in a complex conserved across the plant and animal kingdoms. *Genes & development*, 21(17575050):1484–1493. ISSN 1549-5477.

Pan, J., Wang, G., Yang, H.-Q., Hong, Z., Xiao, Q., Ren, R.-J., Zhou, H.-Y., Bai, L., and Chen, S.-D., 2007. K252a prevents nigral dopaminergic cell death induced by 6-hydroxydopamine through inhibition of both mixed-lineage kinase 3/c-Jun NH2-terminal kinase 3 (JNK3) and apoptosis-inducing kinase 1/JNK3 signaling pathways. *Molecular pharmacology*, 72:1607–18.

Pan, Q., Shai, O., Lee, L. J., Frey, B. J., and Blencowe, B. J., 2008. Deep surveying of alternative splicing complexity in the human transcriptome by high-throughput sequencing. *Nature Genetics*, 40:1413.

Papp, I., Mur, L. A., Dalmadi, A., Dulai, S., and Koncz, C., 2004. A mutation in the Cap Binding Protein 20 gene confers drought tolerance to Arabidopsis. *Plant molecular biology*, 55:679–86.

Park, S.-Y., Fung, P., Nishimura, N., Jensen, D. R., Fujii, H., Zhao, Y., Lumba, S., Santiago, J., Rodrigues, A., Chow, T.-F. F., Alfred, S. E., Bonetta, D., Finkelstein, R., Provart, N. J., Desveaux, D., Rodriguez, P. L., McCourt, P., Zhu, J.-K., Schroeder, J. I., Volkman, B. F., and Cutler, S. R., 2009. Abscisic acid inhibits type 2C protein phosphatases via the PYR/PYL family of START proteins. *Science (New York, N.Y.)*, 324:1068–71.

Park, S. Y., Seo, S. B., Lee, S. J., Na, J. G., and Kim, Y. J., 2001. Mutation in PMR1, a Ca(2+)-ATPase in Golgi, confers salt tolerance in Saccharomyces cerevisiae by inducing expression of PMR2, an Na(+)-ATPase in plasma membrane. *The Journal of biological chemistry*, 276:28694–9.

Parker, R., 2012. RNA Degradation in *Saccharomyces cerevisae*. *Genetics*, 191(3):671.

Parker, R. and Sheth, U., 2007. P bodies and the control of mRNA translation and degradation. *Molecular cell*, 25:635–46.

Parsell, D. A., Kowal, A. S., Singer, M. A., and Lindquist, S., 1994. Protein disaggregation mediated by heat-shock protein Hsp104. *Nature*, 372:475–8.

Patharkar, O. R. and Cushman, J. C., 2000. A stress-induced calcium-dependent protein kinase from Mesembryanthemum crystallinum phosphorylates a two-component pseudo-response regulator. *The Plant journal : for cell and molecular biology*, 24:679–91.

Paulsen, M. T., Veloso, A., Prasad, J., Bedi, K., Ljungman, E. A., Magnuson, B., Wilson, T. E., and Ljungman, M., 2014. Use of Bru-Seq and BruChase-Seq for genome-wide assessment of the synthesis and stability of RNA. *Methods (San Diego, Calif.)*, 67(23973811):45–54. ISSN 1046-2023.

Pei, Z.-M., Murata, Y., Benning, G., Thomine, S., Klüsener, B., Allen, G. J., Grill, E., and Schroeder, J. I., 2000. Calcium channels activated by hydrogen peroxide mediate abscisic acid signalling in guard cells. *Nature*, 406:731.

Pei, Z. M., Ward, J. M., and Schroeder, J. I., 1999. Magnesium Sensitizes Slow Vacuolar Channels to Physiological Cytosolic Calcium and Inhibits Fast Vacuolar Channels in Fava Bean Guard Cell Vacuoles. *Plant physiology*, 121(10557247):977–986. ISSN 0032-0889.

Pelechano, V., Wei, W., and Steinmetz, L. M., 2015. Widespread Co-translational RNA Decay Reveals Ribosome Dynamics. *Cell*, 161:1400–12.

Pereverzev, A. P., Gurskaya, N. G., Ermakova, G. V., Kudryavtseva, E. I., Markina, N. M., Kotlobay, A. A., Lukyanov, S. A., Zaraisky, A. G., and Lukyanov, K. A., 2015. Method for quantitative analysis of nonsense-mediated mRNA decay at the single cell level. *Scientific Reports*, 5:7729.

Pestova, T. V. and Hellen, C. U. T., 2003. Translation elongation after assembly of ribosomes on the Cricket paralysis virus internal ribosomal entry site without initiation factors or initiator tRNA. *Genes & development*, 17:181–6.

Phukan, U. J., Jeena, G. S., and Shukla, R. K., 2016. WRKY Transcription Factors: Molecular Regulation and Stress Responses in Plants. *Frontiers in plant science*, 7(27375634):760–760. ISSN 1664-462X.

Pittman, J. K. and Hirschi, K. D., 2001. Regulation of CAX1, an Arabidopsis Ca(2+)/H+ antiporter. Identification of an N-terminal autoinhibitory domain. *Plant physiology*, 127(11706183):1020–1029. ISSN 1532-2548.

Pomeranz, M. C., Hah, C., Lin, P.-C., Kang, S. G., Finer, J. J., Blackshear, P. J., and Jang, J.-C., 2010. The Arabidopsis tandem zinc finger protein AtTZF1 traffics

between the nucleus and cytoplasmic foci and binds both DNA and RNA. *Plant physiology*, 152:151–65.

Poovaiah, B. W. and Reddy, A. S., 1993. Calcium and signal transduction in plants. *Critical reviews in plant sciences*, 12:185–211. NASA: Grant numbers: NAG-10-0061S/1.

Popp, M. W.-L. and Maquat, L. E., 2013. Organizing principles of mammalian nonsense-mediated mRNA decay. *Annual review of genetics*, 47:139–65.

Posé, D., Verhage, L., Ott, F., Yant, L., Mathieu, J., Angenent, G. C., Immink, R. G. H., and Schmid, M., 2013. Temperature-dependent regulation of flowering by antagonistic FLM variants. *Nature*, 503:414.

Presnyak, V., Alhusaini, N., Chen, Y.-H., Martin, S., Morris, N., Kline, N., Olson, S., Weinberg, D., Baker, K. E., Graveley, B. R., and Coller, J., 2015. Codon optimality is a major determinant of mRNA stability. *Cell*, 160:1111–24.

Price, A. H., Taylor, A., Ripley, S. J., Griffiths, A., Trewavas, A. J., and Knight, M. R., 1994. Oxidative Signals in Tobacco Increase Cytosolic Calcium. *Plant Cell*, 6(9):1301.

Prickett, T. D. and Brautigan, D. L., 2006. The alpha4 regulatory subunit exerts opposing allosteric effects on protein phosphatases PP6 and PP2A. *The Journal of biological chemistry*, 281:30503–11.

Pritchard, J., Jones, R. G. W. Y. N., and Tomos, A. D., 1991. Turgor, Growth and Rheological Gradients of Wheat Roots Following Osmotic Stress. *Journal of Experimental Botany*, 42(8):1043–1049. ISSN 0022-0957. doi:10.1093/jxb/42.8.1043.

Protter, D. S. W. and Parker, R., 2016. Principles and Properties of Stress Granules. *Trends in cell biology*, 26:668–679.

Pérez-Martín, M., Pérez-Pérez, M. E., Lemaire, S. D., and Crespo, J. L., 2014. Oxidative Stress Contributes to Autophagy Induction in Response to Endoplasmic Reticulum Stress in *Chlamydomonas reinhardtii*. *Plant Physiol.*, 166(2):997.

Qin, F., Kakimoto, M., Sakuma, Y., Maruyama, K., Osakabe, Y., Tran, L.-S. P., Shinozaki, K., and Yamaguchi-Shinozaki, K., 2007. Regulation and functional analysis of ZmDREB2A in response to drought and heat stresses in Zea mays L. *The Plant journal : for cell and molecular biology*, 50:54–69.

Qiu, Q.-S., Guo, Y., Dietrich, M. A., Schumaker, K. S., and Zhu, J.-K., 2002. Regulation of SOS1, a plasma membrane Na+/H+ exchanger in *Arabidopsis thaliana*, by SOS2 and SOS3. *Proc Natl Acad Sci USA*, 99(12):8436.

Qiu, Q.-S., Guo, Y., Quintero, F. J., Pardo, J. M., Schumaker, K. S., and Zhu, J.-K., 2004. Regulation of vacuolar Na+/H+ exchange in Arabidopsis thaliana by the salt-overly-sensitive (SOS) pathway. *The Journal of biological chemistry*, 279:207–15.

Quan, R., Lin, H., Mendoza, I., Zhang, Y., Cao, W., Yang, Y., Shang, M., Chen, S., Pardo, J. M., and Guo, Y., 2007. SCABP8/CBL10, a putative calcium sensor, interacts with the protein kinase SOS2 to protect Arabidopsis shoots from salt stress. *The Plant cell*, 19:1415–31.

Quan, R., Wang, J., Yang, D., Zhang, H., Zhang, Z., and Huang, R., 2017. EIN3 and SOS2 synergistically modulate plant salt tolerance. *Scientific Reports*, 7:44637.

Quintero, F. J., Martinez-Atienza, J., Villalta, I., Jiang, X., Kim, W.-Y., Ali, Z., Fujii, H., Mendoza, I., Yun, D.-J., Zhu, J.-K., and Pardo, J. M., 2011. Activation of the plasma membrane Na/H antiporter Salt-Overly-Sensitive 1 (SOS1) by phosphorylation of an auto-inhibitory C-terminal domain. *Proc Natl Acad Sci USA*, 108(6):2611.

Quintero, F. J., Ohta, M., Shi, H., Zhu, J.-K., and Pardo, J. M., 2002. Reconstitution in yeast of the Arabidopsis SOS signaling pathway for Na+ homeostasis. *Proc Natl Acad Sci USA*, 99(13):9061.

Raczynska, K. D., Simpson, C. G., Ciesiolka, A., Szewc, L., Lewandowska, D., McNicol, J., Szweykowska-Kulinska, Z., Brown, J. W. S., and Jarmolowski, A., 2010. Involvement of the nuclear cap-binding protein complex in alternative splicing in Arabidopsis thaliana. *Nucleic acids research*, 38:265–78.

Radhakrishnan, A., Chen, Y.-H., Martin, S., Alhusaini, N., Green, R., and Coller, J., 2016. The DEAD-Box Protein Dhh1p Couples mRNA Decay and Translation by Monitoring Codon Optimality. *Cell*, 167:122–132.e9.

Raimondeau, E., Bufton, J. C., and Schaffitzel, C., 2018. New insights into the interplay between the translation machinery and nonsense-mediated mRNA decay factors. *Biochem Soc Trans*:BST20170427.

Rayapuram, N., Bigeard, J., Alhoraibi, H., Bonhomme, L., Hesse, A.-M., Vinh, J., Hirt, H., and Pflieger, D., 2018. Quantitative Phosphoproteomic Analysis Reveals Shared and Specific Targets of Arabidopsis Mitogen-Activated Protein Kinases

(MAPKs) MPK3, MPK4, and MPK6. *Molecular & cellular proteomics : MCP*, 17:61–80.

Rayapuram, N., Bonhomme, L., Bigeard, J., Haddadou, K., Przybylski, C., Hirt, H., and Pflieger, D., 2014. Identification of novel PAMP-triggered phosphorylation and dephosphorylation events in Arabidopsis thaliana by quantitative phosphoproteomic analysis. *Journal of proteome research*, 13:2137–51.

Raychaudhuri, S. P., Sanyal, M., Weltman, H., and Kundu-Raychaudhuri, S., 2004. K252a, a high-affinity nerve growth factor receptor blocker, improves psoriasis: an in vivo study using the severe combined immunodeficient mouse-human skin model. *The Journal of investigative dermatology*, 122:812–9.

Rayson, S., Arciga-Reyes, L., Wootton, L., De Torres Zabala, M., Truman, W., Graham, N., Grant, M., and Davies, B., 2012a. A role for nonsense-mediated mRNA decay in plants: pathogen responses are induced in Arabidopsis thaliana NMD mutants. *PloS one*, 7(22384098):e31917–e31917. ISSN 1932-6203.

Rayson, S., Ashworth, M., de Torres Zabala, M., Grant, M., and Davies, B., 2012b. The salicylic acid dependent and independent effects of NMD in plants. *Plant signaling & behavior*, 7(22990450):1434–1437. ISSN 1559-2316.

Reddy, A. S. N., Marquez, Y., Kalyna, M., and Barta, A., 2013. Complexity of the alternative splicing landscape in plants. *The Plant cell*, 25:3657–83.

Reinisch, K. M. and Wolin, S. L., 2007. Emerging themes in non-coding RNA quality control. *Current Opinion in Structural Biology*, 17(2):209–214. ISSN 0959-440X.

Ren, M., Qiu, S., Venglat, P., Xiang, D., Feng, L., Selvaraj, G., and Datla, R., 2011. Target of rapamycin regulates development and ribosomal RNA expression through kinase domain in Arabidopsis. *Plant physiology*, 155:1367–82.

Rentel, M. C. and Knight, M. R., 2004. Oxidative stress-induced calcium signaling in Arabidopsis. *Plant physiology*, 135(15247375):1471–1479. ISSN 1532-2548.

Reverdatto, S., Dutko, J., Chekanova, J., Hamilton, D., and Belostotsky, D., 2004. mRNA deadenylation by PARN is essential for embryogenesis in higher plants. *RNA*.

Riehs, N., Akimcheva, S., Puizina, J., Bulankova, P., Idol, R. A., Siroky, J., Schleiffer, A., Schweizer, D., Shippen, D. E., and Riha, K., 2008. Arabidopsis SMG7 protein is required for exit from meiosis. *Journal of cell science*, 121:2208–16.

Riehs-Kearnan, N., Gloggnitzer, J., Dekrout, B., Jonak, C., and Riha, K., 2012. Aberrant growth and lethality of Arabidopsis deficient in nonsense-mediated RNA decay factors is caused by autoimmune-like response. *Nucleic acids research*, 40(22379136):5615–5624. ISSN 0305-1048.

Riese, M., Höhmann, S., Saedler, H., Münster, T., and Huijser, P., 2007. Comparative analysis of the SBP-box gene families in P. patens and seed plants. *Gene*, 401(1):28–37. ISSN 0378-1119.

Rigby, R. E. and Rehwinkel, J., 2015. RNA degradation in antiviral immunity and autoimmunity. *Trends in immunology*, 36(25709093):179–188. ISSN 1471-4906.

Roberts, D. M. and Harmon, A. C., 1992. Calcium-Modulated Proteins: Targets of Intracellular Calcium Signals in Higher Plants. *Annu. Rev. Plant. Physiol. Plant. Mol. Biol.*, 43(1):375–414. ISSN 1040-2519. doi:10.1146/annurev.pp.43.060192.002111.

Rodríguez-Navarro, A. and Rubio, F., 2006. High-affinity potassium and sodium transport systems in plants. *Journal of experimental Botany*, 57(5):1149–1160. ISSN 0022-0957.

Roitinger, E., Hofer, M., Kocher, T., Pichler, P., Novatchkova, M., Yang, J., Schlogelhofer, P., and Mechtler, K., 2015. Quantitative phosphoproteomics of the ataxia telangiectasia-mutated (ATM) and ataxia telangiectasia-mutated and rad3-related (ATR) dependent DNA damage response in Arabidopsis thaliana. *Molecular & cellular proteomics : MCP*, 14:556–71.

Ron, D. and Walter, P., 2007. Signal integration in the endoplasmic reticulum unfolded protein response. *Nature reviews. Molecular cell biology*, 8:519–29.

Roshandel, P. and Flowers, T., 2009. The ionic effects of NaCl on physiology and gene expression in rice genotypes differing in salt tolerance. *Plant and Soil*, 315(1):135–147. ISSN 1573-5036.

Rougemaille, M., Villa, T., Gudipati, R., and Libri, D., 2008. mRNA journey to the cytoplasm: attire required. *Biol. Cell*.

Rus, A., Yokoi, S., Sharkhuu, A., Reddy, M., Lee, B. H., Matsumoto, T. K., Koiwa, H., Zhu, J. K., Bressan, R. A., and Hasegawa, P. M., 2001. AtHKT1 is a salt tolerance determinant that controls Na(+) entry into plant roots. *Proceedings of the National Academy of Sciences of the United States of America*, 98:14150–5.

Rusnak, F. and Mertz, P., 2000. Calcineurin: form and function. *Physiological reviews*, 80:1483–521.

Russo, J., Heck, A. M., Wilusz, J., and Wilusz, C. J., 2017. Metabolic labeling and recovery of nascent RNA to accurately quantify mRNA stability. *Methods (San Diego, Calif.)*, 120(28219744):39–48. ISSN 1046-2023.

Rymarquis, L. A., Souret, F. F., and Green, P. J., 2011. Evidence that XRN4, an Arabidopsis homolog of exoribonuclease XRN1, preferentially impacts transcripts with certain sequences or in particular functional categories. *RNA (New York, N.Y.)*, 17(21224377):501–511. ISSN 1355-8382.

Rädle, B., Rutkowski, A. J., Ruzsics, Z., Friedel, C. C., Koszinowski, U. H., and Dölken, L., 2013. Metabolic labeling of newly transcribed RNA for high resolution gene expression profiling of RNA synthesis, processing and decay in cell culture. *Journal of visualized experiments : JoVE*, (23963265):50195. ISSN 1940-087X.

Sachs, A., 1990. The role of poly(A) in the translation and stability of mRNA. *Current Opinion in Cell Biology*, 2(6):1092–1098. ISSN 0955-0674.

Sachs, A. B. and Deardorff, J. A., 1992. Translation initiation requires the PAB-dependent poly(A) ribonuclease in yeast. *Cell*, 70(6):961–973. ISSN 0092-8674.

Sagi, M. and Fluhr, R., 2006. Production of reactive oxygen species by plant NADPH oxidases. *Plant physiology*, 141:336–40.

Saidi, Y., Finka, A., and Goloubinoff, P., 2011. Heat perception and signalling in plants: a tortuous path to thermotolerance. *The New phytologist*, 190:556–65.

Saidi, Y., Finka, A., Muriset, M., Bromberg, Z., Weiss, Y. G., Maathuis, F. J. M., and Goloubinoff, P., 2009. The Heat Shock Response in Moss Plants Is Regulated by Specific Calcium-Permeable Channels in the Plasma Membrane. *Plant Cell*, 21(9):2829.

Saidi, Y., Peter, M., Finka, A., Cicekli, C., Vigh, L., and Goloubinoff, P., 2010. Membrane lipid composition affects plant heat sensing and modulates Ca(2+)-dependent heat shock response. *Plant signaling & behavior*, 5(21139423):1530–1533. ISSN 1559-2316.

Saijo, Y., Hata, S., Kyozuka, J., Shimamoto, K., and Izui, K., 2000. Over-expression of a single Ca2+-dependent protein kinase confers both cold and salt/drought tolerance on rice plants. *The Plant journal : for cell and molecular biology*, 23:319–27.

Sakuraba, Y., Kim, Y.-S., Han, S.-H., Lee, B.-D., and Paek, N.-C., 2015. The Arabidopsis Transcription Factor NAC016 Promotes Drought Stress Responses

by Repressing AREB1 Transcription through a Trifurcate Feed-Forward Regulatory Loop Involving NAP. *Plant Cell*, 27(6):1771.

Sammeth, M., Foissac, S., and Guigó, R., 2008. A general definition and nomenclature for alternative splicing events. *PLoS computational biology*, 4(18688268):e1000147–e1000147. ISSN 1553-734X.

Sanchez, S. E., Petrillo, E., Beckwith, E. J., Zhang, X., Rugnone, M. L., Hernando, C. E., Cuevas, J. C., Godoy Herz, M. A., Depetris-Chauvin, A., Simpson, C. G., Brown, J. W. S., Cerdan, P. D., Borevitz, J. O., Mas, P., Ceriani, M. F., Kornblihtt, A. R., and Yanovsky, M. J., 2010. A methyl transferase links the circadian clock to the regulation of alternative splicing. *Nature*, 468:112–6.

Sanders, D., Pelloux, J., Brownlee, C., and Harper, J. F., 2002. Calcium at the crossroads of signaling. *The Plant cell*, 14 Suppl:S401–17.

Sangwan, V., Orvar, B. L., Beyerly, J., Hirt, H., and Dhindsa, R. S., 2002. Opposite changes in membrane fluidity mimic cold and heat stress activation of distinct plant MAP kinase pathways. *The Plant journal : for cell and molecular biology*, 31:629–38.

Santiago, J., Dupeux, F., Round, A., Antoni, R., Park, S.-Y., Jamin, M., Cutler, S. R., Rodriguez, P. L., and Marquez, J. A., 2009. The abscisic acid receptor PYR1 in complex with abscisic acid. *Nature*, 462:665–8.

Sarowar, S., Oh, H. W., Cho, H. S., Baek, K.-H., Seong, E. S., Joung, Y. H., Choi, G. J., Lee, S., and Choi, D., 2007. Capsicum annuum CCR4-associated factor CaCAF1 is necessary for plant development and defence response. *The Plant journal : for cell and molecular biology*, 51:792–802.

Schepetilnikov, M. and Ryabova, L. A., 2018. Recent Discoveries on the Role of TOR (Target of Rapamycin) Signaling in Translation in Plants. *Plant Physiol.*, 176(2):1095.

Schmidt, S. A., Foley, P. L., Jeong, D.-H., Rymarquis, L. A., Doyle, F., Tenenbaum, S. A., Belasco, J. G., and Green, P. J., 2015. Identification of SMG6 cleavage sites and a preferred RNA cleavage motif by global analysis of endogenous NMD targets in human cells. *Nucleic Acids Research*, 43(1):309–323. ISSN 0305-1048. doi:10.1093/nar/gku1258.

Schneider-Poetsch, T., Ju, J., Eyler, D. E., Dang, Y., Bhat, S., Merrick, W. C., Green, R., Shen, B., and Liu, J. O., 2010. Inhibition of eukaryotic translation elongation by cycloheximide and lactimidomycin. *Nature chemical biology*, 6:209–217.

Schoenberg, D. R. and Maquat, L. E., 2012. Regulation of cytoplasmic mRNA decay. *Nature reviews. Genetics*, 13:246–59.

Schroeder, J. I., Allen, G. J., Hugouvieux, V., Kwak, J. M., and Waner, D., 2001. Guard cell signal transduction. *Annu. Rev. Plant. Physiol. Plant. Mol. Biol.*, 52(1):627–658. ISSN 1040-2519. doi:10.1146/annurev.arplant.52.1.627.

Schulze, L. M., Dev, B. T., Li, M., and Kronzucker, H. J., 2012. A pharmacological analysis of high-affinity sodium transport in barley (*Hordeum vulgare* L.): a 24Na+/42K+ study. *Journal of Experimental Botany*, 63(7):2479–2489. ISSN 0022-0957.

Schweingruber, C., Rufener, S. C., Zund, D., Yamashita, A., and Muhlemann, O., 2013. Nonsense-mediated mRNA decay - mechanisms of substrate mRNA recognition and degradation in mammalian cells. *Biochimica et biophysica acta*, 1829:612–23.

Seiser, C., Posch, M., Thompson, N., and C. Kü, h., 1995. Effect of Transcription Inhibitors on the Iron-dependent Degradation of Transferrin Receptor mRNA. *Journal of Biological Chemistry*, 270(49):29400–29406. doi:10.1074/jbc.270.49.29400.

Seo, P. J., Park, M.-J., Lim, M.-H., Kim, S.-G., Lee, M., Baldwin, I. T., and Park, C.-M., 2012. A self-regulatory circuit of CIRCADIAN CLOCK-ASSOCIATED1 underlies the circadian clock regulation of temperature responses in Arabidopsis. *The Plant cell*, 24:2427–42.

Sesma, A., Castresana, C., and Castellano, M. M., 2017. Regulation of Translation by TOR, eIF4E and eIF2α in Plants: Current Knowledge, Challenges and Future Perspectives. *Frontiers in Plant Science*, 8:644. ISSN 1664-462X.

Shahid, S. A., Zaman, M., Heng, L., Zaman, M., Shahid, S. A., and Heng, L., 2018. Soil Salinity: Historical Perspectives and a World Overview of the Problem. In *Guideline for Salinity Assessment, Mitigation and Adaptation Using Nuclear and Related Techniques*. Springer International Publishing, Cham, pp. 43–53.

Shalgi, R., Hurt, J. A., Krykbaeva, I., Taipale, M., Lindquist, S., and Burge, C. B., 2013. Widespread regulation of translation by elongation pausing in heat shock. *Molecular cell*, 49(23290915):439–452. ISSN 1097-2765.

Shang, Z., Laohavisit, A., and Davies, J. M., 2009. Extracellular ATP activates an Arabidopsis plasma membrane Ca(2+)-permeable conductance. *Plant signaling & behavior*, 4(19826233):989–991. ISSN 1559-2316.

Shatkin, A. J., 1976. Capping of eucaryotic mRNAs. *Cell*, 9(4, Part 2):645–653. ISSN 0092-8674.

Shavrukov, Y., 2013. Salt stress or salt shock: which genes are we studying? *Journal of Experimental Botany*, 64(1):119–127. ISSN 0022-0957. doi:10.1093/jxb/ers316.

Sheth, U. and Parker, R., 2006. Targeting of aberrant mRNAs to cytoplasmic processing bodies. *Cell*, 125:1095–109.

Shi, H., 2007. Integration Of Ca2+ In Plant Drought And Salt Stress Signal Transduction Pathways. In Jenks, M. A., Hasegawa, P. M., and Jain, S. M., editors, *Advances in Molecular Breeding Toward Drought and Salt Tolerant Crops*. Springer Netherlands, Dordrecht, pp. 141–182.

Shi, H., Bressan, R., Hasegawa, P., and Zhu, J.-K., 2005. *Sodium*. Blackwell Publishing, London.

Shi, H., Ishitani, M., Kim, C., and Zhu, J. K., 2000. The Arabidopsis thaliana salt tolerance gene SOS1 encodes a putative Na+/H+ antiporter. *Proceedings of the National Academy of Sciences of the United States of America*, 97:6896–901.

Shi, H., Lee, B.-h., Wu, S.-J., and Zhu, J.-K., 2003. Overexpression of a plasma membrane Na+/H+ antiporter gene improves salt tolerance in Arabidopsis thaliana. *Nature biotechnology*, 21:81–5.

Shi, H., Quintero, F. J., Pardo, J. M., and Zhu, J.-K., 2002. The putative plasma membrane Na(+)/H(+) antiporter SOS1 controls long-distance Na(+) transport in plants. *The Plant cell*, 14:465–77.

Shigaki, T., Cheng, N. H., Pittman, J. K., and Hirschi, K., 2001. Structural determinants of Ca2+ transport in the Arabidopsis H+/Ca2+ antiporter CAX1. *The Journal of biological chemistry*, 276:43152–9.

Shin, R. and Schachtman, D. P., 2004. Hydrogen peroxide mediates plant root cell response to nutrient deprivation. *Proceedings of the National Academy of Sciences of the United States of America*, 101:8827–32.

Shoemaker, C. J. and Green, R., 2012. Translation drives mRNA quality control. *Nature structural & molecular biology*, 19:594–601.

Sidaway-Lee, K., Costa, M. J., Rand, D. A., Finkenstadt, B., and Penfield, S., 2014. Direct measurement of transcription rates reveals multiple mechanisms for configuration of the Arabidopsis ambient temperature response. *Genome biology*, 15(24580780):R45–R45. ISSN 1465-6906.

Sierla, M., Waszczak, C., Vahisalu, T., and Kangasjärvi, J., 2016. Reactive Oxygen Species in the Regulation of Stomatal Movements. *Plant Physiol.*, 171(3):1569.

Siev, M., Weinberg, R., and Penman, S., 1969. The selective interruption of nucleolar RNA synthesis in HeLa cells by cordycepin. *The Journal of cell biology*, 41(5783871):510–520. ISSN 1540-8140.

Sikorska, N., Zuber, H., Gobert, A., Lange, H., and Gagliardi, D., 2017. RNA degradation by the plant RNA exosome involves both phosphorolytic and hydrolytic activities. *Nature Communications*, 8(1):2162. ISSN 2041-1723.

Simeunovic, A., Mair, A., Wurzinger, B., and Teige, M., 2016. Know where your clients are: subcellular localization and targets of calcium-dependent protein kinases. *Journal of experimental botany*, 67:3855–72.

Simms, C. L., Yan, L. L., and Zaher, H. S., 2017. Ribosome Collision Is Critical for Quality Control during No-Go Decay. *Molecular Cell*, 68(2):361–373.e5. ISSN 1097-2765.

Singh, R., Parihar, P., Singh, S., Mishra, R. K., Singh, V. P., and Prasad, S. M., 2017. Reactive oxygen species signaling and stomatal movement: Current updates and future perspectives. *Redox biology*, 11:213–218.

Sivritepe, N., Sivritepe, H. O., and Eris, A., 2003. The effects of NaCl priming on salt tolerance in melon seedlings grown under saline conditions. *Scientia Horticulturae*, 97(3):229–237. ISSN 0304-4238.

Slomovic, S., Portnoy, V., Liveanu, V., and Schuster, G., 2006. RNA Polyadenylation in Prokaryotes and Organelles; Different Tails Tell Different Tales. *Critical Reviews in Plant Sciences*, 25(1):65–77. ISSN 0735-2689. doi:10.1080/07352680500391337.

Sobell, H. M., 1985. Actinomycin and DNA transcription. *Proceedings of the National Academy of Sciences*, 82(16):5328–5331. ISSN 0027-8424. doi:10.1073/pnas.82.16.5328.

Soma, F., Mogami, J., Yoshida, T., Abekura, M., Takahashi, F., Kidokoro, S., Mizoi, J., Shinozaki, K., and Yamaguchi-Shinozaki, K., 2017. ABA-unresponsive SnRK2 protein kinases regulate mRNA decay under osmotic stress in plants. *Nature Plants*, 3:16204. doi:10.1038/nplants.2016.204.

Sonenberg, N. and Gingras, A.-C., 1998. The mRNA 5- cap-binding protein eIF4E and control of cell growth. *Current Opinion in Cell Biology*, 10(2):268–275. ISSN 0955-0674.

Song, C. J., Steinebrunner, I., Wang, X., Stout, S. C., and Roux, S. J., 2006. Extracellular ATP induces the accumulation of superoxide via NADPH oxidases in Arabidopsis. *Plant physiology*, 140:1222–32.

Song, J., Angel, A., Howard, M., and Dean, C., 2012. Vernalization - a cold-induced epigenetic switch. *Journal of cell science*, 125:3723–31.

Sorenson, R. and Bailey-Serres, J., 2014. Selective mRNA sequestration by OLIGOURIDYLATE-BINDING PROTEIN 1 contributes to translational control during hypoxia in *Arabidopsis*. *Proc Natl Acad Sci USA*, 111(6):2373.

Sorenson, R. S., Deshotel, M. J., Johnson, K., Adler, F. R., and Sieburth, L. E., 2018. Arabidopsis mRNA decay landscape arises from specialized RNA decay substrates, decapping-mediated feedback, and redundancy. *Proceedings of the National Academy of Sciences of the United States of America*, 115(29386391):E1485–E1494. ISSN 0027-8424.

Souret, F. F., Kastenmayer, J. P., and Green, P. J., 2004. AtXRN4 degrades mRNA in Arabidopsis and its substrates include selected miRNA targets. *Molecular cell*, 15:173–83.

Speiser, A., Silbermann, M., Dong, Y., Haberland, S., Uslu, V. V., Wang, S., Bangash, S. A. K., Reichelt, M., Meyer, A. J., Wirtz, M., and Hell, R., 2018. Sulfur Partitioning between Glutathione and Protein Synthesis Determines Plant Growth. *Plant Physiol.*, 177(3):927.

Spriggs, K. A., Bushell, M., and Willis, A. E., 2010. Translational regulation of gene expression during conditions of cell stress. *Molecular cell*, 40:228–37.

Staley, J. P. and Guthrie, C., 1998. Mechanical Devices of the Spliceosome: Motors, Clocks, Springs, and Things. *Cell*, 92(3):315–326. ISSN 0092-8674. doi:10.1016/s0092-8674(00)80925-3.

Stamm, S., Zhu, J., Nakai, K., Stoilov, P., Stoss, O., and Zhang, M. Q., 2000. An Alternative-Exon Database and Its Statistical Analysis. *DNA and Cell Biology*, 19(12):739–756. ISSN 1044-5498. doi:10.1089/104454900750058107.

Stauffer, E., Westermann, A., Wagner, G., and Wachter, A., 2010. Polypyrimidine tract-binding protein homologues from Arabidopsis underlie regulatory circuits based on alternative splicing and downstream control. *The Plant journal : for cell and molecular biology*, 64:243–55.

Steege, D. A., 2000. Emerging features of mRNA decay in bacteria. *RNA (New York, N.Y.)*, 6(10943888):1079–1090. ISSN 1469-9001.

Steinhorst, L. and Kudla, J., 2014. Signaling in cells and organisms – calcium holds the line. *Current Opinion in Plant Biology*, 22:14–21. ISSN 1369-5266.

Stoecklin, G. and Kedersha, N., 2013. Relationship of GW/P-bodies with stress granules. *Advances in experimental medicine and biology*, 768:197–211.

Stowell, J. A. W., Webster, M. W., Kogel, A., Wolf, J., Shelley, K. L., and Passmore, L. A., 2016. Reconstitution of Targeted Deadenylation by the Ccr4-Not Complex and the YTH Domain Protein Mmi1. *Cell reports*, 17:1978–1989.

Streitner, C., Koster, T., Simpson, C. G., Shaw, P., Danisman, S., Brown, J. W. S., and Staiger, D., 2012. An hnRNP-like RNA-binding protein affects alternative splicing by in vivo interaction with transcripts in Arabidopsis thaliana. *Nucleic acids research*, 40:11240–55.

Sugio, A., Dreos, R., Aparicio, F., and Maule, A. J., 2009. The cytosolic protein response as a subcomponent of the wider heat shock response in Arabidopsis. *The Plant cell*, 21:642–54.

Sugliani, M., Abdelkefi, H., Ke, H., Bouveret, E., Robaglia, C., Caffarri, S., and Field, B., 2016. An Ancient Bacterial Signaling Pathway Regulates Chloroplast Function to Influence Growth and Development in Arabidopsis. *The Plant cell*, 28(26908759):661–679. ISSN 1040-4651.

Sun, J., Zhang, X., Deng, S., Zhang, C., Wang, M., Ding, M., Zhao, R., Shen, X., Zhou, X., Lu, C., and Chen, S., 2012. Extracellular ATP Signaling Is Mediated by H2O2 and Cytosolic Ca2+ in the Salt Response of Populus euphratica Cells. *PLOS ONE*, 7(12):e53136. doi:10.1371/journal.pone.0053136.

Sun, M., Schwalb, B., Pirkl, N., Maier, K. C., Schenk, A., Failmezger, H., Tresch, A., and Cramer, P., 2013. Global analysis of eukaryotic mRNA degradation reveals Xrn1-dependent buffering of transcript levels. *Molecular cell*, 52:52–62.

Sundaramoorthy, E., Leonard, M., Mak, R., Liao, J., Fulzele, A., and Bennett, E. J., 2017. ZNF598 and RACK1 Regulate Mammalian Ribosome-Associated Quality Control Function by Mediating Regulatory 40S Ribosomal Ubiquitylation. *Molecular Cell*, 65(4):751–760.e4. ISSN 1097-2765.

Suntres, Z. E., 2002. Role of antioxidants in paraquat toxicity. *Toxicology*, 180:65–77.

Suri, S. and Dhindsa, R., 2007. A heat-activated MAP kinase (HAMK) as a mediator of heat shock response in tobacco cells. *Plant, Cell & Environment*, 31(2):218–226. ISSN 0140-7791. doi:10.1111/j.1365-3040.2007.01754.x.

Suzuki, N., Miller, G., Morales, J., Shulaev, V., Torres, M. A., and Mittler, R., 2011. Respiratory burst oxidases: the engines of ROS signaling. *Current opinion in plant biology*, 14:691–9.

Suzuki, N. and Mittler, R., 2005. Reactive oxygen species and temperature stresses: A delicate balance between signaling and destruction. *Physiologia Plantarum*, 126(1):45–51. ISSN 0031-9317. doi:10.1111/j.0031-9317.2005.00582.x.

Swatek, K. N., Wilson, R. S., Ahsan, N., Tritz, R. L., and Thelen, J. J., 2014. Multisite phosphorylation of 14-3-3 proteins by calcium-dependent protein kinases. *The Biochemical journal*, 459(24438037):15–25. ISSN 0264-6021.

Swidzinski, J. A., Sweetlove, L. J., and Leaver, C. J., 2002. A custom microarray analysis of gene expression during programmed cell death in Arabidopsis thaliana. *The Plant journal : for cell and molecular biology*, 30:431–46.

Swingle, M., Ni, L., and Honkanen, R. E., 2007. Small-molecule inhibitors of ser/thr protein phosphatases: specificity, use and common forms of abuse. *Methods in molecular biology (Clifton, N.J.)*, 365(17200551):23–38. ISSN 1064-3745.

Szádeczky-Kardoss, I., Csorba, T., Auber, A., Schamberger, A., Nyikó, T., Taller, J., Orbán, T. I., Burgyán, J., and Silhavy, D., 2018a. The nonstop decay and the RNA silencing systems operate cooperatively in plants. *Nucleic acids research*, 46(29672715):4632–4648. ISSN 0305-1048.

Szádeczky-Kardoss, I., Gál, L., Auber, A., Taller, J., and Silhavy, D., 2018b. The No-go decay system degrades plant mRNAs that contain a long A-stretch in the coding region. *Plant Science*, 275:19–27. ISSN 0168-9452.

Sánchez-Barrena, M. J., Martínez-Ripoll, M., and Albert, A., 2013. Structural Biology of a Major Signaling Network that Regulates Plant Abiotic Stress: The CBL-CIPK Mediated Pathway. *International journal of molecular sciences*, 14(23481636):5734–5749. ISSN 1422-0067.

Taggart, A. J., DeSimone, A. M., Shih, J. S., Filloux, M. E., and Fairbrother, W. G., 2012. Large-scale mapping of branchpoints in human pre-mRNA transcripts in vivo. *Nature structural & molecular biology*, 19(22705790):719–721. ISSN 1545-9993.

Takeda, S., Gapper, C., Kaya, H., Bell, E., Kuchitsu, K., and Dolan, L., 2008. Local positive feedback regulation determines cell shape in root hair cells. *Science (New York, N.Y.)*, 319:1241–4.

Tan, T., Cai, J., Zhan, E., Yang, Y., Zhao, J., Guo, Y., and Zhou, H., 2016. Stability and localization of 14-3-3 proteins are involved in salt tolerance in Arabidopsis. *Plant molecular biology*, 92:391–400.

Tan, W., Zhang, D., Zhou, H., Zheng, T., Yin, Y., and Lin, H., 2018. Transcription factor HAT1 is a substrate of SnRK2.3 kinase and negatively regulates ABA synthesis and signaling in Arabidopsis responding to drought. *PLOS Genetics*, 14(4):e1007336. doi:10.1371/journal.pgen.1007336.

Tang, M., Liu, X., Deng, H., and Shen, S., 2011. Over-expression of JcDREB, a putative AP2/EREBP domain-containing transcription factor gene in woody biodiesel plant Jatropha curcas, enhances salt and freezing tolerance in transgenic Arabidopsis thaliana. *Plant Science*, 181(6):623–631. ISSN 0168-9452.

Tani, H. and Akimitsu, N., 2012. Genome-wide technology for determining RNA stability in mammalian cells: historical perspective and recent advantages based on modified nucleotide labeling. *RNA biology*, 9(23034600):1233–1238. ISSN 1547-6286.

Tani, H., Mizutani, R., Salam, K. A., Tano, K., Ijiri, K., Wakamatsu, A., Isogai, T., Suzuki, Y., and Akimitsu, N., 2012. Genome-wide determination of RNA stability reveals hundreds of short-lived noncoding transcripts in mammals. *Genome research*, 22(22369889):947–956. ISSN 1088-9051.

Tat, T. T., Maroney, P. A., Chamnongpol, S., Coller, J., and Nilsen, T. W., 2016. Cotranslational microRNA mediated messenger RNA destabilization. *eLife*, 5.

Tennant, P., Fermin, G., Tennant, P., Fermin, G., and Foster, J. E., 2018. Chapter 13 - Viruses as Targets for Biotechnology: Diagnosis and Detection, Transgenesis, and RNAi- and CRISPR/Cas-Engineered Resistance. In *Viruses*. Academic Press, pp. 317–338.

Tester, M. and Davenport, R., 2003. Na+ Tolerance and Na+ Transport in Higher Plants. *Annals of Botany*, 91(5):503–527. ISSN 0305-7364.

Thermann, R., Neu-Yilik, G., Deters, A., Frede, U., Wehr, K., Hagemeier, C., Hentze, M. W., and Kulozik, A. E., 1998. Binary specification of nonsense codons by splicing and cytoplasmic translation. *EMBO J*, 17(12):3484.

Thoreen, C. C., Chantranupong, L., Keys, H. R., Wang, T., Gray, N. S., and Sabatini, D. M., 2012. A unifying model for mTORC1-mediated regulation of mRNA translation. *Nature*, 485:109–13.

Tian, B. and Manley, J. L., 2016. Alternative polyadenylation of mRNA precursors. *Nature Reviews Molecular Cell Biology*, 18:18.

Torres, M. A., Dangl, J. L., and Jones, J. D. G., 2002. Arabidopsis gp91phox homologues AtrbohD and AtrbohF are required for accumulation of reactive oxygen intermediates in the plant defense response. *Proceedings of the National Academy of Sciences of the United States of America*, 99:517–22.

Torres, M. A., Onouchi, H., Hamada, S., Machida, C., Hammond-Kosack, K. E., and Jones, J. D., 1998. Six Arabidopsis thaliana homologues of the human respiratory burst oxidase (gp91phox). *The Plant journal : for cell and molecular biology*, 14:365–70.

Tran, L.-S. P., Urao, T., Qin, F., Maruyama, K., Kakimoto, T., Shinozaki, K., and Yamaguchi-Shinozaki, K., 2007. Functional analysis of AHK1/ATHK1 and cytokinin receptor histidine kinases in response to abscisic acid, drought, and salt stress in Arabidopsis. *Proc Natl Acad Sci USA*, 104(51):20623.

Tsuboi, T., Kuroha, K., Kudo, K., Makino, S., Inoue, E., Kashima, I., and Inada, T., 2012. Dom34:hbs1 plays a general role in quality-control systems by dissociation of a stalled ribosome at the 3' end of aberrant mRNA. *Molecular cell*, 46:518–29.

Tucker, M., Valencia-Sanchez, M. A., Staples, R. R., Chen, J., Denis, C. L., and Parker, R., 2001. The Transcription Factor Associated Ccr4 and Caf1 Proteins Are Components of the Major Cytoplasmic mRNA Deadenylase in Saccharomyces cerevisiae. *Cell*, 104(3):377–386. ISSN 0092-8674.

Uchida, N., Hoshino, S.-I., and Katada, T., 2004. Identification of a human cytoplasmic poly(A) nuclease complex stimulated by poly(A)-binding protein. *The Journal of biological chemistry*, 279:1383–91.

Umezawa, T., Sugiyama, N., Mizoguchi, M., Hayashi, S., Myouga, F., Yamaguchi-Shinozaki, K., Ishihama, Y., Hirayama, T., and Shinozaki, K., 2009. Type 2C protein phosphatases directly regulate abscisic acid-activated protein kinases in Arabidopsis. *Proceedings of the National Academy of Sciences of the United States of America*, 106:17588–93.

Umezawa, T., Yoshida, R., Maruyama, K., Yamaguchi-Shinozaki, K., and Shinozaki, K., 2004. SRK2C, a SNF1-related protein kinase 2, improves drought tolerance by controlling stress-responsive gene expression in Arabidopsis thaliana. *Proceedings of the National Academy of Sciences of the United States of America*, 101:17306–11.

Urao, T., Katagiri, T., Mizoguchi, T., Yamaguchi-Shinozaki, K., Hayashida, N., and Shinozaki, K., 1994. Two genes that encode Ca2+-dependent protein kinases are induced by drought and high-salt stresses in *Arabidopsis thaliana*. *Molecular and General Genetics MGG*, 244(4):331–340. ISSN 1432-1874.

Vacca, R. A., de Pinto, M. C., Valenti, D., Passarella, S., Marra, E., and De Gara, L., 2004. Production of Reactive Oxygen Species, Alteration of Cytosolic Ascorbate Peroxidase, and Impairment of Mitochondrial Metabolism Are Early Events in Heat Shock-Induced Programmed Cell Death in Tobacco Bright-Yellow 2 Cells. *Plant Physiol.*, 134(3):1100.

Vaidyanathan, H., Sivakumar, P., Chakrabarty, R., and Thomas, G., 2003. Scavenging of reactive oxygen species in NaCl-stressed rice (Oryza sativa L.)–differential response in salt-tolerant and sensitive varieties. *Plant Science*, 165(6):1411–1418. ISSN 0168-9452.

Valderrama, R., Corpas, F. J., Carreras, A., Gomez-Rodriguez, M. V., Chaki, M., Pedrajas, J. R., Fernandez-Ocana, A., Del Rio, L. A., and Barroso, J. B., 2006. The dehydrogenase-mediated recycling of NADPH is a key antioxidant system against salt-induced oxidative stress in olive plants. *Plant, cell & environment*, 29:1449–59.

Valmonte, G. R., Arthur, K., Higgins, C. M., and MacDiarmid, R. M., 2014. Calcium-dependent protein kinases in plants: evolution, expression and function. *Plant & cell physiology*, 55:551–69.

Verslues, P. E., Batelli, G., Grillo, S., Agius, F., Kim, Y.-S., Zhu, J., Agarwal, M., Katiyar-Agarwal, S., and Zhu, J.-K., 2007. Interaction of SOS2 with Nucleoside Diphosphate Kinase 2 and Catalases Reveals a Point of Connection between Salt Stress and H2O2 Signaling in *Arabidopsis thaliana*. *Mol. Cell. Biol.*, 27(22):7771.

Vexler, K., Cymerman, M. A., Berezin, I., Fridman, A., Golani, L., Lasnoy, M., Saul, H., and Shaul, O., 2016. The Arabidopsis NMD Factor UPF3 Is Feedback-Regulated at Multiple Levels and Plays a Role in Plant Response to Salt Stress. *Frontiers in plant science*, 7(27746786):1376–1376. ISSN 1664-462X.

Vierling, E., 1991. The Roles of Heat Shock Proteins in Plants. *Annu. Rev. Plant. Physiol. Plant. Mol. Biol.*, 42(1):579–620. ISSN 1040-2519. doi:10.1146/annurev.pp.42.060191.003051.

Volkov, R. A., Panchuk, I. I., Mullineaux, P. M., and Schoffl, F., 2006. Heat stress-induced H(2)O (2) is required for effective expression of heat shock genes in Arabidopsis. *Plant molecular biology*, 61:733–46.

von Koskull-Doring, P., Scharf, K.-D., and Nover, L., 2007. The diversity of plant heat stress transcription factors. *Trends in plant science*, 12:452–7.

Wachter, A., Ruhl, C., and Stauffer, E., 2012. The Role of Polypyrimidine Tract-Binding Proteins and Other hnRNP Proteins in Plant Splicing Regulation. *Frontiers in plant science*, 3:81.

Wada, M., Lokugamage, K. G., Nakagawa, K., Narayanan, K., and Makino, S., 2018. Interplay between coronavirus, a cytoplasmic RNA virus, and nonsense-mediated mRNA decay pathway. *Proc Natl Acad Sci USA*, 115(43):E10157.

Wada, T. and Becskei, A., 2017. Impact of Methods on the Measurement of mRNA Turnover. *International journal of molecular sciences*, 18(29244760):2723. ISSN 1422-0067.

Wagner, E. and Lykke-Andersen, J., 2002. mRNA surveillance: the perfect persist. *J. Cell Sci.*, 115(15):3033.

Wahle, E. and Winkler, G. S., 2013. RNA decay machines: Deadenylation by the Ccr4-Not and Pan2-Pan3 complexes. *Biochimica et Biophysica Acta (BBA) - Gene Regulatory Mechanisms*, 1829(6):561–570. ISSN 1874-9399.

Wall, C., 2017. *Abiotic and Biotic Stress Regulation of Nonsense-Mediated Decay in Arabidopsis*. Master's thesis.

Wallace, E. W. J., Kear-Scott, J. L., Pilipenko, E. V., Schwartz, M. H., Laskowski, P. R., Rojek, A. E., Katanski, C. D., Riback, J. A., Dion, M. F., Franks, A. M., Airoldi, E. M., Pan, T., Budnik, B. A., and Drummond, D. A., 2015. Reversible, Specific, Active Aggregates of Endogenous Proteins Assemble upon Heat Stress. *Cell*, 162(26359986):1286–1298. ISSN 0092-8674.

Walley, J. W., Kelley, D. R., Nestorova, G., Hirschberg, D. L., and Dehesh, K., 2010a. Arabidopsis Deadenylases AtCAF1a and AtCAF1b Play Overlapping and Distinct Roles in Mediating Environmental Stress Responses. *Plant Physiol.*, 152(2):866.

Walley, J. W., Kelley, D. R., Savchenko, T., and Dehesh, K., 2010b. Investigating the function of CAF1 deadenylases during plant stress responses. *Plant Signaling & Behavior*, 5(7):802–805. ISSN null. doi:10.4161/psb.5.7.11578.

Walter, P. and Ron, D., 2011. The Unfolded Protein Response: From Stress Pathway to Homeostatic Regulation. *Science*, 334(6059):1081.

Wang, H., Hill, K., and Perry, S. E., 2004. An Arabidopsis RNA lariat debranching enzyme is essential for embryogenesis. *The Journal of biological chemistry*, 279:1468–73.

Wang, J.-P., Xu, Y.-P., Munyampundu, J.-P., Liu, T.-Y., and Cai, X.-Z., 2016. Calcium-dependent protein kinase (CDPK) and CDPK-related kinase (CRK) gene families in tomato: genome-wide identification and functional analyses in disease resistance. *Molecular genetics and genomics : MGG*, 291:661–76.

Wang, L., Guo, Y., Jia, L., Chu, H., Zhou, S., Chen, K., Wu, D., and Zhao, L., 2014. Hydrogen Peroxide Acts Upstream of Nitric Oxide in the Heat Shock Pathway in Arabidopsis Seedlings. *Plant Physiol.*, 164(4):2184.

Wang, P., Zhao, Y., Li, Z., Hsu, C.-C., Liu, X., Fu, L., Hou, Y.-J., Du, Y., Xie, S., Zhang, C., Gao, J., Cao, M., Huang, X., Zhu, Y., Tang, K., Wang, X., Tao, W. A., Xiong, Y., and Zhu, J.-K., 2018. Reciprocal Regulation of the TOR Kinase and ABA Receptor Balances Plant Growth and Stress Response. *Molecular cell*, 69:100–112.e6.

Wang, X., Bian, Y., Cheng, K., Gu, L.-F., Ye, M., Zou, H., Sun, S. S.-M., and He, J.-X., 2013. A large-scale protein phosphorylation analysis reveals novel phosphorylation motifs and phosphoregulatory networks in Arabidopsis. *Journal of proteomics*, 78:486–98.

Wang, Z., Ji, H., Yuan, B., Wang, S., Su, C., Yao, B., Zhao, H., and Li, X., 2015. ABA signalling is fine-tuned by antagonistic HAB1 variants. *Nature communications*, 6:8138.

Ward, J. M., Hirschi, K. D., and Sze, H., 2003. Plants pass the salt. *Trends in Plant Science*, 8(5):200–201. ISSN 1360-1385.

Waszczak, C., Carmody, M., and Kangasjarvi, J., 2018. Reactive Oxygen Species in Plant Signaling. *Annual review of plant biology*, 69:209–236.

Wawer, I., Golisz, A., Sulkowska, A., Kawa, D., Kulik, A., and Kufel, J., 2018. mRNA Decapping and 5–3- Decay Contribute to the Regulation of ABA Signaling in Arabidopsis thaliana. *Frontiers in Plant Science*, 9:312. ISSN 1664-462X.

Weber, C., Nover, L., and Fauth, M., 2008. Plant stress granules and mRNA processing bodies are distinct from heat stress granules. *The Plant journal : for cell and molecular biology*, 56:517–30.

Webster, M. W., Chen, Y.-H., Stowell, J. A. W., Alhusaini, N., Sweet, T., Graveley, B. R., Coller, J., and Passmore, L. A., 2018. mRNA Deadenylation Is Coupled to Translation Rates by the Differential Activities of Ccr4-Not Nucleases. *Molecular cell*, 70:1089–1100.e8.

Wek, R. C., Jiang, H.-Y., and Anthony, T. G., 2006. Coping with stress: eIF2 kinases and translational control. *Biochemical Society transactions*, 34:7–11.

Weng, Y., Czaplinski, K., and Peltz, S. W., 1996. Genetic and biochemical characterization of mutations in the ATPase and helicase regions of the Upf1 protein. *Molecular and cellular biology*, 16:5477–90.

West, S., Proudfoot, N., and Dye, M., 2008. Molecular dissection of mammalian RNA polymerase II transcriptional termination. *Mol. Cell*.

White, P. J., 2000. Calcium channels in higher plants. *Biochimica et Biophysica Acta (BBA) - Biomembranes*, 1465(1):171–189. ISSN 0005-2736.

White, P. J. and Broadley, M. R., 2003. Calcium in plants. *Annals of botany*, 92:487–511.

Wolf, J. and Passmore, L. A., 2014. mRNA deadenylation by Pan2-Pan3. *Biochemical Society transactions*, 42:184–7.

Wu, H., 2018. Plant salt tolerance and Na+ sensing and transport. *The Crop Journal*, 6(3):215–225. ISSN 2214-5141.

Wu, S. J., Ding, L., and Zhu, J. K., 1996. SOS1, a Genetic Locus Essential for Salt Tolerance and Potassium Acquisition. *Plant Cell*, 8(4):617.

Xiao, X.-H., Yang, M., Sui, J.-L., Qi, J.-Y., Fang, Y.-J., Hu, S.-N., and Tang, C.-R., 2016. The calcium-dependent protein kinase (CDPK) and CDPK-related kinase gene families in Hevea brasiliensis-comparison with five other plant species in structure, evolution, and expression. *FEBS open bio*, 7(28097084):4–24. ISSN 2211-5463.

Xie, C. G., Lin, H., Deng, X. W., and Guo, Y., 2009. Roles of SCaBP8 in salt stress response. *Plant signaling & behavior*, 4(19826238):956–958. ISSN 1559-2316.

Xin, D., Hu, L., and Kong, X., 2008. Alternative Promoters Influence Alternative Splicing at the Genomic Level. *PLOS ONE*, 3(6):e2377. doi:10.1371/journal.pone.0002377.

Xiong, L., Schumaker, K. S., and Zhu, J.-K., 2002. Cell signaling during cold, drought, and salt stress. *The Plant cell*, 14 Suppl(12045276):S165–S183. ISSN 1532-298X.

Xiong, L. and Zhu, J.-K., 2001. Abiotic stress signal transduction in plants: Molecular and genetic perspectives. *Physiologia Plantarum*, 112(2):152–166. ISSN 0031-9317. doi:10.1034/j.1399-3054.2001.1120202.x.

Xiong, Y., McCormack, M., Li, L., Hall, Q., Xiang, C., and Sheen, J., 2013. Glucose-TOR signalling reprograms the transcriptome and activates meristems. *Nature*, 496:181–6.

Xiong, Y. and Sheen, J., 2012. Rapamycin and glucose-target of rapamycin (TOR) protein signaling in plants. *The Journal of biological chemistry*, 287:2836–42.

Xu, F., Huang, Y., Li, L., Gannon, P., Linster, E., Huber, M., Kapos, P., Bienvenut, W., Polevoda, B., Meinnel, T., Hell, R., Giglione, C., Zhang, Y., Wirtz, M., Chen, S., and Li, X., 2015. Two N-terminal acetyltransferases antagonistically regulate the stability of a nod-like receptor in Arabidopsis. *The Plant cell*, 27(25966763):1547–1562. ISSN 1040-4651.

Xu, J. and Chua, N., 2012. Dehydration stress activates Arabidopsis MPK6 to signal DCP1 phosphorylation. *EMBP J.*

Xu, J. and Chua, N.-H., 2009. Arabidopsis decapping 5 is required for mRNA decapping, P-body formation, and translational repression during postembryonic development. *The Plant cell*, 21(19855049):3270–3279. ISSN 1040-4651.

Xu, J. and Chua, N.-H., 2011. Processing bodies and plant development. *Current opinion in plant biology*, 14(21075046):88–93. ISSN 1369-5266.

Xu, J., Yang, J.-Y., Niu, Q.-W., and Chua, N.-H., 2006. Arabidopsis DCP2, DCP1, and VARICOSE form a decapping complex required for postembryonic development. *The Plant cell*, 18:3386–98.

Xue, G.-P. and Loveridge, C. W., 2004. HvDRF1 is involved in abscisic acid-mediated gene regulation in barley and produces two forms of AP2 transcriptional activators, interacting preferably with a CT-rich element. *The Plant journal : for cell and molecular biology*, 37:326–39.

Yamaguchi, T., Aharon, G. S., Sottosanto, J. B., and Blumwald, E., 2005. Vacuolar Na+/H+ antiporter cation selectivity is regulated by calmodulin from within the vacuole in a Ca2+- and pH-dependent manner. *Proceedings of the National Academy of Sciences of the United States of America*, 102(16249341):16107–16112. ISSN 1091-6490.

Yamashita, A., 2013. Role of SMG-1-mediated Upf1 phosphorylation in mammalian nonsense-mediated mRNA decay. *Genes to cells : devoted to molecular & cellular mechanisms*, 18:161–75.

Yamashita, A., Chang, T.-C., Yamashita, Y., Zhu, W., Zhong, Z., Chen, C.-Y. A., and Shyu, A.-B., 2005. Concerted action of poly(A) nucleases and decapping

enzyme in mammalian mRNA turnover. *Nature Structural &Amp; Molecular Biology*, 12:1054.

Yan, C., Yan, Z., Wang, Y., Yan, X., and Han, Y., 2014. Tudor-SN, a component of stress granules, regulates growth under salt stress by modulating GA20ox3 mRNA levels in Arabidopsis. *Journal of experimental botany*, 65:5933–44.

Yan, K., Xu, H., Cao, W., and Chen, X., 2015. Salt priming improved salt tolerance in sweet sorghum by enhancing osmotic resistance and reducing root Na+ uptake. *Acta Physiologiae Plantarum*, 37(10):203. ISSN 1861-1664.

Yan, Y.-B., 2014. Deadenylation: enzymes, regulation, and functional implications. *Wiley interdisciplinary reviews. RNA*, 5:421–43.

Yang, Q., Chen, Z.-Z., Zhou, X.-F., Yin, H.-B., Li, X., Xin, X.-F., Hong, X.-H., Zhu, J.-K., and Gong, Z., 2009. Overexpression of SOS (Salt Overly Sensitive) Genes Increases Salt Tolerance in Transgenic Arabidopsis. *Molecular Plant*, 2(1):22–31. ISSN 1674-2052.

Yang, Z., Wang, C., Xue, Y., Liu, X., Chen, S., Song, C., Yang, Y., and Guo, Y., 2019. Calcium-activated 14-3-3 proteins as a molecular switch in salt stress tolerance. *Nature Communications*, 10(1):1199. ISSN 2041-1723.

Yepiskoposyan, H., Aeschimann, F., Nilsson, D., Okoniewski, M., and Muhlemann, O., 2011. Autoregulation of the nonsense-mediated mRNA decay pathway in human cells. *RNA (New York, N.Y.)*, 17:2108–18.

Yoine, M., Ohto, M.-a., Onai, K., Mita, S., and Nakamura, K., 2006. The lba1 mutation of UPF1 RNA helicase involved in nonsense-mediated mRNA decay causes pleiotropic phenotypic changes and altered sugar signalling in Arabidopsis. *The Plant journal : for cell and molecular biology*, 47:49–62.

Yoshida, R., Hobo, T., Ichimura, K., Mizoguchi, T., Takahashi, F., Aronso, J., Ecker, J. R., and Shinozaki, K., 2002. ABA-activated SnRK2 protein kinase is required for dehydration stress signaling in Arabidopsis. *Plant & cell physiology*, 43:1473–83.

Yoshida, T., Fujita, Y., Maruyama, K., Mogami, J., Todaka, D., Shinozaki, K., and Yamaguchi-Shinozaki, K., 2015a. Four Arabidopsis AREB/ABF transcription factors function predominantly in gene expression downstream of SnRK2 kinases in abscisic acid signalling in response to osmotic stress. *Plant, cell & environment*, 38:35–49.

Yoshida, T., Mogami, J., and Yamaguchi-Shinozaki, K., 2015b. Omics Approaches Toward Defining the Comprehensive Abscisic Acid Signaling Network in Plants. *Plant & cell physiology*, 56:1043–52.

Yu, X., Willmann, M. R., Anderson, S. J., and Gregory, B. D., 2016. Genome-Wide Mapping of Uncapped and Cleaved Transcripts Reveals a Role for the Nuclear mRNA Cap-Binding Complex in Cotranslational RNA Decay in Arabidopsis. *The Plant cell*, 28:2385–2397.

Zakrzewska-Placzek, M., Souret, F. F., Sobczyk, G. J., Green, P. J., and Kufel, J., 2010. *Arabidopsis thaliana* XRN2 is required for primary cleavage in the pre-ribosomal RNA. *Nucleic acids research*, 38(20338880):4487–4502. ISSN 0305-1048.

Zhan, X., Qian, B., Cao, F., Wu, W., Yang, L., Guan, Q., Gu, X., Wang, P., Okusolubo, T. A., Dunn, S. L., Zhu, J.-K., and Zhu, J., 2015. An Arabidopsis PWI and RRM motif-containing protein is critical for pre-mRNA splicing and ABA responses. *Nature communications*, 6:8139.

Zhang, J.-Q., He, G.-J., and Yan, Y.-B., 2013. Biochemical and biophysical characterization of the deadenylase CrCaf1 from Chlamydomonas reinhardtii. *PloS one*, 8:e69582.

Zhang, X. and Guo, H., 2017. mRNA decay in plants: both quantity and quality matter. *Current Opinion in Plant Biology*, 35:138–144. ISSN 1369-5266.

Zhang, X., Zhen, J., Li, Z., Kang, D., Yang, Y., Kong, J., and Hua, J., 2011. Expression Profile of Early Responsive Genes Under Salt Stress in Upland Cotton (Gossypium hirsutum L.). *Plant Molecular Biology Reporter*, 29(3):626–637. ISSN 1572-9818.

Zhang, Y., Wang, Y., Kanyuka, K., Parry, M. A. J., Powers, S. J., and Halford, N. G., 2008. GCN2-dependent phosphorylation of eukaryotic translation initiation factor-2alpha in Arabidopsis. *Journal of experimental botany*, 59:3131–41.

Zhou, H., Lin, H., Chen, S., Becker, K., Yang, Y., Zhao, J., Kudla, J., Schumaker, K. S., and Guo, Y., 2014. Inhibition of the Arabidopsis salt overly sensitive pathway by 14-3-3 proteins. *The Plant cell*, 26:1166–82.

Zhu, F.-Y., Chen, M.-X., Ye, N.-H., Shi, L., Ma, K.-L., Yang, J.-F., Cao, Y.-Y., Zhang, Y., Yoshida, T., Fernie, A. R., Fan, G.-Y., Wen, B., Zhou, R., Liu, T.-Y., Fan, T., Gao, B., Zhang, D., Hao, G.-F., Xiao, S., Liu, Y.-G., and Zhang, J., 2017. Proteogenomic analysis reveals alternative splicing and translation as part of the abscisic acid response in Arabidopsis seedlings. *The Plant journal : for cell and molecular biology*, 91:518–533.

Zhu, J.-K., 2000. Genetic Analysis of Plant Salt Tolerance Using Arabidopsis. *Plant Physiol.*, 124(3):941.

Zhu, J.-K., 2002. Salt and drought stress signal transduction in plants. *Annual review of plant biology*, 53:247–73.

Zhu, J.-K., 2003. Regulation of ion homeostasis under salt stress. *Current Opinion in Plant Biology*, 6(5):441–445. ISSN 1369-5266.

Zhu, J.-K., 2016. Abiotic Stress Signaling and Responses in Plants. *Cell*, 167(2):313–324. ISSN 0092-8674. doi:10.1016/j.cell.2016.08.029.

Zhu, J.-K., Liu, J., and Xiong, L., 1998. Genetic Analysis of Salt Tolerance in Arabidopsis: Evidence for a Critical Role of Potassium Nutrition. *Plant Cell*, 10(7):1181.

Zhuang, Y., Zhang, H., and Lin, S., 2013. Polyadenylation of 18S rRNA in algae. *J. Phycol.*, 49(3):570–579. ISSN 0022-3646. doi:10.1111/jpy.12068.

Supplement

A Measurement of mRNA half-lives in *Arabidopsis thaliana*

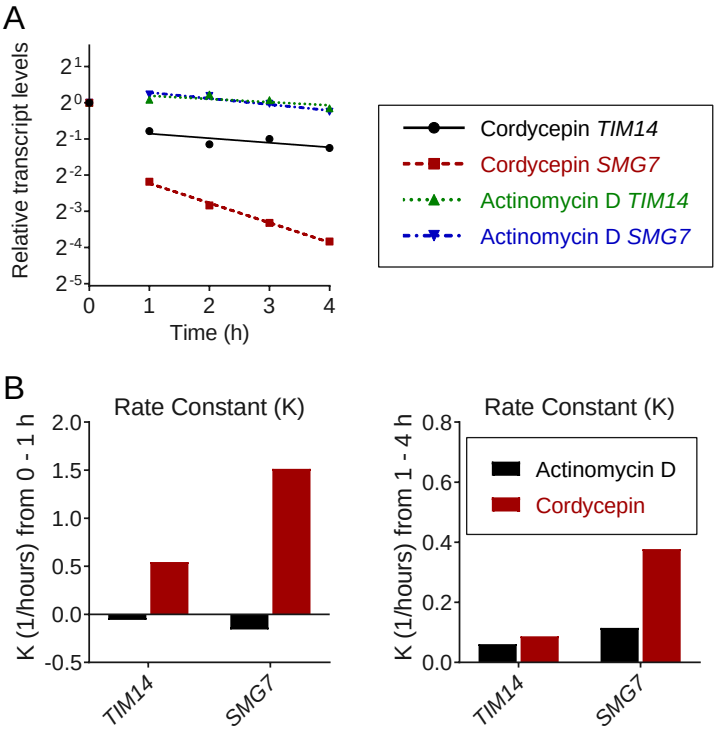

Figure A.1: Rapid decay of NMD target transcript *SMG7* becomes visible with cordycepin treatment in suspension culture cells. (A) Decay curve of *TIM14* and *SMG7* upon treatment with cordycepin or actinomycin D. Dots represent individual values ($n = 1$), lines represent least squares non-linear regression. (B) Rate constant K $(1/hours)$, relation to half-life is $t_{1/2} = ln(2)/K$. As a result, a higher K represents faster degradation. If $K \leq 0$, it is assumed that there is no degradation.

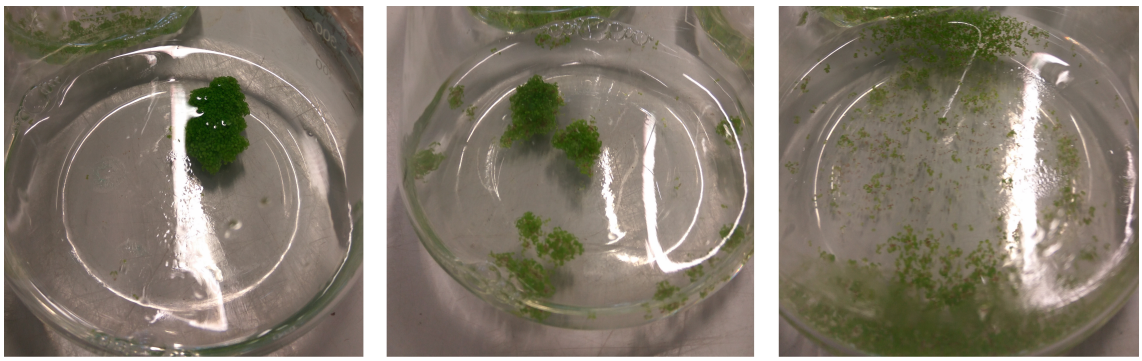

Figure A.2: 7-d-old *A. thaliana* seedlings grown in liquid culture, with various degrees of clumping. Scattered seedlings (far right) were seen in mutants with possible atypical root morphology, for example *rbohc* seedlings.

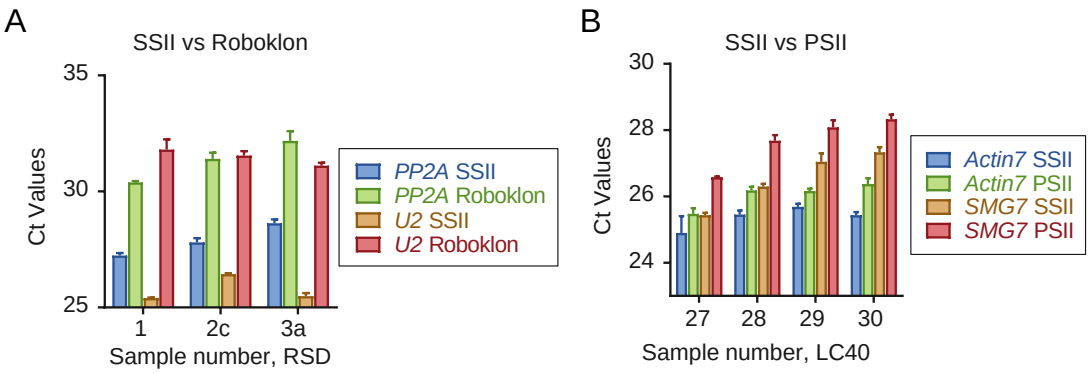

Figure A.3: Reverse transcription from Superscript II (SSII) produces lower Ct values. (A) qPCR data of RT with random hexamers ($d(N)_6$) comparing SSII and Roboklon, housekeeping gene *PP2A* and U2 spliceosomal RNA. Three biological replicates (samples 1, 2c and 3a from working set RSD), error bars represent standard deviation of three technical replicates. (B) qPCR data of RT with oligo dTs ($d(T)_{20}$) comparing SSII and Protoscript II (PSII). Four biological replicates (samples 27, 28, 29, 30 from working set LC40), error bars represent standard deviation from three technical replicates.

B NMD responds dose-dependently to NaCl stress

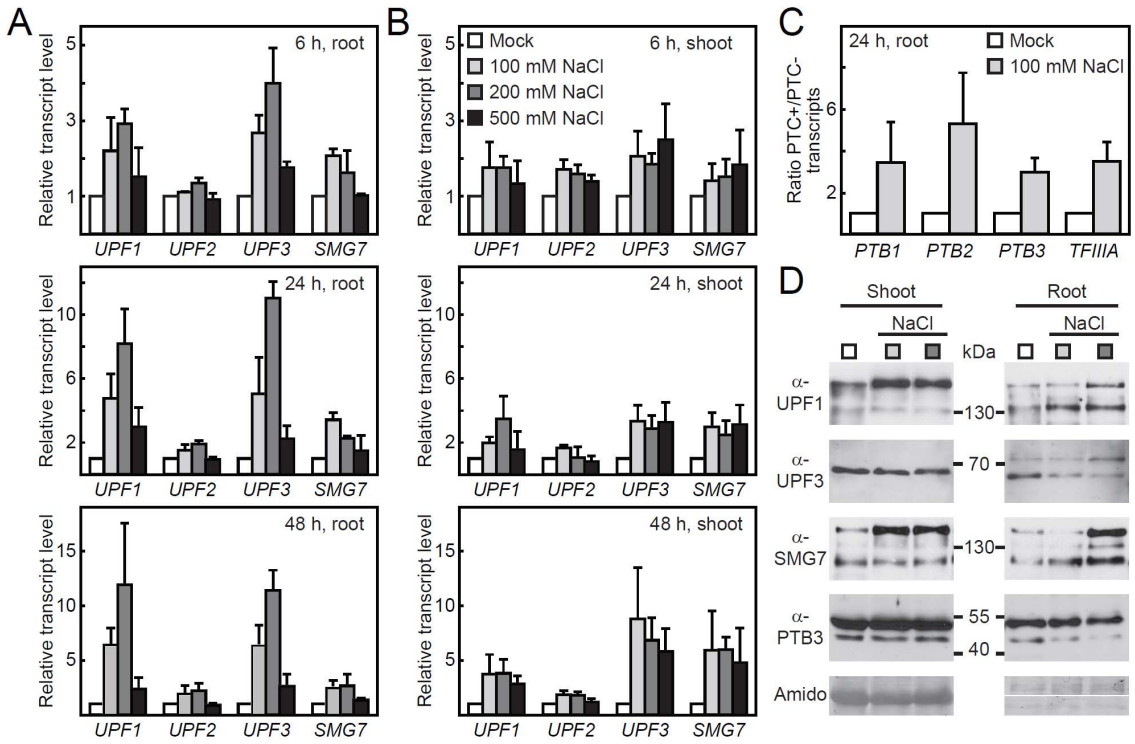

Figure B.1: NMD factor transcript and protein levels in roots and shoots of hydroponically grown *A. thaliana* upon NaCl exposure (Kesarwani, Wachter, et al., unpublished. Figure generated by Prof. Andreas Wachter, data generated by myself and others.) (A, B) levels of NMD factor transcripts in roots (A) and shoots (B) of 4-week-old *A. thaliana* plants exposed for the indicated time periods to different NaCl concentrations (key in (B) applies to all panels) in the liquid medium. Data derived from RT-qPCR (mean values +SD, $n = 3$). (C) Ratios of alternative splicing variants for the indicated genes in samples derived from mock-treated or NaCl exposed (24 h, 100 mM) *A. thaliana* roots. PTC+ and PTC− correspond to previously described NMD target and non-NMD target splicing variants, respectively. Data are normalized to mock and correspond to mean values +SD ($n = 4$). (D) Immunoblot analysis of the NMD factors UPF1, UPF3, SMG7, and the splicing factor PTB3 in shoots (left) and roots (right) of *A. thaliana* exposed for 24 h to 0 (mock, white), 100 mM (light gray), and 200 mM (dark gray) NaCl in the hydroponic system. Sizes and positions of marker bands are indicated. A representative amido black-stained membrane is shown (Amido).

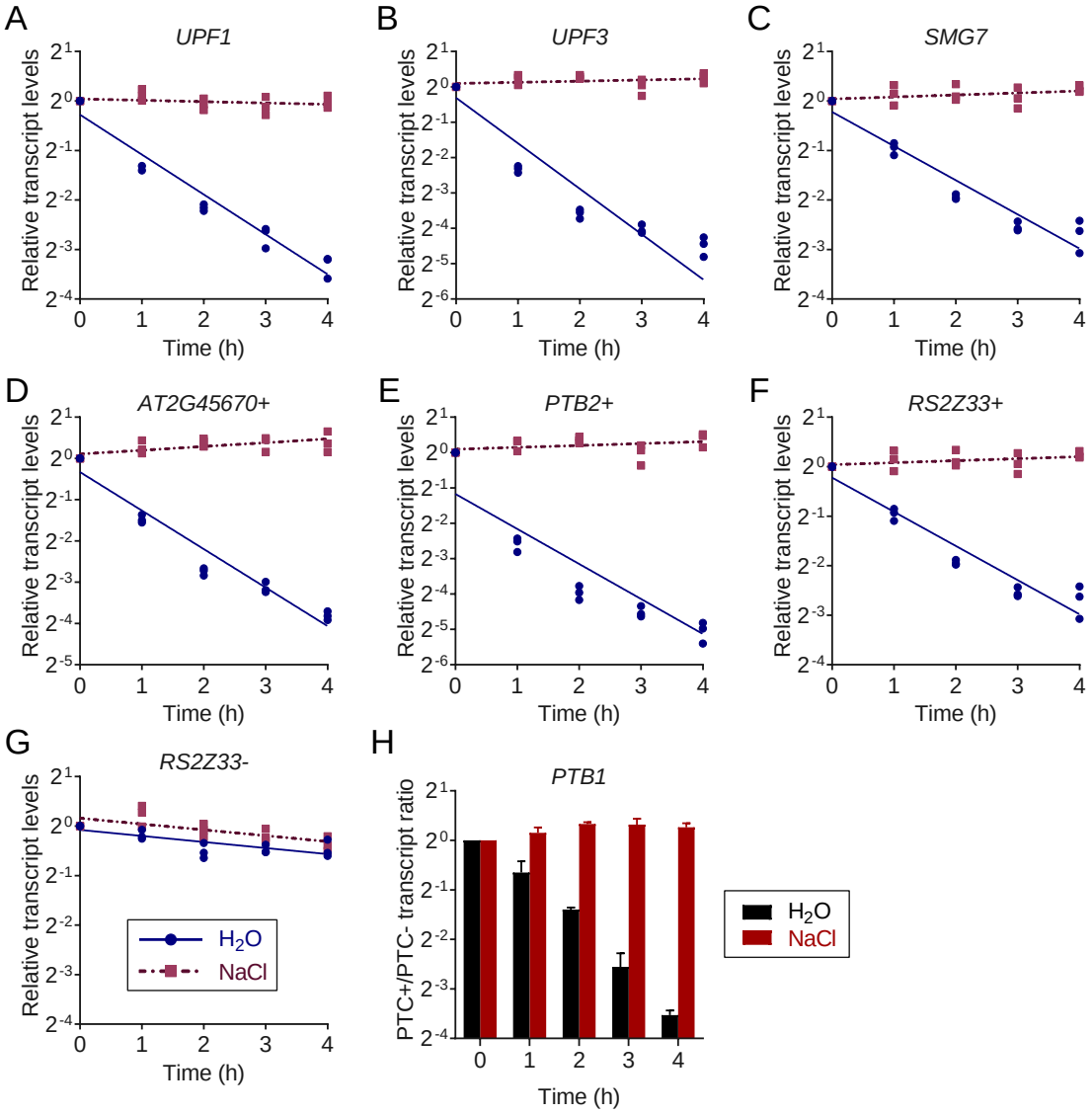

Figure B.2: NaCl stress causes NMD target stabilization. (A-G) RNA stability assays from samples of 7-d-old *A. thaliana* seedlings treated with mock or 500 mM NaCl. Transcript levels were measured using RT-qPCR, data represent individual values ($n = 3$). Color key in (G) applies to all panels. Dots represent individual values, line represents best-fit non-linear regression. (H) Ratio of *PTB1* PTC+/PTC- alternative splicing variants of seedlings treated with mock or 500 mM NaCl as described before, with cordycepin added at 0 h. AS ratios were quantified using a Bioanalyzer. Data are normalized to 0 h time point and represent mean values +SD ($n = 3$).

C NaCl-mediated NMD inhibition is not solely due to osmotic stress

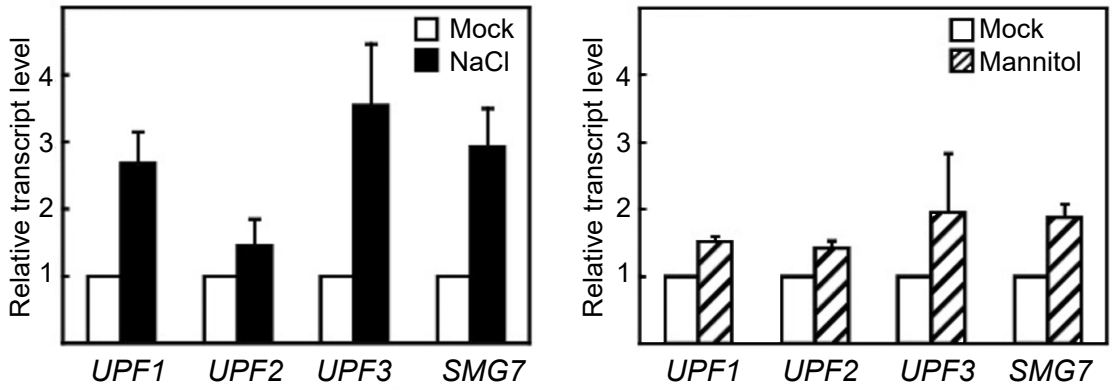

Figure C.1: Steady state NMD factor transcript accumulation in 12-d-old plate grown *A. thaliana* seedlings exposed to 0.5 M NaCl (left) or 1 M mannitol (right), relative to mock treatment (Kesarwani, Wachter, et al., unpublished. Figure generated by Prof. Andreas Wachter, data generated by others than myself.) Data derived from RT-qPCR measurements (mean values + SD, $n = 3$).

D Transcript stabilization by NaCl is likely NMD specific

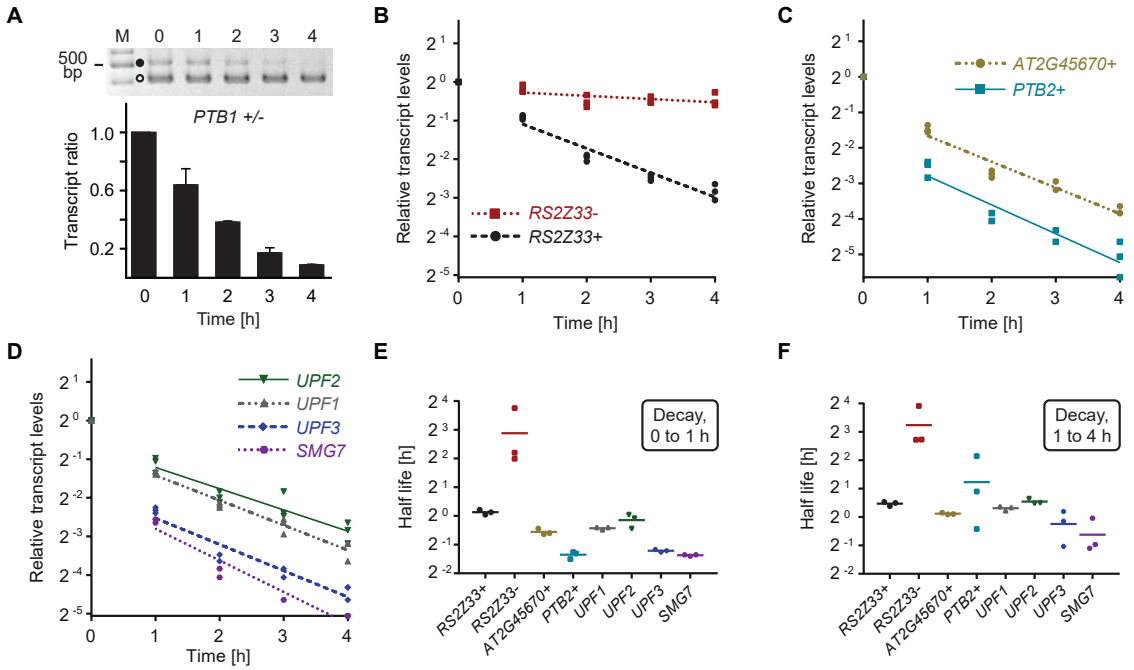

Figure D.1: NMD targets are subject to rapid turnover (Kesarwani, Lee, Ricca et al. (2019). Data and graphs generated by myself, graphs assembled and legend text written by Prof. Andreas Wachter). (A) Coamplification of the PTC− (411 bp, white dot) and the PTC+ (513 bp, black dot) splicing variants of *PTB1* at indicated time points upon transcription inhibition in 7-day-old liquid-grown *A. thaliana* seedlings by cordycepin treatment. Top: gel picture of representative data set, with size marker (M) in 100 bp increments. Bottom: Ratio of PTB1 PTC+/PTC- quantified via Bioanalyzer. Data are normalized to 0 h time point and represent mean values +SD ($n = 3$). (B–D) Transcript decay curves as measured via RT-qPCR from seedlings subjected to transcription inhibition as described in (A). Data are normalized to reference and represent three biological replicates indicated by symbols. Lines show exponential regression starting from 1 h time point. (E–F) Half-lives of indicated transcripts as determined by exponential regression for intervals from 0 to 1 h (E) and 1 to 4 h (F). Symbols show values from three biological replicates each, lines depict mean values.

E NMD target transcripts stabilized in NMD mutants, and further stabilized upon NaCl stress

Figure E.1: 35-d-old soil grown *A. thaliana* Col-0 WT (left) and *smg7-1* (right). The mutant *smg7-1* exhibits strong growth defects, and is sterile when homozygous (Riehs et al., 2008).

F NaCl mediated NMD inhibition involves translation but independent of eIF2α phosphorylation and TOR

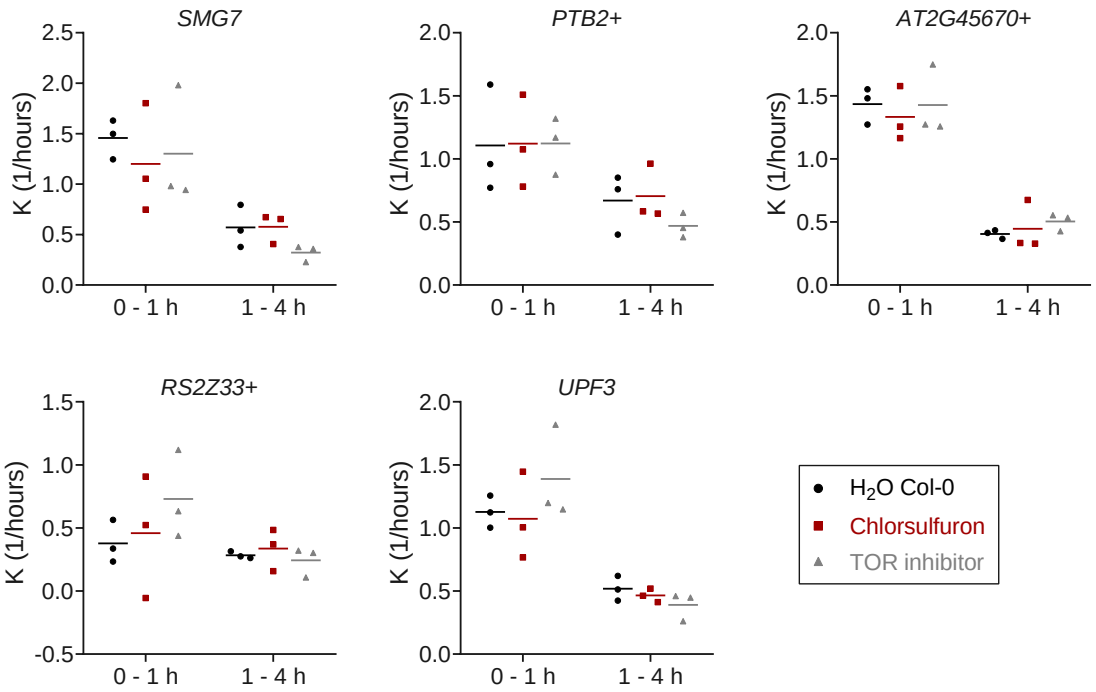

Figure F.1: Rate constants (K) of NMD target transcripts under control conditions, 0.6 μM chlorsulfuron or 5 μM mTOR inhibitor (AZD8055). Unpaired t-tests were performed on both treatments compared to the control, and none were found to be significant ($\alpha = 0.05$). Dots represent individual values, lines represent mean.

G ABA and downstream SnRK2s do not have major involvement in NMD inhibition under NaCl

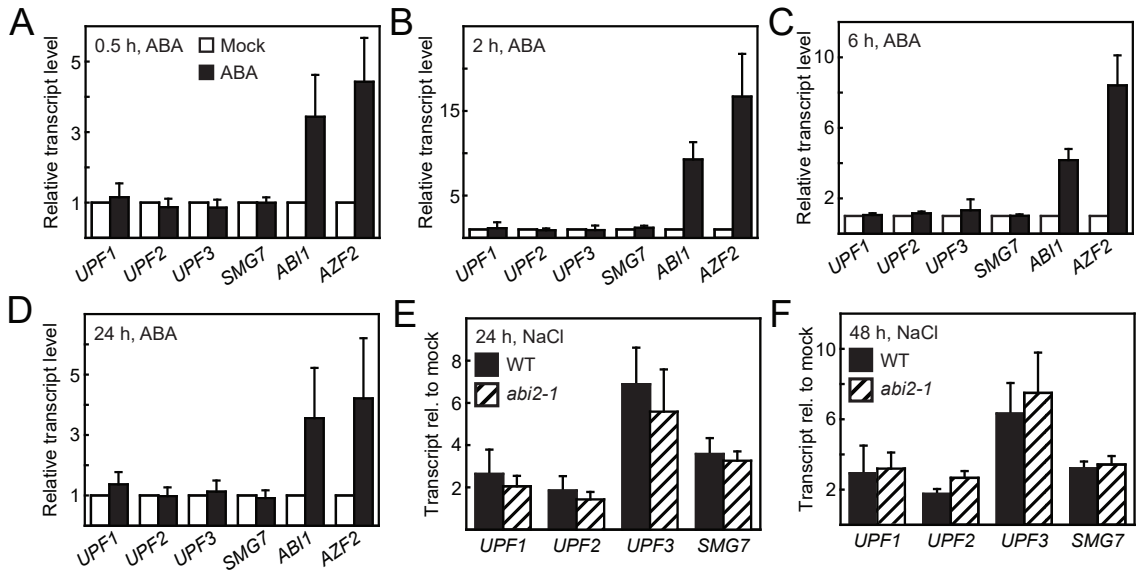

Figure G.1: NaCl-Mediated Induction of NMD Factor Transcripts Is Independent of ABA (Kesarwani, Wachter, et al., unpublished. Figure generated by Prof. Andreas Wachter, data in A–D generated by others than myself). (A–D) 12-day-old, plate-grown *A. thaliana* seedlings were sprayed with 0.01 % Tween 20 (Mock, white) or additionally 100 μM ABA (black), followed by RT-qPCR analysis of the indicated transcripts 0.5 h (A), 2 h (B), 6 h (C), and 24 h (D) after treatment. Data are normalized to mock and are displayed as mean values +SD ($n = 3$). (E, F) 12-day-old *A. thaliana* Landsberg erecta (Ler) seedlings (WT and *abi2-1* mutant) were incubated on plates with mock or 500 mM NaCl solution for 24 h (E) and 48 h (F). Transcript levels were determined by RT-qPCR and normalized to *PP2A* and are presented as means relative to mock values +SD ($n = 3$-4). Color key in (A) applies to all graphs.

H ROS may play a minor role in NMD inhibition under NaCl

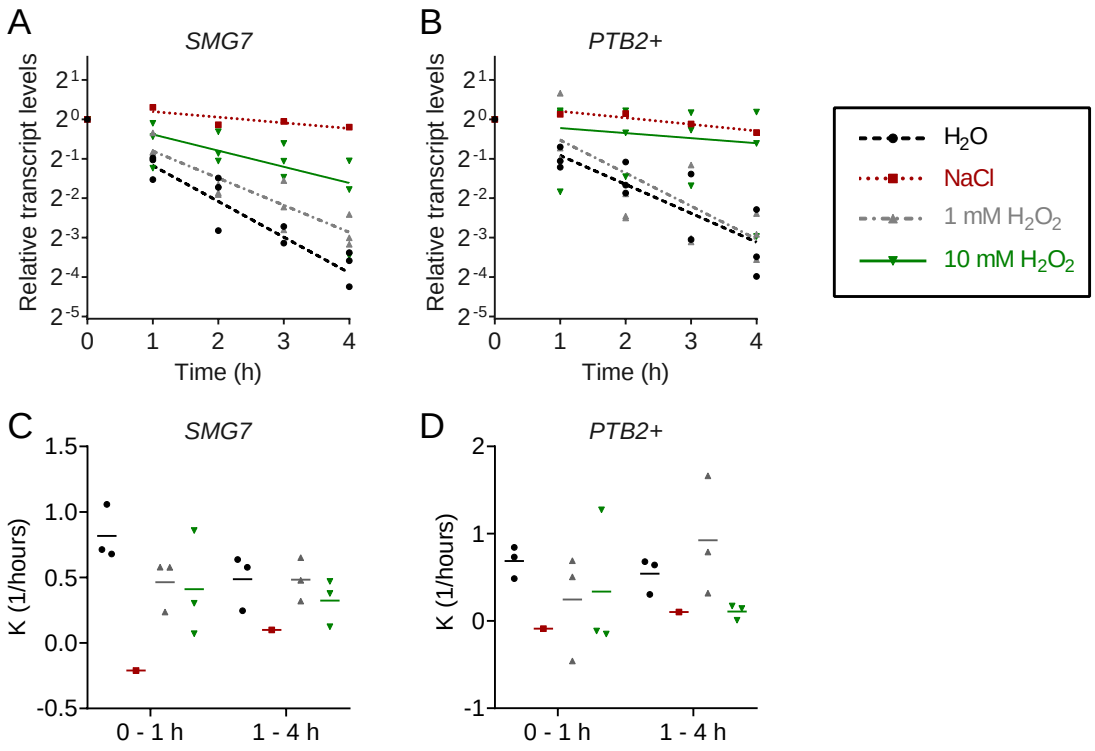

Figure H.1: NMD target transcripts stabilize upon H_2O_2 in a dose-dependent manner. Decay graphs (A–B) and rate constants (C–D) of 7-d-old *A. thaliana* under H_2O control ($n = 3$), 100 mM NaCl ($n = 1$), 1 mM ($n = 3$), or 10 mM ($n = 3$) H_2O_2 treatment. Dots represent individual values, lines represent least squared non-linear regression (A–B) and mean (C–D). Unpaired t-tests performed with 1 mM or 10 mM H_2O_2 against negative control H_2O.

ROS scavengers do not destabilize NMD targets under NaCl

A previous study has shown that ROS production during salt stress was blocked by inhibition of the NADPH oxidase with DPI (Mazel et al., 2004), and that the intracellular ROS produced by NOX is a response to ionic but not osmotic stress (Leshem et al., 2007). This situation is similar to that discussed in Section 4.3, where osmotic stress is shown not to be the major cause of NMD inhibition under NaCl. Therefore three ROS scavengers were selected for this purpose: *N,N'*-dimethylthiourea (DMTU), which is widely used for H_2O_2 suppression (Levine et al., 1994; Böhmer and Schroeder, 2011; Ben Rejeb et al., 2015; Gendreau et al., 2017), DPI, an NOX inhibitor, and DF, an iron/aluminum chelator. Under physiological conditions, H_2O_2 oxidation power is believed to be observed in combination with Fe(II) (Fenton reaction) (Huang et al., 2005). For that reason DF was chosen, because one of the mechanisms of actions for suppressing ROS formation, is by inhibiting the

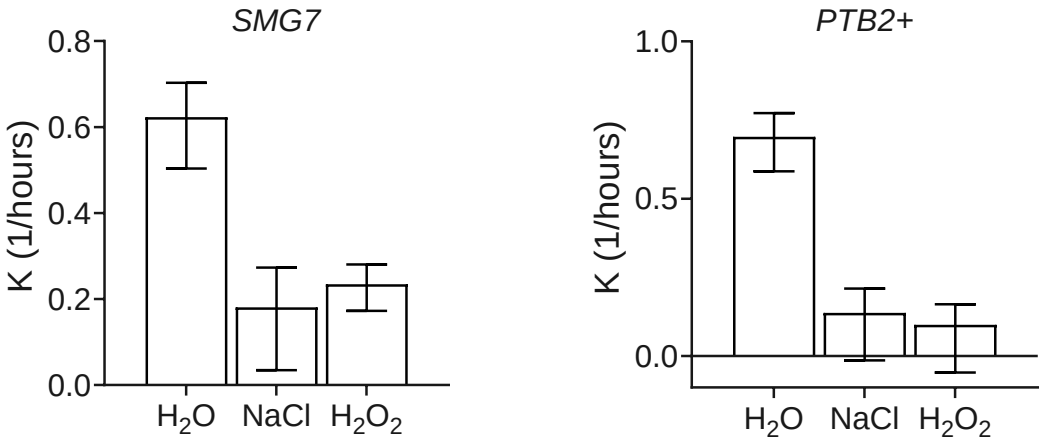

Figure H.2: H_2O_2 treatment stabilizes NMD target transcripts comparibly to NaCl. 90 % confidence interval (CI) of rate constants of *SMG7* (left) and *PTB2+* (right) with 10 mM H_2O_2 and 100 mM NaCl treatment in Figure 29C–D from 0–4 h.

enzyme systems or chelating metal elements which produce free radicals (Carocho and Ferreira, 2013).
DMTU was used in conjunction with NaCl in the half-life assay, and two NMD targets *SMG7* and *PTB2+* were analysed. DMTU stock was solved in methanol (MeOH), therefore the mock for this experiment was equal concentration (% v/v) MeOH. NMD targets in DMTU alone showed slight stabilization compared to mock, particularly during the 1–4 h phase of decay (Figure H.3). Although it is not statistically significant, this could indicate the suppression of H_2O_2 might partially inhibit some aspects of NMD. Upon the addition of NaCl, however, samples that were treated with DMTU did not show significant reduction of stability in NMD target transcripts in either phases (Figure H.3), which indicates the stabilization of NMD targets caused by NaCl acts through a different mechanism besides ROS signaling.

The results from the NOX inhibitor DPI were surprisingly similar. In this case, DPI stock was solved in dimethylsufoxide (DMSO), and therefore mock was equal concentration (% v/v) DMSO. Compared to mock, DPI alone was shown to slightly stabilize NMD target *PTB2+*, particularly in the 1–4 h phase (Figure H.4B, D), while the decay was almost parallel to mock in *SMG7* after the first hour (Figure H.4A, C). Under NaCl treatment, both transcripts show decay within the first hour, but none of the results were significant (Figure H.4).

In the case of the metal chelator DF, three NMD targets *SMG7*, *PTB2+*, and *RS2Z33+* were analysed. At a glance, under NaCl, DF is shown to hyper-stabilize NMD targets (Figure H.5). However since the sample size of both positive and negative controls were $n = 1$, and one 1 h sample point in the positive control was missing due to technical failure in RNA extraction, it would be pre-mature to

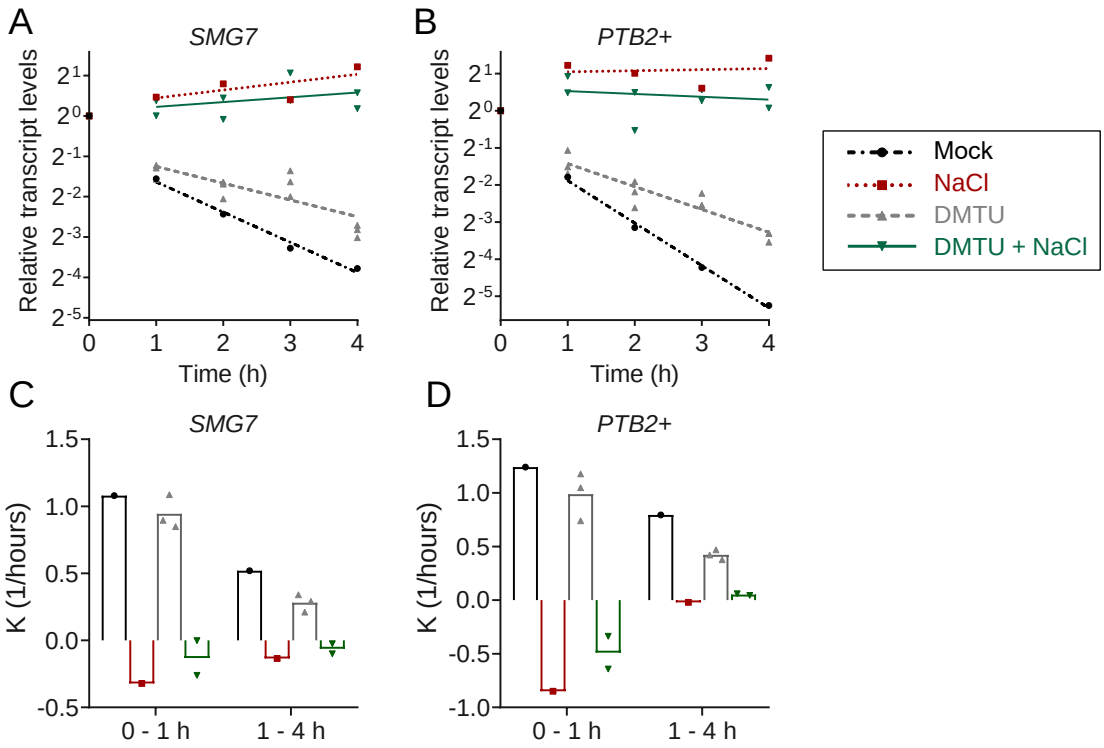

Figure H.3: ROS scavenger DMTU do not significantly destabilize NMD targets under salt stress. Decay graphs (A–B) and rate constants (C–D) of 7-d-old *A. thaliana* seedlings under mock ($n = 1$), 100 mM NaCl ($n = 1$), 15 mM DMTU ($n = 3$), and 15 mM DMTU + 100 mM NaCl ($n = 2$). Dots represent individual values, lines in (A–B) represent least squares non-linear regression, columns in (C–D) represent mean. Unpaired t-tests were performed comparing DMTU samples against their respective controls, i.e DMTU to Mock, NaCl + DMTU to NaCl. Data not significant.

conclude that DF could have astounding effects on NMD under NaCl.

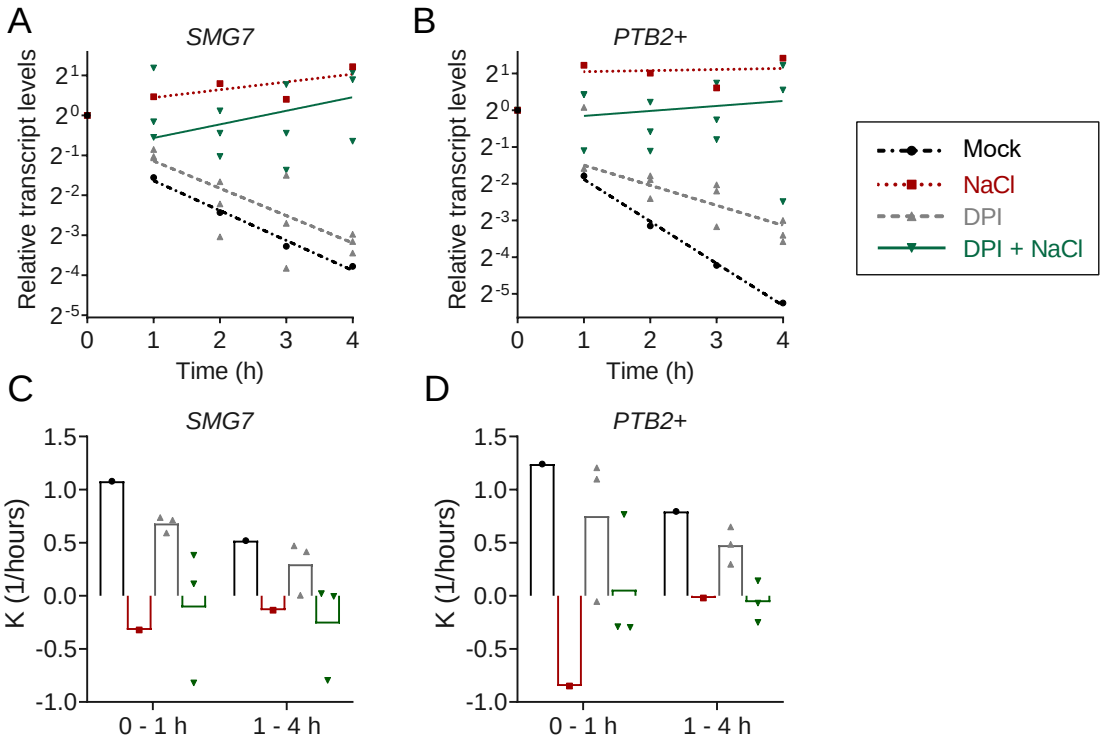

Figure H.4: ROS scavenger DPI do not significantly destabilize NMD targets under salt stress. Decay graphs (A–B) and rate constants (C–D) of 7-d-old *A. thaliana* seedlings under mock ($n = 1$), 100 mM NaCl ($n = 1$), 250 μM DPI ($n = 3$), and 250 μM DPI + 100 mM NaCl ($n = 3$). Dots represent individual values, lines in (A–B) represent least squares non-linear regression, columns in (C–D) represent mean. Unpaired t-tests were performed comparing DPI samples against their respective controls, data not significant.

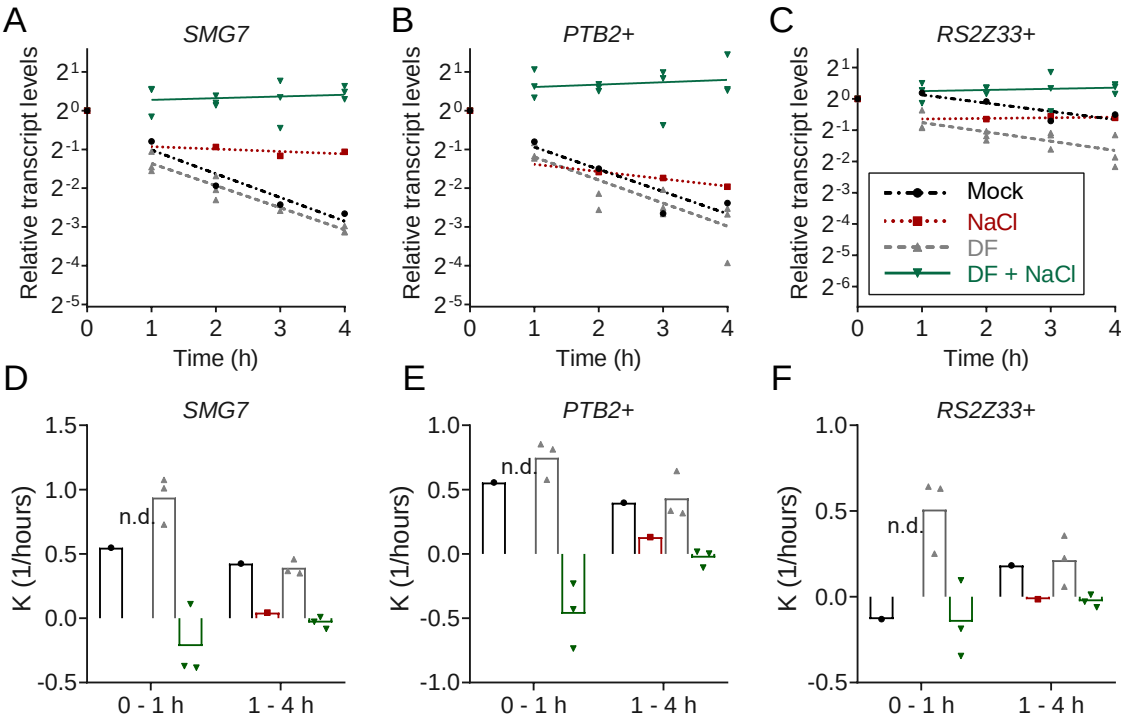

Figure H.5: ROS scavenger DF do not destabilize NMD targets under salt stress. Decay graphs (A–C) and rate constants (D–F) of 7-d-old *A. thaliana* seedlings under mock ($n = 1$), 100 mM NaCl ($n = 1$), 1 mM DF ($n = 3$), and 1 mM DF + 100 mM NaCl ($n = 3$). Dots represent individual values, lines in (A–C) represent least squares non-linear regression, columns in (D–F) represent mean. Unpaired t-tests were performed comparing DF-treated samples against their respective controls, data not significant. Due to technical issues the 1 h sample in NaCl is unavailable, and thus no data (n.d.) was plotted in 0–1 h (D–F). Color key in (C) applies to all graphs.

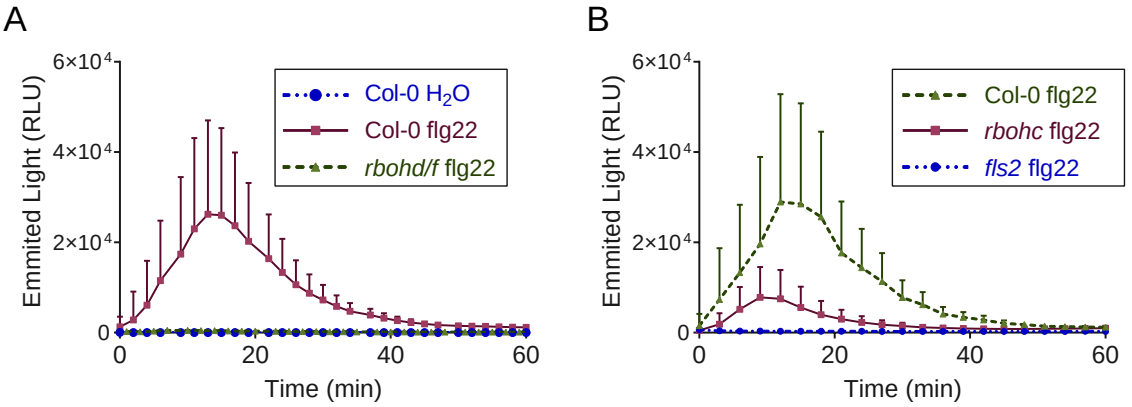

Figure H.6: None or weak oxidative burst triggered in *rboh* mutants under flg22 treatment (Wall, 2017). (A) Oxidative burst assay with 1 μM flg22-treated *A. thaliana* Col-0 WT ($n = 11$), *rbohd/f* ($n = 13$), with Col-0 in H_2O as negative control ($n = 8$). (B) Oxidative burst assays with 1 μM flg22 treated Col-0 WT, *rbohc*, and negative control *fls2* ($n = 8$). Line and dots represent mean, error bars represent +SD. Data adapted from Wall (2017), figures reworked.

I Increases in cytosolic calcium causes NMD target stabilization, and blocked Ca^{2+} channels may increase NMD sensitivity to NaCl

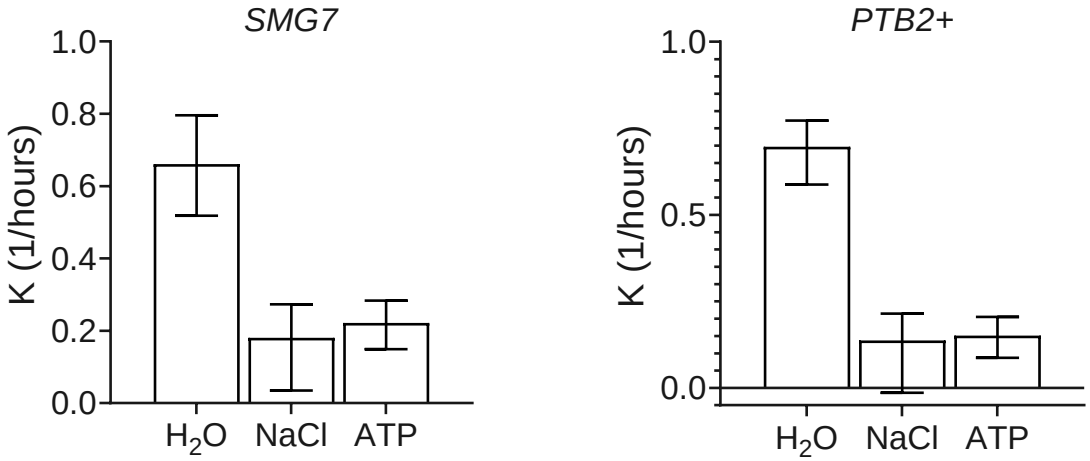

Figure I.1: ATP treatment stabilizes NMD target transcripts comparibly to NaCl. 90 % CI of rate constants of *SMG7* (left) and *PTB2+* (right) with 1 mM ATP and 100 mM NaCl treatement in Figure 38C–D from 0–4 h.

Table I.1: Predicted phosphorylation sites with a score over 0.9 for the 14-3-3-like domain of AtSMG7 (NetPhos 3.1b: http://www.cbs.dtu.dk/services/NetPhos/, Blom et al. (1999))

Position	Context (analysed residue centered)	Score (range [0.000–1.000])
12 S	KTTASSSWE	0.925
14 S	TASSSWERA	0.998
20 S	ERAKSIYDE	0.997
22 Y	AKSIYDEIA	0.945
93 S	VLASSTSTA	0.917
105 S	VKGPSKAEQ	0.924
156 S	SQNLSDKDG	0.997
195 S	AEGDSRSRQ	0.943
231 S	VASYSRDEF	0.966
268 S	KNRQSYEKL	0.996

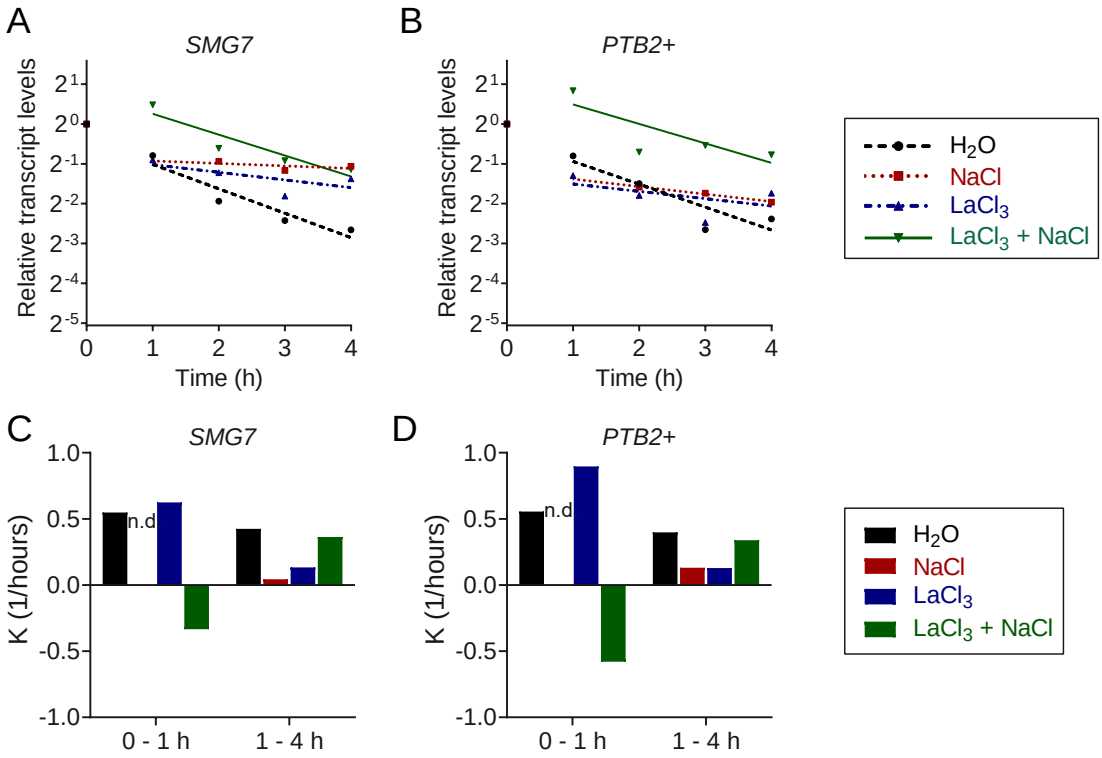

Figure I.2: $LaCl_3$ treatment may enhance NaCl sensitivity of NMD in *A. thaliana*. Decay graphs (A–B) and rate constants (C–D) of 7-d-old *A. thaliana* seedlings treated with 1 mM $LaCl_3$ with or without 100 mM NaCl, with mock as negative control, and 100 mM NaCl treatment as positive control ($n = 1$). Dots represent individual values, lines in (A–B) represent least squared non-linear regression, lines in (C–D) represent mean. Unpaired t-tests were performed against their respective controls, data not statistically significant. Due to technical issues the 1 h sample in NaCl is unavailable, and thus no data (n.d.) was plotted in 0–1 h (C–D). Color key next to B applies to A–B, color key next to D applies to C–D.

J Stress granules are involved in mRNA decay

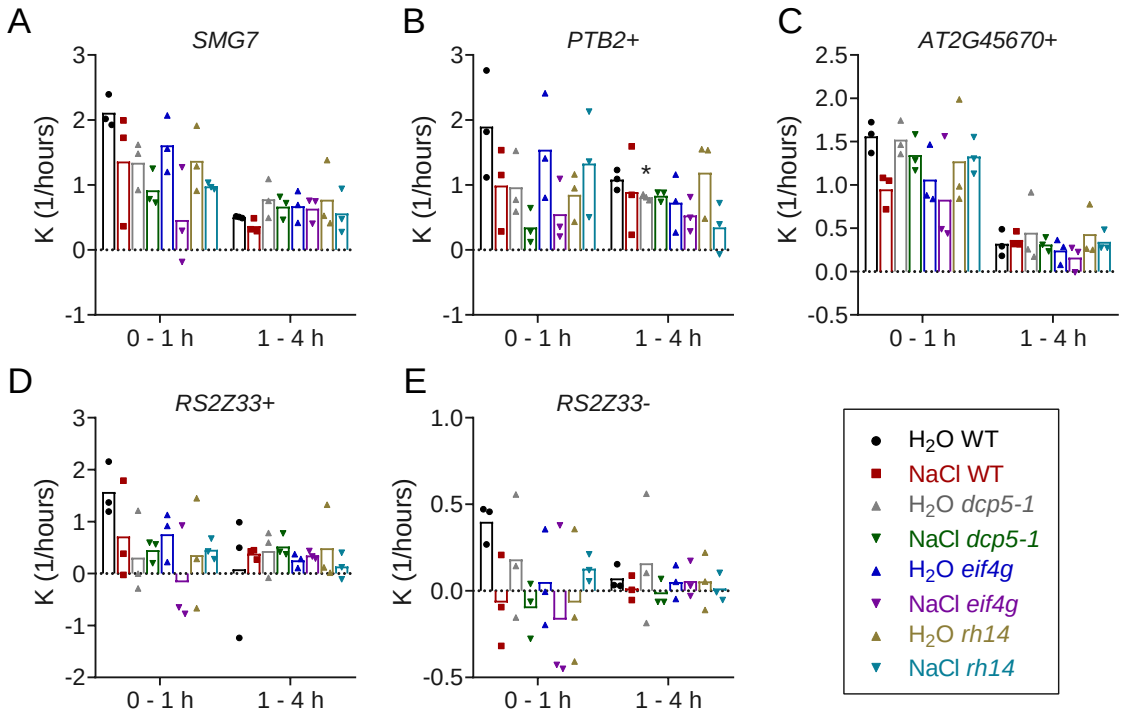

Figure J.1: Rate constants of WT, *dcp5-1*, *eif4g* and *rh14* samples with and without NaCl, corresponding to decay graphs in Figure 45, Figure 46 and Figure 47 respectively. Dots represent individual values, column represents mean. *, $P < 0.05$, unpaired t-test against the respective control: (B) H_2O *dcp5-1* vs WT.